Department of Mathematics and Statistics

Deterministic Modelling of Whole-Body Sheep Metabolism

Emma Catherine Smith

This thesis is presented for the Degree of

Doctor of Philosophy

of

Curtin University

February 2014

Declaration

To the best of my knowledge and belief this thesis contains no material previously published by any other person except where due acknowledgement has been made.

This thesis contains no material which has been accepted for the award of any other degree or diploma in any university.

Emma Smith

February 2014

Acknowledgements

First, I would like to thank my Supervisor, Associate Professor Volker Rehbock. He has shown great patience and belief in me over the years, and prioritised my work at times when it would have been reasonable to not do so. He holds his own work to a very high standard and encourages and inspires me to do the same. The completion of this thesis would not have been possible without his guidance and respect.

I would also like to thank the late Dr Norman Adams of CSIRO. Dr Adams was a leader in the Australia livestock research community, and this project originated with him. In the early stages of my doctorate he provided friendly and considered advice, and I never felt I'd asked a silly question, although I'm quite sure I did from time to time. To quote a tribute written by his Officer-in-Charge Dr Rob Kelly, he was a "man with passion, commitment and time for us all".

Thank you to all the staff and students at the Department of Mathematics and Statistics, past and present, for making it such an interesting and supportive environment to work in. I'd particularly like to thank my friend and Co-Supervisor Dr Ian van Loosen, for giving me a hard time when it was needed, and for having a beer with me when that was needed.

I was given great support from my workplace, Data Analysis Australia, and without the time, patience and trust they provided me, both in my training and specifically for this work, I would not have completed this thesis. Particular thanks must go to Director Dr John Henstridge, Consulting Manager Anna Munday and Senior Consultant Statistician Donna Hill, thank you for your tolerance and your chocolate.

On a personal note, I must thank my partner and best friend Jarrod Black, for looking after me on every level both during the course of this work and always. Thanks to my mother Christine, who didn't follow the technical details but bought me a lot of sheep paraphernalia. She has always believed in me and provided great friendship and encouragement in all of my pursuits. Finally, a heartfelt thanks to my late father Maxwell. In endeavouring to make you proud I have achieved more in my life than I could have ever expected or hoped for.

Publications and Presentations

E. Smith and V. Rehbock, *Deterministic modelling of whole-body sheep metabolism*, Abstracts for the Conference of the Australasian Region of the International Biometric Society, 1–5 December 2013, Mandurah, Australia.

E. Smith, V. Rehbock and N. Adams, *Deterministic modeling of whole-body sheep metabolism*, Journal of Industrial and Management Optimization, **5** (2009), 61–80.

E. Smith, V. Rehbock and N. Adams, *Deterministic modeling of whole-body sheep metabolism*, Abstracts for the 7^{th} International Conference on Optimization: Techniques and Applications, 12–15 December 2007, Kobe, Japan.

Abstract

A deterministic model of whole-body sheep metabolism relies on biochemical knowledge on how pools in the body (e.g. amino acids) absorb nutrients from feed intake and interact with other pools (e.g. are utilised to form body protein). As such it is, where possible, based on accepted facts with regard to biochemical reactions, rather than empirical results from field experiments involving sheep. It is a proactive approach that has the potential to not just replicate experiences from the field, but to provide new information or theories with regard to sheep growth.

In working parallel to field testing of sheep, a deterministic model could be used as a first step, a chance to adjust hypotheses and hence the experimental design to optimise the application of the field results. The model has the advantage of running in a continuous fashion, such that the state of the sheep at any time can be reviewed. Field testing of whole-body sheep is limited to discrete intervals, and data is right-censored due to slaughter being a necessary component of assessing the whole-body. A deterministic model could assist in "filling in the gaps" left by a field experiment. In some situations, field testing of a hypothesis may not be possible, due to ethical, time or monetary constraints for the researcher. In this case, the model would provide an avenue for the research to be conducted, where it may not otherwise be possible.

A review of previous work in the development of whole-body deterministic growth models was undertaken, with the more comprehensive of these having been published in the late 1980s and early 1990s. It is without doubt a difficult problem to tackle, as it requires both a strong mathematical modelling background as well as an understanding of the biochemical processes involved. It does not come as a surprise that progress has been limited in the last 20-30 years. However, with sheep (both the meat and wool sub-industries) being one of the most enduring and prolific in Australia, the development of an accepted sheep model to use in the situations described would be of great benefit.

One of the more comprehensive sheep models published, as developed by Sainz and Wolff [83] in 1990, forms the base of the work in this thesis. It had some limitations that were immediately apparent, such as it being designed only to track lamb growth from 20 to 40kg, as well as other limitations that only became apparent later in this thesis. Sainz and Wolff [83] were forthcoming in their paper with regard to the estimation of the parameters used in their model and the approach in some instances was quite crude. This provided a window of opportunity for the use of dynamic optimisation techniques, in particular optimal parameter selection formulations and their numerical solutions, to improve the model using logical

expected outcomes of a reasonable model that didn't necessitate a strong biological or biochemical background.

The approach in this thesis is to provide the mathematical assistance to improve the model such that it produces reasonable results for both a 20 to 40 kg lamb, as well as growth into steady-state adulthood. To achieve this, the model from Sainz and Wolff [83], which primarily consists of a set of differential equations governing transactions between pools in the body, is implemented in the MISER3.3 [48] software. MISER3.3 is capable of both conducting general simulation and solving optimal control problems. The use of MISER3.3 as a simulation tool for the Sainz and Wolff [83] model was achieved by Hon [45], but coding errors in the derivatives (required to be defined explicitly) meant that the associated optimisation problems were not able to be solved in [45]. The work in this thesis includes correction of these errors and the subsequent use of MISER3.3 to solve various dynamic optimisation problems relating to the whole-body metabolism model.

The approach of the work described in this thesis is primarily mathematical and logical in nature, but it has used results from biological and agricultural literature to support adjustments to the model where this information was available. Whilst there is no guarantee that some of the results presented here are biologically sound, there also wasn't any evidence found to the contrary. The work provides a good starting point and elevates the model beyond some of the mathematical and programming issues that has previously held back its development. If reasonable growth and subsequent steady-state adulthood could not be achieved by the model with the structure outlined by Sainz and Wolff [83] and assuming flexibility in parameters, then a "biologically realistic" version under the same structure would clearly also not be achievable. That in itself would be a significant result. However, this work has achieved extension of the model into steady-state adulthood via dynamic optimisation techniques.

Whilst the work presented remains at a base level in the model development - there are many limitations still present in the application of the model with consequent recommendations for future research - it demonstrates that optimal control of such systems is possible with the appropriate level of mathematical expertise. A reliable, accepted model to replicate whole-body sheep growth throughout its life-cycle may still be a long-term goal, but the massive potential advantages of such a model in an industry worth billions in Australia alone ensures that incremental progress such as this is very important.

Contents

1 Introduction

The livestock industry is one of the most enduring and prolific in Australia, and yet whole-body approaches to understanding and modelling animal growth and development are not commonly found in agricultural literature. The problem can seem overwhelmingly complex as there are many unanswered questions with regards to nature versus nurture, genetic predisposition, and so on. Due to the complicated nature of a model of a living creature, it seems an impossible task to create a base of work in this area that couldn't be critiqued by even those who are not experts in the biology or mathematics fields, and so perhaps it is understandable that little work of this nature is readily available for review and comment. Whilst shortcomings are inevitable, improvements are not possible without there being substantial baseline work that can be improved upon. The aim of this study is to present a modelling, optimal control and simulation approach to the understanding of the development of a single animal to maturity. It will put forward a new direction for the livestock industry, using a generic sheep model as an example where optimal control theory can be applied to livestock objectives. It is expected to raise the interest of other scientists in the field of deterministic modelling of whole-body metabolism.

1.1 Advantages of Whole-Body Metabolism Modelling

There have been many research studies involving sheep and livestock in general that investigate the effects of different factors on the biological and nutritional state of sheep. However, most of these studies deal with only one or two factors at a time and observe the effects of these factors in only a limited number of areas in the body. By definition, this kind of research leaves many unknowns. Whole-body metabolism modelling is a more comprehensive approach to tracking animal development. Expertise in the area of biochemistry that would allow such modelling has been available for some time. As quoted from Bastianelli and Sauvant [15] relating to pig growth, a whole-body metabolism approach gives "fuller integration of present-day knowledge concerning growth mechanisms (than other approaches)". By integrating the underlying mechanisms of growth, it allows more complete understanding of the "important phenomena" of growth and ultimately better predictions of responses in animals to a variety of factors.

As an example, whilst a certain type of feed may increase resistance to a certain parasite, there are also potential side effects, both positive and negative. If a whole-body model is being used to initially test the hypothesis prior to field testing, the affects of the feed on the entire system can be reviewed. If a potential side effect is identified, the experiment can be adjusted to test for

this accordingly. This would lead to a more efficient approach to field testing. Additionally, should field testing not be possible due to ethical considerations, a comprehensive metabolism model could give insight into certain outcomes which would otherwise not be possible. Another limitation of field testing is that once a sheep has been slaughtered and its components analysed, it is clearly not able to resume further growth. A whole-body metabolism model gives the advantage of tracking the state of the sheep in continuous time, rather than at discrete intervals with an ever-decreasing sample pool.

A whole-body approach could not only indicate potential side effects for a proposed study, but it could also be used to test theories or anecdotal evidence as a base step prior to entering the field. If it is implemented into a software system, there is also the potential for new theories to be *established* using the whole-body model itself. With the advances in technology and computing power seen over the last few decades, iterative applications of inputs or controls on the model producing a numerical method for identifying new concepts has become a reality. For example, in an instance where the development of $x$kg of lean meat by y weeks of age was economically optimal, a whole-body computer model could be used to identify feeds or other control factors needed to achieve this goal within specified constraints. The ability to use numerical techniques in solving such problems and potentially uncovering new approaches to livestock development, where an analytical approach may be too complex and time-consuming and a trial-and-error field test may be infeasible, could be highly useful and lucrative.

Research in this area has the potential to enhance our knowledge of the complex and interdependent aspects involved in energy expenditure and protein metabolism. This information can then be used to improve general animal management strategies and also to ascertain suitable genetic traits for particular environments (weather, economically viable feeds, resistance to local diseases or pests, etc).

One example is wool production in sheep. Wool is a major export industry in Australia worth over $2 billion per year, as shown in Figure 5 (Australian Bureau of Statistics, Catalogue 7503). Wool is predominantly protein and higher wool growth in sheep has been known to come at the cost of lower meat production and poor animal health. A mechanistic dynamic model of protein synthesis would help develop our understanding of the consequences of an increasing amount of protein being supplied to the skin for wool growth. The ultimate goal here would be to advise sheep breeders in how they might achieve optimal wool production while still maintaining healthy, fertile and disease resistant sheep.

There are many advantages to the whole-body metabolism approach in modelling sheep growth. Sheep by-products are a significant industry in the Aus-

tralian economy, and hence improvements in the research area of whole-body metabolism modelling could be of tangible benefit in this context.

1.2 Sheep Industry

The Australia Bureau of Statistics (ABS) produces information on the number of sheep and the amount of wool produced in Australia dating back to the late 1880s, predating independence. This is information can be found in Catalogue 7124, and demonstrates the enduring nature of Australia's livestock industry, and particularly the sheep industry. Figures 1 and 2 display changes in the number of sheep and wool produced over time, for Australia and by State and Territory. The number of sheep in the country itself varies considerably over the years, with records as low as 53.4 million in 1903, following the end of the Boer War, and peaking at 180 million in 1970. There was another high point of 170 million in 1990, and it has been on the decline since. However, the number of sheep in the country is not an absolute reflection of the nature of the sheep industry, as it is also affected by the competing sub-industries of meat and wool production. A higher number of sheep in the country could be representative of periods where the wool industry is more lucrative, as an example. Figure 2 demonstrates this effect. While there is a noticeable correlation between the count of sheep and the kilograms of wool being produced, the wool production itself peaked at just over one million tonnes in 1990, the secondary peak of the number of sheep. This could be an indication of improved efficiency in wool growth on a per sheep basis, via careful breeding selection. New South Wales remains the dominant State in contribution to the sheep industry in both a per head and wool production context. Western Australia and Victoria have also become quite prominent in the industry in recent times, particularly in the wool sub-industry.

While Figures 1 and 2 present information relating to the number of sheep and amount of wool produced, it is also important to assess the value of the industry to the nation itself. Figure 3 displays information released by the ABS under Catalogue 7215 relating to the value and unit value of the highly political live sheep export industry. The frame for this data is restricted to the mid 1980s through mid 2013, with quarterly data points. This demonstrates an industry that is seasonal (generally peaking in the December quarter), but on an annual basis has been relatively steady for the last ten years. The unit value of live export sheep has increased, but the number of live exports has decreased. The recent decrease in live exports could be due to a transitional period following the introduction of the Australian Standard for the Export of Livestock by the Federal Government in July 2011, and the rise in unit value indicates demand

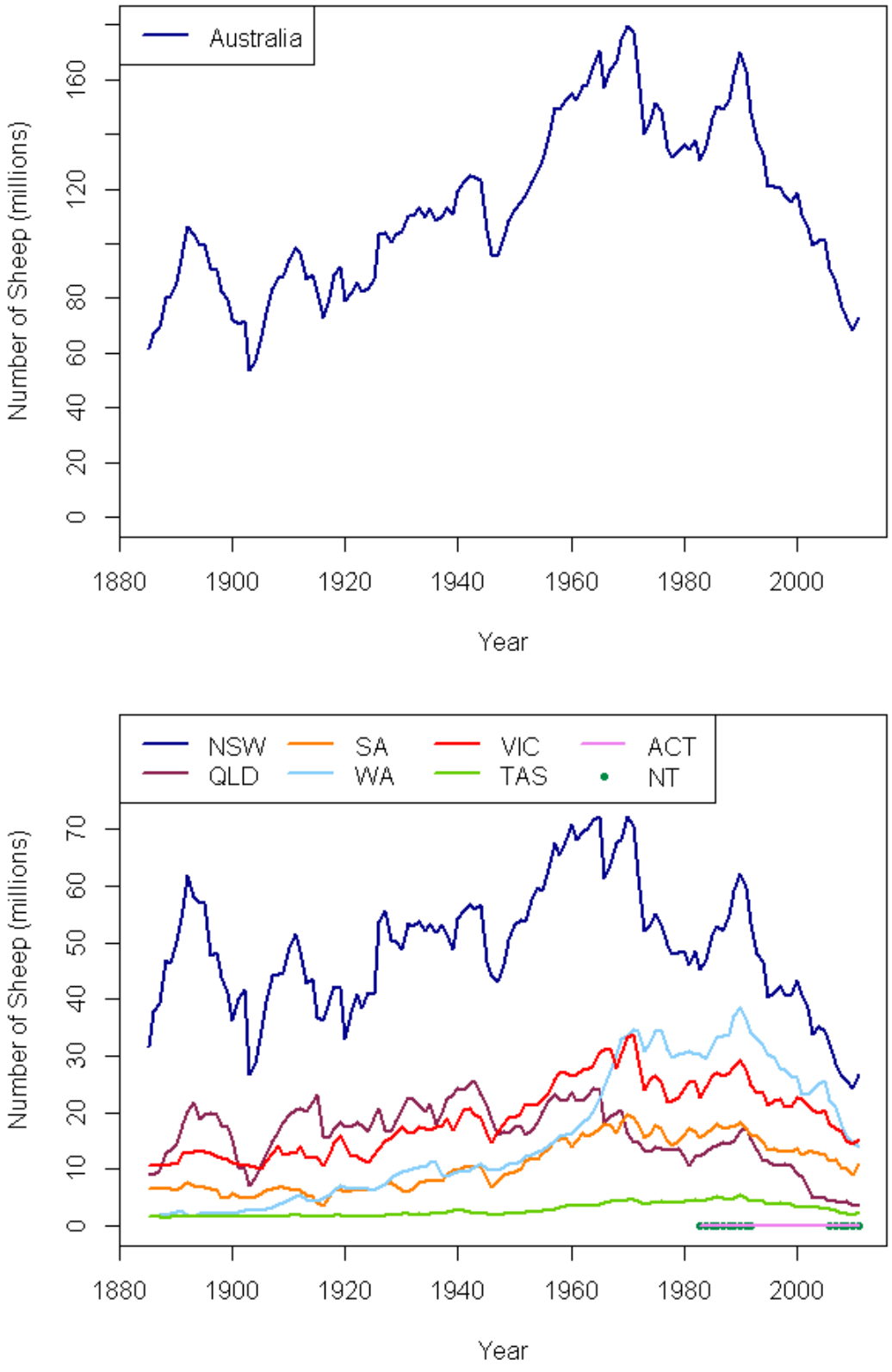

Figure 1: Number of Sheep. *Source: ABS Catalogue 71240DO001_201011 Historical Selected Agricultural Commodities, by State (1861 to Present), 2011.*

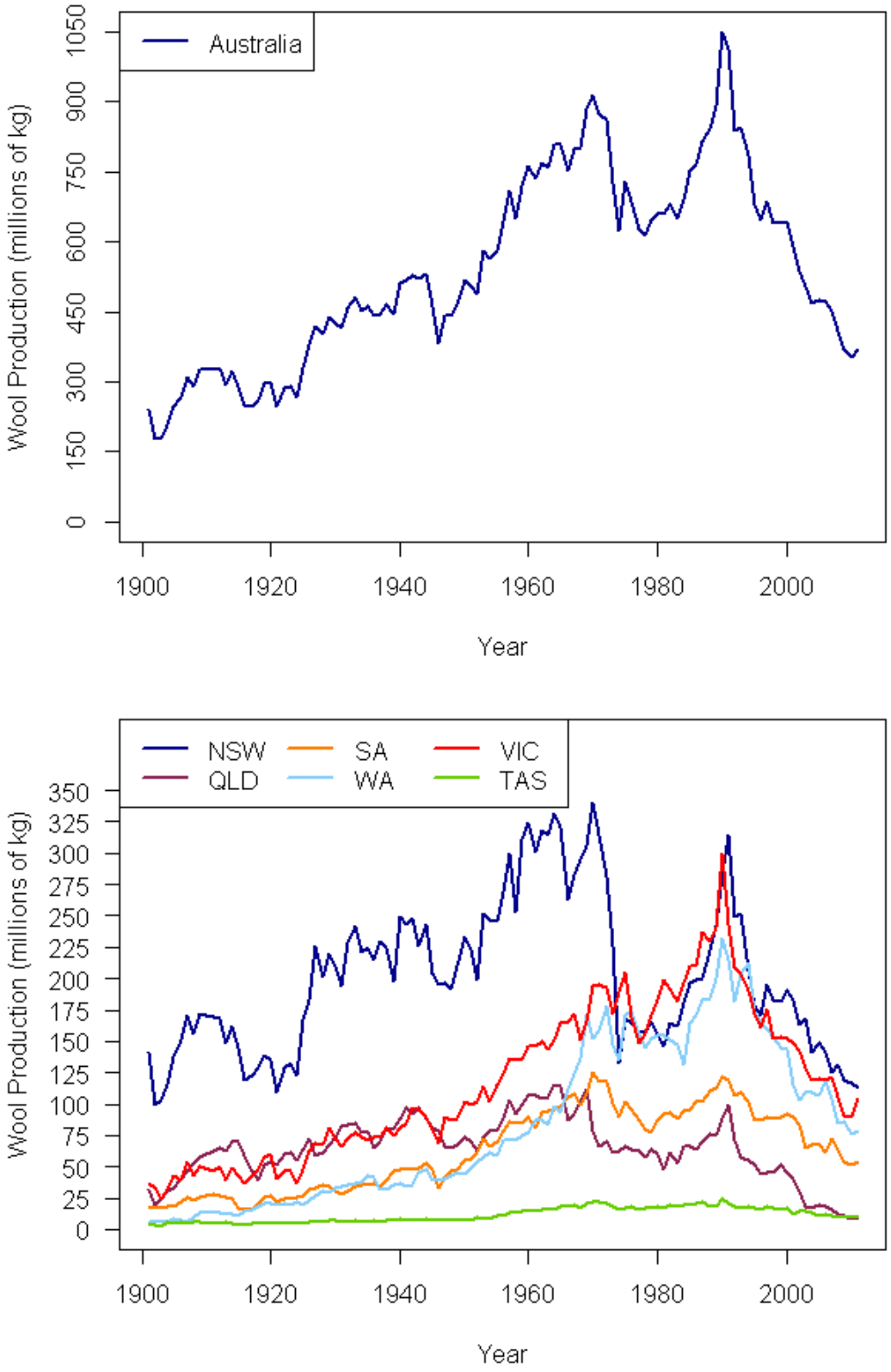

Figure 2: Wool production. *Source: ABS Catalogue 71240DO001_201011 Historical Selected Agricultural Commodities, by State (1861 to Present), 2011.*

has not waned. Information regarding export of mutton and lamb meat is also available under this ABS catalogue, and it shows a steady rise in the tonnes exported from 52,369 tonnes in March 1988 to 97,169 tonnes in June 2013.

Figure 4 shows the value nationally and by State and Territory of slaughtered sheep and lambs via the same ABS catalogue (7215). This shows a reasonably steady gross as well as local value of meat over the last seven years. The gross peak during this period is in the latest presented figure - $2.9 billion in the 2012 financial year. Contrary to number of sheep and wool production, it is Victoria that is the main contributing State to this industry. The value of wool produced has a similar trend, as shown in Figure 5. There has been positive growth in the value of wool being produced nationally, from $2.2 billion in the 2005 financial year to $2.7 billion in the 2012 financial year. Similarly to the wool production breakdown, it is New South Wales that has the highest produced wool value, followed by Victoria and Western Australia.

In its value per capita of population, using 2011 ABS Census of Population and Housing figures, it is South Australia and Western Australia that lead the nation with value of wool produced at $271 and $245 per person per year respectively. For value of slaughtered sheep and lambs it is Western Australia with Victoria, at $216 and $212 per person per year respectively.

To summarise, the sheep industry is enduring and significant to the Australian economy. It is robust, in that it has several sub-industries (wool, meat, live exports) as well as being strong in the local market and in export. It is widespread in its prevalence across the nation. Therefore, research that assists in further understanding the whole-body function of a sheep will be a meaningful contribution to the Australian economy and community as a whole.

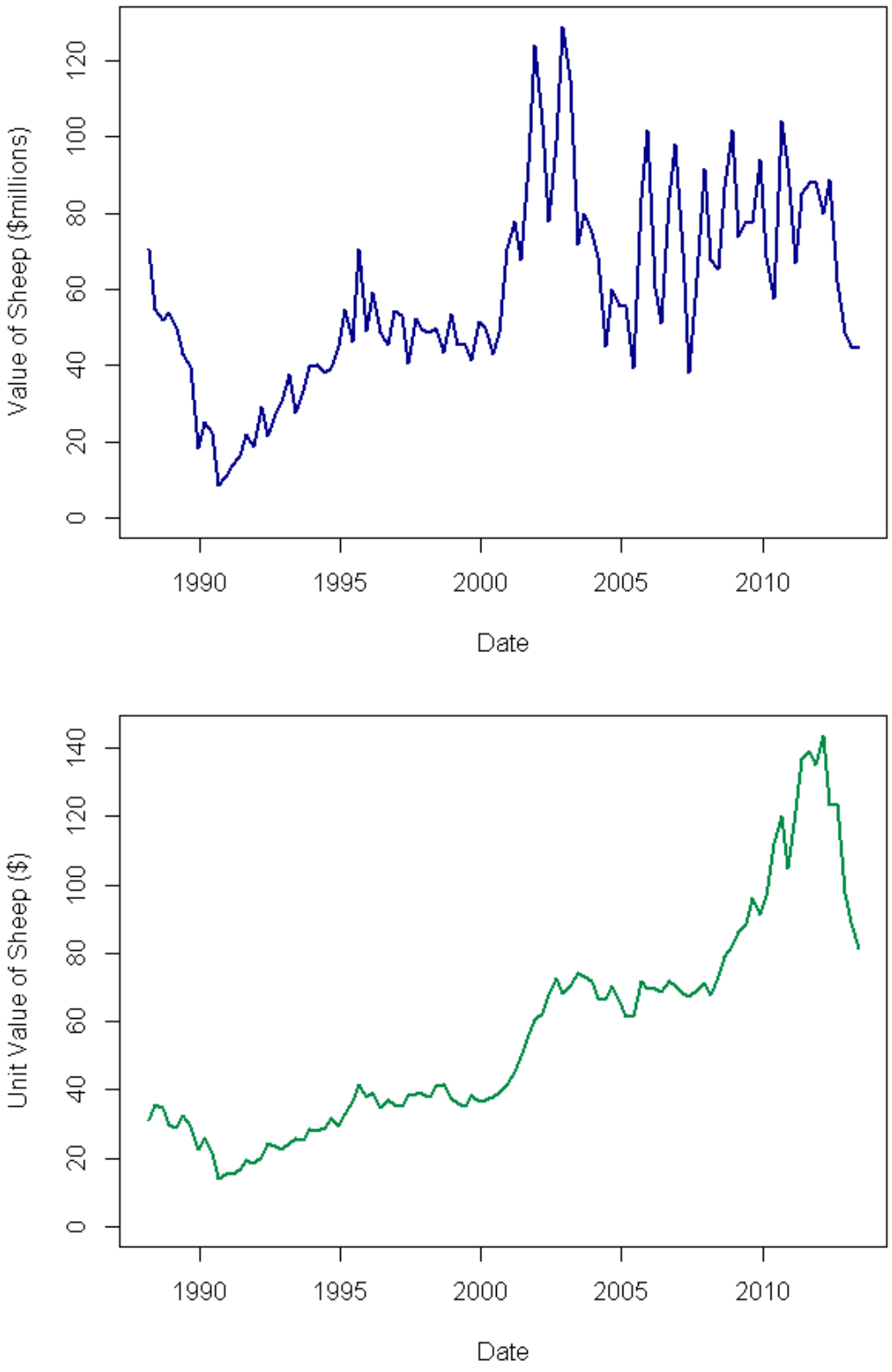

Figure 3: Value and unit value of live sheep exports (Australia). *Source: ABS Catalogue 7215.0, Table 6: Exports of Live Sheep and Cattle: Original.*

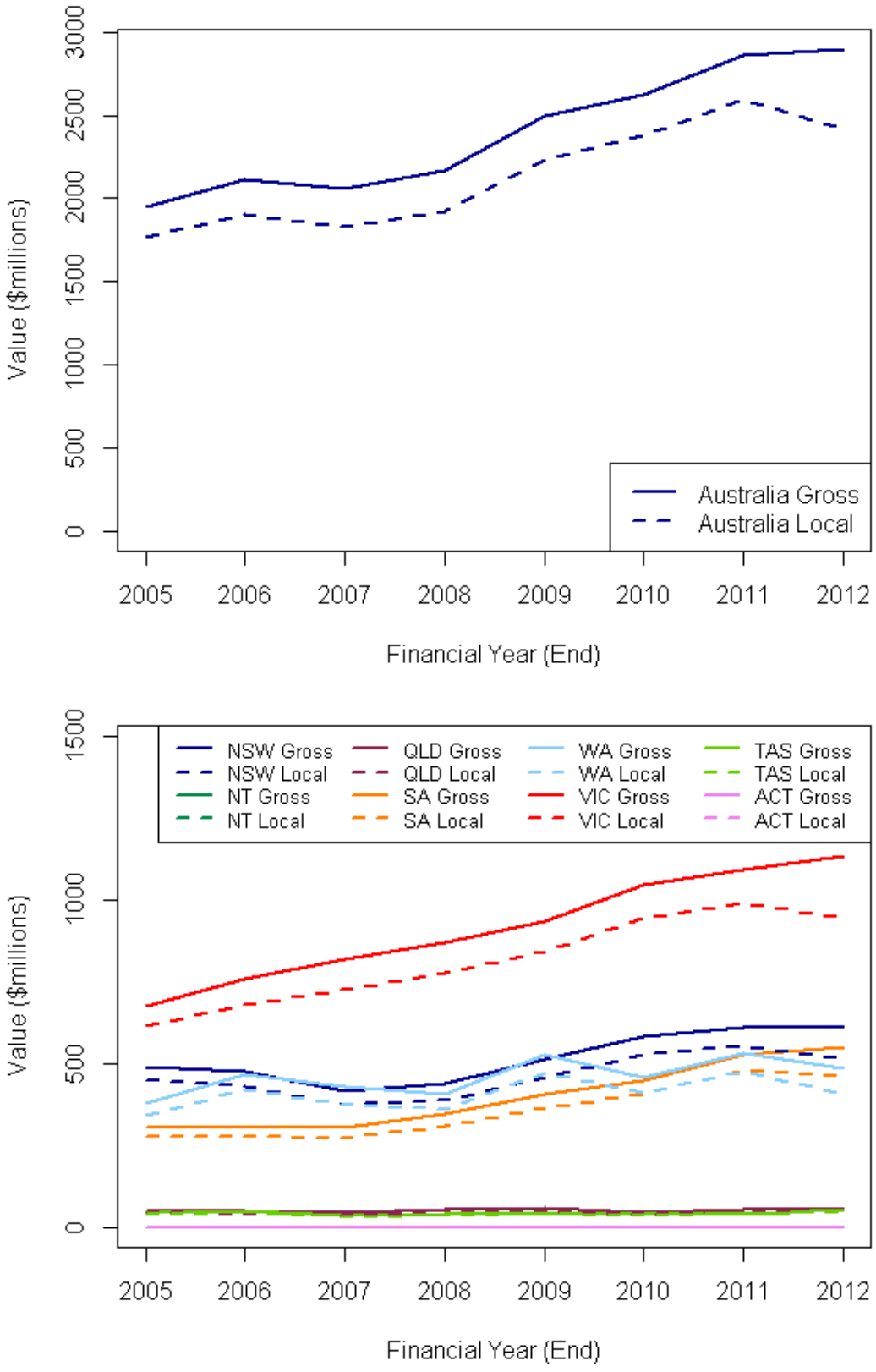

Figure 4: Value of slaughtered sheep and lambs. *Source: ABS Catalogue 7503.0, Value of Agricultural Commodities Produced, Australia.*

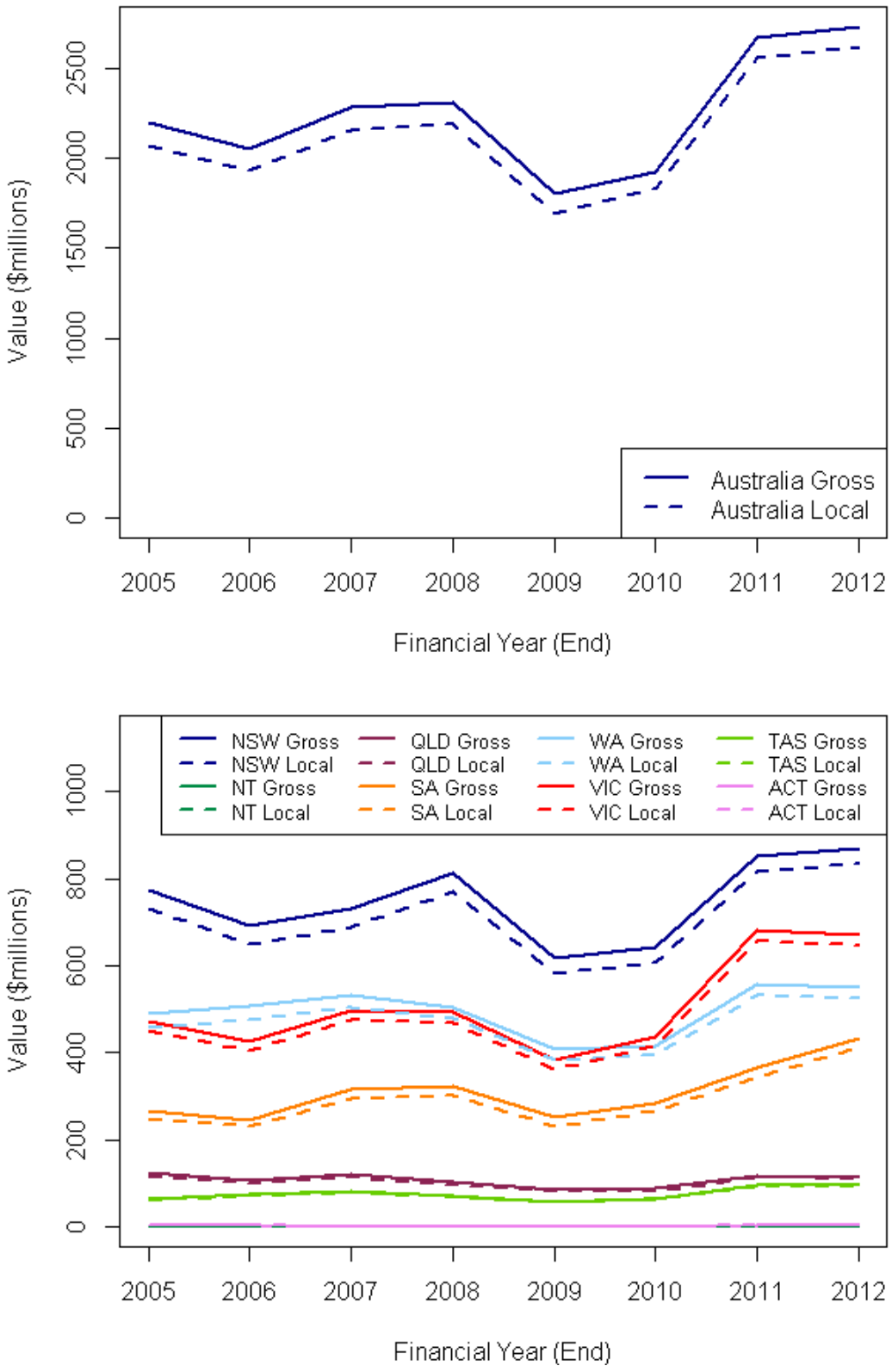

Figure 5: Value of wool produced. *Source: ABS Catalogue 7503.0, Value of Agricultural Commodities Produced, Australia.*

1.3 Review of Work to Date

Principles of basic allometry[1] have been applied to disaggregate growth into body components as far back as the 1920s, with Huxley [46] proposing the study of the relative importance of organs or chemical pools within an animal. Characterising an animal's compartments as body protein, lipid (fat), water and minerals (ash) was an alternative approach that grouped the organs or pools within an animal according to their chemical structure. This approach started appearing in the 1960s and 70s, and Bastianelli and Sauvant [15] described the common conceptual framework of this approach, see Figure 6. Figure 6 depicts a feedback system, in which the body weight and composition of the animal informs the subsequent selection of feed. A component of the absorbed nutrients from the feed is a maintenance requirement (quantity of food of a given quality needed to maintain a constant bodyweight), and the remainder is deposited as either body lipids or protein, leading to animal growth. This framework is a reasonable approximation of the whole-body metabolism, but the nature of how these pools change and inform the change of other pools needs to be defined to complete the model.

Specific to sheep, simplistic models capturing both feed type and availability as well as body and product also appeared in the 1970s. Such environment-pasture-animal systems tracked pasture pools (seed, burrs, etc), environmental conditions (e.g. rainfall and temperature) as well as a basic representation of a sheep by its tissue mass and wool mass. Arnold, Campbell and Galbraith [10] examined a sub-model of this system for sheep, concerned with the consumption of pasture and its use for maintenance, liveweight gain and wool production. This type of model assumes only minimal control over the feed intake of the sheep, with potential intake (relative to body weight) decreasing as the liveweight increases. It is a reflection of the flock maintenance systems at the time, but is limited in its representation of experimental conditions. Including representation of how a sheep might select its own feed under different levels of pasture availability and other factors is clearly problematic. Assumptions are not only required for the diet as selected by the sheep, but also the digestability of the feeds. Hence there is limited control over the inputs to the metabolic system. With a simplistic sheep model covering just tissue mass and wool mass, by definition the inputs need to also be simplistic. The dynamics of the model are based roughly around the relationships between the *digestable organic matter* input to the system and its affects on how close tissue and wool growth is to a pre-defined *maximum potential growth*, which may be dependent on the live weight of the animal, or nitrogen content of the feed.

[1] Allometry is the study of how biological variables scale with changes in body size.

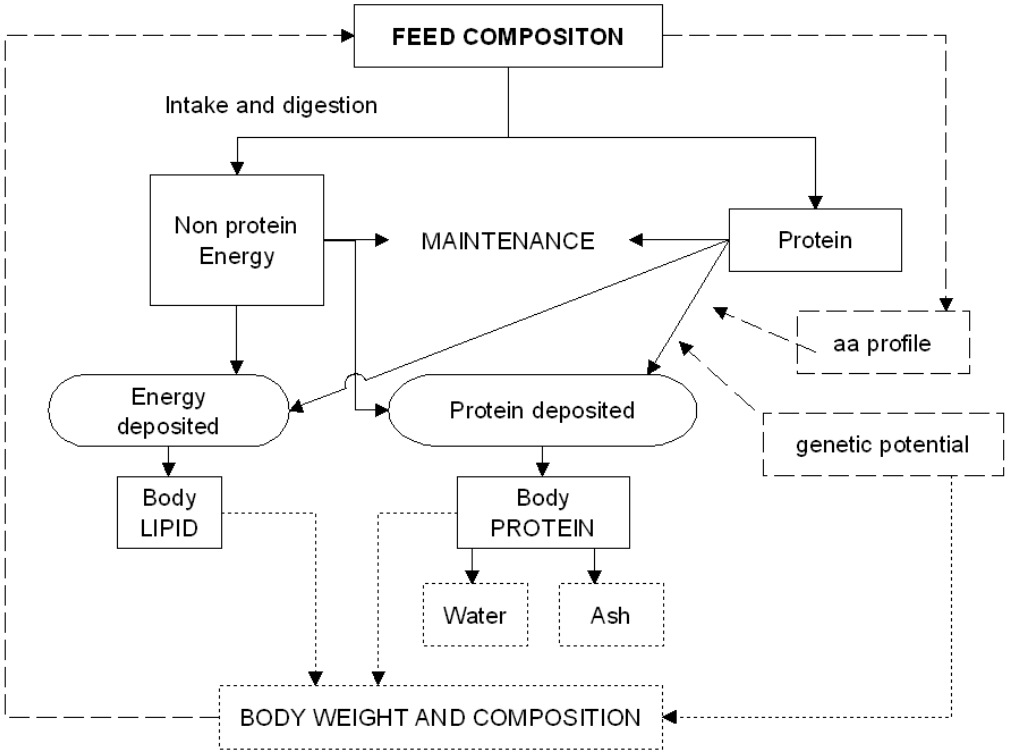

Figure 6: Simplified diagram of nutrient partitioning models. Body protein and body lipid are the state variables; solid arrows correspond with the flows of matter or energy; dotted arrows and boxes correspond with the auxillary variables; broken arrows and boxes correspond with flows of information.

Re-creation of Figure 1 from Bastianelli and Sauvant [15].

Across the 1980s and through the 1990s more sophisticated metabolism models started to emerge. It was known that differences in efficiency with which nutrients were metabolised could not be represented by simplistic models - it was dependent on the general metabolisability of the diet. The Agricultural Research Council [5] published equations for the metabolisability of different types of feed, but differences between these and the metabolisability of other feeds were still being reported in the literature, and models were limited by the availability of field research for the feed in question. Also, it was not abundantly clear *why* these differences in metabolic efficiency existed, and it became increasingly apparent that more sophisticated metabolism models were required to understand what was going on "behind the scenes". A telling example, described in Gill et al. [37], explains how there were contradictory results with regard to the impact of acetate utilisation on the relationship between metabolic efficiency and crude fibre content that were reported in Armstrong and Baxtor [8] and Armstrong et al. [9], as compared to the results in Rook et al. [82] and Ørskov and Allen [71]. In attempting to reconcile this apparent discrepancy, MacRae and Lobley [60] pointed out the need to consider the glucogenic potential of the basal diet when predicting the efficiency with which acetate would be used, and in particular the amino acid supply to the tissues. This example clearly demostrates the need for a whole-body metabolite modelling approach, in order to ensure the full picture of metabolic function is being captured.

A compartmental model that simulates the metabolism of absorbed nutrients in a growing lamb was developed by Gill et al. [37]. Equations within the model were based on enzyme kinetics and the stoichiometry of the biochemical pathways involved. The main flows and interactions between compartments of the model are shown in Figure 7. The model keeps track of the concentrations of different metabolites, and this information along with parameters governing maximum rates of reactions are the main components in the standard biochemical expressions for utilisation or degradation rates of substrates (substances on which an enzyme acts, e.g. glucose). Michaelis-Menton constants, coming from a standard and well-known approach to modelling enzyme kinetics as developed by Leonor Michaelis and Maud Leonora Menten [63], are also used. These constants define the relationship between the current state and the proportion of the maximal i to j reaction velocity that will be achieved between pools at a given point in time. The general structure of these equations are described in Equation (1), where U is the utilisation rate of a substrate, s is the concentration of the substrate, V is the maximal velocity of the reaction, and K is the appropriate Michaelis-Menton constant.

$$U = V\frac{s}{K+s} = \frac{V}{1+\frac{K}{s}}. \tag{1}$$

A conceptual interpretation of the Michaelis-Menton constant in this simple example is the concentration of the substrate at which the reaction velocity reaches half its maximum rate. However, there are more complex variations that take into account the common situation where utilisation rates are dependent on the concentrations of multiple substrates, and here the conceptual interpretation is less straightforward. The maximal reaction velocity can also be a constant, or it can be expressed linearly with respect to substrate concentration. The Gill et al. [37] model had mechanical representations of the whole-body metabolism. However, empirical relationships were used to define body fat and protein turnover. Generic expressions for body fat and protein synthesis based on biochemical knowledge would provide for a more flexible model.

Many publications relating to metabolism modelling and simulation of sheep, cows and steers have come via the Department of Animal Science at the University of California Davis (UC Davis) and its collaborators, with similar structures and state variable definitions. Baldwin, France and Gill [12] was a collaboration between Baldwin of UC Davis and representatives from the Animal and Grassland Research Institute in the United Kingdom, including Margaret Gill, the lead author of Gill et al. [37]. The research in Baldwin, France and Gill [12] set up a mechanistic model for a lactating cow. It was described as a "first step in a (modelling) research programme directed toward quantitative and dynamic evaluation of current concepts, hypotheses, and data for probable adequacy as explanations of variations in partition of nutrients in lactating cows". The idea was to set up the structure and parameterise whole-animal models that could be used to evaluate a multitude of factors relating to nutrient utilisation. The structure of the model was not dissimiliar to Gill et al. [37]. Aside from the differences necessary due to the change of species and the requirement for specific representation of lactation, the notable difference between the two was the more explicit representation of rates of protein and body fat synthesis, as opposed to an empirical definition. To facilitate this, the protein pools were broken down into lean body protein, protein in viscera (internal organs), and protein in milk, rather than expressed as a total protein pool that is subsequently divided into protein types. This allowed for rates of reactions to be more specifically linked to hormonal levels, both anabolic and catabolic.

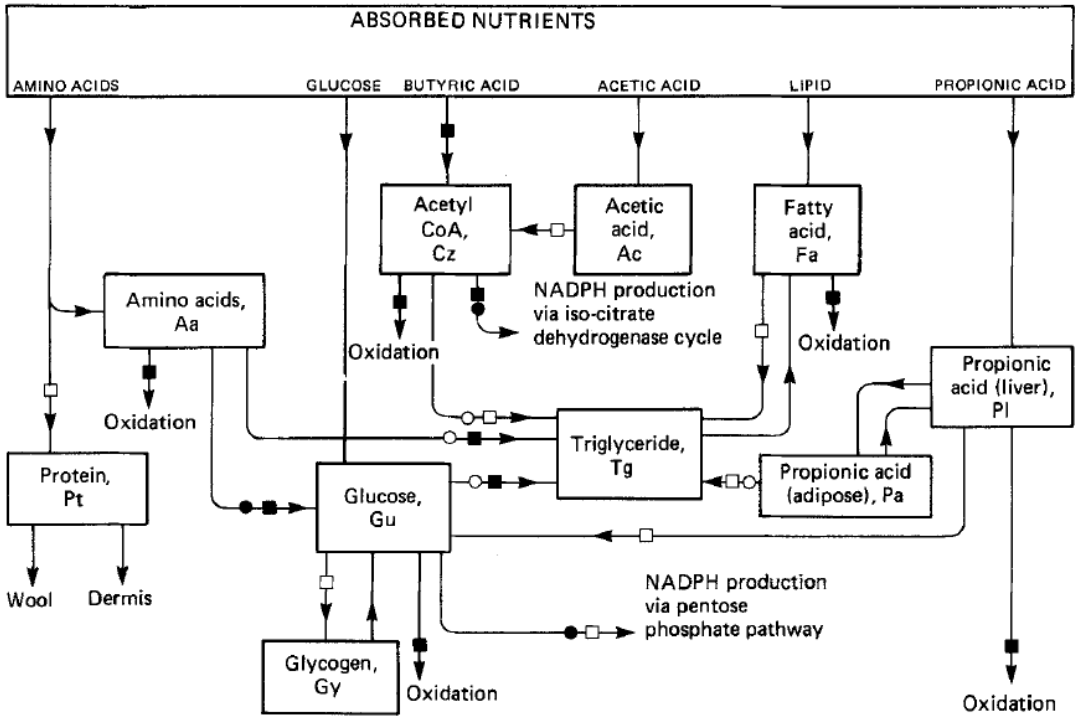

Figure 7: Model for the efficiency of utilisation of absorbed energy. Only the principal substrates and products are shown; carbon dioxide (Cx), oxygen (Ox) and urea (Ur) are also involved in many of these reactions. ATP (At) and NADPH (Np) are two important variables not shown above. The reactions are coded: (■), At-producting; (□), At-requiring; (●), Np-producing; (○), Np-requiring. Maintenance is not shown above, but is a drain on the At pool.

Re-creation of Figure 1 from Gill et al. [37].

A model for growing lambs that was very similar to the lactating cow model of Baldwin, France and Gill [12] was published in 1990 by Sainz and Wolff via the Ministry of Agriculture and Fisheries, New Zealand [83]. Roberto Sainz was also associated with UC Davis, and still was as of 2013. The objectives of the Sainz and Wolff [83] research were:

1. Simulation of lamb growth from 20 to 40kg empty body weight[2] under varying nutritional conditions;

2. Representation of major fundamental processes associated with growth and metabolism, aggregated to the minimal number of necessary pools; and

3. Integration of current knowledge regarding biochemical transformations and metabolic regulation to the whole-animal level.

These objectives appeared to be reached, and the model was subsequently used in analyses relating to growth promotants by Sainz and Wolff themselves [84]. Model details will be discussed further in Chapter 3, and the basic structure can be found in Figure 11, also of Chapter 3. State variables include circulating amino acids, glucose, acetate, lipids, as well as separate protein pools for carcass (or lean body protein), viscera, other tissues (head, skin, etc) and wool. Storage fat is also represented, along with an associated DNA pool for each protein pool (except wool) to govern limitations in genetic capabilities of protein growth. Other supplementary variables are also modelled, but for various reasons do not necessitate specific differential equations.

Following the publication of the Sainz and Wolff papers ([83] and [84]) there have been a number of published works in this field. Bowman, Cottle, White and Bywater ([20] and [21]) developed a model of sheep on a more macro level, including elements such as stocking rates (numbers of livestock in a predefined area) and pasture availability. However, it did have more specific traits for wool, as opposed to just protein in wool, covering the most important clean wool characteristics of fibre diameter, staple length, staple strength and vegetable matter level.

There have been a number of general reviews of existing models, many of which emphasise the need for a whole-body and mechanistic approach. These include Baldwin and Sainz's evaluation of performance and growth models based on feed intake and composition, coming out of UC Davis in 1995 [13]. In 1997, Hanigan et al. [41] reviewed protein synthesis models in ruminants, concluding that a great deal of future effort is required to construct and parameterise models, and

[2]Empty body weight (EBW) is the weight of the shorn animal, less the contents of the digestive tract, the bladder and the fleece (Butler-Hogg [23]).

that tangible improvements at the animal level can be made. Kebreab et al. [51] takes it a step further for dairy cattle in 2004, integrating a number of models and implementing the result into Fortran based software. However, the specific focus is on dietary manipulation to reduce pollution from livestock. Similarly in 2004, McNamara of Washington State University emphasises the advantages of mechanistic, biochemical, dynamic models of metabolism in dairy cattle ([58]). Model results are tested against observations and limitations, particularly with regard to accurate modelling of energy accumulation and energy use (most specifically in early lactation). McNamara's focus is leaning more towards research paving the way to adequate food supply for developing nations. Another publication from McNamara, this time in collaboration with Pettigrew [59] in 2002, reviewed the existing mechanistic, deterministic and dynamic models available for lactating sows.

Other examples of models published in recent years include a more generic mammalian two-dimensional representation (mass and energy) published by Vetharaniam et al. ([95] and [96]) from New Zealand in 2001. Whilst its structure is simplistic, it does attempt to model growth all the way from conception to maturity for mammals, and is described as having potential to be expanded to include details regarding body composition. In 2004, Fox et al. [36] developed a cattle requirement model based on a combination of animal, environmental and feed compositional information. It was a herd-level model that did not have the intricacies of an animal-level model, but did have the practical advanatages of being able to represent diverse production situations and different physiological states (growth, lactation, pregnancy). In 2005, Moen and Boomer [64] from Cornell University published a model for annual energy metabolism rhythms in free-ranging mammals. Whilst the animals were not livestock (white-tailed deer, black bears and golden-mantled ground squirrels), it did raise the interesting issue of variation in metabolism needs according to season.

In 2008, Upton [94] from the Royal Adelaide Hospital took an allometric approach to prepare organ weight and blood flow data for use in modelling the effect of drugs on the system of animals, such as sheep and pigs, in preclinical trials. The paper attempts to describe the relative components of a "standard sheep", which is then used to establish a simulated population. At the micro level, Sarnyai and Boros [86] model cellular energy metabolism and drug metabolism using systems biology. Their claim is that "(in order to) understand how the parts (genes, proteins and metabolites) make up the whole organism, a systemic view is required, with genes and proteins seen more as parts of a highliy interactive network with the potential to affect the network - and be affected by it - in many certain and sometimes unexpected ways, instead of as isolated entities entirely

or largely determining cell function". Also at the micro level, Fleming et al. [34] looked at models for steady-state metabolism for simple organisms in 2010. The work assumes time invariant reaction rates and concentration of metabolites to develop feasible reaction fluxes via constraint equations, and discusses the trade-off between imposing a multitude of physical laws, and the ability to solve the resulting equations.

The 4^{th} International Symposium on Energy and Protein Metabolism and Nutrition, hosted by UC Davis, was held in September 2013. Proceedings of the previous symposium in 2010 included a chapter on "Evaluation and modeling of feed value and requirements: ruminants". These proceedings contained papers from Tedeschi et al. [91] discussing the principal factors affecting the partial efficency of use of metabolisable energy, and from Cannas et al. [24] regarding the energy costs of maintenance of a herd. In the same chapter, De Angelis [30] evaluates the protein and energy value of hay and wheat straw diets for lambs of four different breeds (Sarda, Appenninica, Bergamasca and Leccese), and Oltjen et al. [69] reviews the integration of the UC Davis Sheep (UCDS), a mechanistic, dynamic model predicting lamb growth, with the Small Ruminant Nutrition System (SRNS), to predict dietary energy and protein values to input in the UCDS.

Whole-animal metabolism modelling for ruminants, and sheep in particular, is an ongoing research area. Existing models still lack flexibility. With respect to sheep, Sainz and Wolff's model from 1990 [83] seems to be the quintessential model, with mechanistic equations based on known biochemical processes, where parameters and inputs could potentially be manipulated to a multitude of conditions. However, it is limited in its scope of lamb growth from 20 to 40kg, and has only very basic representation of wool. It is not known how well the model could be extended into steady-state, whether issues exist relating to the representation of energy accumulation, as noted for dairy cattle by McNamara [58], or how feasible its implementation into software to assess various growth trajectories could be. The objective of this work is to investigate these issues, and propose a way forward to an integrated whole-body sheep metabolism model that can be readily used in a programmable context.

1.4 Approach and Outline

The potential benefits of the whole-body metabolism modelling approach are clear, but in order for it to have much worth it must achieve a reasonable level of accuracy. The definition of a reasonable level in itself does not have an obvious answer. At the very least, there must be a strong underlying biological and

chemical aspect to the model that is defensible. It should not yield significantly different results to those of peer-reviewed field studies. In this thesis, the following steps are taken towards achieving this reasonable level of accuracy.

- Review of previous work in this and related areas (see previous Section 1.3);
- Analysis of one of the more comprehensive mathematical models of sheep metabolism published thus far, from Sainz and Wolff [83];
- Implementation of the Sainz and Wolff [83] model into Fortran code and debugging;
- Utilisation of optimal control software MISER3.3 [48] to solve optimal model parameter selection problems;
- The use of MISER3.3 to validate and adjust the model;
- The use of MISER3.3 to solve optimal control problems, with the model as a constraint over various objectives; and
- Review of the work and recommendations for future work in the area.

2 Optimal Control

The approach outlined in Section 1.4 indicates the use of optimal control methods in both the determination of parameters and achieving given objectives. Therefore it is necessary to have a reasonable level of background knowledge in this area in order to understand and interpret the body of the thesis. Hence an introduction to optimal control problems and solution procedures is covered in this Chapter.

Optimal control as a name is quite self-explanatory, it refers to choosing a control function that will yield an optimal result. The results themselves are graded using an objective functional, or a performance measure, which we are seeking to optimise. This typically involves the selection of controls such that the objective functional is either minimised or maximised, and the objective functional can be defined in terms of a selection or combination of aspects of the system. For example, the objective functional could be structured for minimising the total control required (minimal effort). Or there could be a cost related to controls, which may also be dependent on time, and the objective functional could be structured for minimising the total cost of the control process. Objective functionals can also be weighted combinations of different objectives, to obtain an overall objective to optimised. Typically an objective functional has two components - one that is

expressed in terms of the final state of the system, and another that is expressed in terms of the state of the system and its controls over the length of the time period in question.

There is usually a set of constraints under which the system can operate, and constraints that govern the types of control that can be implemented. For example, irrigative control can only add water to a field, it cannot influence evaporation (at least not with regular irrigation). The constraints under which the system can operate can be a set of dynamic or algebraic equations. An algebraic constraint generally governs the allowed scope of the system, for example our field could have no water present, but it cannot have a negative quantity of water present, hence $y \geq 0$, where y represents water level in the field, may be an algebraic constraint of the system. There are also dynamic equations that may be constraints, these govern how the system will progress in relation to the controls. In the absence of control, it becomes a simple simulation where the system will flow naturally from one state to the next, as determined by these dynamic equations.

The dynamic equations can take several different forms. They could be a set of difference equations, relating the state of the system to previous states using a recurrence relation. Differential equations can be present in the continuous time context, and may be ordinary or partial. Ordinary differential equations are where the state variable is a function of a *single* independent variable, whereas partial differential equations are where the state variable is a function of *multiple* independent variables, and they involve partial derivatives with respect to said independent variables. The focus of this study is on continuous optimal control problems with sets of ordinary differential equations governing the change in the state vector with respect to time and current conditions of the state vector itself.

Optimal control problems with systems of ordinary differential equations have many applications. As the problems become more complex, analytical solutions are no longer feasible and numerical techniques must be employed. However, we will start with a simple example.

2.1 The Minimum Effort Control Problem

There are several interpretations of this problem, but the version we consider here is the problem of transferring state x_0 to x_T in time T using a minimum effort control $u(t)$. In keeping with the topic of this work, let us assume that this represents a farmer trying to achieve a certain amount of body weight growth in a sheep, using a minimal amount of feed. The objective functional $g(u)$, a function of the control, can therefore be defined as:

Minimise

$$g(u) = \int_0^T u(t)dt.$$

There are some constraints to be considered in this problem, firstly let us consider the constraints on the controls themselves and presume that one cannot actively remove feed from a sheep. Hence, the controls must be non-negative. It is also reasonable to assume some upper bound u_L on the feed rate. Therefore we have

$$0 \leq u(t) \leq u_L, \ \forall t \in [0, T).$$

Clearly, we have the restrictions of the sheep weight at the start and end of the time period:

$$x(0) = x_0 > 0,$$

and

$$x(T) = x_T > 0.$$

Let us also assume that $x_T \geq x_0$, that the rate of weight gain is a linear function of the rate of feed (with a positive gradient), and that a sheep will lose a certain proportion of their body weight as time progresses (in absence of feed). This gives the following, simple definition of a dynamic constraint:

$$\frac{dx(t)}{dt} = au(t) - bx(t), \text{ where } a > 0, \ 0 < b \ll 1.$$

This is a very simple example, and it is not difficult to come up with potential issues with the assumptions, or to think of more realistic versions. One such version would be to assume that the farmer has a minimum weight target, rather than an exact weight target in mind. It could also be desired that the rate of change of feed rate is kept quite low.

Another reasonable assumption is that as the weight increases a higher level of feed rate is required to increase the weight. For example, energy expenditure is likely to increase with weight, hence a higher feed rate would be required. This could be implemented by adjusting the coefficient of the control term in the dynamic equation to be in terms of the current state (for example, $a_1 - a_2x(t)$). This would change the dynamic constraint to:

$$\frac{dx(t)}{dt} = (a_1 - a_2x(t))\, u(t) - bx(t), \text{ where } a_1 > 0, \ a_2 > 0, \ 0 < b \ll 1.$$

An alternative objective would be to maximise

$$g(u) = \gamma_1 x(T) - \int_0^T \left(\gamma_2 u(t) + \gamma_3 \left| \frac{du(t)}{dt} \right| \right) dt,$$

where γ_1, γ_2 and γ_3 are non-negative constants weighting the relative importance of the three objectives: maximising the final weight, minimising the total amount of feed, and minimising the absolute value of the rate of change in the feed rate. The restriction of the sheep weight at the end of the time period would change to $x(T) \geq x_T$.

One could continue to increase the complexity of the model. In reality, the objective functional is highly dependent on the particular needs of the farmer. This in turn is highly dependent on the market for sheep by-products, and so for flexibility, a more comprehensive set of state variables is desirable.

2.2 Generic Optimal Control Problem

A general formulation of an optimal control problem can be represented as follows:

Minimise

$$g(\mathbf{u}) = \phi_1(\mathbf{x}(T)) + \int_0^T \phi_2 \left(t, \mathbf{x}(t), \mathbf{u}(t)\right) dt, \tag{2}$$

where $\mathbf{x}(0) = \mathbf{x_0} \in \mathbb{R}^n$, $\mathbf{x}(t) = [x_1(t), x_2(t), \ldots, x_n(t)]^\top$ are the states and $\mathbf{u}(t) = [u_1(t), u_2(t), \ldots, u_r(t)]^\top$ are the controls. ϕ_1 is a continuously differentiable function, and ϕ_2 is continuously differentiable with respect to $\mathbf{x}$ and $\mathbf{u}$ and piecewise continuous with respect to t. The dynamic constraints are defined as:

$$\frac{d\mathbf{x}(t)}{dt} = \mathbf{f}(t, \mathbf{x}(t), \mathbf{u}(t)), \ t \in [0, T], \tag{3}$$

where $\mathbf{f} = [f_1, \ldots, f_n]^\top \in \mathbb{R}^n$ are given functions that are continuously differentiable with respect to all their arguments. The process may also be subject to a set of m equality and/or inequality constraints of the form in Equation (4).

$$G_j(\mathbf{u}) = \psi_{1j}\left(\mathbf{x}(t_j|\mathbf{u})\right) + \int_0^{t_j} \psi_{2j}\left(t, \mathbf{x}(t|\mathbf{u}), \mathbf{u}(t)\right) dt \begin{cases} = 0, & j = 1, 2, \ldots, m_e, \\ \geq 0, & j = m_{e+1}, \ldots, m. \end{cases} \tag{4}$$

Note that $\geq$ could be replaced with $\leq$ in Equation (4) with no loss of generality simply by changing the sign of the ψ_1 and ψ_2 functions. Similarly, while the aim of the problem is to *minimise* the objective functional, this produces no loss of

generality, as it is the equivalent of *maximising* the objective funciton in Equation (2) with the sign changed for both ϕ_1 and ϕ_2.

The equality and inequality constraints given in Equation (4), and indeed the objection function in Equation (2), are said to be in canonical form. Many system constraints can be expressed as special transcriptions of this canonical form, and hence it is a convenient framework to express the constraints for a generic optimal control problem. In addition to the canonical constraints, optimal control problems usually involve bounds on the control. These may be written as:

$$u_{min_k} \leq u_k(t) \leq u_{max_k}, \ \forall t \in [0, T], \ k = 1, 2, \ldots, r. \tag{5}$$

2.3 Solution Strategies

There is clearly a large range of optimal control problems that could be posed, ranging from the very simple through to the highly complex. In the case of the former, there are some analytical solution strategies that may be applied. However, most real-world scientific problems are not very simple, and hence numerical methods for solving optimal control problems must be utilised. In this Section an outline of both analytical and numeric solutions will be presented.

2.3.1 Analytical Solutions

As numerical methods will be required for optimal control problems relating to whole-body sheep metabolism, only some basic theory and examples of analytical solutions will be presented here. We now consider the basic unconstrained problem of minimising the objective in Equation (2) subject to the dynamics described by Equation (3), i.e. minimise

$$g(\mathbf{u}) = \phi_1(\mathbf{x}(T)) + \int_0^T \phi_2\left(t, \mathbf{x}(t), \mathbf{u}(t)\right) dt,$$

subject to $\frac{d\mathbf{x}(t)}{dt} = \mathbf{f}(t, \mathbf{x}(t), \mathbf{u}(t))$, $\mathbf{x}(0) = \mathbf{x}_0$. As shown in Equation (6), the dynamic constraint can be added to the objective functional via the use of a multiplier, $\boldsymbol{\lambda}(t) \in \mathbb{R}^n$, which is akin to a Lagrange multiplier, and no actual change has occurred from $g(\mathbf{u})$ to $g^*(\mathbf{u})$ as long as the dynamic equations hold.

$$g^*(\mathbf{u}) = \phi_1(\mathbf{x}(T)) + \int_0^T \left[\phi_2(t, \mathbf{x}(t)\mathbf{u}(t)) + (\boldsymbol{\lambda}(t))^\top \left(\mathbf{f}(t, \mathbf{x}(t), \mathbf{u}(t)) - \frac{d\mathbf{x}(t)}{dt}\right)\right] dt. \tag{6}$$

If the Hamiltonian function is defined as:

$$H(t, \mathbf{x}, \mathbf{u}, \boldsymbol{\lambda}) = \phi_2(t, \mathbf{x}, \mathbf{u}) + \boldsymbol{\lambda}^\top \mathbf{f}(t, \mathbf{x}, \mathbf{u}), \tag{7}$$

and this is substituted into Equation (6), we have

$$g^*(\mathbf{u}) = \phi_1(\mathbf{x}(T)) + \int_0^T \left[H(t, \mathbf{x}, \mathbf{u}, \boldsymbol{\lambda}) - (\boldsymbol{\lambda}(t))^\top \frac{d\mathbf{x}(t)}{dt} \right] dt.$$

By applying integration by parts to the second term of the integrand, we have

$$\begin{aligned} g^*(\mathbf{u}) &= \phi_1(\mathbf{x}(T)) - \left[(\boldsymbol{\lambda}(t))^\top \mathbf{x}(t) \right]_0^T + \int_0^T \left[H(t, \mathbf{x}, \mathbf{u}, \boldsymbol{\lambda}) - (\frac{d(\boldsymbol{\lambda}(t))^\top}{dt} \mathbf{x}(t)) \right] dt \\ &= \phi_1(\mathbf{x}(T)) - (\boldsymbol{\lambda}(T))^\top \mathbf{x}(T) + (\boldsymbol{\lambda}(0))^\top \mathbf{x}(0) \\ &\quad + \int_0^T \left[H(t, \mathbf{x}, \mathbf{u}, \boldsymbol{\lambda}) - (\frac{d(\boldsymbol{\lambda}(t))^\top}{dt} \mathbf{x}(t)) \right] dt. \end{aligned} \tag{8}$$

At a local minimum, $\delta g^* = 0$. Therefore, we divert attention to δg^*. By use of the chain rule, it follows from Equation (8) that

$$\begin{aligned} \delta g^* &= \left[\frac{\partial \phi_1(\mathbf{x}(T))}{\partial \mathbf{x}} - (\boldsymbol{\lambda}(T))^\top \right] \delta \mathbf{x}(T) + (\boldsymbol{\lambda}(0))^\top \delta \mathbf{x}(0) \\ &\quad + \int_0^T \left[\left(\frac{\partial H(t, \mathbf{x}, \mathbf{u}, \boldsymbol{\lambda})}{\partial \mathbf{x}} + \frac{d(\boldsymbol{\lambda}(t))^\top}{dt} \right) \delta \mathbf{x}(t) + \frac{\partial H(t, \mathbf{x}, \mathbf{u}, \boldsymbol{\lambda})}{\partial \mathbf{u}} \delta \mathbf{u}(t) \right] dt. \end{aligned} \tag{9}$$

As the Lagrange multiplier $\boldsymbol{\lambda}$, also known as the costate, is arbitrary, we can set the definition of its derivative with respect to t and its end point such that the first term of Equation (9), and the first term of the integrand vanish. As $\mathbf{x}_0$ is fixed, $\delta \mathbf{x}_0 = 0$. That is, set:

$$\frac{d\boldsymbol{\lambda}(t)}{dt} = - \left[\frac{\partial H(t, \mathbf{x}, \mathbf{u}, \boldsymbol{\lambda})}{\partial \mathbf{x}} \right]^\top, \tag{10}$$

and

$$\boldsymbol{\lambda}(T) = \left[\frac{\partial \phi_1(\mathbf{x}(T))}{\partial \mathbf{x}} \right]^\top, \tag{11}$$

such that

$$\delta g^* = \int_0^T \left[\frac{\partial H(t, \mathbf{x}, \mathbf{u}, \boldsymbol{\lambda})}{\partial \mathbf{u}} \delta \mathbf{u} \right] dt. \tag{12}$$

As discussed previously, at a local minimum, $\delta g^* = 0$. This must hold regardless of $\delta \mathbf{u}$ and t. Therefore for Equation (12) to hold, we must have:

$$\left[\frac{\partial H(t, \mathbf{x}, \mathbf{u}, \boldsymbol{\lambda})}{\partial \mathbf{u}} \right]^\top = \mathbf{0}, \ \forall t \in [0, T]. \tag{13}$$

These are the familiar Euler-Lagrange equations. These only hold when the control $\mathbf{u}$ is unconstrained. In practice, the control will be limited with regard to the whole-body metabolism system. In this more general situation, the control values are restricted to a set of the form

$$U = \left\{ \mathbf{u} = [u_1, \ldots, u_r]^\top \in \mathbb{R}^r \mid u_{min_k} \leq u_k \leq u_{max_k},\ k = 1, \ldots, r \right\},$$

and the Euler-Lagrange equations are replaced by the Pontryagin Minimum Principle [76]. A particular case (for problems also involving a terminal state constraint $\mathbf{x}^*(T) = \mathbf{x_T}$) solved by Pontryagin and his colleagues is given below, without proof. If $\mathbf{u}^*$ is an optimal control, and $\mathbf{x}^*(t)$ and $\boldsymbol{\lambda}^*(t)$ are the corresponding optimal state and costate, then it is necessary that

$$\frac{d\mathbf{x}^*(t)}{dt} = \left[\frac{\partial H(t, \mathbf{x}^*(t), \mathbf{u}^*(t), \boldsymbol{\lambda}^*(t))}{\partial \boldsymbol{\lambda}} \right]^\top = f(t, \mathbf{x}^*(t), \mathbf{u}^*(t)),$$

$$\mathbf{x}^*(0) = \mathbf{x_0},$$

$$\mathbf{x}^*(T) = \mathbf{x_T},$$

$$\frac{d\boldsymbol{\lambda}^*(t)}{dt} = -\left[\frac{\partial H(t, \mathbf{x}^*(t), \mathbf{u}^*(t), \boldsymbol{\lambda}^*(t))}{\partial \mathbf{x}} \right]^\top,$$

and

$$\begin{aligned} &\min_{\mathbf{v} \in U} \ H(t, \mathbf{x}^*(t), \mathbf{v}, \boldsymbol{\lambda}^*(t)) = H(t, \mathbf{x}^*(t), \mathbf{u}^*(t), \boldsymbol{\lambda}^*(t)), \end{aligned} \tag{14}$$

for all $t \in [0, T]$, except possibly on a finite subset of $[0, T]$.

Example 1 - Solving an Optimal Control Problem Using the Pontryagin Minimum Principle

Let us consider the minimum effort control problem posed in Section 2.1.

Minimise

$$g(u) = \int_0^T u(t)dt,$$

subject to $\frac{dx(t)}{dt} = au(t) - bx(t)$, where $a > 0,\ 0 < b \ll 1,\ x(0) = x_0,\ x(T) = x_T$ and $x_T \geq x_0$. It also makes practical sense to limit the feed intake to some upper bount u_L, as well as limit it to non-negative values:

$$0 \leq u \leq u_L.$$

The Hamiltonian function for this optimal control problem is:

$$H(t, x, u, \lambda) = u + \lambda(au - bx). \tag{15}$$

The costate equation is

$$\frac{d\lambda}{dt} = -\left[\frac{\partial H}{\partial x}\right] = b\lambda, \tag{16}$$

which yields

$$\lambda(t) = Ae^{bt}, \tag{17}$$

where $A \in \mathbb{R}$ is a constant. The Hamiltonian may thus be written as

$$H = u + Ae^{bt}(au - bx) = u(1 + Aae^{bt}) - Abxe^{bt}. \tag{18}$$

To minimise the Hamiltonian in (18), if $(1 + Aae^{bt})$ is negative, u should be as large as possible (i.e. u_L). If $(1 + Aae^{bt})$ is positive, u should be as small as possible (i.e. 0). The resulting optimal control u^* is therefore of bang-bang type, where u^* is piecewise constant, being either 0 or u_L for all $t \in [0, T]$. As $(1+Aae^{bt})$ is monotonic in t, regardless of whether $A < 0$ or $A > 0$, there will be *at most* one switch in u^*. Now we consider the two possibilities:

(i) $u^*(t) = u_L$ for $t \in [0, t^*)$, followed by $u^*(t) = 0$ for $t \in [t^*, T]$, where $t^* < T$. For this to produce an optimal solution, at $t = 0$ we require $1 + Aae^{bt} = 1 + Aa < 0$. This implies $A < -1/a$ and hence $A < 0$. The implication of this is that $1 + Aae^{bt}$ is decreasing in t. However, if $1 + Aae^{bt}$ is negative at $t = 0$ and decreasing, it will never get to 0 and the control cannot change from u_L to 0. Due to this contradiction, an optimal solution of this form cannot exist.

(ii) $u^*(t) = 0$ for $t \in [0, t^*)$, followed by $u^*(t) = u_L$ for $t \in [t^*, T]$. Note that we can again assume $t^* < T$, as the case $t = t^*$ is not feasible ($u(t) = 0$ for the entire time horizon leads to a strict decrease in $x(t)$ which violates the requirement $x_T \geq x_0$).

Let us consider case (ii) more closely. For $t \in [0, t^*)$, we have $u^*(t) = 0$, so $\frac{dx}{dt} = -bx$ which, together with the initial condition $x(0) = x_0$, yields the optimal state $x^*(t) = x_0 e^{-bt}$. For $t \in [t^*, T]$, $u^*(t) = u_L$, so $\frac{dx}{dt} = au_L - bx$. This linear equation can be solved together with the terminal condition $x(T) = x_T$ to yield $x^*(t) = \frac{1}{b}\left[au_L - (au_L - bx_T)e^{b(T-t)}\right]$.

Therefore:

$$x^*(t) = \begin{cases} x_0 e^{-bt}, \ t \in [0, t^*), \\ \\ \frac{1}{b}\left[au_L - (au_L - bx_T)e^{b(T-t)}\right], \ t \in [t^*, T], \end{cases} \tag{19}$$

and t^* can be determined as that time for which $x_1(t^*) = x_2(t^*)$ holds. Note that (19) also allows for the special case of $t^* = 0$ (i.e. $u^*(t) = u_L$ for all $t \in [0, T]$), but only if the model constants satisfy

$$u_L = \frac{\left(x_0 - x_T e^{bT}\right) b}{\left(1 - e^{bT}\right) a}. \tag{20}$$

By selecting the intial weight as $x_0 = 20kg$, the final time as $T = 12$ weeks, $a = 1$ and $b = 0.08$ it can be shown that an optimal solution is possible using Equations (19) and (20), provided that $u_L \geq 4.2$ (1dp). The optimal state trajectory with $u_L = 6$ is defined by:

$$x^*(t) = \begin{cases} 20e^{-\frac{2t}{25}}, \ t \in [0, t^*), \\ \\ 75 - 35e^{\frac{2(12-t)}{25}}, \ t \in [t^*, 12], \end{cases} \tag{21}$$

where

$$t^* = -\frac{25}{2} \ln \left[\frac{75}{20 + 35e^{24/25}}\right] \approx 4.95. \tag{22}$$

The optimal state and control trajectories are displayed in Figure 8.

Example 2 - Solving an Optimal Control Problem Using the Euler-Lagrange Equations

Let us consider another variation of the minimum effort control problem given in Section 2.1, in which we have competing objectives of maximising growth whilst minimising the magnitude of our controls. In this case, the inclusion of the term to minimise magnitude of controls prevents the optimal solution being driven towards an infinite control. We thus drop the requirement of bounds on the control, and hence the Euler-Lagrange equations can be used rather than Pontryagin's Minimum Principle. Again, let us assume that this represents a farmer trying to achieve body weight growth in a sheep, using a minimal amount of feed.

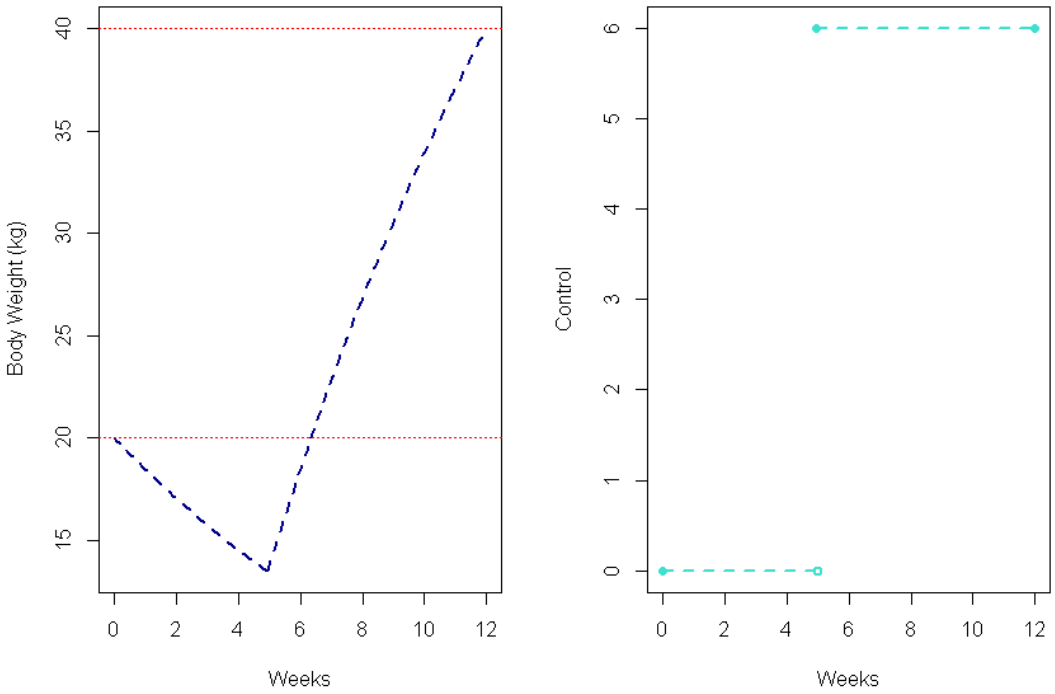

Figure 8: Example 1 - Optimal state and control trajectories.

The objective $g(u)$, a function of the control and the final state, can therefore be defined as:

Minimise

$$g(u) = -\gamma x(T) + \int_0^T (u(t))^2 dt.$$

The weight parameter $\gamma > 0$ is selected according to the relative importance of maximising final body weight as opposed to minimising the cost of control action. Clearly, we have an initial given sheep weight at the start of the time period:

$$x(0) = x_0 > 0.$$

Let us also assume that the rate of weight gain is defined by the feed intake control, and that a sheep will lose a certain proportion of its body weight as time progresses (in the absence of feed). For simplicity, we will also assume that the control is defined as the rate of growth in body weight due to the feed, with no loss of generality caused as compared to the previous definition, where body weight gain was a scalar multiple of the feed intake. Essentially this redefines the control as a nutrient uptake, rather than a feed intake rate. This gives the following, simple definition of a dynamic constraint:

$$\frac{dx(t)}{dt} = u(t) - bx(t), \text{ where } 0 < b \ll 1.$$

The Hamiltonian can thus be defined as:

$$H(x, u, t, \lambda) = u^2 + \lambda(u - bx). \tag{23}$$

The Euler-Lagrange equations require that the optimal solution to this problem minimises the Hamiltonian, which requires

$$\frac{\partial H}{\partial u} = 2u^* + \lambda = 0.$$

Hence we have:

$$u^* = -\frac{\lambda}{2}. \tag{24}$$

We also know the following about the optimal costate λ:

$$\frac{d\lambda}{dt} = -\left[\frac{\partial H}{\partial x}\right] = b\lambda, \tag{25}$$

which indicates that $\lambda(t)$ is of the form $A_1 e^{bt}$, where $A_1 \in \mathbb{R}$ is a constant. As we haven't assumed a terminal constraint on the weight in this example, the Euler-Lagrange equations also define the final costate:

$$\lambda(T) = \left[\frac{\partial(-\gamma x(T))}{\partial x}\right] = -\gamma.$$

It follows that:

$$\begin{aligned} \lambda(T) = A_1 e^{bT} &= -\gamma \\ \Rightarrow A_1 &= -\gamma e^{-bT} \\ \Rightarrow \lambda(t) &= -\gamma e^{b(t-T)}. \end{aligned} \tag{26}$$

By substituting Equation (26) into Equation (24) we have:

$$u^*(t) = \frac{\gamma}{2} e^{b(t-T)}. \tag{27}$$

Now, by substituting Equation (27) into the dynamic constraint, we have:

$$\begin{aligned} \frac{dx(t)}{dt} &= u(t) - bx(t) \\ \Rightarrow x' + bx &= \frac{\gamma}{2} e^{b(t-T)}. \end{aligned} \tag{28}$$

Using the integrating factor method we can derive a general solution to this differential equation:

$$\frac{d}{dt}\left[e^{bt}x\right] = \frac{\gamma}{2}e^{b(2t-T)}$$

$$\Rightarrow e^{bt}x = \frac{\gamma}{4b}e^{b(2t-T)} + A_2 \tag{29}$$

$$\Rightarrow x(t) = \frac{\gamma}{4b}e^{b(t-T)} + A_2e^{-bt},$$

where $A_2 \in \mathbb{R}$ is a constant. We can solve for A_2 by using the initial condition $x(0) = x_0$:

$$x(0) = x_0 = \frac{\gamma}{4b}e^{-bT} + A_2,$$

which, in turn, yields,

$$A_2 = x_0 - \frac{\gamma}{4b}e^{-bT}. \tag{30}$$

Thus, the optimal state is given by

$$x^*(t) = \frac{\gamma}{4b}e^{b(t-T)} + \left(x_0 - \frac{\gamma}{4b}e^{-bT}\right)e^{-bt}. \tag{31}$$

By selecting the initial weight as $x_0 = 20$kg, the final time as $T = 12$ weeks, $b = 0.08$ and assuming $\gamma = 12.1$, it can be shown that the optimal state trajectory culminates in $x_T = 40$kg, roughly mimicking the 20 to 40kg growth from Sainz and Wolff [83]. This result, along with the optimal control, is plotted in Figure 9 alongside the solution where $b = 0.1$, representing a higher level of body weight decline. There is essentially a trade-off between maximising the final state whilst minimising the controls to get it there, and with careful selection of γ, an optimal trajectory can be determined for a reasonable selection of desired final states.

When comparing the solution with that of Example 1, the state and control trajectories are considerably smoother here. Note also that the solution of Example 1 involves starving the sheep at the start of the period, which may not be ethical in practice.

Whilst an analytical solution was able to be determined in these simple examples, in reality, most optimal control problems are too complex to be solved in such a manner, and numerical procedures are required. This will certainly be the case for any optimal control problems with a whole-body metabolism model representing the system dynamics.

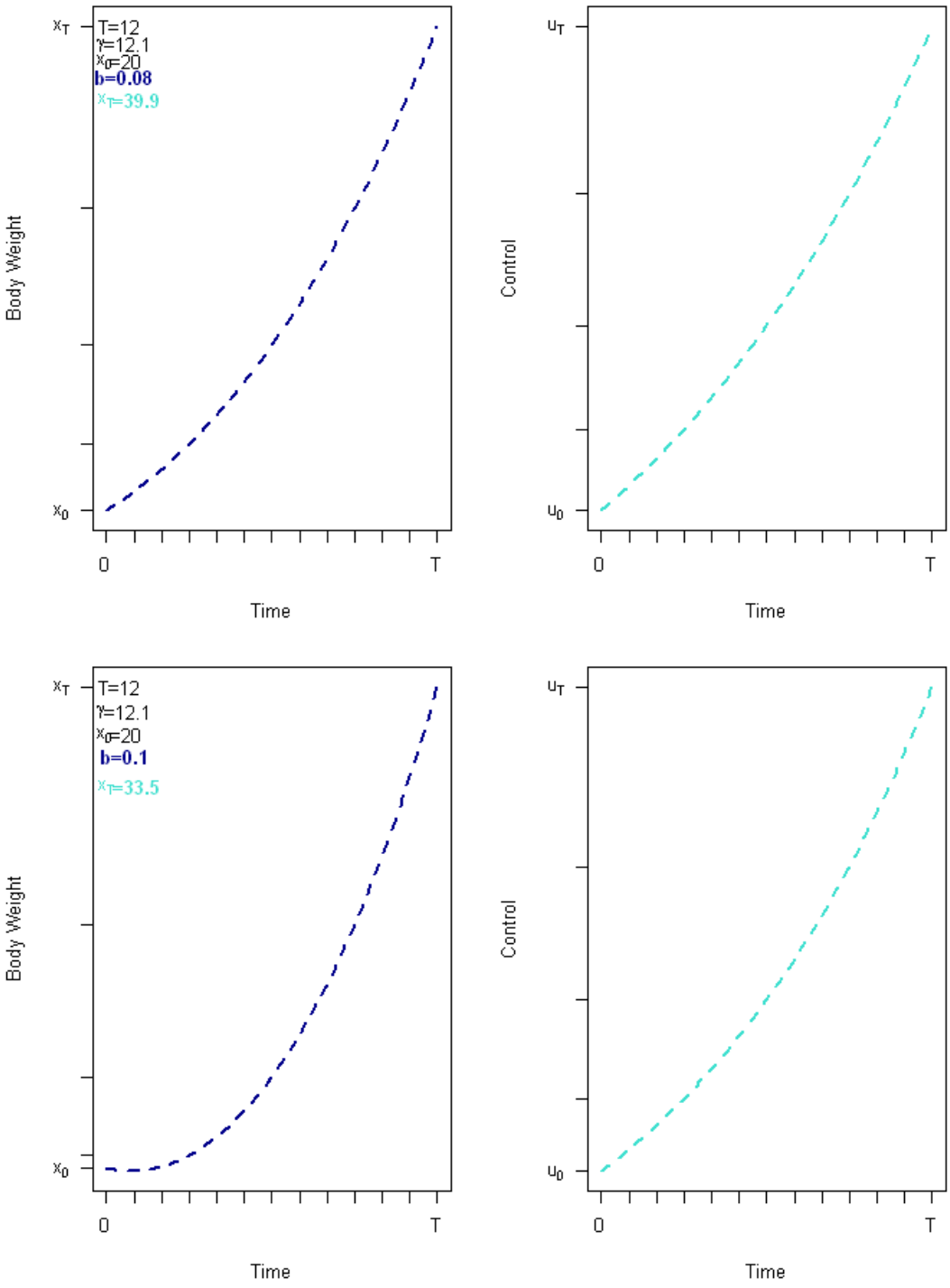

Figure 9: Example 2 - Optimal state and control trajectories.

2.3.2 Numerical Solutions

As most practical problems are too complex to be solved via the analytical solutions discussed in Section 2.3.1, there is a continued need for numerical solution methods. This Section provides an overview of a selection of numerical solution methods culminating in a detailed discussion of control parameterisation, which will be utilised for the whole-body metabolism problem.

Direct Collocation

Direct collocation is a special transcription method, which transforms a constrained optimal control problem into a finite dimensional nonlinearly constrained optimisation problem (NLP) by an appropriate discretisation of both control and state variables, see Von Stryk [97]. The entire time horizon is divided into a finite number of phases, then each phase is subdivided by grid points. In each phase the controls are approximated by a continuously differentiable piecewise cubic function. At the switching points control and state variables may be discontinuous. The problem is solved by standard sequential quadratic programming (SQP) methods (see Fletcher [35]). Although it can readily solve small scale problems, the discretisation of both control and state variables can lead to excessive computations when solving larger scale problems.

Luus-Jaakola Method

The Luus-Jaakola (LJ) optimisation procedure is a direct search optimisation technique based on the use of randomly chosen sample points and adaptive reduction of the search space. In the context of optimal control problems, an initial control estimate is taken at each of a pre-determined number of stages. At the same time, an initial region size is chosen for the control used at each of these stages. Then, in each iteration of the procedure, a set of control values is generated randomly using the initial control estimate and a random diagonal matrix as a multiplying factor. The control values are improved from iteration to iteration through the evaluation of an augmented objective functional over the generated set of control values. This is repeated until a pre-specified number of iterations is reached. The search region is contracted concurrently by a chosen region contraction factor. This process can be repeated until some convergence criterion is satisfied. The method is versatile and reliable, although it usually requires a large number of function evaluations. Refer to Luus and Jaakola [55] and Wang and Luus [98] for an introduction and subsequent improvement to the original LJ method.

Switching Time Computation

The Switching Time Computation (STC) method is a computational procedure to find suitable switching times for single-input nonlinear systems. A concatenation of constant input arcs is used to take the system from an initial point to a target terminal state. The STC method can be fast when compared to other general optimal control software packages [49]. In [50], the authors employ the STC method in a new algorithm (known as the time optimal switchings algorithm (TOS)) to solve a general class of nonlinear minimum time optimal control problems with a single control input. Penalty methods can be readily used to extend these algorithms to more general constrained optimal control problems.

Control Parameterisation

This concept is based on each of the control functions being approximated by a series of either piecewise constant or piecewise linear functions over a number of partitions of the time horizon. The parameters that define these sets of piecewise constant or piecewise linear functions are referred to as *control parameters*, and essentially the optimal control problem can be generalised into an optimal parameter selection problem. This can be considered as a mathematical programming problem, and there are software packages available with proven records of solving problems of this nature.

Consider the generic optimal control problem as presented in Equations (2) through (4). The piecewise constant or piecewise linear control approximations would be defined over a set of knots, which may or may not be equally spaced. The simplest parameterisation is to construct, for each k, a partition of $[0, T]$ such that

$$0 < t_1^k < t_2^k < \ldots < t_{M_k}^k < T,$$

and assume that $u_k(\cdot)$ is piecewise constant on each subinterval. Letting $t_0^k = 0$ and $t_{M_{k+1}}^k = T$, we may write:

$$u_k(t) = \sum_{i=0}^{M_k} h_i^k \chi_{\left[t_i^k, t_{i+1}^k\right]}(t), \tag{32}$$

where the indicator function χ is defined as:

$$\chi_I(t) = \begin{cases} 1, \ t \in I, \\ 0, \ \text{otherwise.} \end{cases}$$

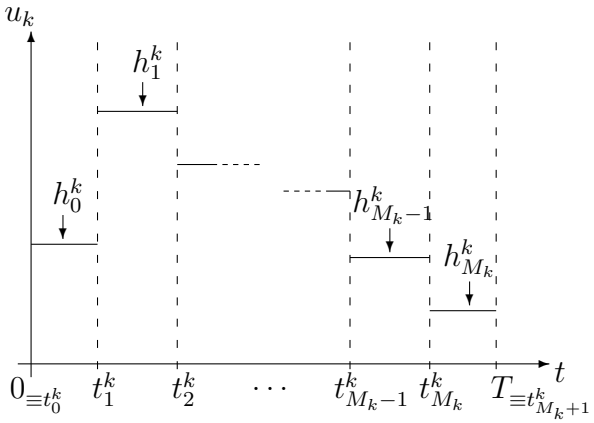

Figure 10: A piecewise constant parameterisation of the k^{th} component of the control vector $\mathbf{u}(t)$.

For convenience, let

$$\boldsymbol{\sigma}^k = \left[h_0^k, h_1^k, \ldots, h_{M_k}^k\right]^\top, \ k = 1, \ldots, r, \text{ and} \tag{33}$$

$$\boldsymbol{\sigma} = \left[(\boldsymbol{\sigma}^1)^\top, (\boldsymbol{\sigma}^2)^\top, \ldots, (\boldsymbol{\sigma}^r)^\top\right]^\top. \tag{34}$$

With this choice of parameterisation, we can restrict the control as follows:

$$a_i^k \leq h_i^k \leq b_i^k, \ i = 0, 1, \ldots, M_k, \ k = 1, \ldots, r.$$

Let $M = \sum_{k=1}^r M_k$. Let $C \subset \mathbb{R}^M$ be the set of all $\boldsymbol{\sigma}$ which satisfy these boundedness constraints and let $\mathcal{U}$ be the set of all piecewise constant control functions which are consistent with the partitions defined above and which satisfy these boundedness constraints. Then each $\boldsymbol{\sigma} \in C$ corresponds to a unique control $\mathbf{u} \in \mathcal{U}$ and vice versa. The generic optimal control problem as presented in Equations (2) through (4) with $\mathbf{u} \in \mathcal{U}$ is thus equivalent to the optimal parameter selection problem given in Equations (35) through (37), as follows.
Choose $\boldsymbol{\sigma} \in C$ to minimise

$$\tilde{g}(\boldsymbol{\sigma}) = \phi_1(\mathbf{x}(T)) + \int_0^T \tilde{\phi}_2\left(t, \mathbf{x}(t), \boldsymbol{\sigma}\right) dt, \tag{35}$$

subject to:

$$\dot{\mathbf{x}} = \tilde{\mathbf{f}}\left(t, \mathbf{x}(t), \boldsymbol{\sigma}\right), \tag{36}$$

$$\mathbf{x}(0) = \mathbf{x_0},$$

and

$$\tilde{G}_j(\mathbf{u}) = \psi_{1j}\left(\mathbf{x}(t_j)\right) + \int_0^{t_j} \tilde{\psi}_{2j}(t, \mathbf{x}(t), \boldsymbol{\sigma})\, dt \begin{cases} = 0, j = 1, 2, \ldots, m_e, \\ \geq 0, j = m_{e+1}, \ldots, m, \end{cases} \tag{37}$$

where

$$\tilde{\phi}_2(t,\mathbf{x}(t),\boldsymbol{\sigma}) \equiv \phi_2\left(t,\mathbf{x}(t),\sum_{i=0}^{M_k} h_i^k \chi_{[t_i^k,t_{i+1}^k]}(t)\right),$$

$$\tilde{\psi}_{2j}(t,\mathbf{x}(t),\boldsymbol{\sigma}) \equiv \psi_{2j}\left(t,\mathbf{x}(t),\sum_{i=0}^{M_k} h_i^k \chi_{[t_i^k,t_{i+1}^k]}(t)\right),$$

$$\tilde{\mathbf{f}}_j(t,\mathbf{x}(t),\boldsymbol{\sigma}) \equiv \mathbf{f}_j\left(t,\mathbf{x}(t),\sum_{i=0}^{M_k} h_i^k \chi_{[t_i^k,t_{i+1}^k]}(t)\right).$$

If we define the following for each $j = 1, 2, \ldots, m$:

$$H_j\left(t,\mathbf{x}(t),\mathbf{u}(t),\boldsymbol{\lambda}_j(t)\right) = \psi_{2j}(t,\mathbf{x}(t),\mathbf{u}(t)) + \boldsymbol{\lambda}_j^\top(t)\mathbf{f}(t,\mathbf{x}(t),\mathbf{u}(t)), \tag{38}$$

$$H_0(t,\mathbf{x}(t),\mathbf{u}(t),\boldsymbol{\lambda}_0(t)) = \phi_2(t,\mathbf{x}(t),\mathbf{u}(t)) + \boldsymbol{\lambda}_0^\top(t)\mathbf{f}(t,\mathbf{x}(t),\mathbf{u}(t)),$$

$$\psi_{1,0} = \phi_1,$$

$$\psi_{2,0} = \phi_2,$$

$$t_0 = T,$$

where for $b = 0, 1, \ldots, m$,

$$\dot{\boldsymbol{\lambda}}_b(t) = -\left[\frac{\partial H_b(t,\mathbf{x}(t),\mathbf{u}(t),\boldsymbol{\lambda}_b(t))}{\partial \mathbf{x}}\right]^\top, \tag{39}$$

$$\boldsymbol{\lambda}_b(t_b) = \left[\frac{\partial \psi_{1b}(\mathbf{x}(t_b)}{\partial \mathbf{x}}\right]^\top, \tag{40}$$

then for each functional g_b, $b = 0, 1, \ldots, m$, its gradient is given by

$$\frac{\partial g_b(\mathbf{u})}{\partial \mathbf{u}} = \int_0^{t_b} \frac{\partial H_b(t,\mathbf{x}(t),\mathbf{u}(t),\boldsymbol{\lambda}_b(t))}{\partial \mathbf{u}} dt. \tag{41}$$

Consequently the gradient for each functional $\tilde{g}_b$ is:

$$\frac{\partial \tilde{g}_b}{\partial \boldsymbol{\sigma}} = \int_0^T \frac{\partial \tilde{H}(t,\mathbf{x}(t),\boldsymbol{\sigma},\boldsymbol{\lambda}_b(t))}{\partial \boldsymbol{\sigma}} dt,\ b = 0, 1, \ldots, m, \tag{42}$$

where $\tilde{H}_b = \tilde{\psi}_{2b} + \boldsymbol{\lambda}_b^\top \tilde{\mathbf{f}}$. An equivalent, more suitable form for implementation is:

$$\frac{\partial g_b}{\partial h_i^k} = \int_{t_i^k}^{t_{i+1}^k} \frac{\partial H_b(t,\mathbf{x}(t),\mathbf{u}(t),\boldsymbol{\lambda}_b(t))}{\partial u_k} dt, \tag{43}$$

for $b = 0, 1, \ldots, m$, $k = 1, \ldots, r$ and $i = 1, \ldots, M_k$. As control parameterisation results in a mathematical programming problem with gradients given by Equation

(43), standard mathematical programming software can now be used to determine the numerical solution. However, note that in order to solve for the costates numerically (on the basis of Equations (39) and (40)), derivatives of the functions $\mathbf{f}$ with respect to $\mathbf{x}$ and $\mathbf{u}$ must be determined analytically. The same applies for derivatives of the objective functional with respect to $\mathbf{x}$ and $\mathbf{u}$. In many cases, this is not a trivial task.

The generic optimal control problem presented in Equations (2) through (4) can also be expanded to include a *system parameter vector* $\mathbf{z}$ that is independent of time, as shown below. System parameters are optimisation variables for the problem (in contrast to the controls - components of $\mathbf{u}$ - which are functions of time t). In later Chapters, we will be seeking to optimise several model parameters in the metabolic sheep model in order to improve the behaviour of the model. These are an instance of system parameters as described here, and will also be referred to as such in these Chapters.

Minimise

$$g(\mathbf{u}, \mathbf{z}) = \phi_1(\mathbf{x}(T), \mathbf{z}) + \int_0^T \phi_2\left(t, \mathbf{x}(t), \mathbf{u}(t), \mathbf{z}\right) dt, \tag{44}$$

where

$$\mathbf{x}(t) = [x_1(t), x_2(t), \ldots, x_n(t)]^\top \in \mathbb{R}^n,$$

is the transposed vector of state variables,

$$\mathbf{u}(t) = [u_1(t), u_2(t), \ldots, u_r(t)]^\top \in \mathbb{R}^r,$$

is the transposed vector of controls, and

$$\mathbf{z} = [z_1, z_2, \ldots, z_s]^\top \in \mathbb{R}^s,$$

is the transposed vector of system parameters. ϕ_1 is a continuously differentiable function. ϕ_2 and its partial derivatives with respect to $\mathbf{x}$, $\mathbf{u}$ and $\mathbf{z}$ are piecewise continuous, and with respect to t are continuous.
The dynamic constraints are defined as:

$$\dot{\mathbf{x}} = \mathbf{f}\left(t, \mathbf{x}(t), \mathbf{u}(t), \mathbf{z}\right), \tag{45}$$

and the intial conditions, which may be variable, are:

$$\mathbf{x}(0) = \mathbf{x_0}(\mathbf{z}). \tag{46}$$

The process may also be subject to a set of m equality and/or inequality con-

straints of the following form:

$$G_j(\mathbf{u},\mathbf{z}) = \psi_{1j}(\mathbf{x}(t_j|\mathbf{u},\mathbf{z})) + \int_0^{t_j} \psi_{2j}(t,\mathbf{x}(t|\mathbf{u},\mathbf{z}),\mathbf{u}(t),\mathbf{z})dt \begin{cases} = 0, j = 1,2,\ldots,m_e, \\ \geq 0, j = m_{e+1},\ldots,m. \end{cases} \tag{47}$$

The same control parameterisation approach to approximate the control as that outlined above can be used to formulate an approximate version of this problem. If we again set:

$$\psi_{1,0} = \phi_1,$$

$$\psi_{2,0} = \phi_2, \text{ and}$$

$$t_0 = T,$$

then for each $b = 0, 1, \ldots, m$, we can define

$$H_b(t,\mathbf{x}(t),\mathbf{u}(t),\mathbf{z},\boldsymbol{\lambda}_b(t)) = \psi_{2b}(t,\mathbf{x}(t),\mathbf{u}(t),\mathbf{z}) + \boldsymbol{\lambda}_b^\top(t)\mathbf{f}(t,\mathbf{x}(t),\mathbf{u}(t),\mathbf{z}), \tag{48}$$

where

$$\dot{\boldsymbol{\lambda}}_b(t) = -\left[\frac{\partial H_b(t,\mathbf{x}(t),\mathbf{u}(t),\mathbf{z},\boldsymbol{\lambda}_b(t))}{\partial \mathbf{x}}\right]^\top, \tag{49}$$

and

$$\boldsymbol{\lambda}_b(t_b) = \left[\frac{\partial \psi_{1b}(\mathbf{x}(t_b),\mathbf{z})}{\partial \mathbf{x}}\right]^\top. \tag{50}$$

Then for each functional g_b, $b = 0, 1, \ldots, m$, its gradients are given by Teo, Goh and Wong [92] as:

$$\frac{\partial g_b}{\partial \mathbf{z}} = \frac{\partial \psi_{1b}(\mathbf{x}(t_b),\mathbf{z})}{\partial \mathbf{z}} + \boldsymbol{\lambda}_b^\top(0)\frac{\partial \mathbf{x}_0(\mathbf{z})}{\partial \mathbf{z}} + \int_0^{t_b} \frac{\partial H_b(t,\mathbf{x}(t),\mathbf{u}(t),\mathbf{z},\boldsymbol{\lambda}_b(t))}{\partial \mathbf{z}}\, dt, \tag{51}$$

and

$$\frac{\partial g_b}{\partial h_i^k} = \int_{t_i^k}^{t_{i+1}^k} \frac{\partial H_b(t,\mathbf{x}(t),\mathbf{u}(t),\mathbf{z},\boldsymbol{\lambda}_b(t)}{\partial u_k} dt, \tag{52}$$

where $i = 1, 2, \ldots, M_k$ and $k = 1, 2, \ldots, r$ and u_k is as defined in Equation (32).

By defining $\boldsymbol{\sigma}$ as in Equations (33) and (34), we have the following approximate optimal control problem:

Minimise

$$\tilde{g}(\mathbf{z},\boldsymbol{\sigma}) = \phi_1(\mathbf{x}(T)) + \int_0^T \tilde{\phi}_2(t,\mathbf{x}(t),\mathbf{z},\boldsymbol{\sigma})dt, \tag{53}$$

subject to:

$$\dot{\mathbf{x}} = \tilde{\mathbf{f}}(t,\mathbf{x}(t),\mathbf{z},\boldsymbol{\sigma}), \tag{54}$$

$$\mathbf{x}(0) = \mathbf{x_0}(\mathbf{z}).$$

The equivalent gradient formulae are:

$$\frac{\partial \tilde{g}_b(\mathbf{z}, \boldsymbol{\sigma})}{\partial \boldsymbol{\sigma}} = \int_0^{t_b} \frac{\tilde{H}_b(t, \mathbf{x}(t), \mathbf{z}, \boldsymbol{\sigma}, \boldsymbol{\lambda}_b(t))}{\partial \boldsymbol{\sigma}} dt, \quad \text{and} \tag{55}$$

$$\frac{\partial \tilde{g}_b(\mathbf{z}, \boldsymbol{\sigma})}{\partial \mathbf{z}} = \frac{\partial \psi_{1b}(\mathbf{x}(t_b), \mathbf{z})}{\partial \mathbf{z}} + \boldsymbol{\lambda}_b^\top(0) \frac{\partial \mathbf{x}_0(\mathbf{z})}{\partial \mathbf{z}} + \int_0^{t_b} \frac{\partial \tilde{H}_b(t, \mathbf{x}(t), \mathbf{z}, \boldsymbol{\sigma}, \boldsymbol{\lambda}_b(t))}{\partial \mathbf{z}} dt, \tag{56}$$

where $b = 0, 1, \ldots, m$ and $\tilde{H} = \psi_{2b} + \boldsymbol{\lambda}_b^\top \tilde{\mathbf{f}}$. Once again, the parameterised problem is a mathematical programming problem. With the gradient formulae (55) and (56), standard mathematical programming software can now be used to determine the numerical solution.

MISER3.3

The control parameterisation method turns the infinite-dimensional optimal control problem into a finite-dimensional mathematical programming problem. In MISER3.3 [48] this is then solved with a sequential quadratic programming algorithm (SQP). Any constraints involving the state variables or nonlinear constraints involving the control functions are transformed into the standard canonical form, as seen in Equation 47. The numerical solution of the state and costate systems is conducted using the Livermore Solver for Ordinary Differential Equations - Automatic (LSODA), see Petzold [75]. This is a Fortran subroutine package developed from the Livermore Solver for Ordinary Differential Equations (LSODE), see Hindmarsh [44], a 6^{th} order Runge-Kutta solution method which essentially replaces the ordinary differential equations with difference equations and then solves them step by step. The LSODA is an adaption which accommodates automatic switching between methods specific for solving stiff and nonstiff problems. MISER3.3 displays a warning to indicate when it is switching between a stiff and nonstiff integrator. The automatic switching capability is useful in a number of different situations, such as where the user is not aware their problem is stiff, or where a problem becomes stiff during the solution process. Optimal control problems relating to whole-body metabolism can be stiff and difficult to solve, and hence the LSODA is an appropriate solution tool. The integrals in the objective, constraints and gradient formulae are approximated using quadratures and the ODE software computes the states and costates, with user supplied analytical gradients utilised in this process.

The MISER3.3 user is warned in Jennings et al. [48] that not every optimal control problem is solvable and that the algorithm may converge to some local Kuhn-Tucker point, which may not even be a local minima, let alone the global minima. For this reason, it is essential that the initial solution (an input to

MISER3.3) is carefully considered, and that allowable ranges for controls and system parameters are not excessively broad. However, it is not straightforward to define a "good" initial guess, nor a range. Therefore the use of MISER3.3 for problems as complex as those relating to whole-body metabolism will often require an extensive amount of evaluation of the specifics of the problem prior to the MISER3.3 run, and even then multiple iterations with varying initial guesses and ranges may be needed to have confidence in the results. Jennings et al. [48] advise that users exercise their intuition, experience and intelligent judgment before accepting the solution obtained.

3 Dynamic Model of Whole-Body Metabolism

The way in which the whole-body metabolism dynamics vary from those in the simple examples in Section 2.1 is that a *set* of state variables are defined, and the associated dynamics represent the way in which these are affected by the feed intake, how they interact with each other, and how they change over time. The feed intake (F_{intake}) is defined as the multiple of maintenance feed requirements. The objective functional is left open at this point, as it is highly subjective. The dynamics can be represented as:

$$\frac{dx_i(t)}{dt} = f_i\left(\mathbf{x}(t), t\right), \; i = 1, \ldots, n, \tag{57}$$

$$\mathbf{x}(0) = \mathbf{x_0},$$

where n is the number of state variables.

This general formulation is easy to pose, however the definition of the functions f_i is very complicated. As discussed in Section 1.3, one of the most comprehensive mathematical models of sheep metabolism published thus far is from Sainz and Wolff [83]. It is aimed at following a lamb's development to maturity and it forms the starting point of our work. The main focus of [83] was to produce a dynamic, mechanistic model of lamb metabolism and growth in order to assess theories concerning the facilitation of particular developmental characteristics. The model relates tissue growth to simulated DNA progression and protein synthesis. There are twelve state variables, including circulating amino acids (Aa), glucose (Gl), lipids (Tg) and acetate (Ac), four protein pools (representing the carcass, Pb, viscera (internal organs), Pv, other tissues, Pz and wool, Pw) and storage triacylglycerol (Ts). The remaining state variables are DNA pools in the carcass (Db), viscera (Dv) and other tissues (Dz). The ordinary differential equations (ODEs) for these twelve state variables are given in Equations (58)

through (65) in the sections that follow.

These pools are chosen as state variables due to their integral necessity in representing the development of the organism when considered as a system. Other pools are omitted from the state variables, either as they are *zero pools* that maintain constant levels across the system and balance system stoichiometrics, or to reduce model complexity. Ultimately, growth represented here, as in any model, is "potential" and not actual growth, and a line must be drawn between sophistication and complexity. As the complexity increases, so does not only the difficulty in implementing the model into the appropriate software, but also the difficulty in finding numerical solutions of the model dynamics. This is a highly relevant issue for metabolism modelling. There will be some factors that are not explicitly taken into account - gender, genotypes, environmental parameters, pregnancy and lactation, parasite infestation, etc - integration of all possible situations and environments is not feasible. However, it may be possible to adjust the model parameters appropriately to imitate certain conditions that are not accommodated in the whole-body metabolism model presented here, but that is not part of the scope for this study.

Tables 40 – 43 in Appendix A along with the description of the dynamics adapted from Sainz and Wolff [83] and Figure 11 in the Sections that follow give a basic overview of variables and parameters used in the model which define the dynamic equations of the whole-body metabolism model.

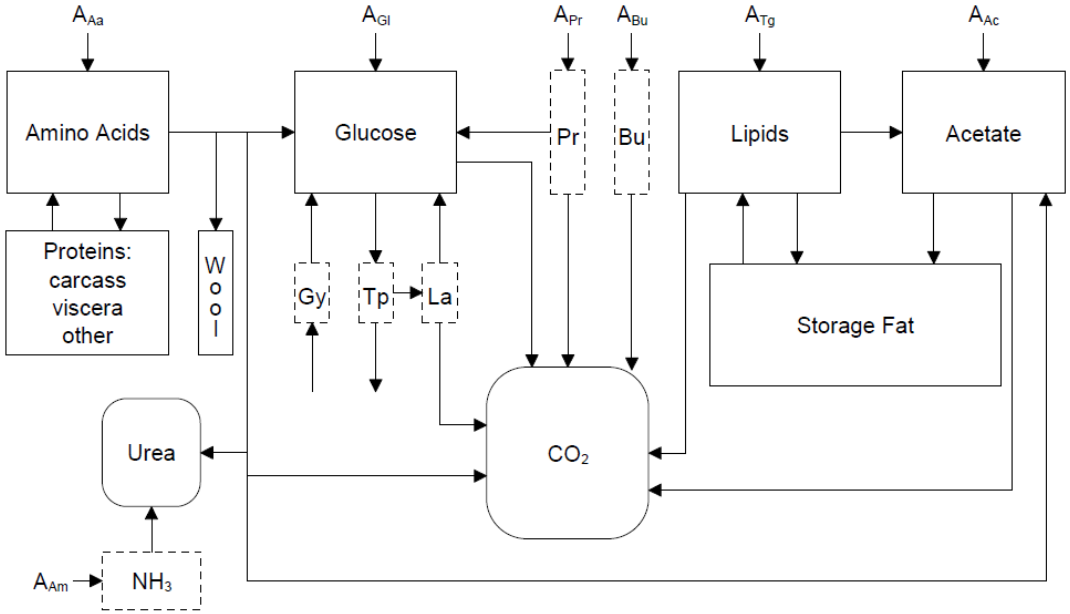

Figure 11: Block diagram of model structure. State variables are depicted as boxes enclosed by solid lines, whilst broken lines denote zero pools. DNA pools in carcass, viscera and other tissues, ADP and ATP were omitted for clarity.

Re-creation of Figure 1 from Sainz and Wolff [83].

The interchange between the different pools is represented by differential equations, mostly of the Michaelis-Menton form. A general example given in [83] is:

$$U = \frac{V_{max}}{1 + \frac{k_{0.5}}{[S]}}.$$

Here, U is the rate of utilisation of substrate S, V_{max} is the maximum velocity for the reaction, $k_{0.5}$ is the substrate concentration at which velocity is one-half maximal and $[S]$ denotes the actual substrate concentration in the blood. For reactions with more than one substrate (eg. S_1 and S_2), a general example is:

$$U = \frac{V_{max}}{1 + \frac{k_{0.5,1}}{[S_1]} + \frac{k_{0.5,2}}{[S_2]}}.$$

Alternatively, a reaction may proceed linearly with respect to substrate availability, in which case

$$U = KS,$$

or, for substrate concentration

$$U = K[S],$$

where K is the first-order rate constant. Substrate concentration can either be defined as the ratio of a circulating metabolite to total extra-cellular fluid (e.g. amino acids in Section 3.1), or the ratio of a solid state to the total empty body weight (e.g. storage triacylglycerol, or body fat, in Section 3.5). Maximal reaction velocities often depend on tissue protein mass and hormonal state, such that

$$V_{max} = V'_{max} P_x^{\theta} H,$$

where V'_{max} is a constant, P_x is one of the protein pools and H is an index of hormonal state. Protein mass is raised to an exponent less than one (θ) in accordance with the observation by Munro [65] that enzymatic capacities vary with tissue mass to the 0.75 power. Sainz and Wolff [83] explain that the exponent values were estimated at 0.75 but are expected to vary. Hence the use of the parameter θ, rather than simply 0.75. Substrate affinity may also be regulated by the hormonal state, as in

$$k_{0.5} = \frac{k'_{0.5}}{H},$$

where $k'_{0.5}$ is a constant. Hormonal controls are limited to two groups having anabolic (H_A) or catabolic (H_C) functions. Anabolic reactions define those where simpler substances are combined to form more complex molecules, and catabolic

reactions involve the breakdown of complex organic molecules into simpler substances. Their respective hormonal controls are defined according to the system's instantaneous concentration of glucose, as in

$$H_A = \left(\frac{C_{Gl}}{C_{Gl,ref}}\right)^2,$$

and

$$H_C = \left(\frac{C_{Gl,ref}}{C_{Gl}}\right)^2,$$

where C_{Gl} and $C_{Gl,ref}$ are the current and reference blood glucose concentrations respectively. Absorption rates of nutrients, such as amino acids (A_{Aa}), glucose (A_{Gl}), volatile fatty acids (VFA; A_{Ac}, A_{Pr} and A_{Bu}) and lipids (A_{Tg}) are given in moles per day, and are approximated as

$$A_i = F_{intake} D_i W_{EB}^{0.75}.$$

in which i is the absorbed nutrient and D_i is the parameter determining the absorption rate of i for the particular dietary regime being simulated. W_{EB} and F_{intake} represent empty body weight and multiples of maintenance feed rate respectively. The 0.75 power applied to W_{EB} reflects the metabolic body weight, and a similar index is applied in Gill et al. [37].

3.1 Amino Acids

Amino acids are the building blocks of protein, which itself is the primary component of the commercial sheep products of meat and wool. It is hence critical to the metabolism model. Inputs to the amino acid (Aa) pool are the absorbed levels of Aa via feed intake (A_{Aa}), and Aa resulting from the degradation of body proteins in the carcass, viscera and other tissues (Pb, Pv and Pz). Protein in wool is not reabsorbed into the body. Conversely, Aa levels are reduced by the synthesis of body proteins, and the synthesis of wool protein (Pw). A component representing gluconeogenesis (conversion into glucose) is also present. The differential equation governing the level of amino acids is given below, where t represents time in days. Note that $P_{i,jk}$ and $U_{i,jk}$ are the production and utilisation respectively of i in the $j \to k$ reaction, measured in moles per day, and K_{jk} is the rate constant for the $j \to k$ reaction on a per-day basis.

$$\begin{aligned}\frac{dAa}{dt} = {} & A_{Aa} + P_{Aa,PbAa} + P_{Aa,PvAa} + P_{Aa,PzAa} - U_{Aa,AaPb} \\ & - U_{Aa,AaPv} - U_{Aa,AaPz} - U_{Aa,AaPw} - U_{Aa,AaGl}.\end{aligned} \tag{58}$$

Equations representing protein turn-over are presented in Section 3.6. Gluconeogenesis is represented as:

$$\begin{aligned} U_{Aa,AaGl} &= K_{AaGl} C_{Aa}, \\ K_{AaGl} &= K'_{AaGl} \left(\frac{C_{Aa}}{C_{Aa,ref}} \right) P v^{\theta 1} H_C, \text{ and} \\ C_{Aa} &= \frac{Aa}{v_{ECF}}, \end{aligned}$$

where $v_{ECF} = 0.24 W_{EB}$ is the assumed volume of extra-cellular fluid, defined as relative to empty body weight. The ratio of 0.24 corresponds to the proportional value of 0.20 of live weight (of which empty body weight represents 83%) for the volume of extra-cellular fuild reported by Hecker [42]. (This information was given by Sainz and Wolff [83], but a copy of Hecker [42] could not be obtained.)

3.2 Glucose

As discussed in the introduction to Chapter 3, glucose concentration in blood is the primary indicator of hormonal controls. These hormonal control levels contribute to rates of reactions throughout the body, and hence the level of glucose is required to be tracked continuously. The rate of change of glucose is governed by gluconeogenesis (as mentioned in Section 3.1), primarily from propionate, lactate and glycerol, but can also be from amino acids. Factors are also present for the conversion of glucose to triose phosphates and oxidation to carbon dioxide. Inputs and outputs to the glucose pool contribute to its rate of change as follows. Note that $Y_{i,jk}$ is the yield of i measured in moles i per mole j utilised in the $j \rightarrow k$ reaction. V_{jk} is the maximum velocity of the $j \rightarrow k$ reaction in moles j per day, and $k_{i,jk}$ is the Michaelis-Menton constant for the $j \rightarrow k$ reaction with respect to i.

$$\begin{aligned} \frac{dGl}{dt} = A_{Gl} + P_{Gl,AaGl} + P_{Gl,PrGl} + P_{Gl,LaGl} \\ + P_{Gl,GyGl} - U_{Gl,GlTp} - U_{Gl,GlCd}. \end{aligned} \tag{59}$$

Net glucose production rates are of the form $P_{Gl,AaGl} = U_{Aa,AaGl} Y_{Gl,AaGl}$, where $Y_{Gl,AaGl}$ is the respective stoichiometric yield coefficient.

Equations governing glucose conversion to triose phosphates ($U_{Gl,GlTp}$) are:

$$U_{Gl,GlTp} = \frac{V_{GlTp}}{\left(1 + \frac{k_{GlTp}}{C_{Gl}}\right)},$$

$$V_{GlTp} = V'_{GlTp} P b^{\theta 2},$$

$$k_{GlTp} = \frac{k'_{GlTp}}{H_A},$$

and

$$C_{Gl} = \frac{Gl}{v_{ECF}}.$$

Oxidation of glucose into carbon dioxide ($U_{Gl,GlCd}$) is presented in Section 7.3.

3.3 Acetate

Acetate plays a role in several key metabolic functions, including gluconeogenesis of amino acids and the oxidation of fatty acids, and is an input to the storage fat pool - a key component of the empty body weight of the sheep - via *de novo* lipogenesis. Acetate can also be directly oxidised to carbon dioxide. The rate of change of acetate levels is modelled as:

$$\frac{dAc}{dt} = A_{Ac} + P_{Ac,TgCd} + P_{Ac,AaGl} - U_{Ac,AcTs} - U_{Ac,AcCd}, \tag{60}$$

where

$$P_{Ac,TgCd} = U_{Tg,TgCd} Y_{Ac,TgCd},$$

and

$$P_{Ac,AaGl} = U_{Aa,AaGl} Y_{Ac,AaGl}.$$

In addition to acetate levels, the rate of *de novo* lipogenesis is also limited by the availability of glucose and circulating lipids:

$$U_{Ac,AcTs} = \frac{V_{AcTs}}{\left(1 + \frac{k_{Ac,AcTs}}{C_{Ac}} + \frac{k_{Gl,AcTs}}{C_{Gl}} + \frac{C_{Tg}}{k_{Tg,AcTs}}\right)},$$

$$V_{AcTs} = V'_{AcTs} H_A \left(Pb + Pv\right)^{\theta 3},$$

$$k_{Gl,AcTs} = \frac{k'_{Gl,AcTs}}{H_A},$$

and

$$C_{Ac} = \frac{Ac}{v_{ECF}}.$$

3.4 Lipids

Lipids are essentially circulating fatty acids acting as energy storage and they are the building blocks for storage triacylglycerol (body fat). Inputs to the lipids pool come from absorption via the feed intake (A_{Tg}), as well as the degradation of storage triacylglycerol. Lipids are consumed in the lipogenesis to storage fats, and can be directly oxidised to carbon dioxide. The dynamics of circulating lipids

(Tg) are represented by:

$$\frac{dTg}{dt} = A_{Tg} + P_{Tg,TsTg} - U_{Tg,TgTs} - U_{Tg,TgCd}, \tag{61}$$

where

$$P_{Tg,TsTg} = U_{Ts,TsTg},$$

$$U_{Tg,TgTs} = \frac{V_{TgTs}}{\left(1 + \frac{k_{Tg,TgTs}}{C_{Tg}} + \frac{k_{Gl,TgTs}}{C_{Gl}}\right)},$$

$$V_{TgTs} = V'_{TgTs}\left(Pb + Pv\right)^{\theta 4},$$

and

$$C_{Tg} = \frac{Tg}{v_{ECF}}.$$

3.5 Storage Triacylglycerol

Storage triacylglycerol is also referred to as storage fat or body fat, and it is a key component of empty body weight. Its dynamics have already been covered in Sections 3.3 and 3.4, namely the deposition of storage triacylglycerol from the *de novo* lipogenesis of acetate and lipogenesis of lipids, and degradation via lipolysis to lipids. The maximum achievable rate for degradation of storage triacylglycerol to circulating lipids is governed by catabolic (degradative) hormonal controls, plus the levels of protein in the carcass and viscera (internal organs). The exponent $\theta 5$ (given a value of five in Sainz and Wolff [83]) is included to ensure that lipolysis cannot proceed when body fat reaches very low levels. It effectively limits $U_{Ts,TsTg}$ to zero rapidly as C_{Ts} decreases. The equation governing temporal variations of levels of storage triacylglycerol (T_s) is:

$$\frac{dTs}{dt} = P_{Ts,AcTs} + P_{Ts,TgTs} - U_{Ts,TsTg}, \tag{62}$$

where

$$P_{Ts,AcTs} = U_{Ac,AcTs} Y_{Ts,AcTs},$$

$$P_{Ts,TgTs} = U_{Tg,TgTs},$$

$$U_{Ts,TsTg} = \frac{V_{TsTg}}{\left(1 + \left(\frac{k_{TsTg}}{C_{Ts}}\right)^{\theta 5}\right)},$$

$$V_{TsTg} = V'_{TsTg} H_C \left(Pb + Pv\right)^{\theta 6},$$

and

$$C_{Ts} = \frac{Ts}{W_{EB}}.$$

3.6 Protein Pools

Protein pools are clearly a critical component of the metabolism model, consisting of both the carcass protein (meat) and wool protein that are essential in the sheep industry. There are four protein pools in the Sainz and Wolff [83] model: protein in the carcass (Pb), viscera (internal organs - Pv), other tissues (head, skin, feet, etc - Pz) and wool (Pw). Growth of the internal protein pools is limited by an associated DNA pool, ensuring growth does not exceed that which is genetically possible, regardless of other factors. Note that, as the level of protein is present as a factor in both the synthesis and degradation rate equations, the appropriate selection of parameters such as $\theta 7$, V'_{AaPb}, k'_{AaPb} and K_{PbAa} (as well as the viscera and other tissues equivalents) ensures that degradation rates exceed synthesis rates once the protein level is beyond a certain point. Protein synthesis and degradation equations are similar, therefore for simplification, generic Px and equations are given here, where possible, along with equations for Pw. Note that protein synthesis in wool is no dependent on anabolic hormone, and is regulated by the other tissues protein pool. The Px variable represents each of the three body protein pool state variables (Pb, Pv, Pz):

$$\frac{dPx}{dt} = P_{Px,AaPx} - U_{Px,PxAa}, \tag{63}$$

$$\frac{dPw}{dt} = P_{Pw,AaPw}, \tag{64}$$

$$P_{Px,AaPx} = \frac{V_{AaPx}}{\left(1 + \frac{k_{AaPx}}{C_{Aa}}\right)},$$

$$P_{Pw,AaPw} = \frac{V_{AaPw}}{\left(1 + \frac{k_{AaPw}}{C_{Aa}}\right)},$$

$$V_{AaPb} = V'_{AaPb} Pb^{\theta 7} Db,$$

$$V_{AaPv} = V'_{AaPv} Pv^{\theta 8} Dv,$$

$$V_{AaPz} = V'_{AaPz} Pz^{\theta 9} Dz,$$

$$V_{AaPw} = V'_{AaPw} Pz^{\theta 10} Dz,$$

$$k_{AaPx} = \frac{k'_{AaPx}}{H_A}, \text{ and } k_{AaPw} \text{ is a constant.}$$

Protein degradation rates, with the exception of wool which does not degrade to internalised amino acids, are first order functions of protein mass, such as:

$$U_{Px,PxAa} = K_{PxAa} Px.$$

Also, the ultilisation and production rates are equivalent for both protein and amino acids:

$$P_{Aa,PxAa} = U_{Px,PxAa},$$

$$P_{Px,AaPx} = U_{Aa,AaPx},$$

and

$$P_{Pw,AaPw} = U_{Aa,AaPw}.$$

3.7 DNA Pools

The DNA pools provide functions to both drive and limit tissue growth, with identical equations representing each of the protein pools (with the exception of wool). The rate of accumulation of tissue DNA is dependent on the proximity of the tissue DNA to its given maximum, the level of anabolic (constructive) hormonal control, and a rate constant. The structure of each of the DNA pool dynamics is the same, therefore for simplicity, a generic Dx equation is given here, representing Db, Dv and Dz:

$$\frac{dDx}{dt} = K_{Dx}\left(Dx_{MAX} - Dx\right) H_A, \tag{65}$$

where Db_{MAX}, Dv_{MAX} and Dz_{MAX} are the maximum DNA contents achievable in the carcass, viscera and other tissues respectively.

3.8 Zero Pools

Zero pools are those where the utilisation is equal to the production at each instant. As such, they do not need to be state variables, but they are included in the model to maintain stoichiometric balance. These include proprionate, butyrate, glycerol, triose phosphates, lactate, ADP and ATP, with the latter two addressed in Section 3.9. Propionate and butyrate enter the system from absorption via feed intake, with butyrate being completely oxidised. More realistically, absorption occurs via the ingestion of food and depends on the nature of the microbial population present in the digestive system. However, these details are considered outside the scope of this model. Two-thirds of the absorbed proprionate is also oxidised, with the remainder converted to glucose by way of gluconeogenesis. Glycerol is assumed to be completely converted to glucose following its release during lipolysis. Triose phosphates are formed from glucose and are partially consumed in the esterification of fatty acids ($Ts \leftrightarrow Tg$), with the remainder converted to lactate. Half of the lactate is then converted to glucose, while the other half is oxidised. These proportions, however, are arbitrary (effect on model be-

haviour was expected to be negligible by Sainz and Wolff [83], this is reviewed in Section 8.1). Behaviour of the zero pools is governed by the following equations:

$$U_{Pr,PrGl} = 0.333A_{Pr},$$

$$U_{Pr,PrCd} = 0.667A_{Pr},$$

$$U_{Bu,BuCd} = A_{Bu},$$

$$U_{Gy,GyGl} = U_{Ts,TsTg} + U_{Tg,TgTs} + U_{Tg,TgCd},$$

$$P_{Tp,GlTp} = U_{Gl,GlTp}Y_{Tp,GlTp},$$

$$U_{Tp,TpLa} = P_{Tp,GlTp} - U_{Tg,TgTs} - U_{Ts,TsTg} - P_{Ts,AcTs},$$

$$P_{La,TpLa} = U_{Tp,TpLa},$$

$$U_{La,LaGl} = 0.5P_{La,TpLa},$$

and

$$U_{La,LaCd} = 0.5P_{La,TpLa}.$$

3.9 Energy Expenditure

Each body protein tissue type has an associated energy expenditure ($U_{At,carcass}$, $U_{At,viscera}$ and $U_{At,other}$). These are all defined similarly, so only $U_{At,carcass}$ is stated below. Also, the equations regulating the utilisation and production rates of ATP are listed below. Here, Px is used to represent generalised tissue protein mass. Note that $R_{i,jk}$ is the requirement in moles i per mole j utilised in the $j \rightarrow k$ reaction.

$$U_{At,carcass} = K_{carcass}Pb,$$

$$\begin{aligned}
U_{At,AtAd} &= U_{At,carcass} + U_{At,viscera} + U_{At,other} \\
&\quad + A_{Aa}R_{At,A_{Aa}} + A_{Gl}R_{At,A_{Gl}} + A_{Tg}R_{At,A_{Tg}} \\
&\quad + U_{Aa,AaPb}R_{At,AaPx} + U_{Aa,AaPv}R_{At,AaPx} + U_{Aa,AaPz}R_{At,AaPx} \\
&\quad + U_{Aa,AaPw}R_{At,AaPx} + U_{Gl,GlTp}R_{At,GlTp} + U_{Tg,TgTs}R_{At,TgTs} \\
&\quad + U_{Ts,TsTg}R_{At,TsTg} + U_{Ac,AcTs}R_{At,AcTs} + U_{La,LaGl}R_{At,LaGl} \\
&\quad + U_{Pr,PrGl}R_{At,PrGl},
\end{aligned}$$

$$\begin{aligned}
P_{At,AdAt} &= U_{Aa,AaGl}Y_{At,AaGl} + U_{Gy,GyGl}Y_{At,GyGl} + U_{Tp,TpLa}Y_{At,TpLa} \\
&\quad + U_{La,LaCd}Y_{At,LaCd} + U_{Pr,PrCd}Y_{At,PrCd} + U_{Bu,BuCd}Y_{At,BuCd}.
\end{aligned}$$

3.10 Oxidation of Alternative Substrates

In the following equations N_{AdAt} is the net rate of ATP utilisation and N_{Ox} represents oxygen uptake necessary to satisfy energy requirements. $Q_{P:Ox}$ is the ratio of high energy phosphate bonds formed per mole oxygen consumed, $Q_{Gl:Ac}$ is the ratio in the Michaelis-Menton equations for oxidation of glucose and acetate and similarly $Q_{Tg:Ac}$ is the ratio of oxygen uptake due to oxidation of fatty acids and acetate. The equations given below depend on the following assumptions:

1. Uptake and utilisation of metabolites are saturable processes (that is, they can reach a maximum level) conforming to Michaelis-Menton kinetics;

2. Maximum rates of oxidative phosphorylation are equal for different substrates, being limited by the electron transport system; and

3. Absolute rates of oxidative phosphorylation (the pathway generating ATP from ADP) are limited by availability of ADP, and therefore by the rate of ATP hydrolysis.

$$N_{AdAt} = U_{At,AtAd} - P_{At,AdAt},$$

$$N_{Ox} = \frac{N_{AdAt}}{Q_{P:Ox}},$$

$$Q_{Gl:Ac} = \frac{C_{Gl}\,(C_{Ac} + k_{AcCd})}{C_{Ac}\,(C_{Gl} + k_{GlCd})},$$

$$k_{GlCd} = \frac{k'_{GlCd}}{H_A},$$

$$Q_{Tg:Ac} = \frac{C_{Tg}\,(C_{Ac} + k_{AcCd})}{C_{Ac}\,(C_{Tg} + k_{TgCd})},$$

$$U_{Gl,GlCd} = \frac{\left(\frac{N_{Ox}Q_{Gl:Ac}}{1+Q_{Gl:Ac}+Q_{Tg:Ac}}\right)}{R_{Ox,GlCd}},$$

$$U_{Tg,TgCd} = \frac{\left(\frac{N_{Ox}Q_{Tg:Ac}}{1+Q_{Gl:Ac}+Q_{Tg:Ac}}\right)}{R_{Ox,TgCd}},$$

$$U_{Ac,AcCd} = \frac{\left(\frac{N_{Ox}}{1+Q_{Gl:Ac}+Q_{Tg:Ac}}\right)}{R_{Ox,AcCd}},$$

$$Q_{P:Ox} = \frac{U_{Ac,AcCd}Y_{At,AcCd} + U_{Gl,GlCd}Y_{At,GlCd} + U_{Tg,TgCd}Y_{At,TgCd}}{U_{Ac,AcCd}R_{Ox,AcCd} + U_{Gl,GlCd}R_{Ox,GlCd} + U_{Tg,TgCd}R_{Ox,TgCd}}.$$

4 Implementation

In order for optimal control and optimal parameter selection problems relating to whole-body metabolism models such as that outlined in Chapter 3 to be solved numerically in MISER3.3, it is necessary to complete a number of non-trivial tasks, including elaborating on some of the dynamic components. For example, an equation for empty body weight was not given in Sainz and Wolff [83]. Also, the units of the state variables are in moles, yet the empty body weight is in kilograms, therefore appropiate molecular weights need to be determined. This is also necessary for comparisons between state variables, such as the protein pools and storage tricylglycerol, with quantities reported in the literature, since grams and kilograms are the most commonly reported units. Additionally, whilst the model can run without an objective functional, it cannot proceed without a given initial state. Initial conditions can naturally be adjusted to suit different starting points of the model, and are treated as an input as opposed to being ingrained in the model itself, but even a test run needs defensible initial conditions. This Chapter covers all the necessary requirements for the model to run in MISER3.3, which includes:

- Determining molecular weights for the protein pools (carcass, viscera, other tissues and wool);
- Developing an equation for empty body weight based on the state variables;
- Determining preliminary initial conditions for the state variables; and
- Constructing derivatives of the model dynamics with respect to the state variables to allow for the control parameterisation method to be applied.

4.1 Molecular Weights and the Empty Body Weight Equation

The Sainz and Wolff [83] paper does not specify an equation to determine empty body weight from the state variables. This quantity is an integral part of the model in calculating concentrations, and it is also required in order to make comparisons between data predicted from the model and observed data found in the literature. The code provided by Hon [45] defines an empty body weight equation as given in Equation (66) below.

$$W_{EB} = \frac{(4.134\,(Pb + Pv + Pz) \times 0.142 + Ts \times 0.807)}{0.95}. \tag{66}$$

Accompanying comments from Hon describe the equation as giving empty body weight in kilograms, and assumes the following:

- Ash (minerals) consists of a constant 5% of empty body weight;
- The molecular weight of amino acids (in all body proteins) is 142g/mol;
- The molecular weight of storage triacylglycerol is 807g/mol; and
- Water mass is equal to 3.134 times the body protein mass.

Similarly, the Sainz and Wolff [83] paper does not explicitly state the initial conditions of the model. As there is uncertainty around the initial conditions, they are not used in the first instance to help develop the empty body weight equation, but rather as a check "after the fact". They are briefly discussed here, with further discussion and analysis in Section 4.2. The initial conditions for Sainz and Wolff [83] *can* be estimated from other information presented in the paper, with the exception of protein in wool. There is some reference to potential sources of these initial conditions (Hammond [40] and Hecker [42]), but copies of these references could not be obtained, so a review of how these were determined was not possible. Hon [45] presents initial conditions, as shown in Table 1, but does not give reference to their source. It is straightforward to confirm that these intial conditions produce an empty body weight of 20kg when applied to the empty body weight equation (66). However, it is not clear whether the initial conditions or the empty body weight equation may have been tweaked to produce this result. The initial conditions of Hon have similarities to, but are not precisely those that can be estimated for a $W_{EB} = 20$kg sheep from Sainz and Wolff [83]. It is only the value of protein in the viscera and other tissues that is consistent between the two. It is understood that the initial conditions and the empty body weight equation used by Hon [45] were derived via consultation with the late Dr Norm Adams of CSIRO Livestock Industries in Wembley, Western Australia. Dr Adams was a co-author of [1], [2] and [3] amongst many other publications, and was considered an expert in the area. For the sake of completeness, the empty body weight equation is reviewed here as it is an integral part of the model. The initial conditions will be considered in Section 4.2.

Searle [88] provides some careful estimates of body composition at different ages of a mixed group of sheep, including forty-six wether (castrated male) Merino sheep, thirteen Corriedales (five wethers, eight ewes), and two cross-bred wethers. Searle groups body composition into four main areas: body water, fat, protein and ash. The state variables that can be defined as part of the circulating fluids (Aa, Gl, Tg, Ac) are represented in the body water component and storage triacylglycerol (Ts) is essentially body fat. It is clear that the body water is

State Variable	**Initial Value - 20kg W_{EB}**
Amino Acid	0.012
Glucose	0.0144
Lipids	0.01152
Acetate	0.0048
Protein (Carcass)	14.8771
Protein (Viscera)	6.84
Protein (Other Tissues)	5.743
Protein (Wool)	0
Storage Triacylglycerol	3.5901
DNA (Carcass)	0.0061
DNA (Viscera)	0.0075
DNA (Other Tissues)	0.0044

Table 1: Initial state variable values from Hon [45].

not wholly represented by the state variables, and so it must be estimated from the state variables in some manner. Searle [88] states that fat is probably the most variable component in the body. Therefore it follows that body protein is probably the right choice for use in predicting the total body water. Body protein is a combination of protein in the carcass (Pb), viscera (Pv) and other tissues (Pz). As empty body weight excludes fleece weight, protein in the wool (Pw) is not included. Table 2 has been constructed from the mid-points of ranges of Table 1 and Table 2 in Searle [88], restricted to ages of three months and older. This is due to the fact that the 20kg empty body weight sheep that is used as the starting point in Sainz and Wolff [83] is 12 weeks of age, so it is keeping within the frame of reference of the model. The problem with Searle is that empty body weights are not presented, rather the total body weight is given and this is inclusive of gut content. The total body water that is presented is also inclusive of water in the gut content, of which Atti et al. [11] gives a mean of 5.8kg in a 36.4kg empty body weight sheep, or 22.3% of the total body water. Clearly this cannot be considered an insignificant quantity, and so whilst the general components and approach used in Equation (66) seem to be valid, the information in Searle [88] cannot be used to verify the multiplier of 3.134 in relating water mass to protein mass.

The results in Atti et al. [11] regarding body water are based on sixteen adult dry ewes of the fat-tailed Barbary breed, where dry indicates that they have not yet bred. Details of the body composition of the sheep involved in the study are presented in Table 3. It can be seen the that ratio of water to protein in empty body weight is 3.811, slightly higher than the 3.134 proposed, but not substantially different. Graham [38] conducted fasting experiments on six Merino

Age (months)	No. of sheep	Total Body Weight (kg)	Protein (% of fat free BW)	Ash (% of fat free BW)
3	7	19.45	19.6	4.6
4	9	23.00	19.0	4.5
6	7	23.70	20.1	5.2
9	4	22.35	21.0	5.8
12	4	31.25	21.3	5.2
15	4	33.90	21.0	5.7
18	7	36.45	20.3	5.6

Table 2: Sheep whole body composition, 3 to 18 months, from Searle [88]. *Protein and ash estimates have average standard errors of* ± 0.2 *within age groups.*

wethers, aged 5–7 years, in order to estimate maintenance feed requirements. Over the course of the experiment, body weights of the sheep dropped from the 61kg mark down to 29kg. Despite this large weight loss, the water to protein ratios remain quite steady over time, as can be seen in Table 4. A similar result is seen in McCann et al. [56], where both lean and obese adult Dorset ewes showed similar water to protein ratios (3.549 and 3.577 respectively). It is hence concluded that the water to protein ratio is a stable parameter, that does not differ substantially with body weight, and while the figure of 3.134 seems reasonable, it is perhaps more appropriate to select a ratio that can be supported by literature in a documented fashion. By assigning equal weight to the average water to protein ratios in Atti et al. [11] (3.811), Graham [38] (3.266) and McCann et al. [56] (3.563) this gives a water to protein ratio of **3.547**.

It stands to reason that the assumption regarding percentage of body weight being ash can be assessed using the same approach as the water to protein ratio. If the average weight of the tail in the fat-tailed Barbary ewes of Atti et al. [11] is excluded from the average empty body weight (as it is the trait of a specific breed), this gives an expected ash percentage of 4.99, as seen in Table 3. Whilst the calculated ash percentages in Table 4 using data from Graham [38] are only indicative, due to the integer rounding applied to the water, fat and protein percentages, they do not discount the theory that 5% body ash is appropriate. The lowest body weight category in Table 4 only has an estimated body ash percentage of 2%. However, this record is only approximate, it is based on the difference between the sum of rounded percentages and 100, and was taken after a long period of fasting for the sheep. It should be kept in mind that the model *may* be limited in its ability to represent substantially under-nourished sheep. This is examined in more detail in Chapter 8.

Components	**Mean ± S.D.**	**Min**	**Max**
Slaughter body weight (kg)	43.1 ± 6.4	32.5	55.0
Body weight without tail (kg)	40.8 ± 5.7	31.3	52.5
Empty body weight (EBW) (kg)	36.4 ± 6.6	27.1	49.8
Total body water (kg)	26.0 ± 2.6	21.8	29.7
Gut content of water (kg)	5.8 ± 1.8	2.3	8.8
Lipid without tail (kg)	7.7 ± 3.5	3.4	15.9
Protein(kg)	5.3 ± 0.8	4.3	7.2
Ash (kg)	1.7 ± 0.2	1.4	2.0
	Mean only		
Tail weight (kg)	*2.3*	-	-
EBW, excluding tail (kg)	*34.1*	-	-
Water in EBW (kg)	*20.2*	-	-
Ash in EBW (%)	*4.67*	-	-
Ash in EBW, excluding tail (%)	*4.99*	-	-
Ratio of water to protein, in EBW	*3.811*	-	-

Table 3: Weights of body components in the fat-tailed Barbary ewes of Atti et al. [11], plus *calculated fields*.

Body Weight (kg)	**Water (%)**	**Fat (%)**	**Protein (%)**	***Ash (%)***	***Ratio of Water to Protein***
61	49	32	15	*4*	*3.267*
48	51	29	16	*4*	*3.188*
39	59	19	17	*5*	*3.471*
29	69	7	22	*2*	*3.136*

Table 4: Empty body weight and composition of fasting adult Merino wethers of Graham [38], plus *calculated fields*.

The ash percentages that are presented in Table 2 are from Searle [88] and are expressed in terms of fat free body weight, whereas the ash percentage being determined is of the *whole empty body weight* and hence they are not comparable.

If we define body water (BW) and body protein (BP) as the amount of water and protein in a sheep's empty body weight then we have the following formula:

$$BW = 3.547BP.$$

Therefore an initial formula for determining empty body weight is:

$$W_{EB} = \frac{4.547BP + BF}{0.95}, \tag{67}$$

where BF (body fat) is the amount of fat in a sheep's empty body weight, and all

variables are given in kilograms. This addresses the first and the last assumption, as itemised at the start of Section 4.1 regarding the development of the empty body weight equation.

The model in Sainz and Wolff [83] describes Pb, Pv, Pz and Ts in moles and their molecular weights must be approximated in order to utilise the empty body weight formula. Hon [45] gave a molecular weight of 142g for body protein, which was applied to the combined moles of Pb, Pv and Pz, and 807g for storage triacylglycerol (Ts), but these figures need to be reviewed.

First, the molecular weights to use for the respective proteins will be estimated. This is not a straightforward process, as molecular weight is a concept generally applied to *molecules* whereas "protein" is not just a mixture of different types of proteins, but within each type of protein there are different chains of amino acid molecules present. The molecular weight proposed by Hon [45] (142g/mol for all body proteins), which was used by Hon to run the model with some success, is within the range of an amino acid molecular weight, rather than a chain of many amino acids (protein). Therefore it is assumed that what is meant by the number of moles of protein in the model is the number of moles of *amino acids in protein*. This makes sense given the structure of the model, where the amino acid pool interchanges directly with the protein pools, see Figure 11 for illustration. Therefore it is the "average" molecular weight of amino acids in the protein of each tissue type that needs to be determined.

Some consideration has been made on the most appropriate way to approach this task. Conceptually, it has been assumed that the relative presence of amino acids in proteins of different areas of the body is the best way forward in determining a generic molecular weight for protein. This approach is what is known as a *number average molecular weight*. Another approach would be to use the relative *weight* of amino acids present, creating a *weighted average molecular weight*. However, this was considered a representation of the "average weight of all amino acids in a protein estimated by choosing an amino acid at random, with probability of selection directly proportional to weight" rather than the "overall average molecular weight of amino acids in protein" (the desired result).

MacRae et al. [61] found that for any particular tissue (protein in carcass, wool, skin, gut and liver were examined) the amino acid composition was similar regardless of slaughter weight or diet, therefore a constant molecular weight could be used for each tissue type. Table 5 is an extract from MacRae et al.. [61]. Table 6 uses that data, as well as molecular weights for individual amino acids as sourced from Nelson and Cox [66], to estimate number average molecular weights for the amino acids in the three body protein pools. Note that skin and a combination of gut and liver were used to find weights for other tissues and viscera respectively.

Amino Acid	Carcass	Wool	Skin	Gut	Liver
Aspartate	89	66	69	88	94
Threonine	50	60	39	51	54
Serine	40	83	50	47	46
Glutamate	135	142	120	126	121
Glycine	93	52	124	88	57
Alanine	80	40	86	74	61
Valine	49	55	3	49	61
Isoleucine	38	30	24	37	43
Leucine	75	74	57	76	90
Tyrosine	31	52	27	36	41
Phenylalanine	39	36	32	41	55
Histidine	26	12	14	23	33
Lysine	70	35	48	69	69
Arginine	73	91	79	67	59
Proline	61	65	83	61	47
Methionine	18	6	10	22	32
Cysteine	9	98	35	14	25
Hydroxyproline	31	0	57	22	8

Table 5: Mean amino acid composition (g/kg total amino acid) from MacRae et al. [61].

Table 6 gives approximations for the molecular weights for Pb, Pv and Pz as well as Pw. The weights of each amino acid present (from Table 5) are translated into numbers of moles using their respective molecular weights. The total weight of the protein is divided by the total number of amino acid moles to determine an average molecular weight for amino acids in each protein type. For completeness, the weighted average molecular weights were also calculated. The ratio of the two is a measure of the heterogeneity of the sizes of the amino acid molecules, and is called the polydispersity index. The weighted average molecular weights and the polydispersity indices are presented in Table 44 and Table 45 of Appendix B respectively. They show a less than six percent difference between the molecular weights for each body area between the two approaches for calculating molecular weights.

The number average molecular weights in Table 6 do not seem to differ greatly between tissue types, with the body proteins being very similar and wool protein having a slightly higher weight. However, all of the number average molecular weights are lower than the 142g/mol figure used by Hon [45]. This brings the assumption regarding the 142g/mol molecular weight of amino acids in body protein into question, and hence the figures presented in Table 6 will be used in the empty body weight formula in its place.

Amino Acid	**MW (g/mol)**	**Carcass**	**Viscera**	**Other**	**Wool**
Aspartate	133	0.6692	1.015	0.6617	0.7068
Theonine	119	0.4202	0.8319	0.4286	0.4538
Serine	105	0.381	1.2667	0.4476	0.4381
Glutamate	147	0.9184	1.7823	0.8571	0.8231
Glycine	75	1.24	2.3467	1.1733	0.76
Alanine	89	0.8989	1.4157	0.8315	0.6854
Valine	117	0.4188	0.4957	0.4188	0.5214
Isoleucine	131	0.2901	0.4122	0.2824	0.3282
Leucine	131	0.5725	1	0.5802	0.687
Tyrosine	181	0.1713	0.4365	0.1989	0.2265
Phenylalanine	165	0.2364	0.4121	0.2485	0.3333
Histidine	155	0.1677	0.1677	0.1484	0.2129
Lysine	146	0.4795	0.5685	0.4726	0.4726
Arginine	174	0.4195	0.977	0.3851	0.3391
Proline	115	0.5304	1.287	0.5304	0.4087
Methionine	149	0.1208	0.1074	0.1477	0.2148
Cysteine	121	0.0744	1.0992	0.1157	0.2066
Hydroxyproline	131	0.2366	0.4351	0.1679	0.0611
Total Moles		**8.2456**	**16.0567**	**8.0963**	**7.8794**
Total Grams		**1007**	**997**	**1987**	**957**
Estimated MW (g/mol)		***122.13***	***123.75***	***122.40***	***126.41***

Table 6: Calculation of number average molecular weights of amino acids in protein, using data from MacRae et al. [61] and Nelson and Cox [66].

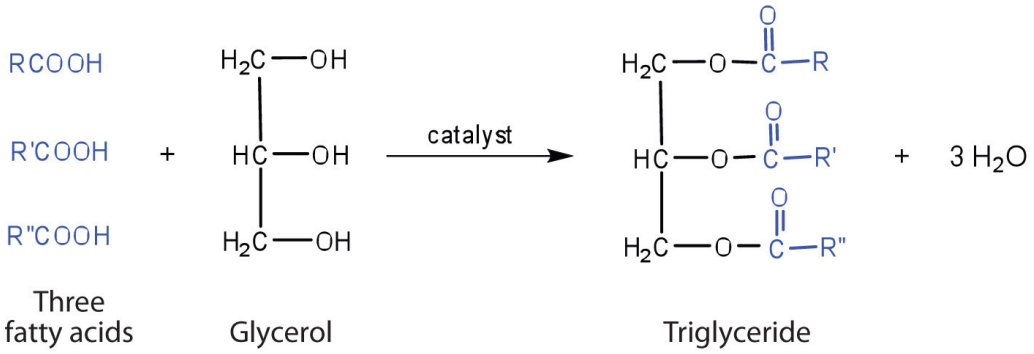

Figure 12: Balanced equation of the formation of a triglyceride (D.W. Ball et al. [14]).

Now an estimate of the molecular weight for storage triacylglycerol is required. Triacylglycerols are glycerides in which the glycerol is esterified with three fatty acids. This reaction is illustrated in Figure 12. Therefore the molecular weight of triacylglycerol is dependent on its fatty acid profile, or the relative proportion of different fatty acids that are present. Similar to the amino acids in protein, a number average molecular weight is sought, based on the relative number of fatty acid molecules expected to be present in triacylglycerides. The glycerol component not included in the fatty acid, as given in Nelson and Cox [66], has a base molecular weight of 38.05g/mol. This is the equivalent of three carbon atoms and two hydrogen atoms. The reaction in which glycerol bonds with the three fatty acids creates the triacylglycerol and three water molecules. The difference between the number of atoms present when the three water molecules are removed from the triacylglycerol is the three carbon and two hydrogen atoms in question. The overall molecular weight depends on which fatty acids glycerol bonds with. Jackson and Winkler [47] give the percentages of total fatty acids in adipose tissue in sheep (before fasting), which are similar to those also given in Hilditch and Shrivastava [43] and Ogilvie, McClymont and Shorland [68]. Using this information, and molecular weights for the fatty acids as sourced from Nelson and Cox [66], Table 7 has been constructed.

This gives a weighted average for the fatty acid molecular weight at approximately 271.4g/mol. As there are three fatty acids bonded to the glycerol base to form the triacylglycerol, this gives an estimate for the molecular weight of the storage fat as 852g/mol. A formula for determining the empty body weight (kg) from the state variables can now be given as follows:

$$W_{EB} = \frac{4.547\,(0.122Pb + 0.124Pv + 0.122Pz) + 0.852Ts}{0.95}. \tag{68}$$

Fatty Acid	Proportion of Total	Molecular Weight
Palmitic acid	0.36	256.433
Oleic acid	0.33	282.461
Stearic acid	0.25	284.477
Myristic acid	0.03	228.371
Palmitoleic acid	0.02	254.408
Linoleate acid	< 0.02 (estimated at 0.01)	280.446

Table 7: Fatty acids present in storage triacylglycerol and their relative proportions and molecular weights, using data from Jackson and Winkler [47] and Nelson and Cox [66].

4.1.1 Further Discussion and Verification

It is important to be confident that the empty body weight equation developed (Equation (68)) can be assumed to be relevant across a number of different scenarios. Upton [94] collates information from a variety of sources to produce a table outlining the body composition of a standard sheep. In Upton's paper, a "standard sheep" is a 45kg Merino ewe, as these are the most commonly used in biomedical research. As Upton states, it has been shown that organ volumes scale with body weight with an allometric coefficient of 1 (citing Anderson and Holford [6] and West et al. [99]). Allometry is the study of how biological variables scale with changes in body size, so this means that for adult sheep the organ volumes will on average be a fixed ratio of body weight. Whilst our focus in this model is on weights rather than volumes, Upton [94] also points out that organ volumes can be estimated from weight by adjusting for tissue density, which itself can be assumed to be a constant. Therefore it can also be assumed that for adult sheep the organ weights will on average be a fixed ratio of body weight. It hence follows that regardless of the "standard sheep" concept applied in this work, the proportion presented by Upton should still be relevant. Components of Upton's Table 1 are presented in Table 8. Note that the original table also contains data with regards to blood flow and cardiac output, which is not shown here.

In order to make meaningful comparisons between the collation from Upton [94] in Table 8 and our top-level formula for empty body weight in Equation (67), the proportions must be adjusted to represent empty body weight, rather than what Upton describes as total body weight. The obvious exclusions are the gastro-intestinal contents and the fleece. The components that contribute to empty body weight are listed in Table 10, and some are grouped. The idea is to be able to show that Equation (67) holds under an independent determination. In order to achieve this, the components from Upton [94] will be broken down into protein, fat, water and ash, using results from other publications.

Component	Ratio of Total Body Weight	Weight (kg)
Blood	0.057	2.56
Lung	0.010	0.45
Brain	0.002	0.09
Heart	0.0037	0.167
Liver (PDV + artery)	0.016	0.72
PDV - stomach	0.032	1.45
PDV - small intestine	0.017	0.79
PDV - large intestine	0.015	0.69
PDV - spleen	0.0023	0.105
Kidneys	0.0046	0.207
Fat	0.168	7.56
Muscle	0.277	12.47
Other (skin, marrow)	0.103	4.64
Bone	0.070	3.15
GI contents	0.130	5.85
Fleece	0.091	4.10

Table 8: Data and references for a 45kg standard sheep, from Upton [94]. *PDV = Portal drained viscera*

Muscle

Pearce et al. [74] quotes Offer and Knight [67] in stating that lean muscle contains approximately 75% water. The other components include protein (approximately 20%), lipids (approximately 5%), carbohydrates (approximately 1%) and vitamins and minerals (ash, approximately 1%). Due to the approximate figures given, the total percentages sum to 102%. These approximate percentages are scaled back proportionately to give an overall total of 100% before being applied in Table 10 and carbohydrates are grouped with ash.

Portal Drained Viscera (PDV) and Other Organs of the Abdominal and Thoracic Cavities

Bhaskar et al. [18] gives average fresh visceral mass (consisting of stomach, small and large intestines) as 85.53% moisture, 5.20% fat, 9.45% protein and 0.90% ash. These are approximate g/100g visceral mass figures, and are based on a sample size of four animals. As such they do not sum exactly to 100%, therefore they are also scaled proportionately to give an overall total of 100% before being applied in Table 10. Due to a lack of more specific information, these proportions have also been applied to PDV - spleen, kidneys, lung, heart and liver in Table 10.

Parameter	mmol/l	Molecular Weight	g/l
Glucose	3.00	180.16	0.54
Cholesterol	1.63	386.65	0.63
Urea	8.35	60.06	0.50
Calcium	2.51	40.078	0.10
Chloride	104.39	35.453	3.70
Sodium	148.10	22.99	3.40
Potassium	4.84	39.0983	0.19
Total Ash			**9.06**
Triglycerides	0.19	852	0.16
Total Protein			**66.8**

Table 9: Blood composition calculations, using data from Casamassina et al. [25] and molecular weights from Nelson and Cox [66].

Brain, Other (Skin, Marrow) and Blood

The control group of sheep in Butler-Hogg [23] had an average composition for the "remainder" (including head, hide, feet and blood) of 18.1% protein, 8.8% fat, 5.2% ash and 67.9% water. These percentages are applied to the brain, other (skin and marrow) and blood in Table 10. Blood composition was assessed in lactating Comisana ewes in Casamassina et al. [25], and the control group had an average of 66.8g/l of total proteins present in the samples. All other non-protein blood parameters (glucose, triglycerides, calcium, etc) given were in units of mmol/l, and these are presented in Table 9. Every non-protein blood parameter other than triglycerides was grouped as "ash". Using blood density of 1060g/l (Cutnell and Johnson [29]), and assuming components not listed could be grouped into body water, this gave proportions of blood as: 6.30% protein, 0.85% ash, 0.015% fat and 92.83% water. However, as independent breakdowns for other (skin and marrow) and brain were not able to be sourced, the composition for the "remainder" in Butler-Hogg [23] was used for these components, along with blood. The information from Casamassima et al. [25] does provide a useful yet minor check, however, that the water content in the combined blood, brain and other (skin and marrow) should be at least 2.38kg (92.83% of the 2.56kg blood component). As it is 4.95kg using the results in Butler-Hogg [23], this has not been violated.

Bone

Field et al. [33] fit a least-squares regression model to bone composition data in Rambouillet $\times$ Columbia cross sheep at three different ages, 5 to 6 months, 10 to 12 months and 48 to 96 months. However, there were only four animals in each group, and marrow seemed to be included in the analysis, whereas marrow is

treated separately in the breakdown given by Upton [94]. An interesting outcome of the study in Field et al. [33] was that the composition of bone across the different ages had significant differences between means ($p < 0.05$). In general, the bones had less moisture as the animals aged, and other components, such as fat and ash, increased with age. The mean compositions of bone in the 48 to 96 month old group in Field et al. [33] are assumed to be stable adult measurements that are likely to be the most applicable to the standard sheep described by Upton [94]. These were 77.45% "dry matter", 16.13% fat, and an assumed remainder of 6.42% moisture. It is assumed that the fat content of fresh bone is already taken into account via the general body fat and marrow estimates from Upton [94], and hence it is the dry matter and the moisture that is of interest. Simple calculations give a moisture content of 7.65% in fat-free fresh bone. The percentage of dry-fat-free bone that is ash is given as 62.86%. When multiplied by 92.35% (dry-fat-free bone to fat-free fresh bone adjustment), this gives 58.05% of fat-free fresh bone being ash. In Aerssens et al. [4], bone samples from sheep aged 1–2 years where taken, cleaned from soft tissue and bone marrow and defatted. Whilst the protein levels presented in Aerssens et al. [4] are too low to be inclusive of non-extractable proteins, the ash % of dry-fat-free bone for sheep is given as a range of 62.6–64.2 for lower density bone, and 68.2–69.7 for higher density bone. The Field et al. [33] result is clearly in the right general area, and with the breed and exact age and number of sheep tested in Aerssens et al. [4] not being known, it is not appropriate to make an exact comparison. The proportions in Fields et al. [33] are applied in Table 10 due to the availability of water content estimates. The remaining proportion of the fat-free bone not covered by ash and moisture is assumed to be collagen (a form of protein) and non-collagenous proteins.

Fat

Robertson, Faulkner and Vernon [80] outline a study of glucose and fatty acid activity in perirenal adipose tissue of 7 to 9 month old Cheviot and Finn × Dorset Horn cross-bred sheep. Similar to the study in Field et al. [33], the sample group consisted of only four animals in each group (in this case group is defined by the breed). The total amount of water per gram of adipose tissue did not change significantly over the two-hour incubation of the tissue, and so the mean value was reported, 255.1μl/g. However, this analysis was only conducted on the Cheviot sheep. Using the standard conversion of 1000g/l for water, this gives a percentage of adipose tissue being water of 25.51%. Water content of adipose tissue was identified between sites in Berthelot et al. [17], for cross-bred (Berrichon du Cher or Suffolk) × INRA 401 male lambs. The sites tested included perirenal (as analysed in Robertson, Faulkner and Vernon [80]), omental, caudal

Organs	**Weight (kg) [94]**	**Body Protein (kg)**	**Body Fat (kg)**	**Body Water (kg)**	**Ash (kg)**
Muscle	12.47	2.4451	0.6113	9.1691	0.2445
PDV - stomach, PDV - small intestine, PDV - large intestine	2.93	0.2739	0.1507	2.4793	0.0261
PDV - spleen, kidneys, lung, heart, liver (PDV + artery)	1.65	0.1543	0.0849	1.3962	0.0147
Other (skin, marrow), brain, blood	7.29	1.3195	0.6415	4.9499	0.3791
Fat	7.56	-	5.7456	1.8144	-
Bone	3.15	1.082	-	0.241	1.827
Total	**35.05**	**5.2748**	**7.234**	**20.05**	**2.4914**

Table 10: 45kg standard sheep empty body weight composition with protein, fat, water and ash proportions as estimated in Section 4.1.1.

and dorsal adipose tissues. The sample group consisted of six lambs, and the water content for perirenal, omental, caudal and dorsal adipose tissues was given as 18.0%, 18.6%, 26.3% and 29.6% respectively. This is quite a broad range, and the 18.0% for perirenal adipose tissue differs substantially from the 25.51% given in Robertson, Faulkner and Vernon [80]. This is not overly surprising, given the small sample sizes, and the differences in breeds and ages used (Berthelot et al. [17] states a slaughter weight of 34.2kg, on average, rather than an age). There is no clear advantage in taking a sophisticated approach to determining a suitable water proportion in adipose tissue, so a rough mid-point of the two extremes in Berthelot et al. [17] of 24% is used in Table 10.

Conclusions

Ideally, these proportions used to break the estimates of Upton [94] down into body protein, fat, water and ash would be available for specific body organs from a large sample size of Australian Merino sheep, but this result was not available in the literature. There is an issue of false precision in Table 10. It is pieced together from different studies involving sheep of different breeds, under different conditions, slaughtered at different ages, and whilst the proportions are probably within a reasonable range for each organ, it is misleading to put the different organs together. The assumption is that the combinations produce a reasonable overall sheep body composition breakdown, and the fact is that this is unlikely to be true. There are other issues that need to be considered, such as that the components of organs (skin in particular) may be related to the fleece

production and the shearing schedule (see Wodzicka [103]), neither of which are considered here. The empty body weight formula needs to be simple rather than sophisticated, such that it gives a reasonable approximation over many scenarios. It also needs to be based on studies that cover each aspect used in the formula - rather than having a study affect one estimate in the formula and not another. There is just too much variability for another approach to be defensible. Therefore the simple approach used in Equation (67) is quite valid. However, it would be beneficial to review the assumptions made with reference to empty body weight and general proportions of body composition should any other biological studies, either simply more recent or relating specifically to Australia Merinos, become available.

As a final defence of Equation (67) before concluding this Section, it can be noted that the body water in Table 10 is approximately 3.8 times the body protein, which is similar to the 3.547 ratio assumption used for Equation (67). The ash proportion is slightly higher at 7.1% rather than 5%, but it had been identified earlier that ash proportion may change under different conditions (note the 2% ash figure for undernourished sheep from Graham [38]). In the Sainz and Wolff [83] paper, Figure 3 displays approximate percentages of body protein and body fat as compared to empty body weight, at the 20, 30 and 40kg reference empty body weights. Using the mid-point of the percentages to estimate the 35kg empty body weight proportions, we have 15.6% body protein and 22.5% body fat. This is not substantially different to the 15% and 20.6% respectively that can be calculated from the figures in Table 10. If Equation (67) is applied to the estimated body protein and body fat at the 20, 30 and 40kg reference empty body weights in Sainz and Wolff [83], then estimates for empty body weight can be compared with the reference weights. This has also been conducted using the original empty body weight equation from Hon [45] (Equation (66)) for comparison, and the results are presented in Table 11. Whilst Equation (67) gives results slightly different to the reference weights, they are notably closer than those produced using Equation (66). As the percentages of body protein and body fat are simply estimated from a Figure, it is concluded that the empty body weight calculated using Equation (67) gives results comparable to those in Sainz and Wolff [83].

4.2 Preliminary Initial Conditions

As discussed in Section 4.1, the initial conditions are essentially an input to the model, a starting point. The initial conditions described by Hon [45] are given in Table 1. These are combined with kilogram estimates of the body proteins and

EBW (Reference)	Body Protein	Body Fat	EBW (67)	EBW (66)
20	3.3 (16.5%)	2.8 (14%)	18.7	17.3
30	4.8 (16%)	6.0 (20%)	29.3	27.2
40	6.1 (15.25%)	10 (25%)	39.7	37.1

Table 11: Empty body weight (EBW) comparisons using Figure 3 in Sainz and Wolff [83], Equation (66) and Equation (67).

the body fat in Table 12. Using Equation (68), the initial conditions given by Hon [45] now give an empty body weight of 19.32kg, which is based on a body protein of 3.3638kg and body fat of 3.0588kg. Using Figure 3 from Sainz and Wolff [83], approximate body protein and body fat percentages for an empty body weight of 20kg are 16.5% and 14% respectively. The initial conditions of Hon [45] give body protein and body fat percentages of 17.4% and 15.8% respectively. The higher percentages are not wholly unexpected, as it was noted that Equation (67) would produce an underestimate of the reference weight of 20kg in Table 11. The ratio of protein to fat is close to the Sainz and Wolff [83] estimates, however for consistency the initial condition for storage triacylglycerol was reduced to 3.35 moles (producing 2.8542kg body fat) such that these ratios are equal. Following this, the initial conditions for both body protein and body fat were adjusted by a constant factor of 1.047 in order to ensure Equation (68) produces an exact 20kg empty body weight (after changing body fat to 2.8542kg the empty body weight was 19.1kg). The adjusted initial values are also presented in Table 12. These initial conditions are simply a point to start from in running the model, and will be revisited in Chapter 5. At this stage, initial conditions for the other state variables will not be adjusted, as this would be purely speculative.

4.2.1 Preliminary Derived Variable Values from Sainz and Wolff [83]

Whilst Sainz and Wolff [83] do not explicitly give the state variable values for a $W_{EB} = 20$kg, 30kg or 40kg sheep, it is possible to estimate the values used, with the exception of protein in wool. These may be considered potential initial conditions for running the model. They can be estimating by using their Table 3 *Definition of major rates in the model* at the $W_{EB} = 20$kg, 30kg and 40kg reference values, in conjunction with model structure formula given in their Methods Section. That is, the rate of utilisation and production equations of the model, as presented in Chapter 3, are analysed along with the values of these rates at certain empty body weights as given by Sainz and Wolff [83] to estimate the values of state variables and other model values at the same empty body weights.

State Variable	**Initial Value (Moles)**	**Initial Value (kg)**	**Initial Value Adj. (kg)**	**Initial Value Adj. (Moles)**
Amino Acid (Aa)	0.012	-	-	0.012
Glucose (Gl)	0.0144	-	-	0.0144
Lipids (Tg)	0.01152	-	-	0.01152
Acetate (Ac)	0.0048	-	-	0.0048
Protein (Carcass) (Pb)	14.8771	1.8150	1.9000	15.5743
Protein (Viscera) (Pv)	6.84	0.8482	0.8879	7.1605
Protein (Other Tissues) (Pz)	5.743	0.7006	0.7335	6.0121
Protein (Wool) (Pw)	0	0	0	0
Storage Triacylglycerol (Ts)	3.35	2.8542	2.9880	3.5070
DNA (Carcass) (Db)	0.0061	-	-	0.0061
DNA (Viscera) (Dv)	0.0075	-	-	0.0075
DNA (Other Tissues) (Dz)	0.0044	-	-	0.0044

Table 12: Review of initial state variable values (20kg empty body weight) from Hon [45], including reduced body fat.

The result is effectively a snapshot of the state variables at certain points of the simulation run by Sainz and Wolff [83]. The derived state variable values (which along with corresponding hormonal controls and concentrations will hereby be collectively referred to as the "variable values") are given in Table 13, with details of the derivation corresponding to $W_{EB} = 20$kg given in the Sections below. This process was repeated for $W_{EB} = 30$kg and $W_{EB} = 40$kg. Sainz and Wolff [83] determined the values in their Table 3 (SW Table 3) from values reported in the literature, and then set the affinity constants (k_{jk}) in a similar manner, finally using least squares regression to determine other parameters. The state variable values derived in this Section are set such that a *select few* of the reference fluxes in SW Table 3 will *fit precisely for each empty body weight*. They cannot be expected to produce an exact fit to other rates from SW Table 3 (that is, where an exact fit is not forced), but we would expect the differences between the reported rate and the rate produced using the derived initial conditions to be representative of a least squares fit. Flux values where an exact match has been forced are highlighted in the relevant tables (Tables 16-18). There was an issue involving the derivation of Dz in that two very different values were determined depending on which rate in Sainz and Wolff's Table 3 [83] was used to derive it. This is discussed further in Section 4.2.1.

Variable Values - Protein

The amount of protein in the carcass, viscera and other tissues (Pb, Pv and Pz respectively) can be estimated by using the rates of $U_{Pb,PbAa}$, $U_{Pv,PvAa}$ and $U_{Pz,PzAa}$. This is demonstrated in Equations (69), (70) and (71). It is not possible to determine the value of Pw (protein in wool) as its value does not feed into the differential equations. There is documented evidence of a relationship between the amount of wool and the attributes of the skin (Wodzicka [103]), and incorporating this is a possible future enhancement to the model.

$$U_{Pb,PbAa} = K_{PbAa} Pb,$$

$$\Rightarrow Pb_{W_{EB}=20} = \frac{U_{Pb,PbAa_{W_{EB}=20}}}{K_{PbAa}} = \frac{0.6020}{0.04}$$

$$\therefore Pb_{W_{EB}=20} = 15.05. \tag{69}$$

$$Pv_{W_{EB}=20} = \frac{U_{Pv,PvAa_{W_{EB}=20}}}{K_{PvAa}} = \frac{2.052}{0.3} = 6.84. \tag{70}$$

$$Pz_{W_{EB}=20} = \frac{U_{Pz,PzAa_{W_{EB}=20}}}{K_{PzAa}} = \frac{0.5743}{0.1} = 5.743. \tag{71}$$

Variable/ Parameter	**Value** $W_{EB} = 20$kg	**Value** $W_{EB} = 30$kg	**Value** $W_{EB} = 40$kg
Aa	0.01064	0.01634	0.02403
Gl	0.01429	0.02141	0.02858
Tg	0.01120	0.01689	0.02206
Ac	0.004925	0.007086	0.009530
Pb	15.05	23.00	31.30
Pv	6.840	8.523	10.30
Pz	5.743	7.837	9.803
Pw	-	-	-
Ts	3.307	7.241	11.4458
Db	0.006162	0.006934	0.007205
Dv	0.007663	0.008071	0.008123
Dz	0.004547	0.004789	0.004790
H_A	0.9848	0.9821	0.9850
H_C	1.104	1.018	1.0153
C_{Aa}	0.002217	0.002270	0.002503
C_{Gl}	0.002977	0.002973	0.002977
C_{Tg}	0.002334	0.002346	0.002298
C_{Ac}	0.001026	0.0009842	0.0009927
C_{Ts}	0.1654	0.2414	0.2861

Table 13: Sainz and Wolff [83] Preliminary derived variable values where $W_{EB} =$ 20kg, 30kg and 40kg (4 s.f.).

Variable Values - Circulating Fluids, Concentrations and Hormonal Controls

The amount of circulating glucose (Gl) can be estimated by using the value of $U_{Gl,GlTp}$, as it only depends on Gl, plus parameters, the value of Pb (already estimated), and other terms such as H_A and C_{Gl} that are derived from Gl and other known values, such as W_{EB}. The values for Gl, C_{Gl} and the hormonal controls of H_A and H_C are derived in Equations (72), (73) and (74).

$$U_{Gl,GlTp} = \frac{V_{GlTp}}{\left(1 + \frac{k_{GlTp}}{C_{Gl}}\right)} = \frac{V'_{GlTp} Pb^{\theta 2}}{\left(1 + \frac{k'_{GlTp}}{C_{Gl} H_A}\right)}$$

$$\Rightarrow (U_{Gl,GlTp}) \left(1 + \frac{k'_{GlTp}}{C_{Gl}\left(\frac{C_{Gl}}{C_{Gl,ref}}\right)^2}\right) = V'_{GlTp} Pb^{\theta 2}$$

$$\Rightarrow \frac{k'_{GlTp} C^2_{Gl,ref}}{C^3_{Gl}} = \frac{V'_{GlTp} Pb^{\theta 2}}{U_{Gl,GlTp}} - 1$$

$$\therefore C_{Gl} = \sqrt[3]{\frac{k'_{GlTp} C^2_{Gl,ref}}{\left(\frac{V'_{GlTp} Pb^{\theta 2}}{U_{Gl,GlTp}} - 1\right)}}$$

$$\Rightarrow C_{Gl_{W_{EB}=20}} = \sqrt[3]{\frac{0.003^3}{\left(\frac{0.0415 Pb^1_{W_{EB}=20}}{U_{Gl,GlTp_{W_{EB}=20}}} - 1\right)}} = \sqrt[3]{\frac{0.003^3}{\left(\frac{0.0415(15.05)}{0.3087} - 1\right)}}$$

$$\therefore C_{Gl_{W_{EB}=20}} = 0.002977$$

$$\Rightarrow Gl_{W_{EB}=20} = v_{ECF_{W_{EB}=20}} C_{Gl_{W_{EB}=20}} = (0.24)(20)(0.002977)$$

$$\therefore Gl_{W_{EB}=20} = 0.01429. \tag{72}$$

$$H_{A_{W_{EB}=20}} = \left(\frac{C_{Gl_{W_{EB}=20}}}{C_{Gl,ref}}\right)^2 = \left(\frac{0.002977}{0.003}\right)^2 = 0.9848. \tag{73}$$

$$H_{C_{W_{EB}=20}} = \left(\frac{C_{Gl,ref}}{C_{Gl_{W_{EB}=20}}}\right)^2 = \left(\frac{0.003}{0.002977}\right)^2 = 1.0154. \tag{74}$$

The amount of circulating amino acids (Aa) can be estimated by using the value of $U_{Aa,AaGl}$, as it only depends on Aa, plus parameters and the values of Pv and Gl (already estimated). The values of Aa and C_{Aa} are derived in Equation (75).

$$U_{Aa,AaGl} = K_{AaGl} C_{Aa} = \frac{K'_{AaGl} C^2_{Aa} Pv^{\theta 1} H_C}{C_{Aa,ref}}$$

$$\therefore C_{Aa} = \sqrt{\frac{C_{Aa,ref} U_{Aa,AaGl}}{K'_{AaGl} Pv^{\theta 1} H_C}}$$

$$\Rightarrow C_{Aa_{W_{EB}=20}} = \sqrt{\frac{(0.0025) U_{Aa,AaGl_{W_{EB}=20}}}{(18) Pv^1_{W_{EB}=20} H_{C_{W_{EB}=20}}}} = \sqrt{\frac{(0.0025)(0.2459)}{(18)(6.84)^1(1.0154)}}$$

$$\therefore C_{Aa_{W_{EB}=20}} = 0.002217$$

$$\Rightarrow Aa_{W_{EB}=20} = v_{ECF_{W_{EB}=20}} C_{Aa_{W_{EB}=20}} = (0.24)(20)(0.002217)$$

$$\therefore Aa_{W_{EB}=20} = 0.01064. \tag{75}$$

The amount of circulating lipids (Tg) can be estimated by using the value of $U_{Tg,TgTs}$, as it only depends on Tg, plus parameters and the values of Pb, Pv and Gl (already estimated). The values of Tg and C_{Tg} are derived in Equation (76).

$$U_{Tg,TgTs} = \frac{V_{TgTs}}{\left(1 + \frac{k_{Tg,TgTs}}{C_{Tg}} + \frac{k_{Gl,TgTs}}{C_{Gl}}\right)} = \frac{V'_{TgTs} \left(Pb + Pv\right)^{\theta 4}}{\left(1 + \frac{k_{Tg,TgTs}}{C_{Tg}} + \frac{k_{Gl,TgTs}}{C_{Gl}}\right)}$$

$$\Rightarrow \frac{V'_{TgTs} \left(Pb + Pv\right)^{\theta 4}}{U_{Tg,TgTs}} = 1 + \frac{k_{Tg,TgTs}}{C_{Tg}} + \frac{k_{Gl,TgTs}}{C_{Gl}}$$

$$\Rightarrow \frac{k_{Tg,TgTs}}{C_{Tg}} = \frac{V'_{TgTs} \left(Pb + Pv\right)^{\theta 4}}{U_{Tg,TgTs}} - \frac{k_{Gl,TgTs}}{C_{Gl}} - 1$$

$$\therefore C_{Tg} = \frac{k_{Tg,TgTs}}{\left(\frac{V'_{TgTs}(Pb+Pv)^{\theta 4}}{U_{Tg,TgTs}} - \frac{k_{Gl,TgTs}}{C_{Gl}} - 1\right)}$$

$$\Rightarrow C_{Tg_{W_{EB}=20}} = \frac{0.0024}{\left(\frac{(0.00518)\left(Pb_{W_{EB}=20} + Pv_{W_{EB}=20}\right)^{0.902}}{U_{Tg,TgTs_{W_{EB}=20}}} - \frac{(0.003)}{C_{Gl_{W_{EB}=20}}} - 1\right)}$$

$$= \frac{0.0024}{\left(\frac{(0.00518)(15.05+6.84)^{0.902}}{0.0276} - \frac{(0.003)}{0.002977} - 1\right)}$$

$$\therefore C_{Tg_{W_{EB}=20}} = 0.002334$$

$$\Rightarrow Tg_{W_{EB}=20} = v_{ECF_{W_{EB}=20}} C_{Tg_{W_{EB}=20}} = (0.24)(20)(0.002334)$$

$$\therefore Tg_{W_{EB}=20} = 0.01120. \tag{76}$$

The amount of circulating acetate Ac can be estimated by using the value of $U_{Ac,AcTs}$, as it only depends on Ac, plus parameters and the values of Pb, Pv, Gl and Tg (already estimated). The values of Ac and C_{Ac} are derived in Equation (77).

$$U_{Ac,AcTs} = \frac{V_{AcTs}}{\left(1 + \frac{k_{Ac,AcTs}}{C_{Ac}} + \frac{k_{Gl,AcTs}}{C_{Gl}} + \frac{C_{Tg}}{k_{Tg,AcTs}}\right)}$$

$$= \frac{V'_{AcTs} H_A \left(Pb + Pv\right)^{\theta 3}}{\left(1 + \frac{k_{Ac,AcTs}}{C_{Ac}} + \frac{k'_{Gl,AcTs}}{H_A C_{Gl}} + \frac{C_{Tg}}{k_{Tg,AcTs}}\right)}$$

$$\Rightarrow \frac{V'_{AcTs} H_A \left(Pb + Pv\right)^{\theta 3}}{U_{Ac,AcTs}} = 1 + \frac{k_{Ac,AcTs}}{C_{Ac}} + \frac{k'_{Gl,AcTs}}{H_A C_{Gl}} + \frac{C_{Tg}}{k_{Tg,AcTs}}$$

$$\therefore \frac{k_{Ac,AcTs}}{C_{Ac}} = \frac{V'_{AcTs} H_A \left(Pb + Pv\right)^{\theta 3}}{U_{Ac,AcTs}} - \frac{k'_{Gl,AcTs}}{H_A C_{Gl}} - \frac{C_{Tg}}{k_{Tg,AcTs}} - 1$$

$$\Rightarrow \frac{0.001}{C_{Ac_{W_{EB}=20}}} = \frac{0.346 H_{A_{W_{EB}=20}} \left(Pb_{W_{EB}=20} + Pv_{W_{EB}=20}\right)^{0.878}}{U_{Ac,AcTs_{W_{EB}=20}}} -$$

$$\frac{0.001}{H_{A_{W_{EB}=20}} C_{Gl_{W_{EB}=20}}} - \frac{C_{Tg_{W_{EB}=20}}}{0.0036} - 1$$

$$= \frac{(0.346)(0.9848)\left(15.05 + 6.84\right)^{0.878}}{1.727} - \frac{0.001}{(0.9848)(0.002977)} - \frac{0.002334}{0.0036} - 1$$

$$\therefore C_{Ac_{W_{EB}=20}} = 0.001026$$

$$\Rightarrow Ac_{W_{EB}=20} = v_{ECF} C_{Ac_{W_{EB}=20}} = (0.24)(20)(0.001026)$$

$$\therefore Ac_{W_{EB}=20} = 0.004925. \tag{77}$$

Variable Values - Storage Triacylglycerol

The amount of storage triacylglycerol (Ts) can be estimated by using the value of $U_{Ts,TsTg}$, as it only depends on Ts, plus parameters and the values of Pb, Pv and Gl (already estimated). The values of Ts and C_{Ts} are derived in Equation (78).

$$U_{Ts,TsTg} = \frac{V_{TsTg}}{1 + \left(\frac{k_{TsTg}}{C_{Ts}}\right)^{\theta 5}} = \frac{V'_{TsTg} H_C \left(Pb + Pv\right)^{\theta 6}}{1 + \left(\frac{k_{TsTg}}{C_{Ts}}\right)^{\theta 5}}$$

$$\Rightarrow \left(\frac{k_{TsTg}}{C_{Ts}}\right)^{\theta 5} = \frac{V'_{TsTg} H_C \left(Pb + Pv\right)^{\theta 6}}{U_{Ts,TsTg}} - 1$$

$$\therefore C_{Ts} = \frac{k_{TsTg}}{\sqrt[\theta 5]{\frac{V'_{TsTg} H_C (Pb+Pv)^{\theta 6}}{U_{Ts,TsTg}} - 1}}$$

$$\Rightarrow C_{Ts_{W_{EB}=20}} = \frac{0.0968}{\sqrt[5]{\frac{0.00546 H_{C_{W_{EB}=20}} \left(Pb_{W_{EB}=20} + Pv_{W_{EB}=20}\right)^{0.75}}{U_{Ts,TsTg_{W_{EB}=20}}} - 1}}$$

$$= \frac{0.0968}{\sqrt[5]{\frac{(0.00546)(1.0154)(15.05+6.84)^{0.75}}{0.0525} - 1}}$$

$$\therefore C_{Ts_{W_{EB}=20}} = 0.1654$$

$$\Rightarrow Ts_{W_{EB}=20} = C_{Ts_{W_{EB}=20}} W_{EB_{W_{EB}=20}}$$
$$\therefore Ts_{W_{EB}=20} = 3.3073. \tag{78}$$

Variable Values - DNA Pools and Adjustment of V'_{APw}

The values of DNA in the carcass, viscera and other tissues variables (Db, Dv and Dz respectively) can be estimated by using the rates of $U_{Aa,AaPb}$, $U_{Aa,AaPv}$ and $U_{Aa,AaPz}$. This is demonstrated in Equations (79), (80) and (81).

$$U_{Aa,AaPb} = \frac{V_{AaPb}}{\left(1 + \frac{k_{AaPb}}{C_{Aa}}\right)} = \frac{V'_{AaPb} Pb^{\theta 7} Db}{\left(1 + \frac{k'_{AaPb}}{H_A C_{Aa}}\right)}$$

$$\therefore Db = \frac{U_{Aa,AaPb}\left(1 + \frac{k'_{AaPb}}{H_A C_{Aa}}\right)}{V'_{AaPb} Pb^{\theta 7}}$$

$$\Rightarrow Db_{W_{EB}=20} = \frac{U_{Aa,AaPb_{W_{EB}=20}}\left(1 + \frac{0.0005}{H_{A_{W_{EB}=20}} C_{Aa_{W_{EB}=20}}}\right)}{21.7 Pb^{0.682}_{W_{EB}=20}}$$

$$= \frac{0.6914\left(1 + \frac{0.0005}{(0.9848)(0.002217)}\right)}{(21.7)(15.05)^{0.682}}$$

$$\therefore Db_{W_{EB}=20} = 0.006162. \tag{79}$$

$$U_{Aa,AaPv} = \frac{V_{AaPv}}{\left(1 + \frac{k_{AaPv}}{C_{Aa}}\right)} = \frac{V'_{AaPv} Pv^{\theta 8} Dv}{\left(1 + \frac{k'_{AaPv}}{H_A C_{Aa}}\right)}$$

$$\therefore Dv = \frac{U_{Aa,AaPv}\left(1 + \frac{k'_{AaPv}}{H_A C_{Aa}}\right)}{V'_{AaPv} Pv^{\theta 8}}$$

$$\Rightarrow Dv_{W_{EB}=20} = \frac{U_{Aa,AaPv_{W_{EB}=20}}\left(1 + \frac{0.0005}{H_{A_{W_{EB}=20}} C_{Aa_{W_{EB}=20}}}\right)}{63.2 Pv^{0.852}_{W_{EB}=20}}$$

$$= \frac{2.028\left(1 + \frac{0.0005}{(0.9848)(0.002217)}\right)}{(63.2)(6.84)^{0.852}}$$

$$\therefore Dv_{W_{EB}=20} = 0.007663. \tag{80}$$

$$U_{Aa,AaPz} = \frac{V_{AaPz}}{\left(1 + \frac{k_{AaPz}}{C_{Aa}}\right)} = \frac{V'_{AaPz} Pv^{\theta 9} Dz}{\left(1 + \frac{k'_{AaPz}}{H_A C_{Aa}}\right)}$$

$$\therefore Dz = \frac{U_{Aa,AaPz}\left(1+\frac{k'_{AaPz}}{H_A C_{Aa}}\right)}{V'_{AaPz} Pz^{\theta 9}}$$

$$\Rightarrow Dz_{W_{EB}=20} = \frac{U_{Aa,AaPz_{W_{EB}=20}}\left(1+\frac{0.0005}{H_{A_{W_{EB}=20}} C_{Aa_{W_{EB}=20}}}\right)}{33.8 Pz^{0.882}_{W_{EB}=20}}$$

$$= \frac{0.5843\left(1+\frac{0.0005}{(0.9848)(0.002217)}\right)}{(33.8)(5.743)^{0.882}}$$

$$\therefore Dz_{W_{EB}=20} = 0.004547. \tag{81}$$

If $U_{Aa,AaPw}$ is used to determine Dz - possible as it depends only on Dz, plus parameters and the values of Pz and Aa (already estimated) - the result is quite different, as shown in Equation (82). One can only assume that an error exists in the presentation of the parameter values in Sainz and Wolff [83], but it is not immediately apparent where that might have occurred. The value of Dz derived in Equation (81) seems the more credible, as it is not only of the same scale as Db and Dz, but it is also less than the predefined maximum value of Dz ($Dz_{MAX} = 0.0048$ in Sainz and Wolff's Table 4). If we assume the value of $Dz_{W_{EB}=20}$ derived in Equation (81) is correct, then an adjustment must be made to one or more of the components of $U_{Aa,AaPw}$. It is logically more likely that one error has taken place in the presentation of data in Sainz and Wolff [83] than multiple, so it is reasonable to look to adjust only one of the components of this formula. Pz, Dz, and Aa are effectively fixed, so that leaves $\theta 10$, V'_{AaPw} or k_{AaPw}, all of which are solely used in the $U_{Aa,AaPw}$ formula in the model definition. (However, it should be noted that $U_{Aa,AaPw}$ is used in the definition of $U_{At,AtAd}$.)

$$U_{Aa,AaPw} = \frac{V_{AaPw}}{\left(1+\frac{k_{AaPw}}{C_{Aa}}\right)} = \frac{V'_{AaPw} Pz^{\theta 10} Dz}{\left(1+\frac{k_{AaPw}}{C_{Aa}}\right)}$$

$$\therefore Dz = \frac{U_{Aa,AaPw}\left(1+\frac{k_{AaPw}}{C_{Aa}}\right)}{V'_{AaPw} Pz^{\theta 10}}$$

$$\Rightarrow Dz_{W_{EB}=20} = \frac{U_{Aa,AaPw_{W_{EB}=20}}\left(1+\frac{0.0025}{C_{Aa_{W_{EB}=20}}}\right)}{0.0145 Pz^{0.916}_{W_{EB}=20}}$$

$$= \frac{0.0325\left(1+\frac{0.0025}{0.002217}\right)}{(0.0145)(5.743)^{0.916}}$$

$$\therefore Dz_{W_{EB}=20} = 0.9616. \tag{82}$$

First, the adjustment of $\theta 10$ is considered, and its corresponding adjusted

value is derived in Equation (83). Whilst this results in a genuine solution, when discussing maximum reaction velocities (in the form of $V_{max} = V'_{max} Px^{\theta} H$), Sainz and Wolff [83] state that *protein mass is raised to an exponent less than one (θ) in accordance with the observation by Munro (1969) ([65]) that enzymatic capacities vary with tissue mass to the 0.75 power.* Sainz and Wolff explain that the exponent values (θ) were estimated empirically, and some variation from 0.75 is expected. However, it is clear the presented value of $\theta 10$ (0.916) is more likely to be correct than the derived value of 3.9791 from Equation (83). Derived values for $\theta 10$ corresponding to $W_{EB} = 30$kg and 40kg (Table 14) have a similar result.

$$U_{Aa,AaPw} = \frac{V'_{AaPw} Pz^{\theta 10} Dz}{\left(1 + \frac{k_{AaPw}}{C_{Aa}}\right)}$$

$$\Rightarrow Pz^{\theta 10} = \frac{U_{Aa,AaPw}\left(1 + \frac{k_{AaPw}}{C_{Aa}}\right)}{V'_{AaPw} Dz}$$

$$\therefore \theta 10 = \frac{\log(U_{Aa,AaPw}) + \log\left(1 + \frac{k_{AaPw}}{C_{Aa}}\right) - \log(V'_{AaPw}) - \log(Dz)}{\log(Pz)}$$

$$\Rightarrow \theta 10_{W_{EB}=20} = \frac{\log(0.0325) + \log\left(1 + \frac{0.0025}{0.002217}\right) - \log(0.0145) - \log(0.004547)}{\log(5.743)}$$

$$\therefore \theta 10_{W_{EB}=20} = 3.9791. \tag{83}$$

Secondly, the adjustment of V'_{AaPw} is considered. Whilst the adjusted value of 3.067 as derived in Equation (84) is significantly greater than its presented value of 0.0145, it is still considerably smaller than its protein in carcass, viscera and other tissues counterparts ($V'_{AaPb} = 21.7$, $V'_{AaPv} = 63.2$ and $V'_{AaPz} = 33.8$). V'_{AaPw} is a factor for calculation of V_{AaPw}, the maximum velocity of an amino acid to protein in wool reaction in moles per day. The specifics of how this reference factor was estimated are not explicitly described in Sainz and Wolff [83], although it does mention the use of least squares regression in fitting V_{jk} maximum capacities, and that protein accretion rates were derived from a publication from the Agricultural Research Council [5]. Unfortunately, a copy of this publication was not able to be sourced. Derived values for V'_{AaPw} corresponding to $W_{EB} = 30$kg and $W_{EB} = 40$kg given in Table 14 give a similar scale of result.

$$U_{Aa,AaPw} = \frac{V'_{AaPw} Pz^{\theta 10} Dz}{\left(1 + \frac{k_{AaPw}}{C_{Aa}}\right)}$$

$$\therefore V'_{AaPw} = \frac{U_{Aa,AaPw}\left(1 + \frac{k_{AaPw}}{C_{Aa}}\right)}{Pz^{\theta 10} Dz}$$

$$\Rightarrow V'_{AaPw_{W_{EB}=20}} = \frac{0.0325\left(1+\frac{0.0025}{0.002217}\right)}{(5.743)^{0.916}(0.004547)}$$
$$\therefore V'_{AaPw} = 3.067. \tag{84}$$

Lastly, the adjustment of k_{AaPw} is considered, this is the Michaelis-Menton constant for the amino acids to protein in wool reaction, with respect to amino acids. Its definition, as given by Sainz and Wolff [83], is the substrate concentation at which velocity is one-half maximal. It is compared with the current concentration of substrate (amino acids) in the blood and this ratio is used to determine the proportion of the maximum reaction velocity that is currently being reached. For the equivalent reaction of protein accretion in the carcass, viscera and other tissues, the Michaelis-Menton constant is also dependent on the hormonal controls. In other words, the substrate concentration at which velocity is one-half maximal varies also with the concentration of circulating glucose. The higher the concentration of circulating glucose, the lesser the concentration of the substrate (amino acids) needs to be in order to achieve half the maximal reaction velocity. The presented value of 0.0025 for k_{AaPw} is the equivalent of k_{AaPb}, k_{AaPv} and k_{AaPz} when the circulating glucose is approximately 45% of its reference value (that is, where $H_A = 0.2$). This does not seem unreasonable, as undernourished sheep are thought to produce greater quantities of wool. Ultimately, k_{AaPw} and V'_{AaPw} are intrinsically related. One is the substrate affinity required to achieve half the maximal velocity of the reaction, the other is a factor relating the amount of protein in skin and other tissues to the maximal velocity of the reaction (the higher the amount of protein in the skin, the faster a certain number of moles of protein in wool can be produced). The focus of Sainz and Wolff [83] was on the growth of lambs, and hence wool was possibly not a primary concern.

As shown in Equation (85), in order to achieve a $U_{Aa,AaPw}$ of 0.0325 with a V'_{AaPw} value of 0.0145, the value of k_{AaPw} would need to be negative. As this represents a concentration, a negative value is illogical. A negative value is also produced in the cases where $W_{EB} = 30$kg and where $W_{EB} = 40$kg, as shown in Table 14. Indeed when considering the numerator of the defining equation of $U_{Aa,AaPw}$ given in the first line of Equation (85), a non-negative k_{AaPw} value gives an upper limit of $U_{Aa,AaPw}$ as $V'_{AaPw}Pz^{\theta 10}Dz = 0.0003269$, assuming $V'_{AaPw} = 0.0145$, $Dz = 0.004547$, $\theta 10 = 0.916$ and $Pz = 5.743$. This leads to the conclusion that either V'_{AaPw} needs to be adjusted, or the reference rate of $U_{Aa,AaPw}$ (0.0325 where $W_{EB} = 20$kg) is too large. Using the molecular weight of wool of 126.41g/mol from Table 6, the actual amount of wool being produced at this rate would be $0.0003269 \times 365 \times 126.41 = 15.1$ grams per year of protein in wool (as compared to 1.5kg per year with $U_{Aa,AaPw} = 0.0325$, and us-

Variable/ Parameter	**Value** $W_{EB} = 20kg$	**Value** $W_{EB} = 30kg$	**Value** $W_{EB} = 40kg$
Dz (via $U_{Aa,AaPw}$)	0.9616	1.000	0.9998
New V'_{AaPw}	3.067	3.028	3.027
New $\theta 10$	3.979	3.510	3.2558
New k_{AaPw}	-0.002195	-0.002247	-0.002479

Table 14: Derived values of V'_{AaPw}, $\theta 10$ and k_{AaPw} if adjusted to ensure consistent Dz values.

ing $k_{AaPw} = 0.0025$ and $C_{Aa} = 0.002217$). The 15.5 gram figure is clearly too low, and the value of 1.5kg per year for lamb wool production seems reasonable given that adult sheep produce approximately three times this weight in wool per year. (According to the Department of Agriculture, Fisheries and Forestry in the Queensland Government [90], an adult Merino sheep produces about 4.5kg of wool per year in Queensland.) For a 30kg sheep this equates to an upper limit of of 21.1 grams achievable with $V'_{AaPw} = 0.0145$ as compared to 2.1kg per year, and an upper limit of 25.9 grams as compared to 2.7kg per year for a 40kg sheep. Hence the logical conclusion is the adjustment of V'_{AaPw}. Wool growth is further discussed in Section 6.2.

$$U_{Aa,AaPw} = \frac{V'_{AaPw} P z^{\theta 10} Dz}{\left(1 + \frac{k_{AaPw}}{C_{Aa}}\right)}$$

$$\therefore k_{AaPw} = C_{Aa} \left(\frac{V'_{AaPw} P z^{\theta 10} Dz}{U_{Aa,AaPw}} - 1 \right)$$

$$\Rightarrow k_{AaPw_{W_{EB}=20}} = (0.002217) \left(\frac{(0.0145)(5.743)^{0.916}(0.004547)}{0.0325} - 1 \right)$$

$$\therefore k_{AaPw_{W_{EB}=20}} = -0.002195. \tag{85}$$

The value of V'_{AaPw} of Sainz and Wolff's Table 4 [83] is presumably derived via least squares regression, but potentially an incorrect value was presented. For testing purposes, as in Section 4.2.2, the derived V'_{AaPw} for each W_{EB} is used. However, going forward the average of the three values of V'_{AaPw} given in Table 14 (equivalent to an equally weighted least squares fit) will be used for V'_{AaPw} (3.04). This is not dissimilar to the adjusted V'_{AaPw} value of 2.9805 as used by Hon [45], although no explanation of this adjustment was provided in the dissertation.

W_{EB}	Ash Proportion
20	0.07991
30	0.05460
40	0.03174

Table 15: Ash proportions in the dummy empty body weight formula of Equation (86) (4 s.f.).

4.2.2 Testing the Derived Variable Values

The values derived in the Equations of Section 4.2.1, and indeed the implementation of the model structure, was tested by setting the initial conditions of the model to the variable values calculated for $W_{EB} = 20$kg, $W_{EB} = 30$kg and $W_{EB} = 40$kg and running the MISER3.3 program with the optimisation disabled and without a control variable implemented. The state variables and model parameters for this testing simulation were the same as those outlined in Chapter 3 with ODEs as presented in Equations (58) through (65). The simulation was run with a terminal time of zero, such that MISER3.3 would calculate and output the value of the relevant rates using the aforemented model structure. The remaining rate values of Sainz and Wolff's Table 3 [83] (that is, those that are not forced to be equal) were thus checked against the corresponding output rates when $t = 0$ for any discrepancies. In order to achieve this, it was necessary to develop a dummy version of the empty body weight formula (not outlined in Chapter 3) such that the initial empty body weight would be exactly 20kg, 30kg or 40kg, as required. This was determined by making some reasonably small adjustments to the parameters in Equation (68) and simplifying, such that it created the desired empty body weight of 20kg when $Pb = 15.05$, $Pv = 6.84$, $Pz = 5.743$ and $Ts = 3.3073$ (rounded to four decimal places), and likewise for $W_{EB} = 30$kg and $W_{EB} = 40$kg. For simplicity, only the ash proportion is adjusted in each case. The result is given in Equation (86), with ash proportions in Table 15.

$$W_{EB} = \frac{(4.55)(0.124)(Pb + Pv + Pz) + 0.85Ts}{1 - (Ash\ Proportion)}. \tag{86}$$

The Sainz and Wolff [83] Table 3, plus the values of these major rates with the model run using the determined initial conditions, are given in Table 16 for $W_{EB} = 20$kg, Table 17 for $W_{EB} = 30$kg and Table 18 for $W_{EB} = 40$kg.

Term	Definition	Major Rates	Re-produced
A_{Aa}	absorption of amino acids	0.4107	0.4086
A_{Gl}	absorption of glucose	0	0
A_{Tg}	absorption of lipid	0.0085	0.008413
A_{Ac}	absorption of acetate	2.675	2.6632
A_{Pr}	absorption of propionate	1.184	1.177
A_{Bu}	absorption of butyrate	0.4146	0.4131
$U_{Bu,BuCd}$	butyrate oxidation	0.4146	0.4131
$U_{Aa,AaGl}$	gluconeogenesis from amino acids	0.2459	0.2459
$U_{Pr,PrGl}$	gluconeogenesis from propionate	0.3942	0.3920
$U_{La,LaGl}$	gluconeogenesis from lactate	0.2328	0.2327
$U_{Gy,GyGl}$	gluconeogenesis from glycerol	0.1142	0.1141
$U_{Gl,GlTp}$	glucose to triose phosphates	0.3087	0.3087
$U_{Tp,TpLa}$	triose phosphates to lactate	0.4653	0.4653
$U_{La,LaCd}$	lactate oxidation	0.2327	0.2327
$U_{Ac,AcTs}$	lipogenesis from acetate	1.727	1.727
$U_{Ts,TsTg}$	lipolysis of storage fat	0.0525	0.0525
$U_{Tg,TgTs}$	esterification of fatty acids	0.0276	0.0276
$U_{Pb,PbAa}$	carcass protein degradation	0.6020	0.6020
$U_{Pv,PvAa}$	visceral protein degradation	2.052	2.052
$U_{Pz,PzAa}$	'other' protein degradation	0.5743	0.5743
$U_{Aa,AaPb}$	carcass protein synthesis	0.6914	0.6914
$U_{Aa,AaPv}$	visceral protein synthesis	2.028	2.028
$U_{Aa,AaPz}$	'other' protein synthesis	0.5843	0.5843
$U_{Aa,AaPw}$	wool protein synthesis	0.0325	0.0325
$U_{At,carcass}$	undef. energy expenditure in carcass	5.117	5.117
$U_{At,viscera}$	undef. energy expenditure in viscera	13.27	13.27
$U_{At,other}$	undef. energy in other tissues	5.308	5.571
$U_{At,AtAd}$	total ATP hydrolysis	58.33	58.58
$P_{At,AdAt}$	partial ATP production	30.05	29.93
$U_{Gl,GlCd}$	glucose oxidation	0.1268	0.1279
$U_{Tg,TgCd}$	lipid oxidation	0.0340	0.03396
$U_{Ac,AcCd}$	acetate oxidation	1.254	1.2884

Table 16: Sainz and Wolff Table 3 Major Rates W_{EB} = 20kg (from [83] and reproduced).

Term	Definition	Major Rates	Re-produced
A_{Aa}	absorption of amino acids	0.5505	0.5538
A_{Gl}	absorption of glucose	0	0
A_{Tg}	absorption of lipid	0.0113	0.0114
A_{Ac}	absorption of acetate	3.587	3.610
A_{Pr}	absorption of propionate	1.587	1.596
A_{Bu}	absorption of butyrate	0.5558	0.5599
$U_{Bu,BuCd}$	butyrate oxidation	0.5558	0.5599
$U_{Aa,AaGl}$	gluconeogenesis from amino acids	0.3220	0.3220
$U_{Pr,PrGl}$	gluconeogenesis from propionate	0.5286	0.5314
$U_{La,LaGl}$	gluconeogenesis from lactate	0.3664	0.3663
$U_{Gy,GyGl}$	gluconeogenesis from glycerol	0.1568	0.1564
$U_{Gl,GlTp}$	glucose to triose phosphates	0.4708	0.4708
$U_{Tp,TpLa}$	triose phosphates to lactate	0.7327	0.7327
$U_{La,LaCd}$	lactate oxidation	0.3663	0.3663
$U_{Ac,AcTs}$	lipogenesis from acetate	2.336	2.336
$U_{Ts,TsTg}$	lipolysis of storage fat	0.0732	0.0732
$U_{Tg,TgTs}$	esterification of fatty acids	0.0384	0.0384
$U_{Pb,PbAa}$	carcass protein degradation	0.9200	0.9200
$U_{Pv,PvAa}$	visceral protein degradation	2.557	2.557
$U_{Pz,PzAa}$	'other' protein degradation	0.7837	0.7837
$U_{Aa,AaPb}$	carcass protein synthesis	1.043	1.043
$U_{Aa,AaPv}$	visceral protein synthesis	2.586	2.586
$U_{Aa,AaPz}$	'other' protein synthesis	0.8127	0.8127
$U_{Aa,AaPw}$	wool protein synthesis	0.0455	0.0455
$U_{At,carcass}$	undef. energy expenditure in carcass	7.820	7.820
$U_{At,viscera}$	undef. energy expenditure in viscera	16.53	16.54
$U_{At,other}$	undef. energy in other tissues	7.602	7.602
$U_{At,AtAd}$	total ATP hydrolysis	78.95	78.96
$P_{At,AdAt}$	partial ATP production	41.46	41.65
$U_{Gl,GlCd}$	glucose oxidation	0.1675	0.1675
$U_{Tg,TgCd}$	lipid oxidation	0.0452	0.04475
$U_{Ac,AcCd}$	acetate oxidation	1.661	1.657

Table 17: Sainz and Wolff Table 3 Major Rates W_{EB} = 30kg (from [83] and reproduced).

Term	Definition	Major Rates	Re-produced
A_{Aa}	absorption of amino acids	0.6928	0.6871
A_{Gl}	absorption of glucose	0	0
A_{Tg}	absorption of lipid	0.0143	0.01415
A_{Ac}	absorption of acetate	4.514	4.479
A_{Pr}	absorption of propionate	1.998	1.980
A_{Bu}	absorption of butyrate	0.6995	0.6948
$U_{Bu,BuCd}$	butyrate oxidation	0.6995	0.6948
$U_{Aa,AaGl}$	gluconeogenesis from amino acids	0.4718	0.4718
$U_{Pr,PrGl}$	gluconeogenesis from propionate	0.6652	0.6593
$U_{La,LaGl}$	gluconeogenesis from lactate	0.5100	0.5096
$U_{Gy,GyGl}$	gluconeogenesis from glycerol	0.1942	0.1945
$U_{Gl,GlTp}$	glucose to triose phosphates	0.6421	0.6421
$U_{Tp,TpLa}$	triose phosphates to lactate	1.109	1.019
$U_{La,LaCd}$	lactate oxidation	0.5097	0.5096
$U_{Ac,AcTs}$	lipogenesis from acetate	3.012	3.012
$U_{Ts,TsTg}$	lipolysis of storage fat	0.0904	0.0904
$U_{Tg,TgTs}$	esterification of fatty acids	0.0490	0.0490
$U_{Pb,PbAa}$	carcass protein degradation	1.252	01.252
$U_{Pv,PvAa}$	visceral protein degradation	3.090	3.090
$U_{Pz,PzAa}$	'other' protein degradation	0.9803	0.9803
$U_{Aa,AaPb}$	carcass protein synthesis	1.361	1.361
$U_{Aa,AaPv}$	visceral protein synthesis	3.113	3.113
$U_{Aa,AaPz}$	'other' protein synthesis	1.008	1.008
$U_{Aa,AaPw}$	wool protein synthesis	0.0587	0.0587
$U_{At,carcass}$	undef. energy expenditure in carcass	10.639	10.642
$U_{At,viscera}$	undef. energy expenditure in viscera	19.98	19.98
$U_{At,other}$	undef. energy in other tissues	9.509	9.509
$U_{At,AtAd}$	total ATP hydrolysis	99.50	99.57
$P_{At,AdAt}$	partial ATP production	53.49	53.17
$U_{Gl,GlCd}$	glucose oxidation	0.2078	0.2096
$U_{Tg,TgCd}$	lipid oxidation	0.0550	0.05509
$U_{Ac,AcCd}$	acetate oxidation	2.046	2.075

Table 18: Sainz and Wolff Table 3 Major Rates W_{EB} = 40kg (from [83] and reproduced).

There are some small differences between the major rates values presented here. However, these are partially due to the initial conditions being determined directly from the values of Tables 3 and 4 in Sainz and Wolff [83], which are highly likely to be rounded figures. This effect can be investigated by further examining the discrepancies of Table 16. For example, we note that A_{Aa} has an initial rate of 0.4107 in Table 3 from Sainz and Wolff [83], yet when reproduced it has a value of 0.4086. The formula governing A_{Aa} is given in Equation (87), where we can see that it has a direct relationship with the empty body weight and model parameters F_{intake} (feed intake as a multiple of maintanence) and D_{Aa} (parameter determining absorption rate of Aa). The initial empty body weight is fixed at 20kg, and F_{intake} is set at 1.6, assuming this is not a rounded figure as only one decimal place is presented, this indicates that perhaps the value of D_{Aa} of 0.027 is a rounded figure, and the cause for the discrepancy in A_{Aa} seen in Table 16. If the value of A_{Aa} rounds to 0.4107, then this implies that $D_{Aa} = 0.02714$, rounded to four significant figures. However, there are some cases where rounding cannot completely explain the discrepancies, and the effect of a least squares fit is present. An example is where D_{Tg} is given as 0.000556 and A_{Tg} as 0.0085. For D_{Tg} to round to 0.000556, then $0.000555 < D_{Tg} < 0.0005565$ and hence $0.008406 < A_{Tg} < 0.008421$. Therefore A_{Tg} could not round to 0.0085. In cases like these it is difficult to determine which is the most accurate representation of D_{Tg} and A_{Tg}.

$$A_{Aa} = F_{intake} D_{Aa} W_{EB}^{0.75}. \tag{87}$$

Some consideration was given to possibly investigating further what portion of the discrepancies between the initial rates reproduced, and those presented by Sainz and Wolff [83] could be attributed to rounding error. However, the discrepancies themselves are of such a small magnitude that there is unlikely to be any contributing factor other than rounding and the least squares approach. Also, there has been inconsistent rounding applied to Table 3 of Sainz and Wolff [83], and without an assumption of consistent rounding, it would be difficult to quantify. For example, the rates of $U_{La,LaGl}$ and $U_{La,LaCd}$ should be identical, since they are both defined as $0.5P_{La,TpLa}$. However, for the $W_{EB} = 40$kg case in Table 3, Sainz and Wolff have rounded $U_{La,LaGl}$ to two significant figures (0.51), whereas $U_{La,LaCd}$ is rounded to four significant figures (0.5097). It is also suspected that there are typographical errors in the data of Table 3, such as in the case of $U_{Tp,TpLa}$, which is reproduced precisely for the $W_{EB} = 20$kg and $W_{EB} = 30$kg case, but for the $W_{EB} = 40$kg case Table 3 has a value of 1.109, whereas the reproduced value is 1.019. If this rate, and the rates that are forced to be equal

to the reproduced figures are excluded, the average differences between the Table 3 rates and the reproduced rates across the empty body weights ranges from -0.4% through to 1.65%, with an average overall difference of just 0.08%. Therefore it can be concluded that the state variable values used by Sainz and Wolff [83] have been derived with an acceptable level of accuracy. This result also gives a strong indication that the model structure, as outlined in Chapter 3, has been reproduced accurately in the Fortran code of MISER3.3.

The state variable values derived from Sainz and Wolff [83] for a $W_{EB} =$ 20kg sheep, as given in Table 13, would not produce 20kg of empty body weight using Equation (68), nor would they match the 16.5% body protein and 14% body fat proportions as described in Section 4.2 using the derived molecular weights in Equation (68). Using Equation (68), the initial empty body weight would be 19.2kg, with 3.38kg (17.7%) body protein and 2.82kg (14.7%) body fat. This is very similar to the result in Section 4.2 for the initial conditions of Hon [45] after lowering the body fat to 2.85kg, although the split between protein in carcass, viscera and other tissues is slightly different. Therefore to prepare for the potential use of the 20kg state variable values derived from Sainz and Wolff [83] as initial conditions for the model, an overall scaling factor of 1.043 will be applied to both the protein and the storage fat variables, such that the empty body weight is precisely 20kg. Again, at this stage, initial conditions for the other state variables will not be adjusted, as this would be purely speculative.

4.3 The Model Derivatives

Whilst the model structure used by Sainz and Wolff [83], presented in Chapter 3, seems to have been coded correctly, in order to take advantage of the optimisation functionality of MISER3.3 [48], derivatives of the right-hand sides of the differential equations for the state variables (Equations (58) through (65)) are required. These derivatives are used to solve the costate equations and the costate values are used to calculate gradients of the objective and constraints functionals. These gradients, in turn, are required to solve the mathematical programming problem which arises when solving the optimal control and parameter selection problems. This issue of having to enter derivatives explicitly into the MISER3.3 code was addressed by Hon [45]. It was discussed here that the Jacobian of the dynamics, $\left[\frac{\partial f_i}{\partial x_j}\right]$, $i = 1, \ldots, n$, $j = 1, \ldots, n$, is non sparse, and many of its elements are very tedious to derive. The twelve state equations are determined from a complicated mixture of 84 parameters and 83 supplementary variables, as well as the twelve state variables. The details of the state equations are given in Chapter 3.

State Variable	**Initial Value (Moles)**	**Initial Value (kg)**	**Initial Value Adj. (kg)**	**Initial Value Adj. (Moles)**
Amino Acid (Aa)	0.01064	-	-	0.01064
Glucose (Gl)	0.01429	-	-	0.01429
Lipids (Tg)	0.01120	-	-	0.01120
Acetate (Ac)	0.004925	-	-	0.004925
Protein (Carcass) (Pb)	15.05	1.836	1.916	15.7038
Protein (Viscera) (Pv)	6.84	0.8482	0.8850	7.1371
Protein (Other Tissues) (Pz)	5.743	0.7006	0.7311	5.9925
Protein (Wool) (Pw)	0	0	0	0
Storage Triacylglycerol (Ts)	3.307	2.8178	2.9402	3.4509
DNA (Carcass) (Db)	0.006162	-	-	0.006162
DNA (Viscera) (Dv)	0.007663	-	-	0.007663
DNA (Other Tissues) (Dz)	0.004547	-	-	0.004547

Table 19: Review of initial state variable values (20kg empty body weight) estimated from Sainz and Wolff [83].

Whilst Hon [45] made some progress, a match between the entries of the Jacobian and MISER3.3's inbuilt numerical derivative check was not achieved. Some errors were not resolved, and in using the code produced by Hon, MISER3.3's internal derivative check showed significant to severe discrepancies in over 40 of the 144 Jacobian entries, with an unacceptable maximum error of 2.0977×10^6. Hon [45] suggested that a more efficient approach may have been to use an automatic differentiation software package such as ADIFOR [19], but due to delays in obtaining a copy of the software, it was not investigated further. The work of Hon [45] was expanded on by Ramsey [78] in which ADIFOR [19] was utilised to determine the Jacobian matrix. With this in place, MISER3.3's internal derivative check showed up similarly severe discrepancies. Although these only appeared in 13 of the Jacobian entries (maximum error not given), it was still unacceptable. Ramsey [78] concluded that these errors were likely due to limitations in the ADIFOR code.

It was decided for this work that satisfactory results from the derivative check were more likely to be obtained by editing the original, manually developed derivatives. This was an immense task, and after no less than fifteen major revisions of the code there were only minor discrepancies in six of the Jacobian entries with the maximum error at 7.6×10^{-6}. With some errors to be attributed to numerical noise in MISER3.3's own derivative check, this was accepted as workable. An example of the manual derivative task is given in Section 4.3.1.

4.3.1 Glucose Example

To gain insight into the nature of these derivatives, circulating glucose is used as an example to examine in depth. Let us focus on the equation governing glucose conversion to triose phosphates ($U_{Gl,GlTp}$) from Section 3.2. We start by fully expanding the definition of $U_{Gl,GlTp}$ so that it is only expressed in terms of input parameters and state variables, see Equation (88). Secondly, substituting in parameter values and simplifying gives the resulting Equation (89).

Using the initial values of the sheep and varying only one state variable from the $U_{Gl,GlTp}$ equation at a time we have the relationships displayed in Figures 13 – 17. These Figures show the nonlinearity in the relationship between the initial values and the example reaction rate $U_{Gl,GlTp}$, and indicate the complexity of the analytic user gradients required for the control parameterisation method. These Figures also outline an example of sensitivity of initial rates of utilisation to the initial values of state variables.

$$U_{Gl,GlTp} = \frac{V_{GlTp}}{\left(1+\frac{k_{GlTp}}{C_{Gl}}\right)} = \frac{V'_{GlTp}Pb^{\theta 2}}{\left(1+\frac{k_{GlTp}}{C_{Gl}}\right)} = \frac{V'_{GlTp}Pb^{\theta 2}}{\left(1+\frac{\left(\frac{k'_{GlTp}}{H_A}\right)}{C_{Gl}}\right)}$$

$$= \frac{V'_{GlTp}Pb^{\theta 2}}{\left(1+\frac{\left(\frac{k'_{GlTp}}{H_A}\right)}{\left(\frac{Gl}{v_{ECF}}\right)}\right)} = \frac{V'_{GlTp}Pb^{\theta 2}}{\left(1+\frac{k'_{GlTp}v_{ECF}}{H_A Gl}\right)} = \frac{V'_{GlTp}Pb^{\theta 2}}{\left(1+\frac{k'_{GlTp}v_{ECF}}{\left(\frac{C_{Gl}}{C_{Gl,ref}}\right)^2 Gl}\right)}$$

$$= \frac{V'_{GlTp}Pb^{\theta 2}}{\left(1+\frac{k'_{GlTp}v_{ECF}C^2_{Gl,ref}}{C^2_{Gl}Gl}\right)} = \frac{V'_{GlTp}Pb^{\theta 2}}{\left(1+\frac{k'_{GlTp}v_{ECF}C^2_{Gl,ref}}{\left(\frac{Gl}{v_{ECF}}\right)^2 Gl}\right)} \tag{88}$$

$$= \frac{V'_{GlTp}Pb^{\theta 2}}{\left(1+\frac{k'_{GlTp}v^3_{ECF}C^2_{Gl,ref}}{Gl^3}\right)} = \frac{V'_{GlTp}Pb^{\theta 2}Gl^3}{\left(Gl^3+k'_{GlTp}v^3_{ECF}C^2_{Gl,ref}\right)}$$

$$\therefore \frac{V'_{GlTp}Pb^{\theta 2}Gl^3}{U_{Gl,GlTp}} = Gl^3 +$$

$$k'_{GlTp}\left(0.24\left(\frac{4.547\left(0.122Pb+0.124Pv+0.122Pz\right)+0.852Ts}{0.95}\right)\right)^3 C^2_{Gl,ref}.$$

$$\frac{0.0415PbGl^3}{U_{Gl,GlTp}} = Gl^3 +$$

$$\left(0.24\left(\frac{4.547\left(0.122Pb+0.124Pv+0.122Pz\right)+0.852Ts}{0.95}\right)\right)^3 (0.003)^3$$

$$= Gl^3 + \left(4.547\left(0.122Pb+0.124Pv+0.122Pz\right)+0.852Ts\right)^3 \times$$

$$(0.003)^3 (0.24)^3 (0.95)^{-3}. \tag{89}$$

The glucose example given here covers $U_{Gl,GlTp}$, however, to fully define $\frac{dGl}{dt}$ we also require A_{Gl}, $P_{Gl,AaGl}$, $P_{Gl,PrGL}$, $P_{Gl,LaGl}$, $P_{Gl,GyGl}$ and $U_{Gl,GlCd}$ to be defined. This is entered in the Fortran code for MISER3.3 via supplementary variables, which are then combined to produce an overall definition of $\frac{dGl}{dt}$ (see Equation (59)). Similarly derivatives with respect to each state variable have been determined manually for each of the supplementary variables, and are also then combined to produce the derivatives of the dynamic equations, as required for the implementation into MISER3.3. Whilst inclusion of full documentation of this process here is not appropriate, it should be reiterated that this was a substantial amount of work, and provided a signiciant step forward from previous

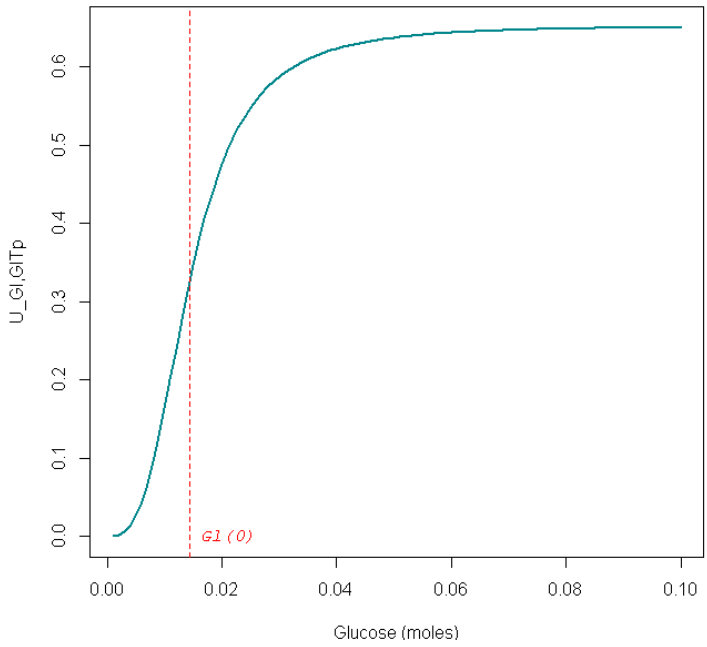

Figure 13: Initial $U_{Gl,GlTp}$ versus glucose.

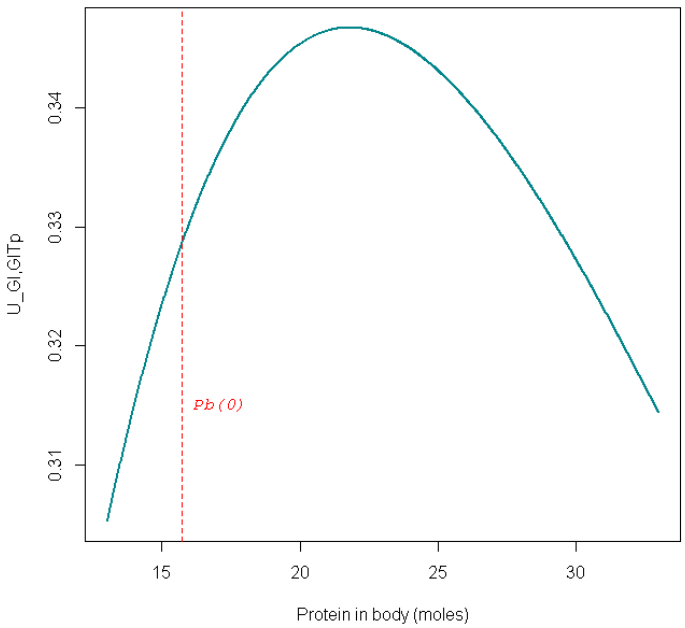

Figure 14: Initial $U_{Gl,GlTp}$ versus carcass protein.

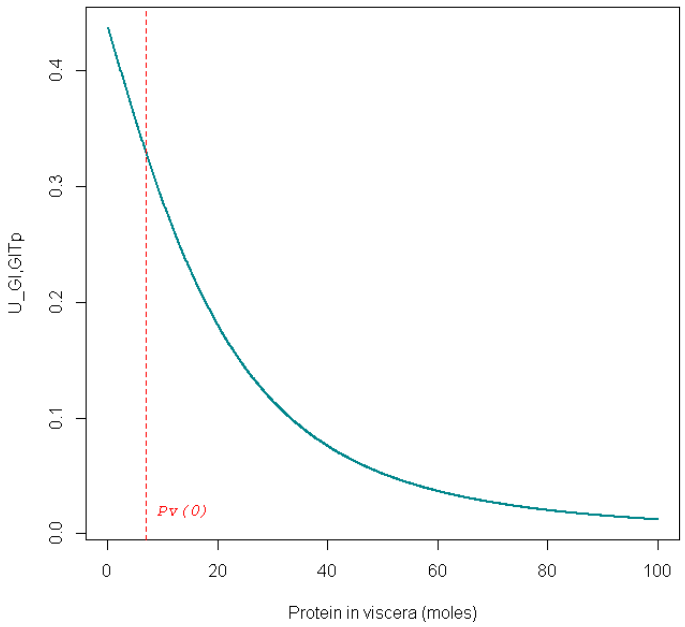

Figure 15: Initial $U_{Gl,GITp}$ versus viscera protein.

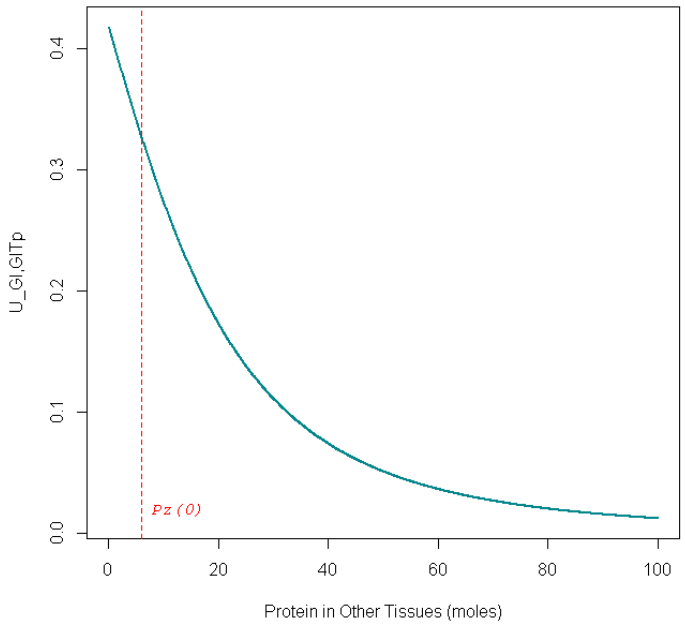

Figure 16: Initial $U_{Gl,GITp}$ versus other tissues protein.

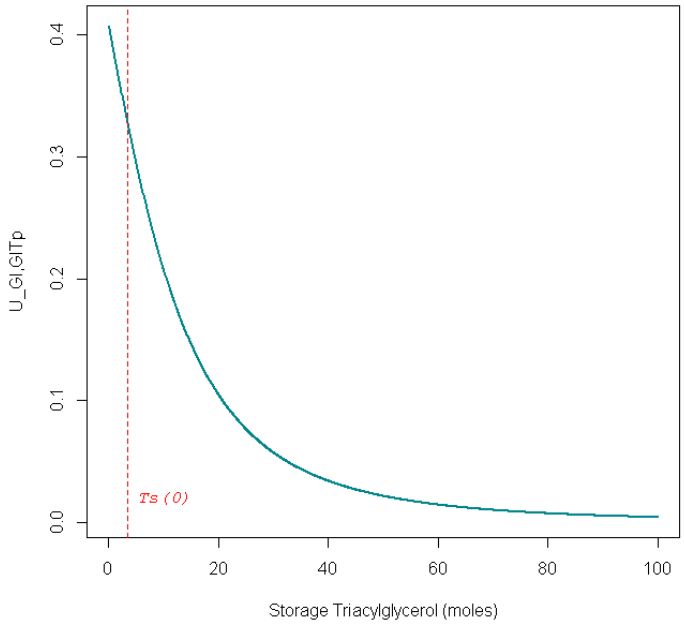

Figure 17: Initial $U_{Gl,GlTp}$ versus storage triacylglycerol.

work, where a functional MISER3.3 model was not able to be produced (Hon [45] and Ramsey [78]). The maximum error identified in MISER3.3's internal derivative check using the code previously developed was 2.0977×10^6. The components of $[\partial f_i/\partial x_j]$ were refined iteratively, resulting in a maximum error of 7.6×10^{-6}, which is assumed negligible when considering inaccuracies are present in the internal derviative check itself (being a numerical procedure). Further detail is provided in the MISER3.3 output regarding the proportion of each of the 1,012 quadrature points assessed for each state dynamic and state variable combination for which a discrepancy has been identified in the user defined derivatives, and therefore it is possible to assess which Jacobian derivatives were improved upon in each adjustment to the code. This process is outlined in Table 20.

There may still be issues with errors in the Jacobian matrix, which can become more prominent when system parameters change during an optimisation process. This can lead to poor convergence to an optimal solution for the optimisation routine built into the MISER3.3 code. It is hoped that future refinements of MISER3.3, the model itself, or processing power may help resolve these issues. However, the Jacobian presently coded into the software does allow for significant progress in the simulation and optimisation of the model.

Iteration	Max. Error	Derivatives Refined
0	2.1×10^6	NA
1	207	df_{Ts}/dAc
2	207	df_{Ts}/dGl, df_{Ts}/dPz, df_{Ts}/dTs
3	207	df_{Gl}/dPz
4	207	df_{Gl}/dPz, df_{Tg}/dPz, df_{Ac}/dPz
5	172	df_{Gl}/dAa, df_{Gl}/dDx, df_{Tg}/dAa, df_{Tg}/dDx
6	26.4	df_{Ac}/dAa, df_{Ac}/dDx
7	26.4	df_{Pv}/dAa, df_{Aa}/dTg, df_{Ac}/dTs
8	0.069	df_{Gl}/dTg, df_{Gl}/dPz, df_{Gl}/dTs, df_{Tg}/dTg, df_{Tg}/dPz, df_{Tg}/dTs, df_{Ac}/dTg
9	0.069	df_{Gl}/dPb, df_{Gl}/dPv, df_{Tg}/dPb, df_{Tg}/dPv, df_{Ts}/dPb, df_{Ts}/dPv
10	2.5×10^{-4}	df_{Gl}/dGl, df_{Gl}/dAc, df_{Tg}/dAc, df_{Ac}/dTg, df_{Ac}/dGl, df_{Ac}/dPx, df_{Ac}/dTs
11	7.6×10^{-6}	df_{Ac}/dAc

Table 20: Details of refinements of user defined df_i/dx_j derivatives and subsequent maximum error for each iteration.Note that Dx represents Db, Dv and Dz collectively.

5 Review of Initial Conditions

The first step in running the model was to replicate the 20kg to 40kg empty body weight growth that the Sainz and Wolff [83] model was designed to represent. To achieve this, the code was adjusted to incoporate the empty body weight equation (Equation (68)) and the initial conditions in Table 12 and Table 19 were implemented in the data inputs. Growth was simulated by running the model (as outlined in Chapter 3) through MISER3.3 with the optimisation disabled and without a control variable. The resulting growth trajectories were analysed, and the initial conditions revised appropriately. Figure 2 in Sainz and Wolff [83] indicates that the simulated sheep should reach an empty body weight of 40kg from 20kg in approximately 20 weeks time (aged 12 weeks through 32 weeks). Therefore the terminal time (t_{final}) was set to 140 days. V'_{AaPw} was set to the average of the adjusted values presented in Table 14 (3.04). The initial conditions as given in Hon [45] are reviewed in Section 5.1, and those derived from the Sainz and Wolff paper [83] in Section 4.2.1, are reviewed in Section 5.2. Subsequent conclusions are given in Section 5.3. Note that the initial condition for protein in wool is discussed in Section 6.2 and is not directly addressed here. There is no feedback of Pw back into the differential equations governing growth (Equations (58) through (65)), therefore it will not affect the review of other initial conditions.

5.1 Initial Conditions as Derived from Hon [45]

The derived initial state variable values from Hon [45], as presented in Table 12, were implemented in the simulation with MISER3.3. Equation (68) was used to define empty body weight, and V'_{AaPw} was set to the average of the adjusted values presented in Table 14 (3.04). Plots of the state variables by sheep age (in weeks) are given in Figures 18, 19 and 20. It seems as though the model is correcting levels of amino acids, glucose, lipids and acetate in the initial stages of the simulation, with tick-like patterns visible in Figure 18. The Sainz and Wolff [83] model appears to be quite sensitive to the initial conditions, and therefore it follows that these should be adjusted such that natural growth patterns can be replicated. This will also reduce the burden on the model for correcting proportions before commencing natural growth. Results for the first four days of the simulation are plotted in Figures 21, 22, 23 and 24 to look closer at what is happening in the initial stages. Note that similar plots for the other state variables are provided in Figures 74 and 75 of Appendix C, as confirmation that this tick-like effect was not present for these variables. For amino acids, glucose and acetate, there is a sharp jump or drop between the preliminary initial condition and the first simulated value, then it flows through a turning point before continuing into a natural looking growth pattern. For lipids, the starting drop is more spread out amongst the first few simulated values. This effect is likely a result of instability in the initial values of the anabolic and catabolic hormonal controls (H_A and H_C), which are presented in Figure 25. The hormonal controls are factors affecting the growth of amino acids, glucose, lipids and acetate and are based on the relationship between the current concentration of glucose in circulating fluids, and the reference concentration. It is assumed that the initial glucose level, and the relative level of amino acids, lipids and acetate, need revision to stabilise the model and proceed accordingly.

For amino acids, glucose, lipids and acetate, by 1.5 days into the simulation the growth trajectories have stabilised. At this point, the proportions of the state variables may be considered to be appropriate. This point is indicated by the dashed line in Figures 18, 19 and 20. Whilst it is only amino acids, glucose, lipids and acetate that exhibit this strange growth trajectory, for consistency the initial conditions for all state variables will be adjusted to match their values after 1.5 days of simulated growth, and then scaled back proportionately such that the empty body weight remains at 20kg at $t = 0$ according to Equation (68). This implicitly assumes linear growth in the other state variables from 12 weeks to 12 weeks and 1.5 days of age, but due to this being a very short period of time, and the uncertainty in the initial conditions and the empty body weight equation,

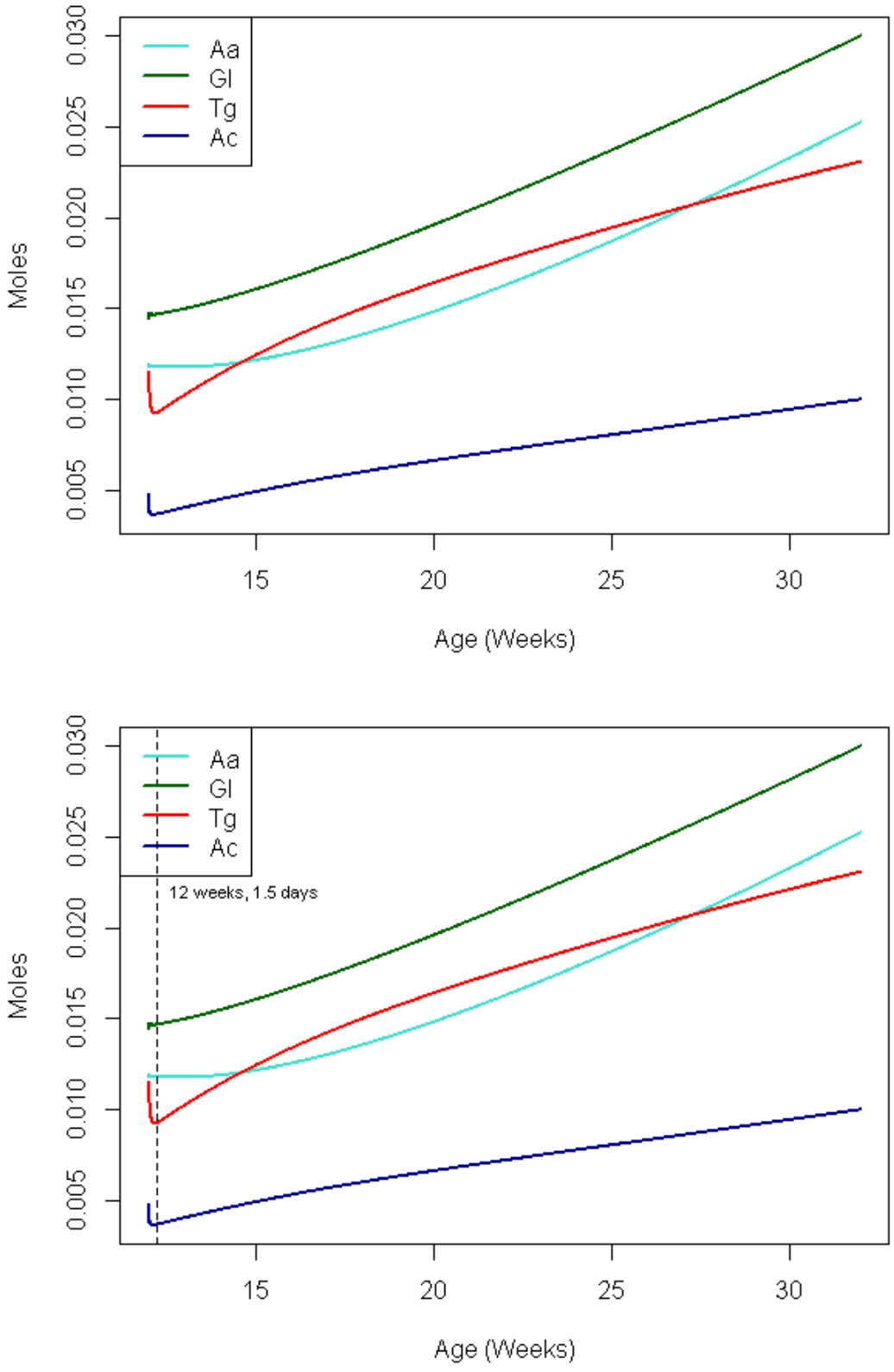

Figure 18: Circulating amino acids (Aa), glucose (Gl), lipids (Tg) and acetate (Ac), using preliminary initial conditions derived from Hon [45].

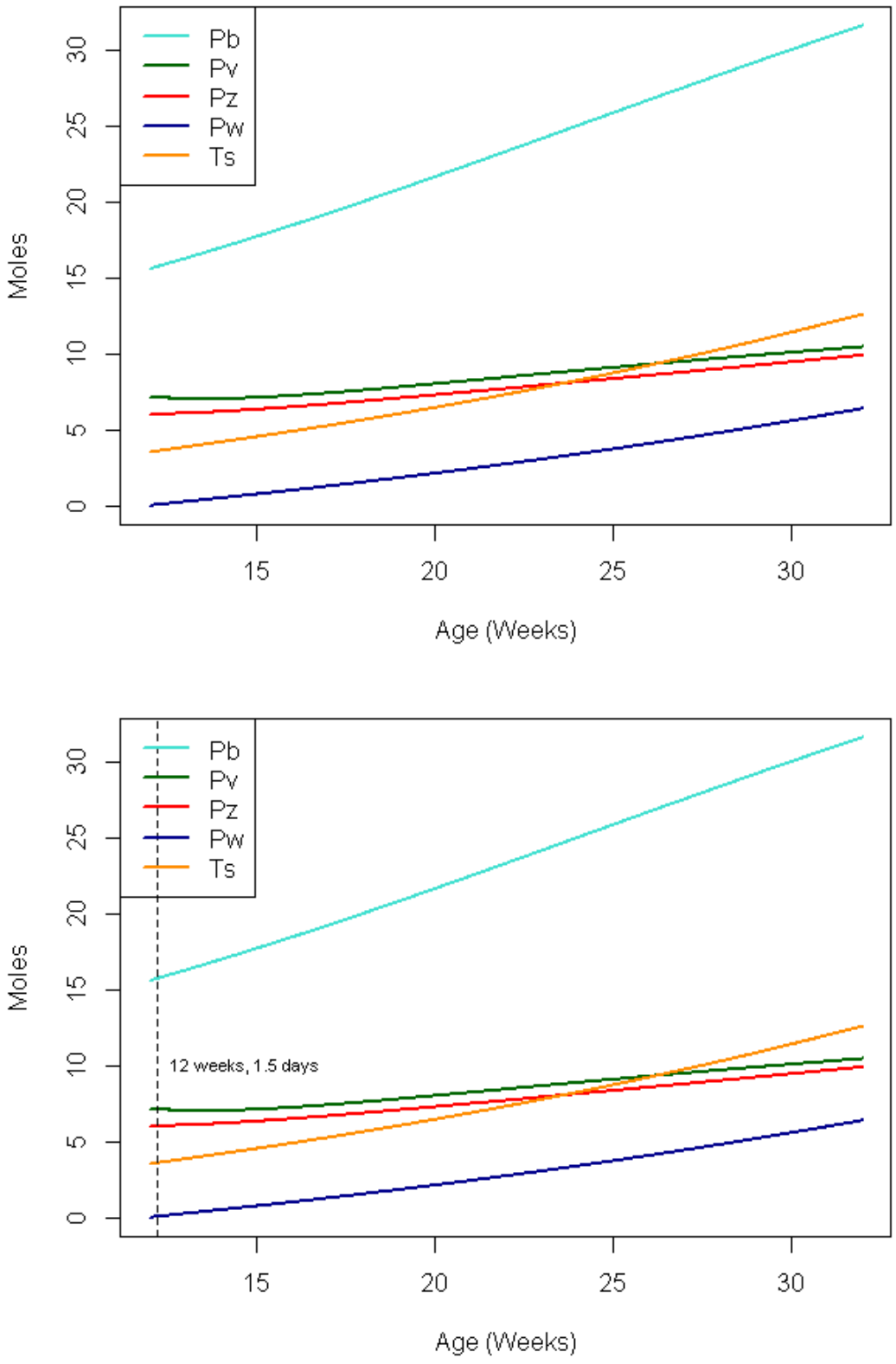

Figure 19: Protein in carcass (Pb), viscera (Pv), other tissues (Pz) and wool (Pw), and storage triacylglycerol (Ts), using preliminary initial conditions derived from Hon [45].

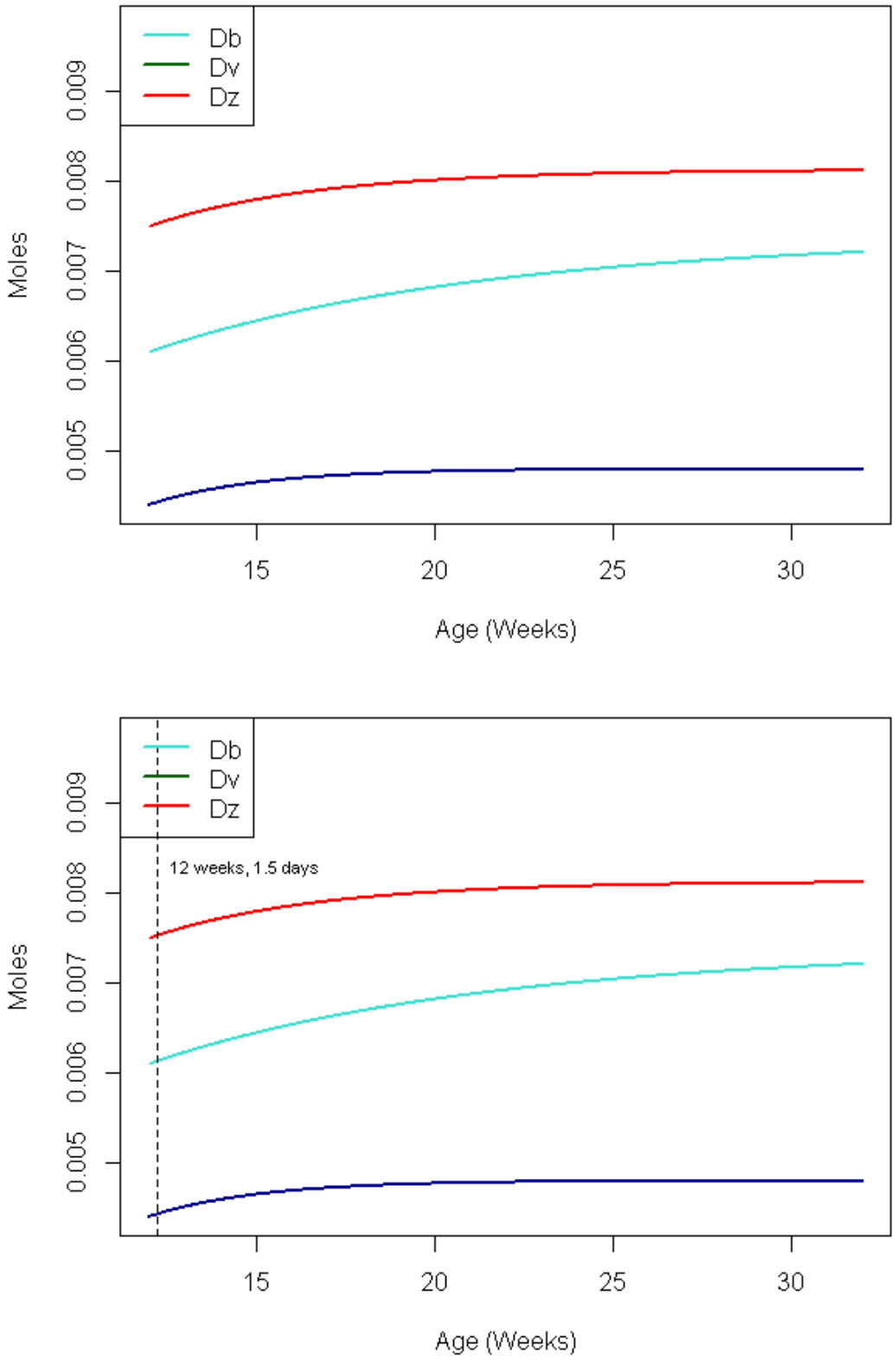

Figure 20: DNA pools Corresponding to carcass (Db), viscera (Dv) and other tissues (Dz), using preliminary initial conditions derived from Hon [45].

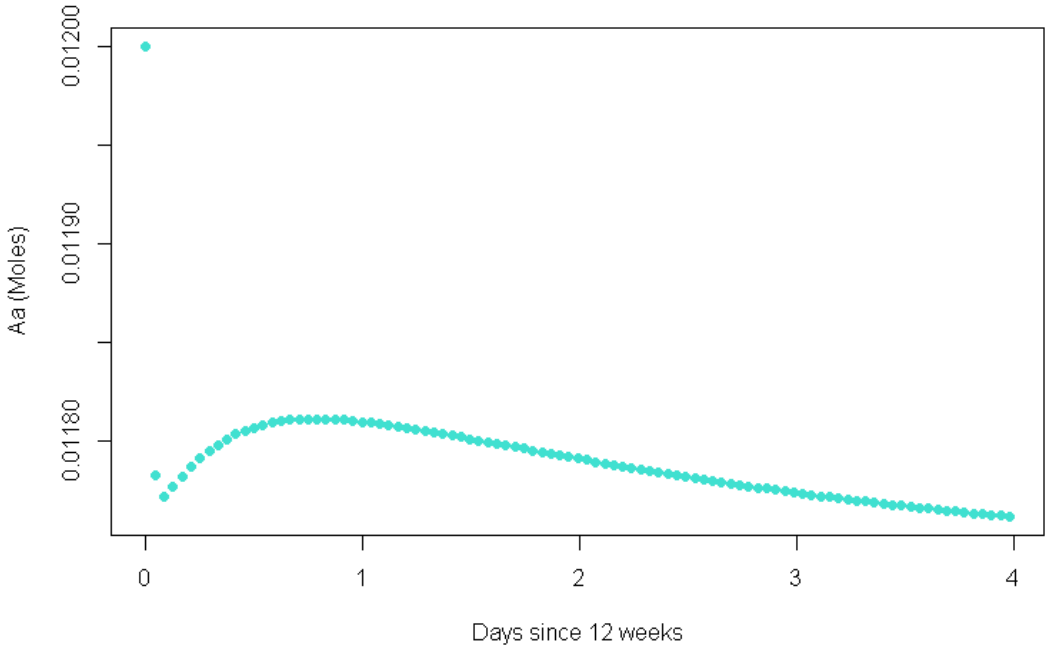

Figure 21: Amino acids (Aa) over first four days of simulation, using preliminary initial conditions derived from Hon [45].

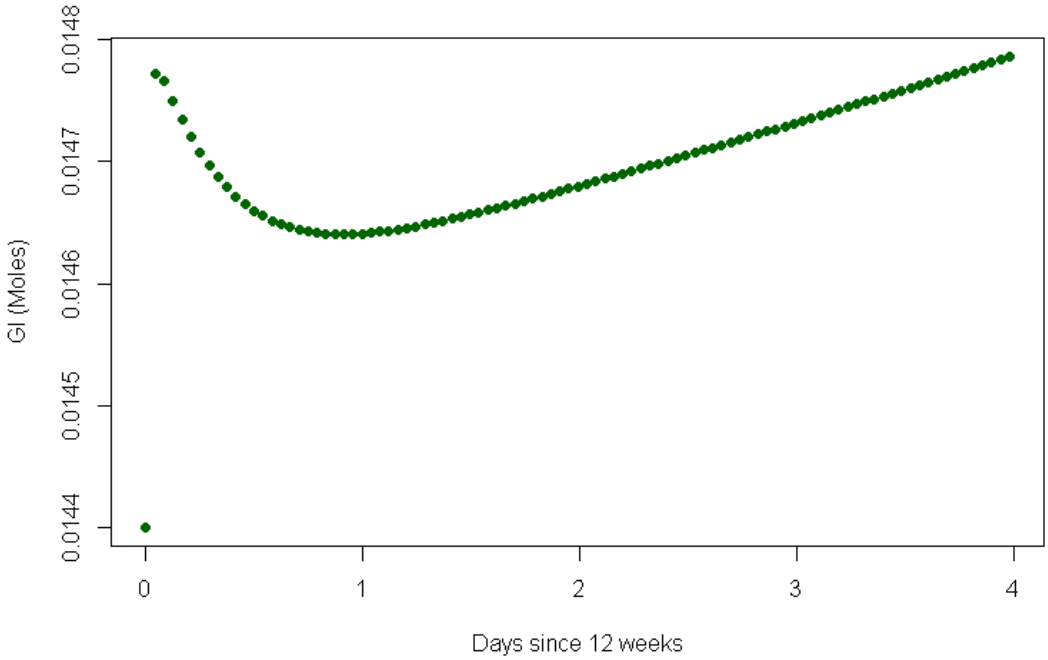

Figure 22: Glucose (Gl) over first four days of simulation, using preliminary initial conditions derived from Hon [45].

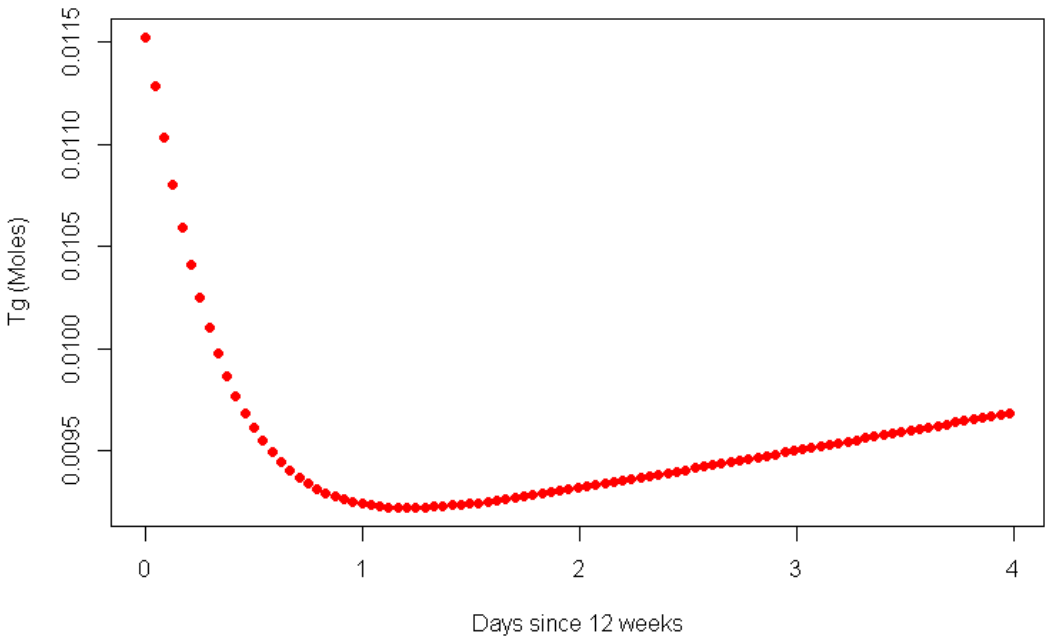

Figure 23: Lipids (Tg) over first four days of simulation, using preliminary initial conditions derived from Hon [45].

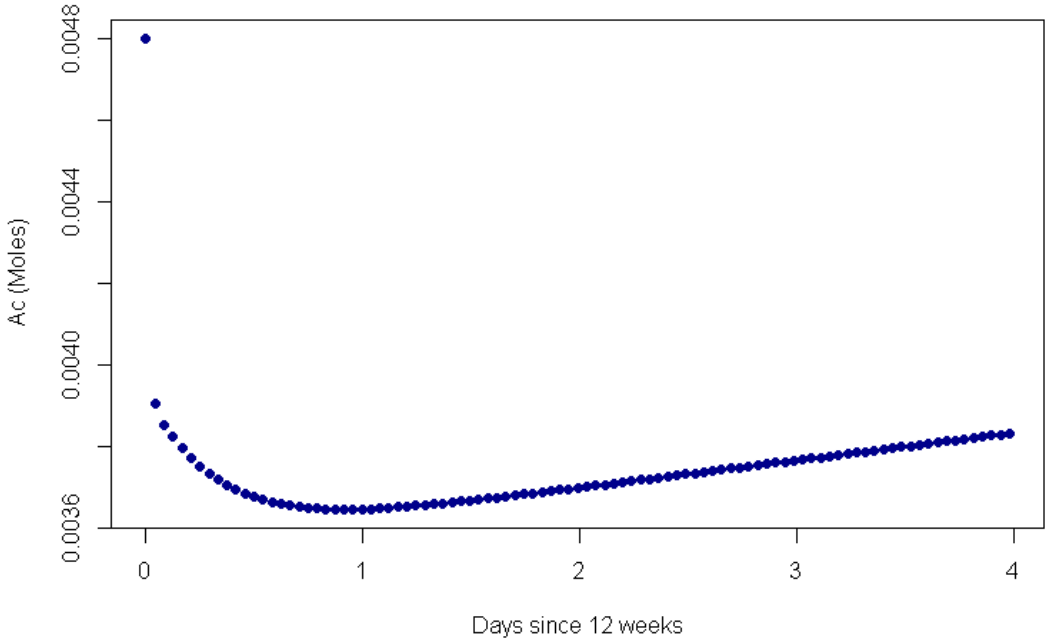

Figure 24: Acetate (Ac) over first four days of simulation, using preliminary initial conditions derived from Hon [45].

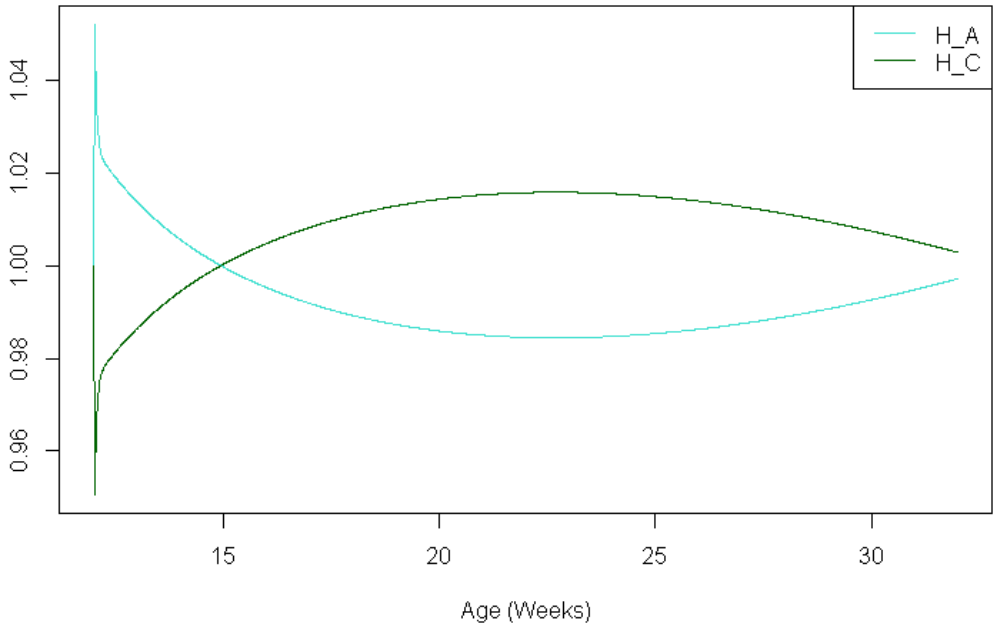

Figure 25: Anabolic (H_A) and catabolic (H_C) hormonal controls, using preliminary initial conditions derived from Hon [45].

this is deemed an acceptable assumption. It is not refuted by the plots of the other state variables in Figures 74 and 75 of Appendix C. Whilst the model is continuous, data can only be extracted at a finite number of points. The output taken nearest to 1.5 days is where the model time is equal to $t = 1.4924$ days, therefore $\mathbf{x}_{t=1.4924}$ is used to determine draft revised initial conditions. Details are presented in Table 21. Note that this adjustment has not substantially altered the body protein to body fat ratio that was imposed in Section 4.2.

The model was run again with the draft revised initial conditions (from Table 21), and whilst the tick effect was certainly reduced, there was still some evidence of it for amino acids, glucose, lipids and acetate. Results for these variables for the first four days of the simulation using the draft revised initial conditions are given in Figures 26, 27, 28 and 29. It can be seen that there is still an issue of a sharp initial jump for amino acids, and a slight jump for glucose. There is some instability in the initial few points, but the turning points are now negligible. There is only one turning point apparent at the start of the period for lipids in Figure 28. Not surprisingly, there is still some apparent instability in the initial values of the hormonal controls, as shown in Figure 30.

State Variable	Initial Conditions (Preliminary)	Value at $t = 1.4924$	Initial Conditions (Revised)
Aa	0.012	0.0118	0.01173
Gl	0.0144	0.01466	0.01456
Tg	0.01152	9.2433×10^{-3}	9.1841×10^{-3}
Ac	4.8×10^{-3}	3.6671×10^{-3}	3.6436×10^{-3}
Pb	15.57429	15.71889	15.61826
Pv	7.16055	7.12178	7.07618
Pz	6.01214	6.01904	5.9805
Pw	0	0.0513	0.05097
Ts	3.50699	3.5777	3.55479
Db	6.1×10^{-3}	6.129×10^{-3}	6.0897×10^{-3}
Dv	7.5×10^{-3}	7.5284×10^{-3}	7.4802×10^{-3}
Dz	4.4×10^{-3}	4.4267×10^{-3}	4.3984×10^{-3}
EBW (kg)	20.00	20.1283	20.00

Table 21: Revision of preliminary initial conditions derived from Hon [45].

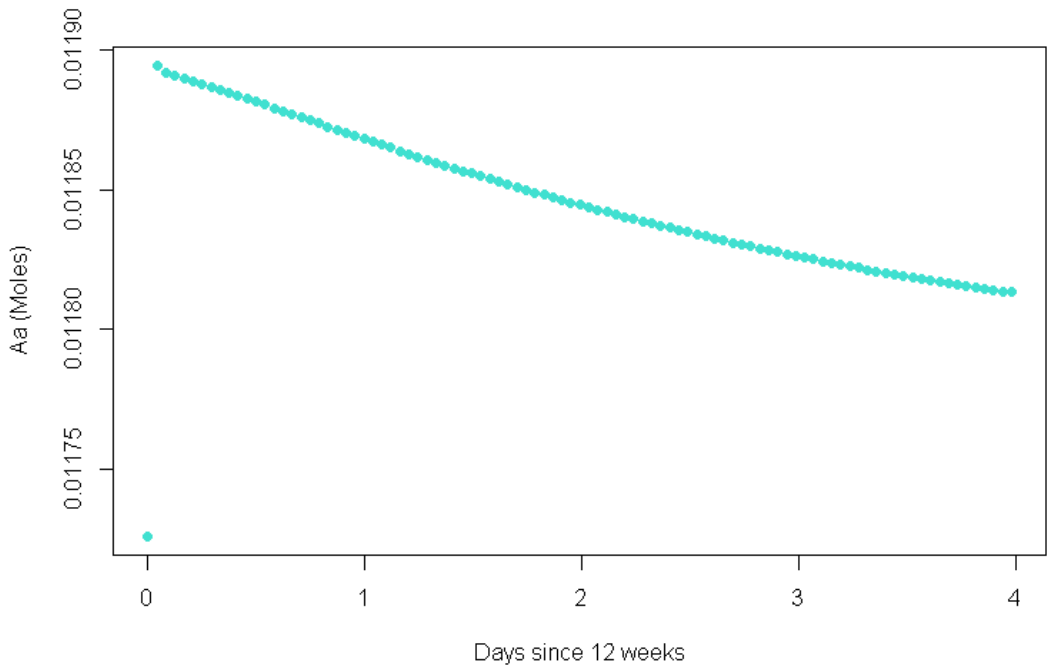

Figure 26: Amino acids (Aa) over first four days of simulation, using draft revised initial conditions derived from Hon [45].

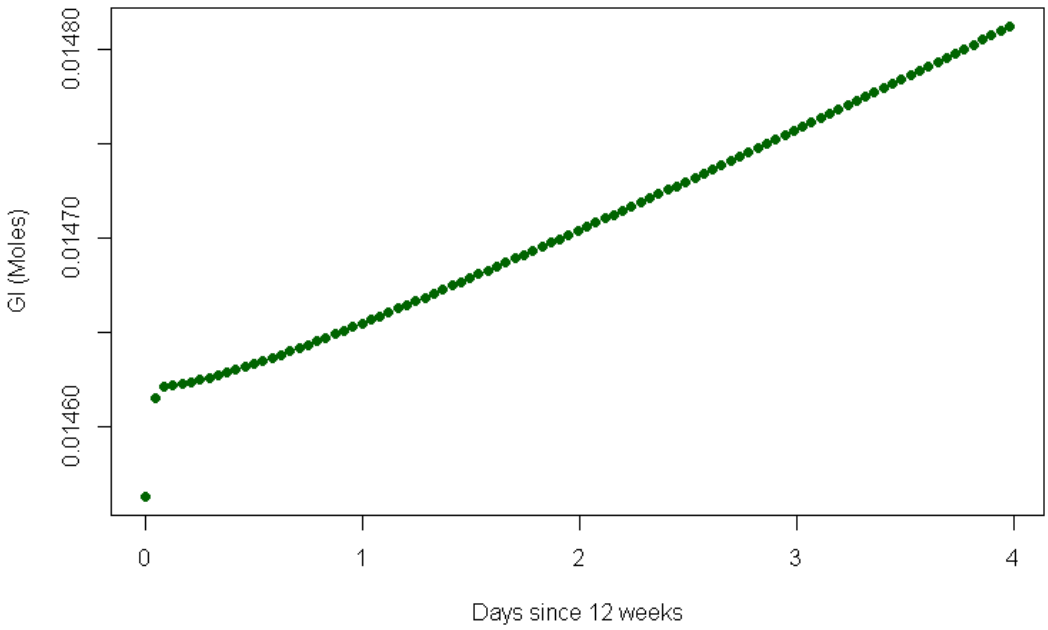

Figure 27: Glucose (Gl) over first four days of simulation, using draft revised initial conditions derived from Hon [45].

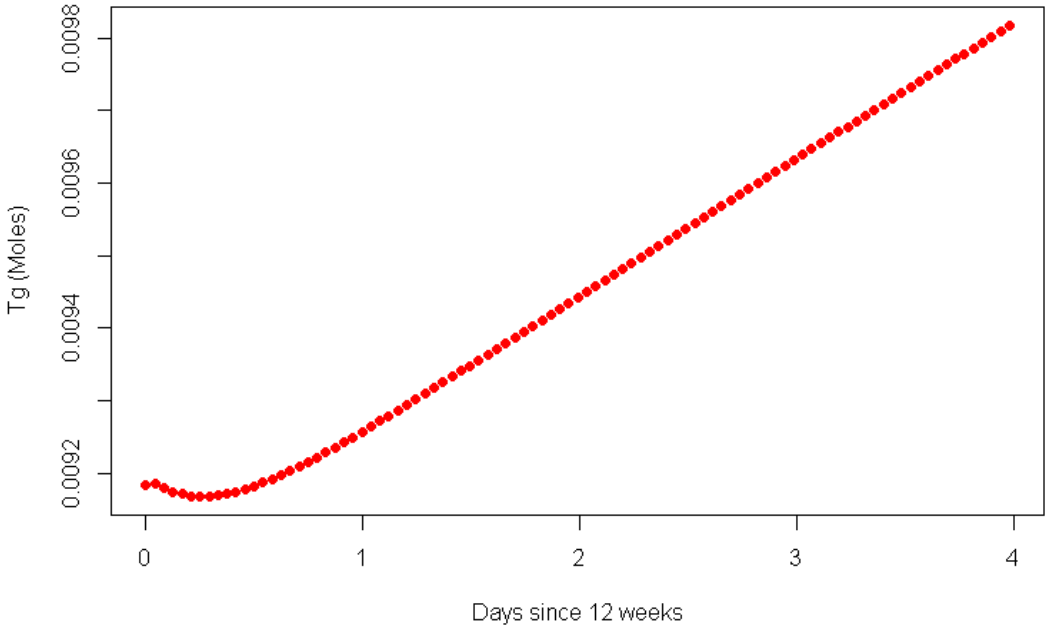

Figure 28: Lipids (Tg) over first four days of simulation, using draft revised initial conditions derived from Hon [45].

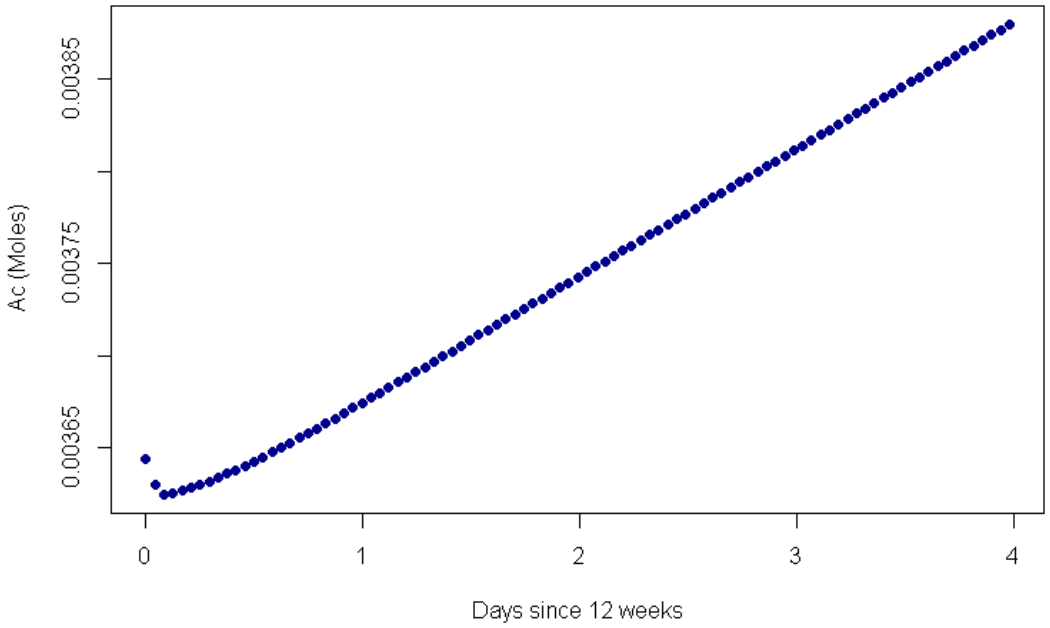

Figure 29: Acetate (Ac) over first four days of simulation, using draft revised initial conditions derived from Hon [45].

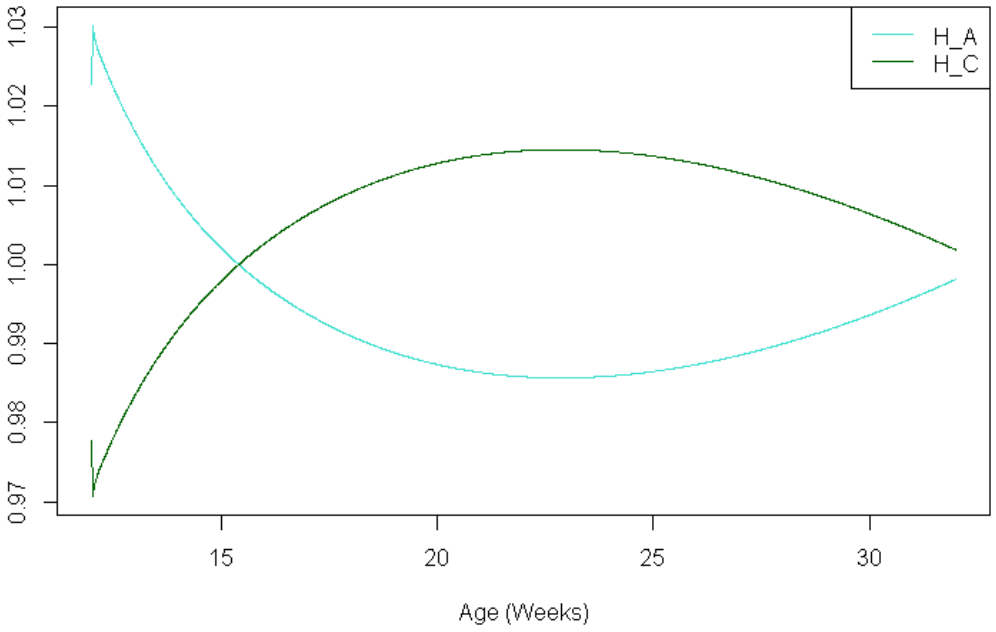

Figure 30: Anabolic (H_A) and catabolic (H_C) hormonal controls, using draft revised initial conditions derived from Hon [45].

State Variable	**Initial Conditions (Revised)**	**Value at $t = 0.0829$**	**Initial Conditions (Further Revised)**
Aa	0.01173	0.01892	0.01892
Gl	0.01456	0.01462	0.01462
Tg	9.1841×10^{-3}	9.1795×10^{-3}	9.1795×10^{-3}
Ac	3.6436×10^{-3}	3.6244×10^{-3}	3.6244×10^{-3}
Pb	15.61826	-	15.61826
Pv	7.07618	-	7.07618
Pz	5.9805	-	5.9805
Pw	0.05097	-	0.05097
Ts	3.55479	-	3.55479
Db	6.0897×10^{-3}	-	6.0897×10^{-3}
Dv	7.4802×10^{-3}	-	7.4802×10^{-3}
Dz	4.3984×10^{-3}	-	4.3984×10^{-3}

Table 22: Further revision of Revised Initial Conditions derived from Hon [45].

In order to rectify the initial instability in the values for amino acid, glucose, lipids and acetate, the initial conditions were further revised to be equal to the third data point for each variable, as generated using the revised initial conditions presented in Table 21. This corresponds to a model time of only $t = 0.0829$ days, or two hours. As this is such a short period, the other initial conditions were not adjusted further to match their value at this time. The further revised initial conditions are presented in Table 22.

Figures 31, 32 and 33 show that this approach has successfully removed the unnatural tick-like patterns in the growth trajectories of the state variables. Figure 34 also demonstrates initial *stability* in the hormonal controls. It is appropriate to note here that the terminal empty body weight is 41.83kg, marginally higher than the 40kg generated by Sainz and Wolff [83]. This issue will be discussed in Chapter 6 and steady-state growth will be discussed in Chapter 7.

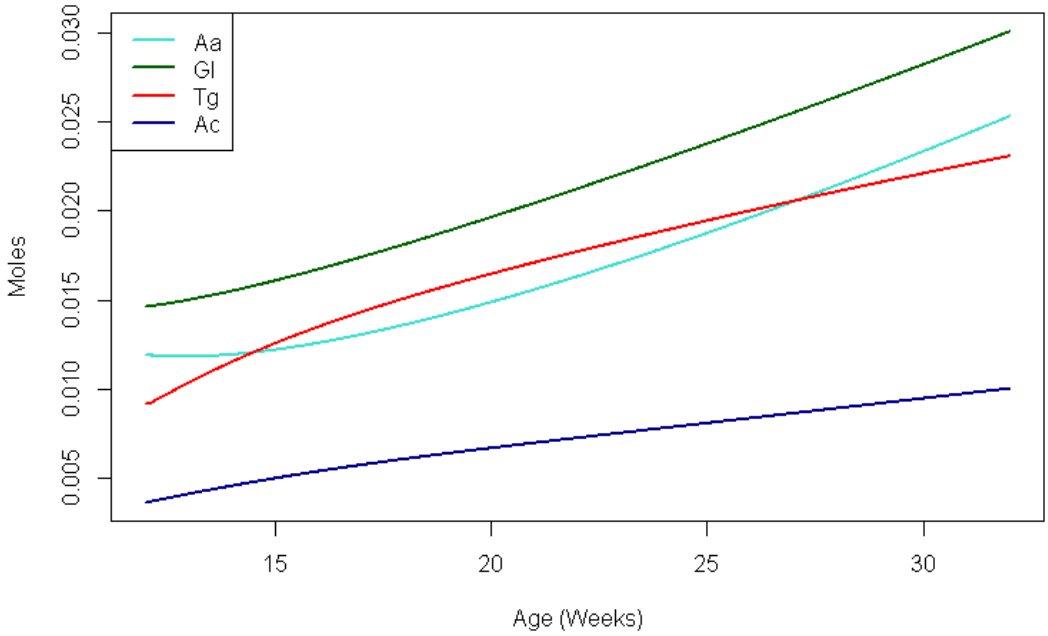

Figure 31: Circulating amino acids (Aa), glucose (Gl), lipids (Tg) and acetate (Ac), using further revised initial conditions derived from Hon [45].

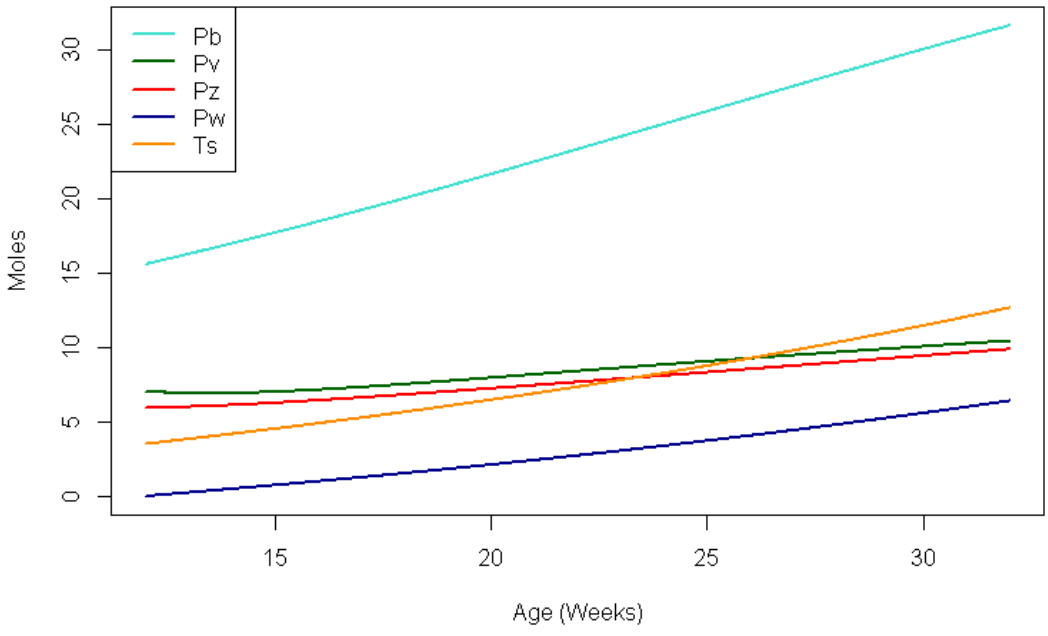

Figure 32: Protein in carcass (Pb), viscera (Pv), other tissues (Pz) and wool (Pw), and storage triacylglycerol (Ts), using further revised initial conditions derived from Hon [45].

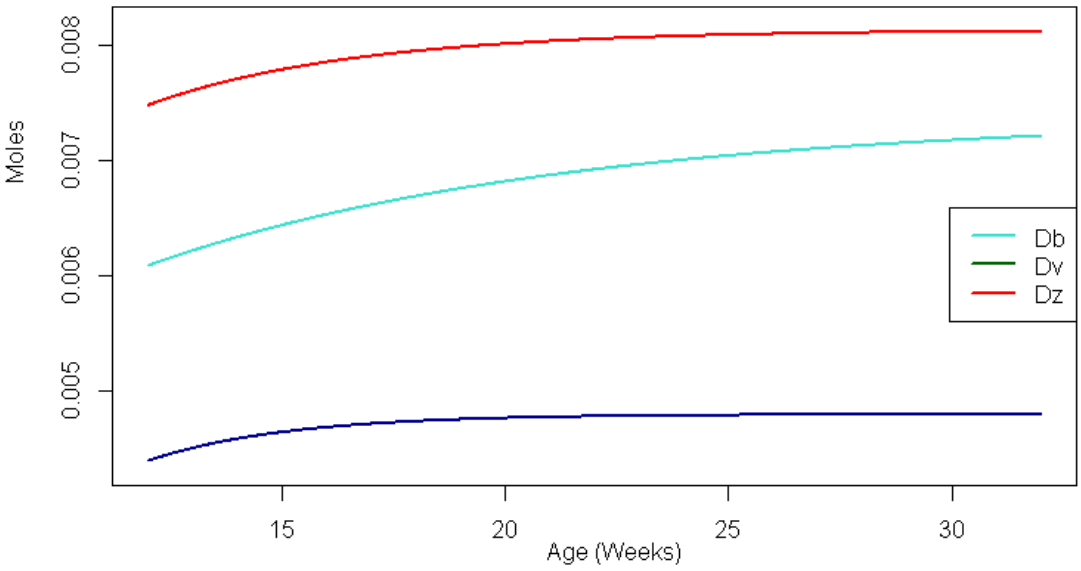

Figure 33: DNA pools corresponding to carcass (Db), viscera (Dv) and other tissues (Dz), using further revised initial conditions derived from Hon [45].

5.2 Initial Conditions as Derived from Sainz and Wolff [83]

The derived initial state variable values from Sainz and Wolff [83], after scaling to produce 20kg empty body weight using Equation (68) as presented in Table 19, were implemented in the simulation with MISER3.3. Definitions of empty body weight and V'_{AaPw} were the same as those used in Section 5.1. Figures of the state variables by sheep age (in weeks) are given in Appendix C. As was seen in the equivalent plots relating to the preliminary initial conditions derived from Hon [45], the model corrects levels of amino acids, glucose, lipids and acetate in the initial stages of the simulation. The glucose, lipids and acetate and hormonal control plots have a similar growth pattern to that which was identified for the preliminary initial conditions derived from Hon [45]. However, the Hon [45] derived amino acids decrease sharply, then after a slight increase have a subsequent decrease, whereas Sainz and Wolff [83] derived amino acids increase sharply before assuming a natural-looking pattern of slight positive growth, as shown in Figure 35 for the first fours days of the simulation. The preliminary initial condition for amino acids as derived from Sainz and Wolff [83] is 11% lower than the preliminary figure for Hon [45], and this is the greatest difference amongst amino acids, glucose, lipids and acetate for the two sets of preliminary initial conditions. Therefore it is not surprising that the initial growth pattern for amino acids differs between the two sets.

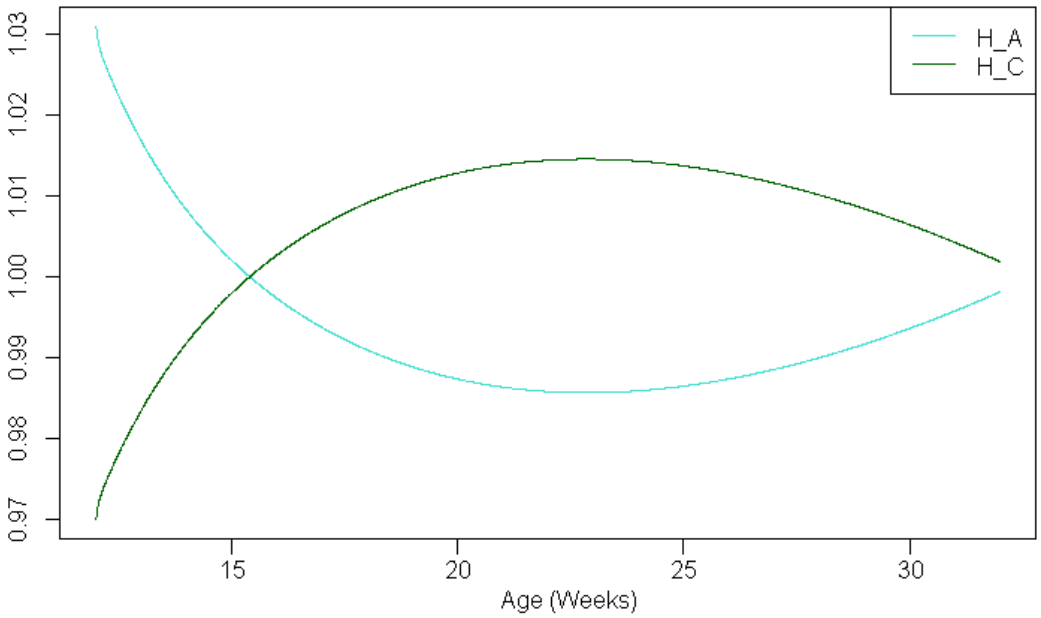

Figure 34: Anabolic (H_A) and catabolic (H_C) hormonal controls, using further revised initial conditions derived from Hon [45].

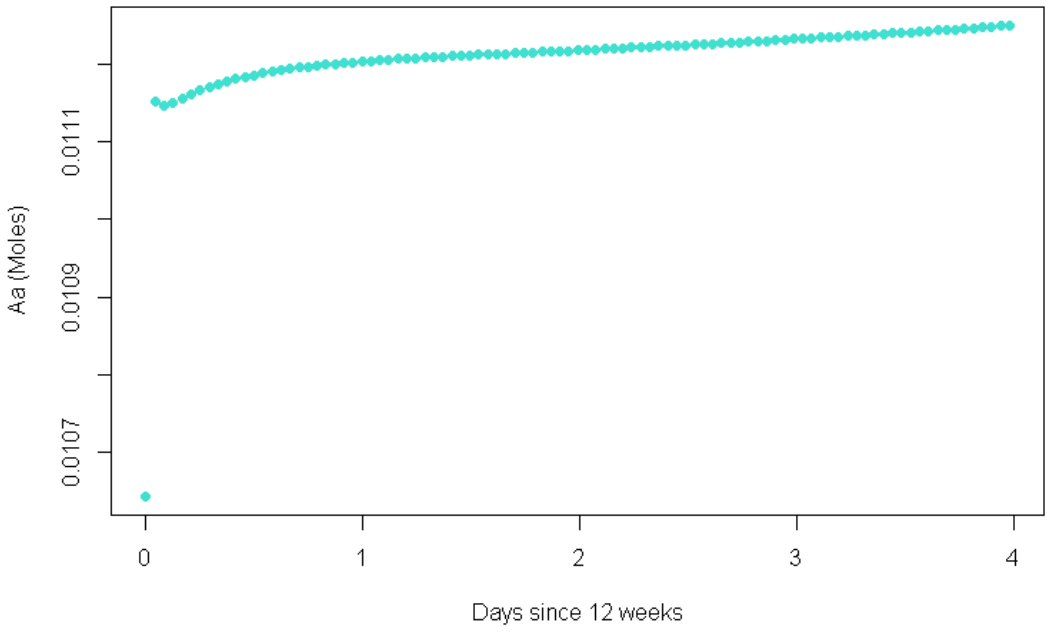

Figure 35: Amino acids (Aa) over first four days of simulation, using Preliminary Initial Conditions derived from Sainz and Wolff [83].

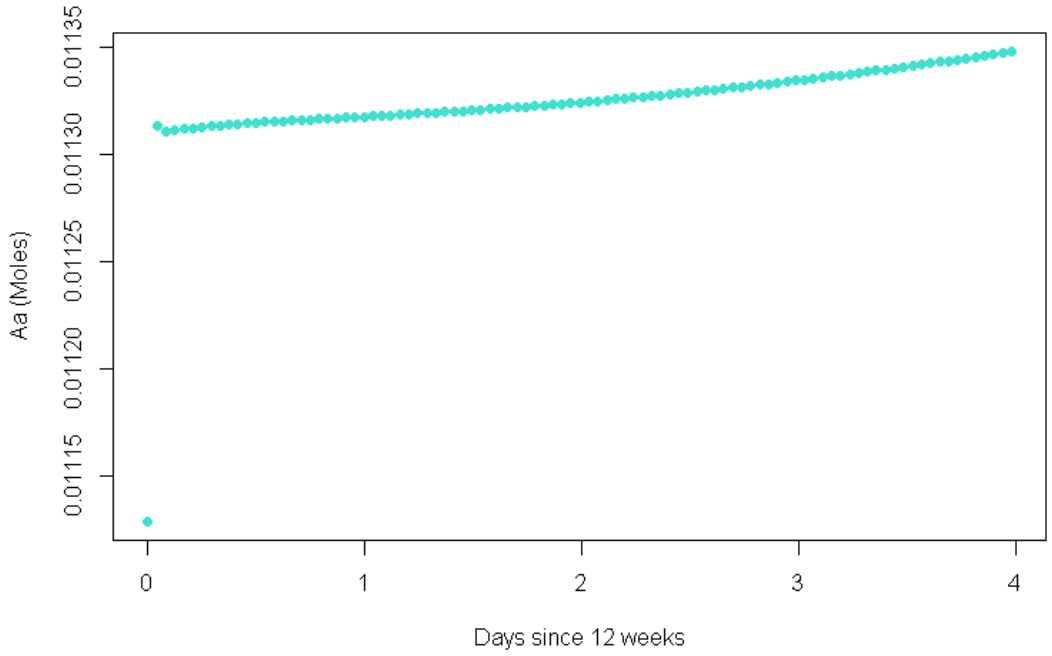

Figure 36: Amino acids (Aa) over first four days of simulation, using draft revised initial conditions derived from Sainz and Wollf [83].

As was the case in the preliminary initial conditions derived from Hon [45], by 1.5 days into the simulation the growth trajectories for the circulating amino acids, glucose, lipids and acetate have stabilised. Again, for consistency the initial conditions for all state variables were adjusted to match their values after 1.5 days of simulated growth, and then scaled back proportionately such that the empty body weight remains at 20kg at $t = 0$ according to Equation (68). Similarly, the scaling back of empty body weight to 20kg by a constant implicitly assumes linear growth in the other state variables from 12 weeks to 12 weeks and 1.5 days of age, but this is deemed an acceptable assumption. It is also not refuted by the plots of the other state variables, see Appendix C. This adjustment has not substantially altered the body protein to body fat ratio that was discussed in Section 4.2.

The model was run again with the draft revised initial conditions, and whilst the tick effect was certainly reduced, there was still some evidence of it for amino acids, glucose, lipids and acetate, with a particularly large relative initial jump for amino acids. This was a similar result to that from Section 5.1, with turning points also now being negligible. The main difference here is again for amino acids, where the slope is positive following the initial jump rather than negative, as seen in Section 5.1, compare Figures 26 and 36, with further graphs available for review in Appendix C.

State Variable	Initial Conditions (Preliminary)	Value at $t = 1.4924$	Initial Conditions (Revised)
Aa	0.01064	0.01121	0.01113
Gl	0.01429	0.01451	0.0144
Tg	0.0112	9.684×10^{-3}	9.6131×10^{-3}
Ac	4.925×10^{-3}	3.8234×10^{-3}	3.7955×10^{-3}
Pb	15.05	15.84298	15.72703
Pv	6.84	7.12302	7.07089
Pz	5.743	6.01607	5.97205
Pw	0	0.05141	0.05103
Ts	3.30727	3.51873	3.49298
Db	6.1621×10^{-3}	6.189×10^{-3}	6.1437×10^{-3}
Dv	7.6634×10^{-3}	7.6839×10^{-3}	7.6277×10^{-3}
Dz	4.5467×10^{-3}	4.5632×10^{-3}	4.5299×10^{-3}
EBW (kg)	20.00	20.1474	20.00

Table 23: Revision of preliminary initial conditions derived from Sainz and Wolff [83].

Again, in order to rectify the sharp jump in the values for amino acid, glucose, lipids and acetate, the initial conditions were further revised to be equal to the third data point for each variable, as generated using the revised initial conditions presented in Table 23.

Figures 89, 90 and 91 of Appendix C show that this approach has successfully removed the unnatural tick-like patterns in the growth trajectories of the state variables, as was the case in Section 5.1. Figure 92 of Appendix C also demonstrates initial stability in the hormonal controls. It is appropriate to note at this stage that the empty body weight at the end of the period is 41.70kg, marginally higher than the 40kg generated by Sainz and Wolff [83], and only slightly lower than that produced by the further revised initial conditions based on Hon [45] (41.83kg). This issue is discussed in Chapter 6, and steady-state growth will be discussed in Chapter 7.

5.3 Initial Conditions Conclusions

The further revised initial conditions developed from Hon [45] and those developed from Sainz and Wolff [83] both appear to provide a reasonable starting point for the model. The growth trajectories within the 140 day period appear natural, and the final body weights (41.83kg and 41.70kg respectively) are not substantially different from the 40kg set by Sainz and Wolff [83]. There are clearly some issues surrounding initial stability of the state variables present in circulating fluids (amino acids, glucose, lipids and acetate), and this is likely related to in-

State Variable	**Initial Conditions (Revised)**	**Value at $t = 0.0829$**	**Initial Conditions (Further Revised)**
Aa	0.01113	0.01131	0.01131
Gl	0.0144	0.01447	0.01447
Tg	9.6131×10^{-3}	9.6054×10^{-3}	9.6054×10^{-3}
Ac	3.7955×10^{-3}	3.7722×10^{-3}	3.7722×10^{-3}
Pb	15.72703	-	15.72703
Pv	7.07089	-	7.07089
Pz	5.97205	-	5.97205
Pw	0.05103	-	0.05103
Ts	3.49298	-	3.49298
Db	6.1437×10^{-3}	-	6.1437×10^{-3}
Dv	7.6277×10^{-3}	-	7.6277×10^{-3}
Dz	4.5299×10^{-3}	-	4.5299×10^{-3}

Table 24: Further revision of Revised Initial Conditions derived from Sainz and Wolff [83].

stability in the hormonal controls of H_A and H_C. It is more than likely that this issue of initial instability was present for Sainz and Wolff [83] and Hon [45], but that it was not noted there due to the use of a slightly coarser numerical solution procedure (fourth-order Runge-Kutta scheme with a larger step size, as compared to the adaptive 6^{th} order scheme used in MISER3.3). The hormonal controls are affected by both the instantaneous concentration of glucose, and the reference concentration of glucose. Sainz and Wolff have set the reference concentration of glucose to 0.003 moles per litre of extra-cellular fluid.

This is the same reference level used by their UC Davis colleague Baldwin in his collaborative work on the metabolism of a lactating cow (Baldwin, France and Gill [12]), but may not necessarily be appropriate for growing lambs. Using a molecular weight for glucose of 180.16g/mol, this reference level is the equivalent of approximately 54mg/dL. This reference level is supported by Elmahdi et al. [32], who states that in most ruminants, blood glucose is 2.5-3.5 mmol/L, assuming that blood and extra-cellular fluid are effectively interchangeable. Panousis et al. [73] gives average plasma glucose concentrations in sheep as 46-69mg/dL (2.6-3.8 mmol/L). Also, Casamassima et al. [25] gives an average blood glucose concentration in the control group of sheep over a 40 day trial as precisely 3mmol/l.

However, results found in the literature relating to *lambs* show more variation:

- 1.93 mmol/L blood glucose concentration in male lambs aged six months from Tripathi et al. [93];
- 4.75 mmol/L plasma glucose concentration in lambs aged seven weeks from Beaufort-Krol et al. [16];
- 5.00 mmol/L plasma glucose concentration in lambs aged seven months from Onischuk and Kennedy [70]; and
- 5.80 mmol/L plasma glucose concentration in lambs aged sixty days from Sanz Sampelayo et al. [85].

Caution should also be exercised when comparing blood glucose levels since the measurement method can affect the relative concentrations. In addition, measurements found in the literature were often in terms of plasma rather than blood concentrations, making comparisons even more difficult. The relative plasma content in blood was researched, but results varied from 61% through to 91%, and were also found to be dependent on infections and other factors (see Clarkson [26] and Anosa and Isoun [7]). This may be an indication of the highly variable environments that sheep seem to be able to exist in, and the survival mechanisms of lambs. Whilst glucose dynamics appear to be quite fast, as seen in the plots relating to hormonal controls in Sections 5.1 and 5.2, and the intention of the model is to work over a relatively long time horizon, a reference level around the mid-range of glucose concentrations is probably the most reasonable choice. It may make sense to define the reference glucose level as a linear function of time to allow for varying concentrations by age of sheep. In addition, hormonal controls for glucose are affected by the fatness of the animals, as demonstrated by Zhang et al. [106] in 2005. Consideration of these effects are among a range of potential improvements to the model to consider for future work.

There are also mathematical models available at the level of responses to individual meals (see Liu and Tang [53]), however, as feed intake is continuous in the Sainz and Wolff [83] model, rather than inputs at specific time intervals, then in the current context it is more appropriate for a generalised glucose model and reference level to be used. Many other parameters and rates in the model depend upon the relative size of the glucose concentration to the reference level, and changing the reference level alone would not be appropriate without then reviewing many other aspects of the model. Whether the 0.003 moles per litre reference level is appropriate would depend upon how it is conceptually defined, as well as how it relates to the other elements in the model. Despite the initial

State Variable	Initial Conditions (Hon [45])	Initial Conditions (Sainz and Wolff [83])	Difference (%)
Aa	0.01892	0.01131	-67.3
Gl	0.01462	0.01447	-1.1
Tg	9.1795×10^{-3}	9.6054×10^{-3}	4.4
Ac	3.6244×10^{-3}	3.7722×10^{-3}	3.9
Pb	15.61826	15.72703	0.7
Pv	7.07618	7.07089	-0.1
Pz	5.9805	5.97205	-0.1
Pw	0.05097	0.05103	0.1
Ts	3.55479	3.49298	-1.8
Db	6.0897×10^{-3}	6.1437×10^{-3}	0.9
Dv	7.4802×10^{-3}	7.6277×10^{-3}	1.9
Dz	4.3984×10^{-3}	4.5299×10^{-3}	2.9

Table 25: Comparison of further revised initial conditions as derived from Hon [45] and from Sainz and Wolff [83].

instabilities (which may simply be a result of sensitivities in the model to relative values of state variables and the feed intake at $t = 0$), which have been addressed in the Sections above, there is no suggestion that the reference level should be changed at this stage.

For the sake of setting some initial conditions going forward, a decision needed to be made between the two sets of further revised initial conditions. Given the suspected sensitivity to relative values of the state variables, it would not be appropriate to choose some conditions from those derived from Hon [45] and combine them with some conditions from those derived from Sainz and Wolff [83]. Therefore each set needs to be assessed on its own merits. Ultimately, there is very little difference between them, with the exception of amino acids where the Sainz and Wolff [83] derived value is 67% lower than that derived from Hon [45], as shown in Table 25. It was also seen in the growth plots for amino acids (see Figure 31 and Figure 89). Further plots in Figure 37 show that the amino acids value derived from Hon [45] results in an initial decrease before aligning very close to the growth with the amino acids value derived from Sainz and Wolff [83]. The Sainz and Wolff [83] initial value for amino acids results in smooth growth from the start, and hence appears to be the more appropriate figure. The initial values derived from Sainz and Wolff [83] also have the advantage of being fully repeatable, with their derivation documented in this work. Therefore the further revised initial conditions from Sainz and Wolff [83] as presented in Table 24 will be used as the starting point for a 20kg empty body weight sheep for the model going forward.

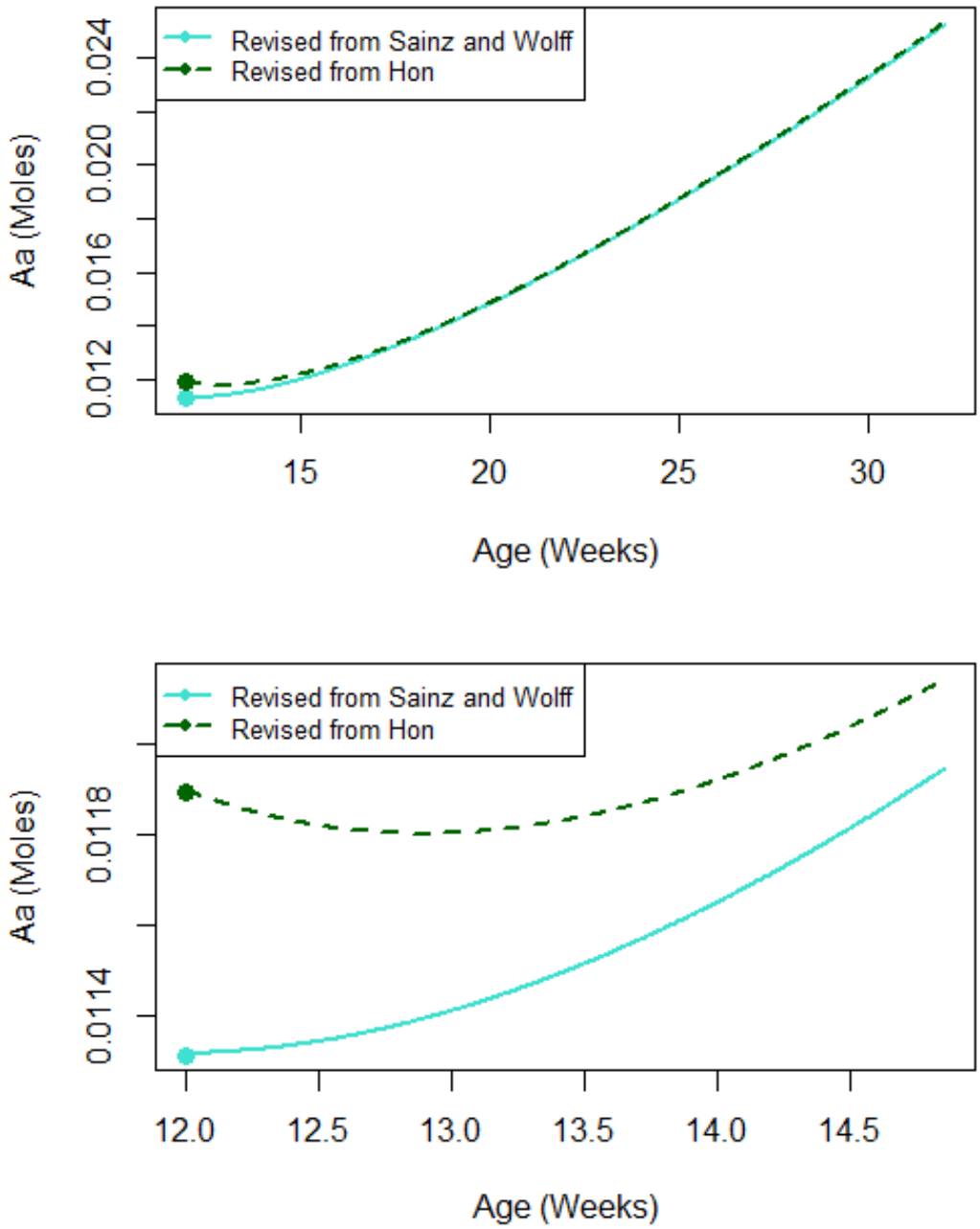

Figure 37: Circulating amino acids (Aa), using further revised initial conditions derived from Hon [45] and from Sainz and Wolff [83].

6 Review of 20kg to 40kg Growth

6.1 Reference State Comparisons

Although the model now runs successfully, without issues obvious to the naked eye, this is no guarantee that the simulation reflects all aspects of growth realistically, or even that the simulated growth matches that reported in Sainz and Wolff [83]. The 30kg and 40kg reference states, along with estimated body protein and fat proportions from their Figure 1, can be used as a comparison with the simulated results. The initial conditions as derived from Sainz and Wolff [83] differ slightly to those implemented, but this is not expected to make a substantial difference. The derived variable values from Sainz and Wolff [83], plus some other calculated terms, are provided for 30kg and 40kg reference states alongside simulated variables in Table 26. It is clear that the empty body weight equation used in Sainz and Wolff must translate state variables into a more modest kilogram weight, as the state variables for $W_{EB} = 30$kg in Table 26 are all lower than those simulated. This will have some effect on the way growth progresses, as many rates depend on the empty body weight. The two reference states are also achieved at different ages. For Sainz and Wolff [83] it can be estimated that the lamb reaches 30kg empty body weight at 22 weeks of age, and 40kg at 32 weeks of age, from their Figure 2. In the simulation, these milestone weights are achieved at 22.3 and 30.7 weeks respectively. The body protein values are all *smaller* in the simulated case at 40kg, however, the body fat is marginally higher. Overall, there are only minor differences between the state variables, hormonal levels and concentrations at the two reference states. At 30kg the simulated values are between 0.2% lower and 4.7% higher than those given in Sainz and Wolff [83], and for 40kg, the simulated values are between 2.1% lower and 1.7% higher from those in Sainz and Wolff [83]. The largest difference is seen in the levels of circulating lipids (Tg), which is 4.7% higher in the simulated case at 30kg. However, by 40kg this has stabilsed to being just 1.7% higher.

It is of interest to compare not just the state variables, but some of the rate values at the reference states of 30kg and 40kg. Using an extract from the simulation along with the Major Rates table from Sainz and Wolff [83] this comparison is presented in Tables 27 and 28. The absorption values differ slightly, as extracts from the simulation are only available at a finite number of points and hence they represent empty body weights of 29.997kg and 39.997kg respectively. As for the state variables, there are only minor differences between the major rates at these reference weights. However, at 30kg the rates are all higher in the simulated results (0.03% to 3.46%) and by 40kg the rates are all lower in the simulated results (-1.2% through -2.9%).

Variable/ Parameter	**S&W [83]** $W_{EB} = 30$kg	**Simulated** $W_{EB} = 30$kg	**S&W [83]** $W_{EB} = 40$kg	**Simulated** $W_{EB} = 40$kg
Aa	0.01634	0.01643	0.02403	0.02387
Gl	0.02141	0.02138	0.02858	0.02867
Tg	0.01689	0.01768	0.02206	0.02244
Ac	0.007086	0.007166	0.009530	0.009567
Pb	23.00	23.61	31.30	30.65
Pv	8.523	8.591	10.30	10.21
Pz	7.837	7.853	9.803	9.637
Pw	-	-	-	-
Ts	7.241	7.276	11.45	11.62
Db	0.006934	0.006952	0.007205	0.007195
Dv	0.008071	0.008074	0.008123	0.008120
Dz	0.004789	0.004790	0.004790	0.00480
H_A	0.9821	0.9797	0.9850	0.9913
H_C	1.018	1.021	1.015	1.009
C_{Aa}	0.002270	0.002282	0.002503	0.002486
C_{Gl}	0.002973	0.002969	0.002977	0.002987
C_{Tg}	0.002346	0.002456	0.002298	0.002337
C_{Ac}	0.0009842	0.000995	0.0009927	0.000997
C_{Ts}	0.2414	0.2425	0.2861	0.2904

Table 26: Sainz and Wolff [83] Preliminary derived variable values where W_{EB} =30kg and 40kg (from Table 13), as compared to simulated results.

Considering the small differences in results expected as the empty body weight equation used in the simulation differs from the (unknown) equation used in Sainz and Wolff [83], it can be concluded that the simulation replicates lamb growth from 20kg through 40kg in an equivalent manner to that produced by Sainz and Wolff. This provides a stable base from which to develop improvements and identify possible limitations in the use of the model.

6.2 Wool Growth

As the Sainz and Wolff [83] model was only intended to model a lamb's growth to maturity, there was a concern that it may not adequately replicate wool growth. The initial condition for protein in wool used by Hon [45] was zero. This was not flagged as an issue in Chapter 5 as a sheep may well have been sheared immediately prior to the simulation commencing, and so it is a reasonable scenario to consider. Similarly, when the initial condition for Pw was revised in Chapter 5 via the rebasing at 12 weeks, 1.5 days, as the scenario was not unreasonable to consider, it wasn't highlighted at the time. Clearly, there would be more of a concern if this initial condition of zero was attached to protein in the carcass, for example. It should be noted again at this stage that the growth rate of protein in wool is not dependent on the amount of protein in wool already present. There is no feedback of Pw back into the differential equations governing growth. Therefore, whilst some consideration should be made about what initial condition would be most useful, it will not actually affect the growth rate. There are two main and independent items with regards to wool growth that need to be considered here:

1. Does the model adequately represent wool growth?; and
2. What is the most appropriate initial value to use for wool, for general research purposes?

In order to assess the simulated wool growth, there must be an understanding of what can be expected of a standard sheep. In Section 4.2.1, it was mentioned that, according to the Department of Agriculture, Fisheries and Forestry in the Queensland Government [90], an adult Merino sheep produces about 4.5kg of wool per year in Queensland, and that seemed roughly level with instantaneous growth rates of wool (with corrected V'_{AaPw}). However, wool growth needs to be researched with a little more depth to be confident in the accuracy of the model. Also, the instantaneous growth rates considered in Section 4.2.1 were based on values of V'_{AaPw} determined individually for a 20kg, 30kg and 40kg empty body weight sheep, as it pre-dates the assignment of a global V'_{AaPw} value of 3.04.

Term	Definition	Major Rates	Simulated
A_{Aa}	absorption of amino acids	0.5505	0.5537
A_{Gl}	absorption of glucose	0	0
A_{Tg}	absorption of lipid	0.0113	0.0114
A_{Ac}	absorption of acetate	3.587	3.609
A_{Pr}	absorption of propionate	1.587	1.596
A_{Bu}	absorption of butyrate	0.5558	0.5599
$U_{Bu,BuCd}$	butyrate oxidation	0.5558	0.5599
$U_{Aa,AaGl}$	gluconeogenesis from amino acids	0.3220	0.3289
$U_{Pr,PrGl}$	gluconeogenesis from propionate	0.5286	0.5313
$U_{La,LaGl}$	gluconeogenesis from lactate	0.3664	0.3761
$U_{Gy,GyGl}$	gluconeogenesis from glycerol	0.1568	0.1605
$U_{Gl,GlTp}$	glucose to triose phosphates	0.4708	0.4824
$U_{Tp,TpLa}$	triose phosphates to lactate	0.7327	0.7522
$U_{La,LaCd}$	lactate oxidation	0.3663	0.3761
$U_{Ac,AcTs}$	lipogenesis from acetate	2.336	2.358
$U_{Ts,TsTg}$	lipolysis of storage fat	0.0732	0.0746
$U_{Tg,TgTs}$	esterification of fatty acids	0.0384	0.0397
$U_{Pb,PbAa}$	carcass protein degradation	0.9200	0.9444
$U_{Pv,PvAa}$	visceral protein degradation	2.557	2.577
$U_{Pz,PzAa}$	'other' protein degradation	0.7837	0.7853
$U_{Aa,AaPb}$	carcass protein synthesis	1.043	1.065
$U_{Aa,AaPv}$	visceral protein synthesis	2.586	2.606
$U_{Aa,AaPz}$	'other' protein synthesis	0.8127	0.8147
$U_{Aa,AaPw}$	wool protein synthesis	0.0455	0.0459
$U_{At,carcass}$	undef. energy expenditure in carcass	7.820	8.028
$U_{At,viscera}$	undef. energy expenditure in viscera	16.53	16.67
$U_{At,other}$	undef. energy in other tissues	7.602	7.617
$U_{At,AtAd}$	total ATP hydrolysis	78.95	79.80
$P_{At,AdAt}$	partial ATP production	41.46	41.90
$U_{Gl,GlCd}$	glucose oxidation	0.1675	0.1675
$U_{Tg,TgCd}$	lipid oxidation	0.0452	0.04616
$U_{Ac,AcCd}$	acetate oxidation	1.661	1.672

Table 27: Sainz and Wolff Table 3 Major Rates W_{EB} = 30kg (from [83] and simulated results).

Term	Definition	Major Rates	Simulated
A_{Aa}	absorption of amino acids	0.6928	0.6871
A_{Gl}	absorption of glucose	0	0
A_{Tg}	absorption of lipid	0.0143	0.0141
A_{Ac}	absorption of acetate	4.514	4.479
A_{Pr}	absorption of propionate	1.998	1.980
A_{Bu}	absorption of butyrate	0.6995	0.6947
$U_{Bu,BuCd}$	butyrate oxidation	0.6995	0.6947
$U_{Aa,AaGl}$	gluconeogenesis from amino acids	0.4718	0.4583
$U_{Pr,PrGl}$	gluconeogenesis from propionate	0.6652	0.6593
$U_{La,LaGl}$	gluconeogenesis from lactate	0.5100	0.5011
$U_{Gy,GyGl}$	gluconeogenesis from glycerol	0.1942	0.1913
$U_{Gl,GlTp}$	glucose to triose phosphates	0.6421	0.6317
$U_{Tp,TpLa}$	triose phosphates to lactate	1.109	1.002
$U_{La,LaCd}$	lactate oxidation	0.5097	0.5011
$U_{Ac,AcTs}$	lipogenesis from acetate	3.012	2.980
$U_{Ts,TsTg}$	lipolysis of storage fat	0.0904	0.0886
$U_{Tg,TgTs}$	esterification of fatty acids	0.0490	0.0485
$U_{Pb,PbAa}$	carcass protein degradation	1.252	01.226
$U_{Pv,PvAa}$	visceral protein degradation	3.090	3.062
$U_{Pz,PzAa}$	'other' protein degradation	0.9803	0.9637
$U_{Aa,AaPb}$	carcass protein synthesis	1.361	1.340
$U_{Aa,AaPv}$	visceral protein synthesis	3.113	3.088
$U_{Aa,AaPz}$	'other' protein synthesis	1.008	0.9948
$U_{Aa,AaPw}$	wool protein synthesis	0.0587	0.0580
$U_{At,carcass}$	undef. energy expenditure in carcass	10.639	10.419
$U_{At,viscera}$	undef. energy expenditure in viscera	19.98	19.80
$U_{At,other}$	undef. energy in other tissues	9.509	9.348
$U_{At,AtAd}$	total ATP hydrolysis	99.50	98.36
$P_{At,AdAt}$	partial ATP production	53.49	52.92
$U_{Gl,GlCd}$	glucose oxidation	0.2078	0.2056
$U_{Tg,TgCd}$	lipid oxidation	0.0550	0.05418
$U_{Ac,AcCd}$	acetate oxidation	2.046	2.024

Table 28: Sainz and Wolff Table 3 Major Rates W_{EB} = 40kg (from [83] and simulated results).

Amino Acid	**MW (g/mol)**	**g/ 109g wool**	**mol/ 109g wool**
Alanine	89	0.0394	0.0483
Arginine	174	0.0926	0.058
Aspartic acid	133	0.0623	0.0511
Cystine	121	0.1036	0.0934
Glutamic acid	147	0.1329	0.0986
Glycine	75	0.0472	0.0687
Histidine	155	0.011	0.0077
Isoleucine	131	0.0339	0.0282
Leucine	131	0.0816	0.0679
Lysine	146.19	0.0302	0.0226
Methionine	149	0.0051	0.0038
Phenylalanine	165	0.0367	0.0242
Proline	115	0.0623	0.0591
Serine	105.09	0.0898	0.0933
Threonine	119	0.0587	0.0538
Tryptophan	204.225	0.0086	0.0046
Tyrosine	181	0.0519	0.0313
Valine	117	0.0522	0.0487
Total	-	**109.12**	**0.8635**
Number average molecular weight (g/mol)			**126.37**

Table 29: Determining number average molecular weight of amino acids in wool protein from Corfield and Robson [28].

Table 6 gives a molecular weight for amino acids in wool protein as 126.41g/mol. Corfield and Robson [28] assessed a sample of Australian Merino 64s quality wool and presented the estimated grams of each amino acid per 100g of wool using slightly different methods in their Table 1. By using the average of the estimates for each amino acid, and applying the molecular weights for the amino acids, a number average molecular weight for amino acids in wool protein of 126.37g/mol is obtained. This gives some independent corroboration of the molecular weight used for Pw. The details of how this is reached are presented in Table 29.

Liu and Masters [52] state that wool is almost entirely composed of protein, and quotes Williams [102] in stating that wool fibre is primarily protein, with as little as 0.5% lipids and minerals. This is supported by Corfield and Robson [28], where the estimated grams of amino acids per 100g of wool actually sums to slightly more than 100g. Therefore it is assumed that the molecular weight of amino acids in protein in wool, along with the number of moles of amino acids in protein in wool generated in the model, can be used as an adequate estimate of what is known as clean fleece weight (CFW), which is wool cleaned of lanolin, dirt, etc.

A formula for determining clean fleece weight (kg) from Pw is hence given in Equation (90).

$$CFW = 0.126 \times Pw. \tag{90}$$

The simulated wool growth from the model using the further revised initial conditions derived from Sainz and Wolff [83] is from 6.43g at 12 weeks of age, to 818.48g at 32 weeks of age - 5.8g/day of clean fleece weight growth. However, the growth in empty body weight over this time must also be considered, from 20kg to 41.7kg, as a larger sheep has a greater amount of skin (Pz), and is likely to produce more wool over the same time period. As wool growth is dependent on both the size of the sheep as well as the time that has passed, it is difficult to set an appropriate initial condition for wool, and to assess the wool growth from 12 to 32 weeks of age (20kg to 41.7kg). The literature relating to wool growth is, unsurprisingly, dominated by breeds of sheep known for high rates of wool growth, whereas the simulated sheep in this work is designed to be somewhat generic. Therefore at this stage, where the focus is on this initial period of lamb growth, we will restrict our attention to setting a reasonable initial condition, and ensuring wool growth over this period is within an acceptable range.

A number of results from studies on wool are presented in Table 30. These are all growth until *first shear*, meaning that it is a cumulative fleece growth from birth. In order to capture full cumulative fleece growth, this is a suitable method for defining the initial condition, particularly when aiming to match simulated growth with results from the literature collected in the same fashion. However, it must be kept in mind that the simulated growth in the model is not dependent on the amount of wool present at any one time. There are also many factors affecting wool growth. Breed has already been mentioned, but there is also feed type and availability, the existence and treatment of parasites, time of year and stocking rates amongst others (refer to White and McConchie [101], McGregor [57], Ramírez-Restrepo et al. [77], Rehbein et al. [79] and White et al. [100]). Whenever possible, a control result from the literature was used. Whilst this is not an exact science, if growth is in the right "ball park", then this will be an indicator of potential model proficiency. Other limitations in the literature also include varying measurements and units used for wool growth. Some of the different measurements include:

- Greasy Fleece Weight (GFW);
- Clean Fleece Weight (CFW); and
- Yield (CFW/GFW as a %).

The units used to describe wool growth are generally either presented as cumulative mass or growth rates, some examples are:

- Weight (g or kg); and
- Growth (g per day, mg cm^{-2} per day).

Depending on what is presented, it may or may not be comparable to the output of the simulation model. For example, there is no connection to surface area of sheep skin in the model, so a mg/cm^2 value is not replicable. CFW was selected as the measurement of interest, due to the frequency with which wool growth is reported in this manner, and the ability to compare its values with the output of the model via Equation (90). However, in order to maximise the usability of the data, if CFW was able to be inferred using GFW and Yield, or an estimate of Yield, then these research papers were also included. In reference to Table 30, Yield was presented in Meyer et al. [62], Rodehutscord et al. [81], Wuliji et al. [105], Scales et al. [87] and Lupton et al. [54]. These percentages by month of age are displayed in Figure 38. It is assumed that yield is not dependent on age, and this is supported by the randomness in Figure 38. The lowest yield is from Lupton et al. [54], which reports on Rambouillet breeds that are raised for both wool and meat production. The other yields are from either Merino or Merino cross breeds - typically wool producing breeds. The mean yield for all the data is approximately 71%, whereas the mean yield for the Merino and Merino cross breeds is about 74%. By applying a yield of 74% to the GFW measurements in Brand and Franck [22] and Ozcan et al. [72] (Merino breeds), CFW estimates can be determined. CFW values that have been estimated in this manner are italicised in Table 30.

The logical starting point would be the amount of clean fleece weight that could be expected for a first shear in a 12 week old lamb. Using Equation (90), estimates for the simulated clean fleece weight being generated through the model are able to be determined. As the simulation at this stage finishes at 32 weeks (approximately 7.4 months), data from Table 30 after this point will not be considered when determining an initial value. This is because, not only would it be outside the age range of focus, but the 20 to 40kg growth is driven with an F_{intake} value of 1.6 (a multiple of maintenance feed rate). Therefore, this is *not* a growth pattern that would be expected beyond this period, and hence we would *expect* growth after this point to be an inaccurate reflection of a standard sheep. The simulated CFW using the initial value from Table 24, alongside field data as at less than 7.4 months of age from Table 30 is displayed in Figure 39.

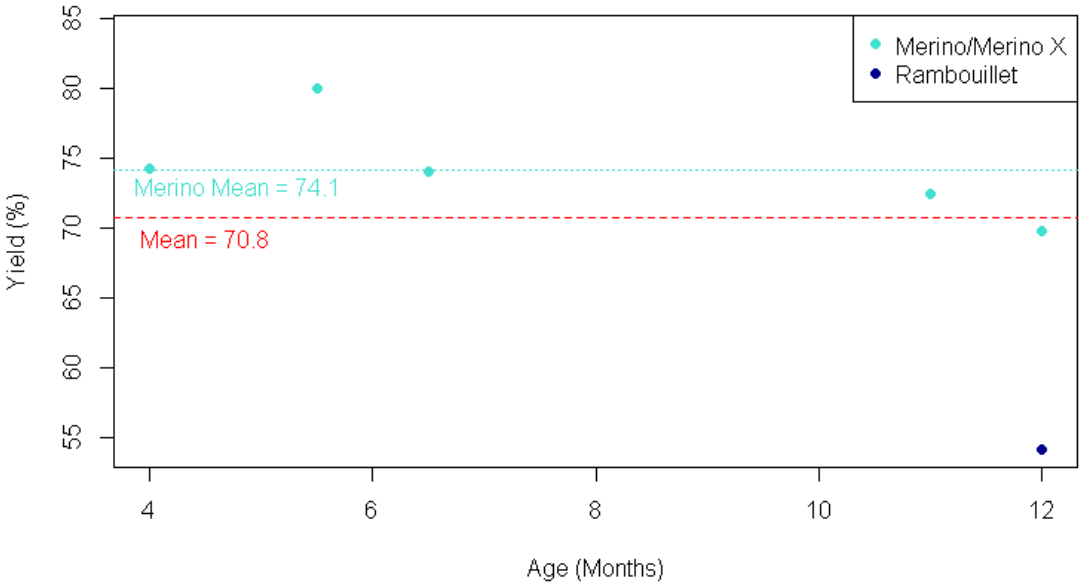

Figure 38: Yield of CFW by age in months from Meyer et al [62], Rodehutscord et al. [81], Wuliji et al. [105], Scales et al. [87] and Lupton et al. [54].

Breed	Age (Months)	GFW (kg)	CFW (kg)	Yield (%)	Source
Merino X	4	1.13	0.839	74.3	Meyer et al [62]
Sth African Merino	4.5	0.85	*0.586*	-	Brand and Franck [22]
Merino	4.5	1.25	*0.862*	-	Brand and Franck [22]
Merino	5.5	-	-	80	Rodehutscord et al. [81]
Muzaffarnagri	6	-	0.511	-	Sinha and Singh [89]
Merino	6.5	-	-	74	Rodehutscord et al. [81]
Merino	11	2.8	2.03	72.4	Wuliji et al. [105]
Merino X	12	3.783	2.641	69.8	Scales et al. [87]
Rambouillet	12	3.61	1.96	54.1	Lupton et al. [54]
Sth African Merino	16.5	-	3.93	-	Cloete et al. [27]
Turkish Merino	18	5.26	*3.722*	-	Ozcan et al. [72]

Table 30: Literature results for wool growth in sheep to first shearing. Italicised elements are estimates of CFW based on the GFW figure.

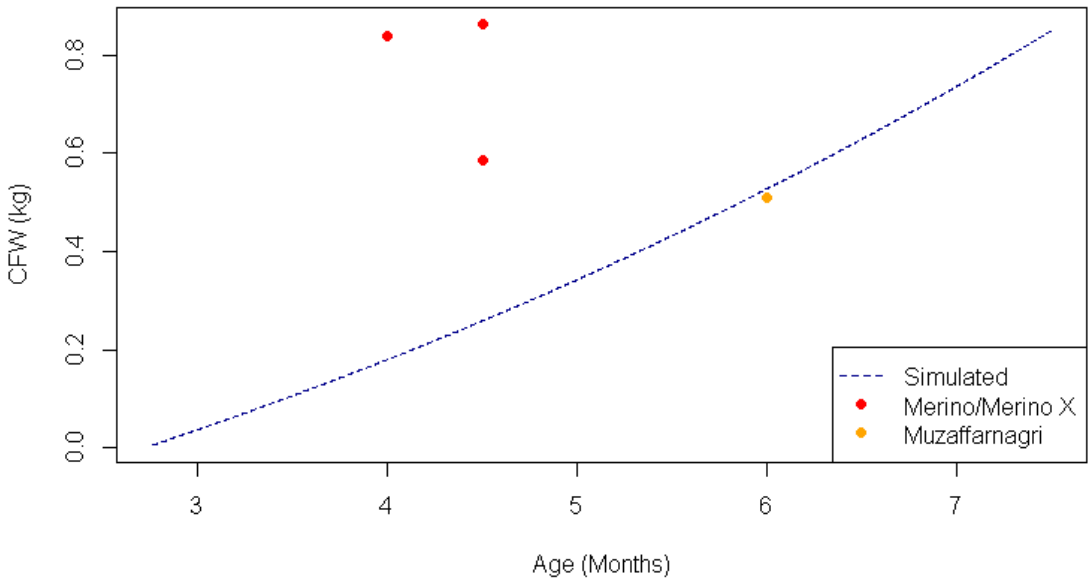

Figure 39: Simulated CFW by age in months, with field data from Meyer et al. [62], Brand and Franck [22], Rodehutscord et al. [81] and Sinha and Singh [89].

Age (Months)	**CFW (Field Data)**	**CFW (Simulated)**	**CFW (Simulated : New)**
4	0.839	0.1806	$0.1806 + x$
4.5	0.586	0.2591	$0.2591 + x$
4.5	0.862	0.2591	$0.2591 + x$
6	0.511	0.5277	$0.5277 + x$

Table 31: Comparison of simulated and literature results for wool growth to first shearing (Meyer et al. [62], Brand and Franck [22] and Sinha and Singh [89]).

Keeping in mind that a change in initial condition will only result in a vertical translation of the simulated CFW growth curve, as protein in wool (Pw) does not feed back into the model, it is possible to determine the initial condition that would minimise the distance between the simulated trajectory and the field data by solving for x where $CFW_{new} = CFW_{current} + x$, using a least squares approach between CFW_{new} and the field data. This problem is posed in Equation (91), with the solution of $x = 0.393$ given in Equation (92). The result is known to be a minimum due to the positive x^2 term. This corresponds to an initial condition of 393g of CFW, or $Pw = 3.167$mol. The solution is plotted alongside field data up to 12 months of age in Figure 40. Whilst the simulated wool growth around 12 months of age is a little on the high side, this is not unexpected considering the sheep is in a high growth phase ($F_{intake} = 1.6$). It can be concluded that the simulated wool growth is within a reasonable range for growing lambs, and no deficiencies in the model structure, the adjusted wool growth parameter V'_{AaPw} or the initial condition for wool are apparent at this stage.

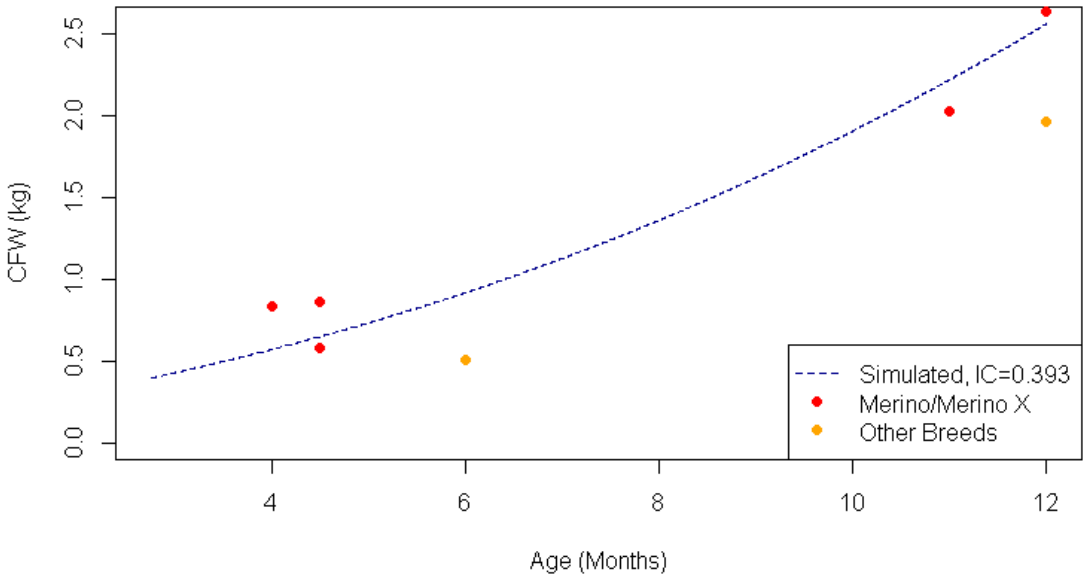

Figure 40: Simulated CFW by age in months using initial value of 393g, with field data from Meyer et al. [62], Brand and Franck [22], Rodehutscord et al. [81], Sinha and Singh [89], Wuliji et al. [105], Scales et al. [87] and Lupton et al. [54].

Minimise

$$\begin{aligned}&(0.839-(0.1806+x))^2+(0.586-(0.2591+x))^2+\\&(0.865-(0.2591+x)^2+(0.511-(0.5277+x))^2\end{aligned} \tag{91}$$

$$\Rightarrow (0.6584-x)^2+(0.3269-x)^2+(0.6059-x)^2+(-0.0167-x)^2.$$

Solve for

$$\frac{d}{dx}\left[(0.6584-x)^2+(0.3269-x)^2+(0.6059-x)^2+(-0.0167-x)^2\right]=0$$

$$\begin{aligned}&\Rightarrow -2(0.6584-x)-2(0.3269-x)-2(0.6059-x)-2(-0.0167-x)=0\\&\Rightarrow 2x-1.3168+2x-0.6538+2x-1.2058+2x+0.334=0\\&\Rightarrow 8x-3.143=0\\&\therefore x=0.3930.\end{aligned} \tag{92}$$

7 Extending the Model to Steady-State Adulthood

The Sainz and Wolff [83] model was concerned with lamb growth from 20kg to 40kg and whether it would accurately model a steady-state adult sheep is a point of interest. Presumably, an F_{intake} value of 1.6 (multiple of maintenance feed level) was not intended to be an indefinite value, but it is not clear at what stage this should be pared back. It is not clear either, that the constant model parameter values as used by Sainz and Wolff [83] are supportive of steady-state for all state variables. In this Chapter, simulation of the Sainz and Wolff [83] model (as defined in Chapter 3) is extended, and dynamic optimisation techniques are utilised, culminating in an adjusted model that replicates sheep growth into steady-state adulthood.

7.1 Extending the Time Horizon for the Sainz and Wolff [83] Model

As a first step, simulation of the Sainz and Wolff [83] model is extended to assess when an appropriate time would be to pare back the initially high F_{intake} value of 1.6. In this step, the optimsation feature of MISER3.3 is disabled and there is no control variable, hence this is not an optimal control problem. One way to investigate is to look at the DNA variables of Db, Dv and Dz to see at which stage they reach their maximum levels of 0.00737, 0.00813 and 0.0048 respectively. According to Sainz and Wolff [83], the remainder (skin, brain, etc) represented by Dz would reach its maximum most rapidly, followed by visceral organs (Pv) and then carcass (Pb). This is the case with the simulated growth trajectory, where Dz converges to 0.00480 at approximately 5.7 months of age, Dv converges to 0.008130 at around 10.3 months, and Db converges to 0.007370 at 18.6 months of age. This suggests that under an excessive feed regime, sheep reach a point where the growth in body protein is small, and it is mainly additional body fat that can be produced. In our simulation, it is not quite that straightforward. Once the growth in protein is limited due to the DNA variables reaching their limit, if the feed rate of 1.6 multiples of maintenance is continued, then the absorbed amino acids and glucose are not able to be fully utilised in growth. This leads to an excessive build up of these circulating nutrients, where growth becomes unstable and the model will have integration failure problems. In a realistic situation, there are likely to be biological feedback mechanisms which prevent sheep from eating excessively, but these have not been considered in the existing model. We will consider more direct changes to the feed rate first. Once

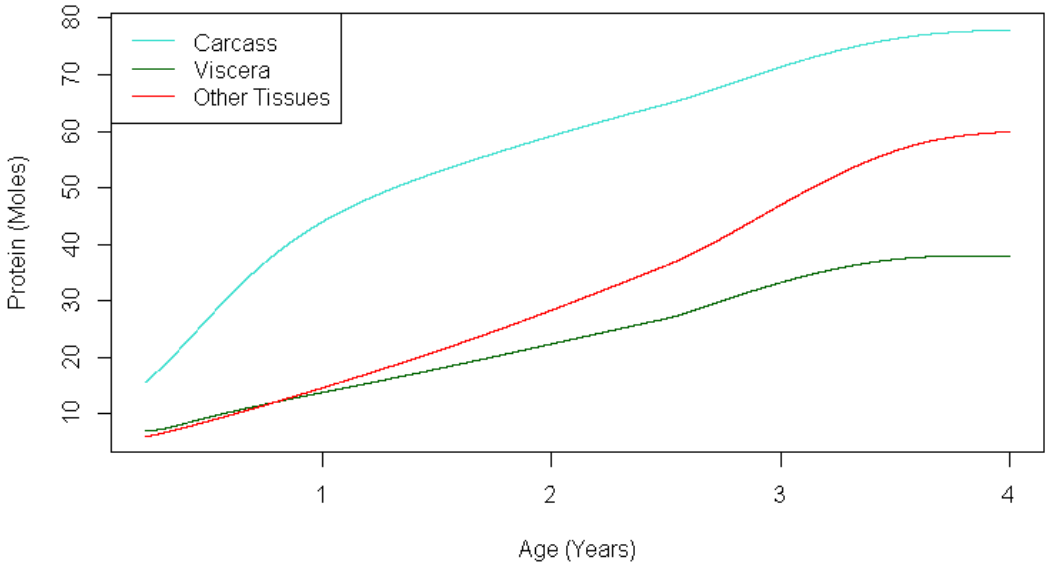

Figure 41: Simulated protein in carcass (Pb), viscera (Pv) and other tissues (Pz) up to 3 years, 9 months of age.

the concentration of circulating glucose reaches a certain point (corresponding to approximately 2.5 years of age), it causes the hormonal control of H_A to increase exponentially, which in turn causes a boost in protein growth. Its effect is limited as protein degradation rates increase more rapidly, such that eventually the protein growth will slow to zero. This causes the circulating glucose and hence H_A levels to increase beyond all reasonable bounds, and model integration failure occurs. Since there are no limiting factors such as a DNA variable for storage fat, it continues to grow over the time period.

$$\begin{aligned}
\frac{dPb}{dt} &= P_{Pb,AaPb} - U_{Pb,PbAa} = U_{Aa,AaPb} - U_{Pb,PbAa} \\
&= \frac{V_{AaPb}}{1 + \frac{k_{AaPb}}{C_{Aa}}} - K_{PbAa}Pb \\
&= \frac{V'_{AaPb}Pb^{\theta 7}Db}{1 + \frac{k'_{AaPb}}{H_A C_{Aa}}} - K_{PbAa}Pb \\
\therefore \frac{dPb}{dt} &\leq (21.7)(Db_{MAX})Pb^{0.682} - (0.04)Pb \qquad (93) \\
&\leq 0.1599Pb^{0.682} - 0.04Pb.
\end{aligned}$$

As shown in Figure 41, protein in carcass, viscera and other tissues all level out near the end of the simulated period. This is due to an intrinsic upper limit in the

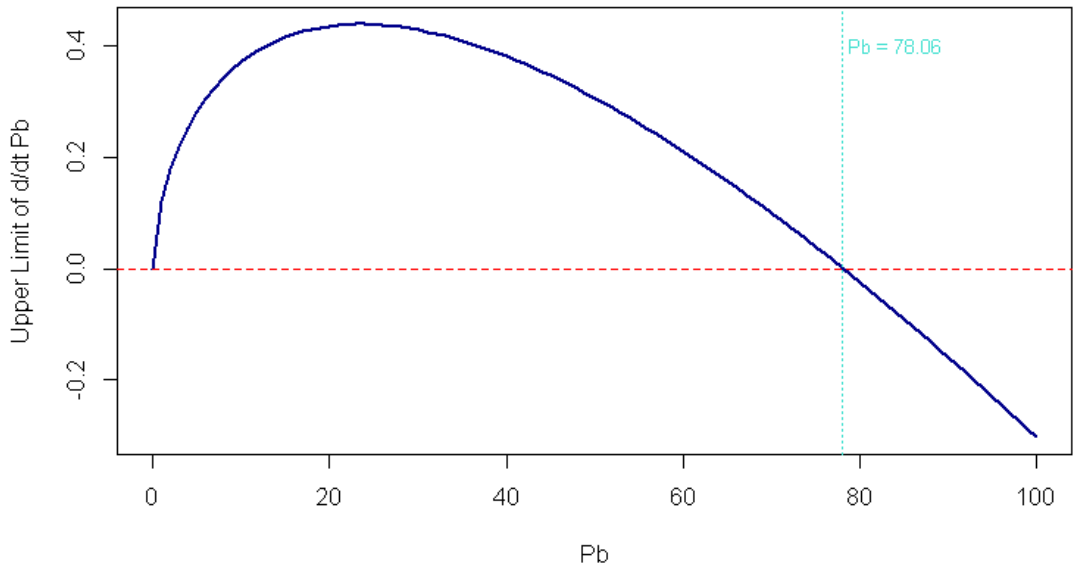

Figure 42: Upper limit of $\frac{dPb}{dt}$ as defined in Equation (93) plotted against Pb.

value of these protein variables. This can be demonstrated for all body proteins, but the example of protein in carcass is given in Equation (93) - first presented via Equation (63) - and Figure 42. Equation (93) shows that, with the current parameter values of $V'_{AaPb} = 21.7$, $Db_{MAX} = 0.00737$, $\theta 7 = 0.682$ and $K_{PbAa} = 0.04$, the growth of protein in carcass is limited by the formula $0.1599Pb^{0.682} - 0.04Pb$. This is displayed graphically in Figure 42, and demonstrates that protein in carcass is not able to sustain positive growth past $Pb \approx 78.1$ once $Db = Db_{MAX}$, regardless of hormonal levels or the concentration of amino acids in circulating fluids. The same approach applied to protein in viscera and other tissues gives positive growth limits of $Pv \approx 37.9$ and $Pz \approx 60.4$ respectively. It is important to note that the model with its current parameter values will not support sheep growth beyond this level. This also means that wool growth has an upper limit of 28.7kg per year. According to the Department of Agriculture, Fisheries and Forestry in the Queensland Government [90], an adult Merino sheep produces about 4.5kg of wool per year in Queensland. However, Wool Producers Australia states that a Peppin Merino ram may produce up to 20 kilograms of wool [104]. While the Peppin Merino sheep may not be representative of the Australian Merino flock, in order to replicate extreme cases of wool producing animals, it may be necessary to adjust parameters of the model such as V'_{AaPw}.

Next, the time horizon was limited to model the sheep up to 2.5 years of age and compared with data provided by Graham, Searle and Griffiths [39] on expected empty body weights and fat-free body weights. The aim was to determine at what point a value of 1.6 for F_{intake} should be modified. Again, the optimisation functionality in MISER3.3 was disabled, no control variable was used,

Age (weeks)	**Body Weight (kg) [39]**	**Predicted W_{EB} (kg)**	**Prior gain [1] (g/day) range [39]**	**Prior gain [1] (g/day) midpoint**	**Predicted gain[1] (g/day)**
18	15–28	25.4	90–230	160	141
27	20–40	35.6	60–160	110	169
39	24–52	50.5	40–160	100	183
57	31–72	75.4	12–130	71	211
66	32–72	89.7	-20–140	60	234
74	33–85	103.8	-20–170	75	261
84	34–90	123.9	10–80	45	302
93	39–98	144.7	0–120	60	345
105	38–109	177.2	0–120	60	412
119	33–94	223	-50–80	15	506

Table 32: Comparison of simulated body weight and growth rates with those given in Graham, Searle and Griffiths [39] for Groups 1 and 2.

and this was a simple simulation. It is already known that, with $F_{intake} = 1.6$, the first DNA variable of Dz reaches its maximum of 0.0048 at a sheep age of approximately 5.7 months. It follows that the feed intake should be pared back before this time, but further detail is required.

The body weights in Graham, Searle and Griffiths [39] are described as fasting liveweight less weight of fleece. It is assumed that fasting liveweight has negligible gut content, and hence the body weights should be directly comparable to the model's predicted empty body weights. The data presented in Table 32 is from Table 1 in Graham, Searle and Griffiths [39] for Groups 1 and 2. These are Border Leceister × Merino crossbred sheep fed either *ad lib.* or half *ad lib.*. The level of feeding was varied amongst the sheep so that there was a wide range in growth rate at each age. The lower value in each body weight and growth range in Table 32 is virtually the average for sheep fed half *ad lib.*, whereas the higher value is the extreme for sheep fed *ad lib.* Therefore, if the simulated empty body weight or its growth are exceeding their respective upper limits, it can be assumed the sheep is growing at a rate that is inconsistent with a reasonable feed intake. This should give some indication of the point where an F_{intake} value of 1.6 becomes infeasible in a real-life situation. Of course, the assumption here is that the model is adequately representing energy expenditure. This assumption is investigated further in Section 7.2. The growth rates in g/day given by Graham, Searle and Griffiths [39] are not instantaneous, but represent average growth in the three weeks leading up to the age given. They are hence referred to as "prior gain".

[1]For Prior gain in Table 32, this is stated in [39] as meaning body weight gain over the

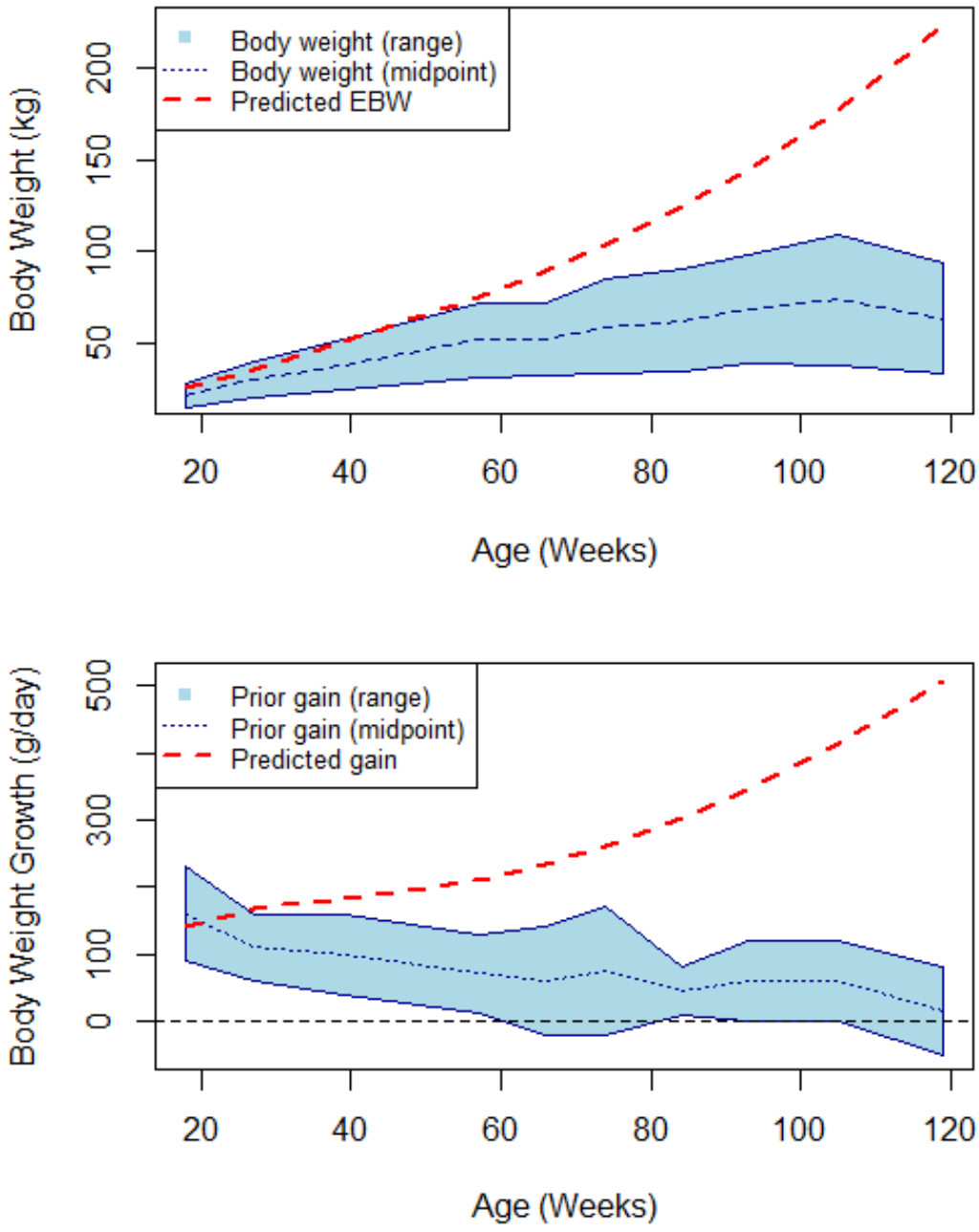

Figure 43: Range and midpoint of body weight and growth from [39] as compared to simulated growth with $F_{intake} = 1.6$.

From Table 32 and Figure 43 it is apparent that predicted empty body weight growth is within the ranges observed by Graham, Searle and Griffiths [39] up until the weeks leading up to an age of 27 weeks. In these weeks, the average predicted gain is 169g/day, whereas the upper limit of that observed in [39] is 160g/day. The predicted growth rate continues to increase as time goes on, whereas the observed growth rate gradually slows, and has reached virtual steady-state by about two years of age. The empty body weight itself stays within the observed body weight range from [39] up until the 57 week mark, but it is clear that the growth before this time exceeds that observed. This is particularly clear in Figure 43. By using linear interpolation between times of measurement, as has been used to determine the range polygons in Figure 43, the upper limit of prior gain in between 18 weeks and 27 weeks of age can be represented as $y = 370 - 70x/9$, where y is growth rate in g/day, and x is age in weeks. Using the average daily simulated growth rate for the three weeks leading up to the age in weeks as the base of comparison, this exceeds the limit at approximately 26.1 weeks. At this point, the upper limit in observed growth is estimated at 167g/day, and the predicted growth rate for the three weeks leading up to 26.1 weeks of age is 167.1g/day.

7.2 Nutrient Intake and Energy Expenditure

For the purposes of testing the model's ability to replicate a basic growth pattern into adulthood, the F_{intake} value was set to 1.6 up until 26 weeks of age, corresponding to a model time of $t = 98$, a week prior to the simulated growth being identified as outside the ranges observed by Graham, Searle and Griffiths [39] in the previous Section. The F_{intake} was set to 1, designed to represent maintenance, at two years of age, which corresponds to a model time of $t = 644$. A linear function between these two points was used to represent a gradual decrease in feed intake as a multiple of maintenance. Therefore the F_{intake} was defined as piecewise linear, as represented in Equation (94), where t is model time. The model was run to two years of age (terminal time $t = 644$), so is expected to be approaching steady-state at the end of the time period. To clarify, in this example the optimsation functionality of MISER3.3 is still disabled, and no control variable is used. As can be seen in Figure 44, the storage triacylglycerol (T_s) is increasing rapidly at the end of the period despite F_{intake} approaching one - which is supposed to be the maintenance feed rate. The values of protein in carcass (P_b), protein in viscera (P_v) and protein in other tissues (P_z) all *decrease* before F_{intake} reaches the maintenance value, and then have a subsequent increase

previous few weeks. To aid comparison, average growth over the previous three weeks is used in the Predicted gain.

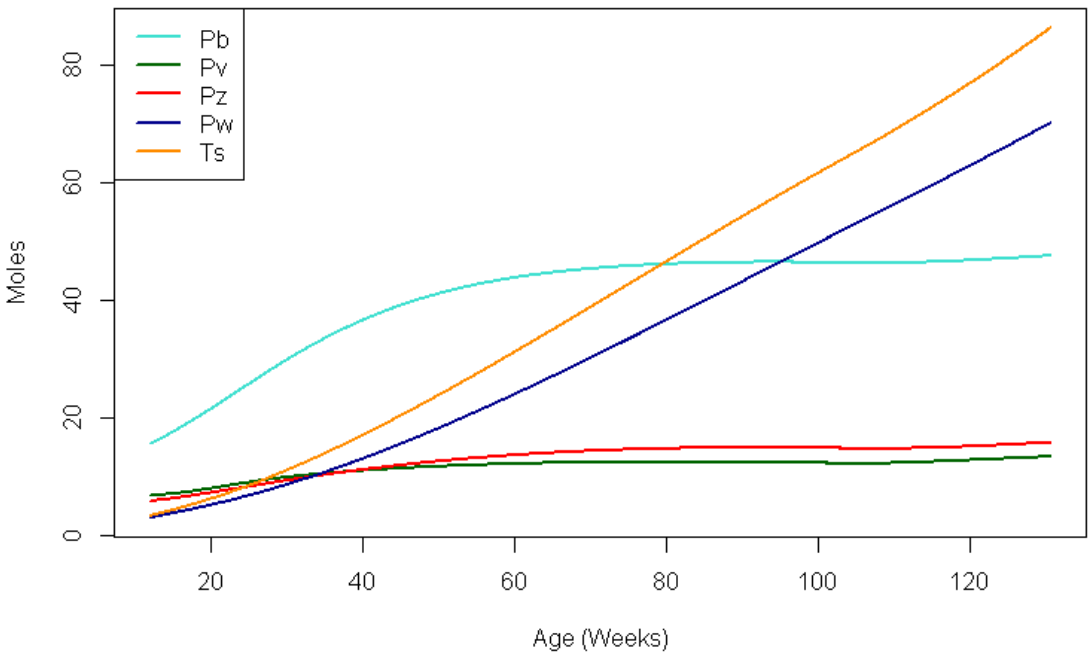

Figure 44: Storage triacylglycerol (Ts) and protein growth with F_{intake} as defined in Equation (94).

towards the end of the period. What can be inferred from this result, is that an F_{intake} of one may be too high to represent maintenance in some instances, and that protein degradation can occur with an F_{intake} variable that is greater than one. This highlights potential issues with both the definition of F_{intake}, and the values of $K_{carcass}$, $K_{viscera}$ and K_{other}, protein degradation (energy expenditure) parameters.

$$F_{intake} = \begin{cases} 1.6, & 0 \leq t < 98, \\ \frac{111}{65} - \frac{t}{910}, & 98 \leq t < 644, \\ 1, & t \geq 644. \end{cases} \tag{94}$$

Ideally, by the end of the two-year period, the sheep should be approaching a steady-state. Therefore an optimal parameter selection problem arises, with the protein degradation parameters to be adjusted. Due to the uncertainty surrounding the F_{intake} parameter, this is modified to a piecewise linear continuous control with nodes at $t = 98$ and $t = 644$. The objective functional to be minimised is defined as the sum of squares of the rates of change of the variables contributing to empty body weight (protein in carcass, viscera and other tissues, as well as storage triacylglycerol) at the end of the time period. In other words, the aim is to drive the model towards a point where the protein pools and the storage triacylglycerol level out as one would expect at steady-state. The optimal control problem described here is formulated in Section 7.2.1 as follows.

7.2.1 Aiming for Steady-State - Optimal Parameter Selection of $K_{carcass}$, $K_{viscera}$ and K_{other} with Optimal Control of F_{intake}

As discussed in Section 7.2, as the feed intake nears one, storage triacylglycerol, and subsequently empty body weight, is still increasing rapidly. This suggests that F_{intake} may not represent maintenance when it is equal to one. It was also identified that protein in carcass, viscera and other tissues degraded while F_{intake} was greater than one, suggesting that the protein degradation parameters of $K_{carcass}$, $K_{viscera}$ and K_{other} may need some adjustment. As shown in Graham, Searle and Griffiths [39], steady-state is expected to be reached at about 2 years of age. Thus we set up an objective functional such that the rates of change of the state variables contributing to empty body weight (the protein pools mentioned above, plus storage triacylglycerol) at the end of the time period are being minimised (with the aim of driving them to zero). Therefore the objective functional is defined as:

Minimise

$$g(u(t), \mathbf{z}) = \Sigma_{i=1}^{12} a_i \left(f_i(T)\right)^2,$$

where

$$a_i \geq 0, \ i = 1, 2, \ldots, 12.$$

The state variables are

$$\mathbf{x} = [Aa, Gl, Tg, Ac, Pb, Pv, Pz, Pw, Ts, Db, Dv, Dz]^\top,$$

and

$$\mathbf{f} = \frac{d\mathbf{x}}{dt} = \left[\frac{dAa}{dt}, \frac{dGl}{dt}, \frac{dTg}{dt}, \frac{dAc}{dt}, \frac{dPb}{dt}, \frac{dPv}{dt}, \frac{dPz}{dt}, \frac{dPw}{dt}, \frac{dTs}{dt}, \frac{dDb}{dt}, \frac{dDv}{dt}, \frac{dDz}{dt}\right]^\top,$$

are the state dynamics as defined in Equations (58) through (65),

$$\mathbf{x}(0) = \big[0.01131, 0.01447, 9.605 \times 10^{-3}, 3.772 \times 10^{-3}, 15.727, 7.0709,$$

$$5.972, 3.167, 3.493, 6.144 \times 10^{-3}, 7.628 \times 10^{-3}, 4.53 \times 10^{-3}\big]^\top, \qquad (95)$$

$$t \in [0, T], \text{ where } T = 644. \qquad (96)$$

System parameters are defined as

$$\mathbf{z} = [K_{carcass}, K_{viscera}, K_{other}]^\top,$$

subject to

$$\begin{aligned} 0.25 \leq K_{carcass} \leq 0.68, \\ 0.97 \leq K_{viscera} \leq 3.92, \\ 0.485 \leq K_{other} \leq 1.94, \end{aligned} \tag{97}$$

with a single control variable of

$$u(t) = F_{intake},$$

where F_{intake} is piecewise linear across two fixed intervals, the values at the end points of these intervals ($t = 0$, $t = 98$ and $t = 644$) are subject to:

$$\begin{aligned} 1.3 \leq F_{intake_{t=0}} \leq 1.6, \\ 1.1 \leq F_{intake_{t=98}} \leq 1.5, \\ 0.85 \leq F_{intake_{t=644}} \leq 1.1. \end{aligned} \tag{98}$$

The model parameters referenced in Equations (58) through (65), with the exception of $V'_{AaPw} = 3.0405$ and those in $\mathbf{z}$, are as defined in Table 43. The model parameters, system parameters and the control variable influence the dynamics of the model as specified within Equations (58) through (65). The weights of the objective functional terms are:

$$\mathbf{a} = [0, 0, 0, 0, 1, 1, 1, 0, 1, 0, 0, 0]^\top,$$

such that the objective functional can be simplified to:

$$g(u(t), \mathbf{z}) = \left(\frac{dPb}{dt}(T)\right)^2 + \left(\frac{dPv}{dt}(T)\right)^2 + \left(\frac{dPz}{dt}(T)\right)^2 + \left(\frac{dTs}{dt}(T)\right)^2. \tag{99}$$

Initial state variable values, with the exception of Pw, are as derived from Sainz and Wolff [83] and given with more significant figures in Table 25. The initial condition for Pw is as derived in Section 6.2 and the parameter V'_{AaPw} is as derived in Section 4.2.1. Completely open ranges for $K_{carcass}$, $K_{viscera}$ and K_{other} tend to cause a numerical problem in that the underlying optimisation routine in MISER3.3 will often choose parameter values far from the initial guess which, in turn, can lead to an unreasonable model that fails to integrate. Hence, allowable ranges were initially defined as between half and double the original values given by Sainz and Wolff [83] (see Table 43 in Appendix A). Some iterations of adjustments of these initial ranges of the energy expenditure parameters were necessary in order to achieve convergence to a solution such that that solution

did not yield an optimal parameter value at one of the bounds of the range used. Details of the allowable range used for the energy expenditure parameters in the final iteration are given in Equation (97).

The control F_{intake} is assumed to be piecewise linear, and follows a similar set-up as used in Section 7.2, with an initial high value for growth which decreases linearly (with the aim of approaching maintenance incrementally). The values of F_{intake} were also subject to bounds which were adjusted incrementally in order to avoid model integration failure. As for the energy expenditure parameters, this incremental process was continued until the final optimal solution for the F_{intake} values was in the interior of the allowed range. The restrictions for the values of F_{intake} used in the final iteration are given in Equation (98).

The optimal solution of (99) obtained was:

$$\begin{aligned} g^* = \; & (1.443 \times 10^{-4})^2 + (-1.185 \times 10^{-5})^2 + (-2.741 \times 10^{-4})^2 \\ & + (-3.480 \times 10^{-7})^2 \\ = \; & 9.61 \times 10^{-8}, \end{aligned} \tag{100}$$

where

$$\begin{aligned} K_{carcass} &= 0.4769, \\ K_{viscera} &= 1.971, \\ K_{other} &= 1.001, \end{aligned} \tag{101}$$

and

$$F_{intake} = \begin{cases} 1.3915 - (2.749 \times 10^{-3)}t, & 0 \leq t < 98, \\ 1.1524 - (3.09 \times 10^{-4})t, & 98 \leq t < 644, \\ 0.9534, & t \geq 644. \end{cases} \tag{102}$$

The growth trajectories of the protein variables and storage triacylglycerol from the optimal solution are presented in Figure 45. The variables that contribute to the empty body weight have evened out over the time period, and the ranges for F_{intake} seem to be reasonable given its definition as multiples of maintenance, but the manner in which the feed is distributed to different pools in the body may be a limiting constraint. It can be seen in Figure 46, that whilst the levels of amino acids and glucose are relatively stable, lipids are increasing rapidly towards the end of the time period and acetate is also increasing. It follows that the optimal solution obtained with the constraints of this problem, which include the model structure and values of other parameters, has not resulted in a steady-state across all the state variables.

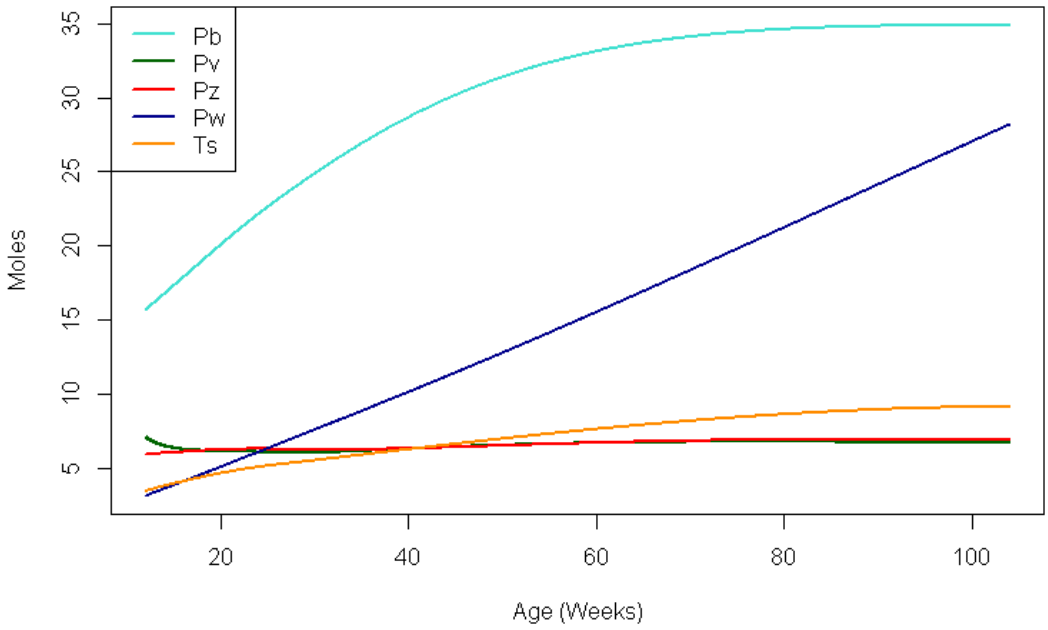

Figure 45: Storage triacylglycerol (Ts) and protein growth with F_{intake} as defined in Equation (102) and protein degradation parameters with values as given in Equation (101).

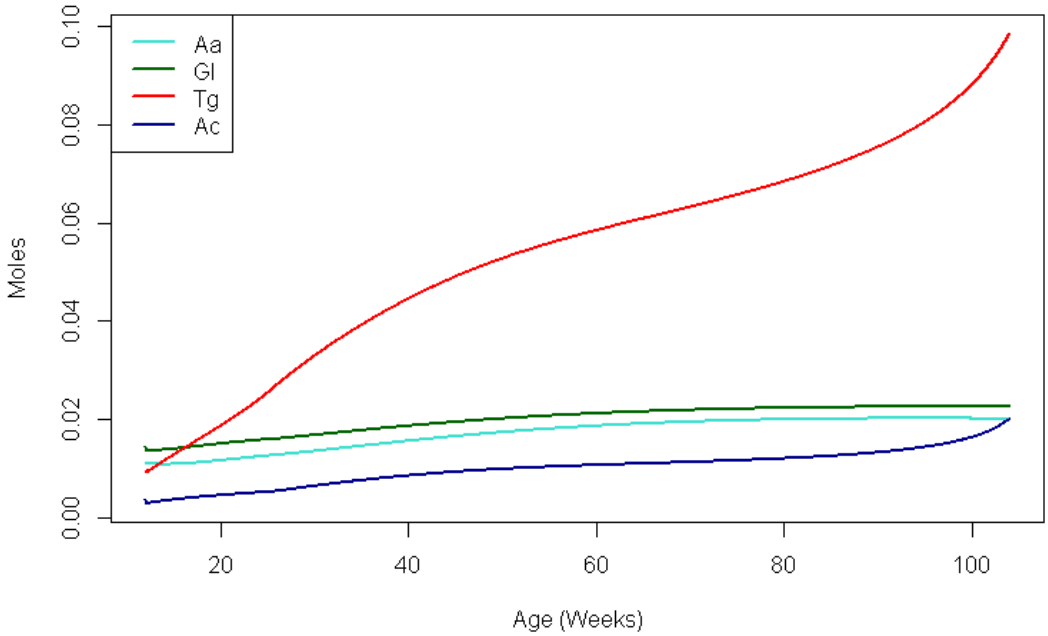

Figure 46: Circulating amino acids (Aa), glucose (Gl), lipids (Tg) and acetate (Ac) with F_{intake} as defined in Equation (102) and protein degradation parameters with values as given in Equation (101).

The parameters D_{Tg} and D_{Ac} control the rate at which lipids and acetate are absorbed into the body, as shown in Equations (103) and (104), and are set by Sainz and Wolff [83] to values of 5.56×10^{-4} and 0.176 respectively. However, it is not known whether these values presented in their paper are rounded in some way. If the model is particularly sensitive, this could have an impact. It is certainly clear that these parameters are based on empirical results from other studies. A similar optimal control and optimal parameter selection problem, including D_{Tg} and D_{Ac} as system parameters, is outlined in the following Section.

$$A_{Tg} = F_{intake} D_{Tg} W_{EB}^{0.75}. \tag{103}$$

$$A_{Ac} = F_{intake} D_{Ac} W_{EB}^{0.75}. \tag{104}$$

7.2.2 Aiming for Steady-State - Optimal Parameter Selection of $K_{carcass}$, $K_{viscera}$, K_{other}, D_{Tg} and D_{Ac} with Optimal Control of F_{intake}

We modify the problem considered in the previous Section by including D_{Tg} and D_{Ac} as system parameters. The resulting problem is defined as:

Minimise

$$g(u(t), \mathbf{z}) = \Sigma_{i=1}^{12} a_i \left(f_i(T)\right)^2,$$

where

$$a_i \geq 0, \ i = 1, 2, \ldots, 12.$$

The state variables are

$$\mathbf{x} = [Aa, Gl, Tg, Ac, Pb, Pv, Pz, Pw, Ts, Db, Dv, Dz]^\top,$$

and

$$\mathbf{f} = \frac{d\mathbf{x}}{dt} = \left[\frac{dAa}{dt}, \frac{dGl}{dt}, \frac{dTg}{dt}, \frac{dAc}{dt}, \frac{dPb}{dt}, \frac{dPv}{dt}, \frac{dPz}{dt}, \frac{dPw}{dt}, \frac{dTs}{dt}, \frac{dDb}{dt}, \frac{dDv}{dt}, \frac{dDz}{dt}\right]^\top,$$

are the state dynamics as defined in Equations (58) through (65),

$$\mathbf{x}(0) = \big[0.01131, 0.01447, 9.605 \times 10^{-3}, 3.772 \times 10^{-3}, 15.727, 7.0709,$$

$$5.972, 3.167, 3.493, 6.144 \times 10^{-3}, 7.628 \times 10^{-3}, 4.53 \times 10^{-3}\big]^\top, \tag{105}$$

$$t \in [0, T], \text{ where } T = 644. \tag{106}$$

System parameters are defined as

$$\mathbf{z} = [K_{carcass}, K_{viscera}, K_{other}, D_{Tg}, D_{Ac}]^\top,$$

subject to

$$\begin{aligned} 0.25 \leq K_{carcass} \leq 0.68, \\ 0.97 \leq K_{viscera} \leq 3.92, \\ 0.485 \leq K_{other} \leq 1.94, \\ 5.55 \times 10^{-4} \leq D_{Tg} \leq 5.57 \times 10^{-4}, \\ 0.175 \leq D_{Ac} \leq 0.177, \end{aligned} \tag{107}$$

with a single control variable of

$$u(t) = F_{intake},$$

where F_{intake} is piecewise linear across two fixed intervals, the values at the end points of these intervals ($t = 0$, $t = 98$ and $t = 644$) are subject to the same constraints as used in Section 7.3.1:

$$\begin{aligned} 1.3 \leq F_{intake_{t=0}} \leq 1.6, \\ 1.1 \leq F_{intake_{t=98}} \leq 1.5, \\ 0.85 \leq F_{intake_{t=644}} \leq 1.1. \end{aligned} \tag{108}$$

The model parameters referenced in Equations (58) through (65), with the exception of $V'_{AaPw} = 3.0405$ and those in $\mathbf{z}$, are as defined in Table 43. The model parameters, system parameters and the control variable influence the dynamics of the model as specified within Equations (58) through (65). The weights of the objective functional terms are:

$$\mathbf{a} = [0, 0, 0, 0, 1, 1, 1, 0, 1, 0, 0, 0]^\top,$$

such that the objective functional can be simplified to:

$$g(u(t), \mathbf{z}) = \left(\frac{dPb}{dt}(T)\right)^2 + \left(\frac{dPv}{dt}(T)\right)^2 + \left(\frac{dPz}{dt}(T)\right)^2 + \left(\frac{dTs}{dt}(T)\right)^2. \tag{109}$$

The optimal solution of (109), which was on the interior of the bounds, was:

$$\begin{aligned} g^* = \; & (1.534 \times 10^{-4})^2 + (-1.330 \times 10^{-5})^2 + (-2.689 \times 10^{-4})^2 \\ & + (-1.081 \times 10^{-6})^2 \\ = \; & 9.60 \times 10^{-8}, \end{aligned} \tag{110}$$

where

$$\begin{aligned} K_{carcass} &= 0.4731, \\ K_{viscera} &= 1.970, \\ K_{other} &= 1.001, \\ D_{Tg} &= 5.554 \times 10^{-4}, \\ D_{Ac} &= 0.17502, \end{aligned} \tag{111}$$

and

$$F_{intake} = \begin{cases} 1.3908 - (2.739 \times 10^{-3)}t, & 0 \leq t < 98, \\ 1.1525 - (3.075 \times 10^{-4})t, & 98 \leq t < 644, \\ 0.9544, & t \geq 644. \end{cases} \tag{112}$$

As the solution is very similar to that achieved in 7.2.1, a subsequent version of this optimal control problem was run, widening the bounds for D_{Tg} and D_{Ac}. The bounds were initially set as varying five per cent on either side of the original values of these parameters (5.56×10^{-4} for D_{Tg} and 0.176 for D_{Ac}), but were incrementally widened to yield an optimal solution on the interior of the bounds. The resulting bounds used are presented in Equation (115). This problem can be defined as:

Minimise

$$g(u(t), \mathbf{z}) = \Sigma_{i=1}^{12} a_i \left(f_i(T)\right)^2,$$

where

$$a_i \geq 0, \ i = 1, 2, \ldots, 12.$$

The state variables are

$$\mathbf{x} = [Aa, Gl, Tg, Ac, Pb, Pv, Pz, Pw, Ts, Db, Dv, Dz]^\top,$$

and

$$\mathbf{f} = \frac{d\mathbf{x}}{dt} = \left[\frac{dAa}{dt}, \frac{dGl}{dt}, \frac{dTg}{dt}, \frac{dAc}{dt}, \frac{dPb}{dt}, \frac{dPv}{dt}, \frac{dPz}{dt}, \frac{dPw}{dt}, \frac{dTs}{dt}, \frac{dDb}{dt}, \frac{dDv}{dt}, \frac{dDz}{dt}\right]^\top,$$

are the state dynamics as defined in Equations (58) through (65),

$$\mathbf{x}(0) = \big[0.01131, 0.01447, 9.605 \times 10^{-3}, 3.772 \times 10^{-3}, 15.727, 7.0709,$$

$$5.972, 3.167, 3.493, 6.144 \times 10^{-3}, 7.628 \times 10^{-3}, 4.53 \times 10^{-3}\big]^\top, \tag{113}$$

$$t \in [0, T], \text{ where } T = 644. \tag{114}$$

System parameters are defined as

$$\mathbf{z} = [K_{carcass}, K_{viscera}, K_{other}, D_{Tg}, D_{Ac}]^\top,$$

subject to

$$\begin{aligned} 0.25 \leq K_{carcass} \leq 0.68, \\ 0.97 \leq K_{viscera} \leq 3.92, \\ 0.485 \leq K_{other} \leq 1.94, \\ 5.282 \times 10^{-4} \leq D_{Tg} \leq 5.838 \times 10^{-4}, \\ 0.1590 \leq D_{Ac} \leq 0.1848, \end{aligned} \tag{115}$$

with a single control variable of

$$u(t) = F_{intake},$$

where F_{intake} is piecewise linear across two fixed intervals, the values at the end points of these intervals ($t = 0$, $t = 98$ and $t = 644$) are subject to the same constraints as used in Section 7.3.1:

$$\begin{aligned} 1.3 \leq F_{intake_{t=0}} \leq 1.6, \\ 1.1 \leq F_{intake_{t=98}} \leq 1.5, \\ 0.85 \leq F_{intake_{t=644}} \leq 1.1. \end{aligned} \tag{116}$$

The model parameters referenced in Equations (58) through (65), with the exception of $V'_{AaPw} = 3.0405$ and those in $\mathbf{z}$, are as defined in Table 43. The model parameters, system parameters and the control variable influence the dynamics of the model as specified within Equations (58) through (65). The weights of the objective functional terms are:

$$\mathbf{a} = [0, 0, 0, 0, 1, 1, 1, 0, 1, 0, 0, 0]^\top,$$

such that the objective functional can be simplified to:

$$g(u(t), \mathbf{z}) = \left(\frac{dPb}{dt}(T)\right)^2 + \left(\frac{dPv}{dt}(T)\right)^2 + \left(\frac{dPz}{dt}(T)\right)^2 + \left(\frac{dTs}{dt}(T)\right)^2. \tag{117}$$

The optimal solution of (117), which was on the interior of the bounds, was:

$$\begin{aligned} g^* = \; & (1.526 \times 10^{-4})^2 + (-1.049 \times 10^{-5})^2 + (-2.634 \times 10^{-4})^2 \\ & + (-7.337 \times 10^{-8})^2 \\ = \; & 9.28 \times 10^{-8}, \end{aligned} \tag{118}$$

where

$$\begin{aligned} K_{carcass} &= 0.4071, \\ K_{viscera} &= 1.956, \\ K_{other} &= 0.9863, \\ D_{Tg} &= 5.307 \times 10^{-4}, \\ D_{Ac} &= 0.1591, \end{aligned} \tag{119}$$

and

$$F_{intake} = \begin{cases} 1.3930 - (2.650 \times 10^{-3)}t, & 0 \leq t < 98, \\ 1.1638 - (3.107 \times 10^{-4})t, & 98 \leq t < 644, \\ 0.9637, & t \geq 644. \end{cases} \tag{120}$$

When comparing this result with that in Section 7.2.1, it can be noted that the optimal solution has only decreased by about 3.4%. The final growth of the body protein and storage triacylglycerol variables, with the exception of carcass protein, is marginally closer to steady-state, but the issue with very sharp final growth of lipids and the high final growth of acetate remains. The tick-like behaviour for acetate shown in Figure 48 also indicates that this solution is only feasible with a lowering of the initial condition for acetate.

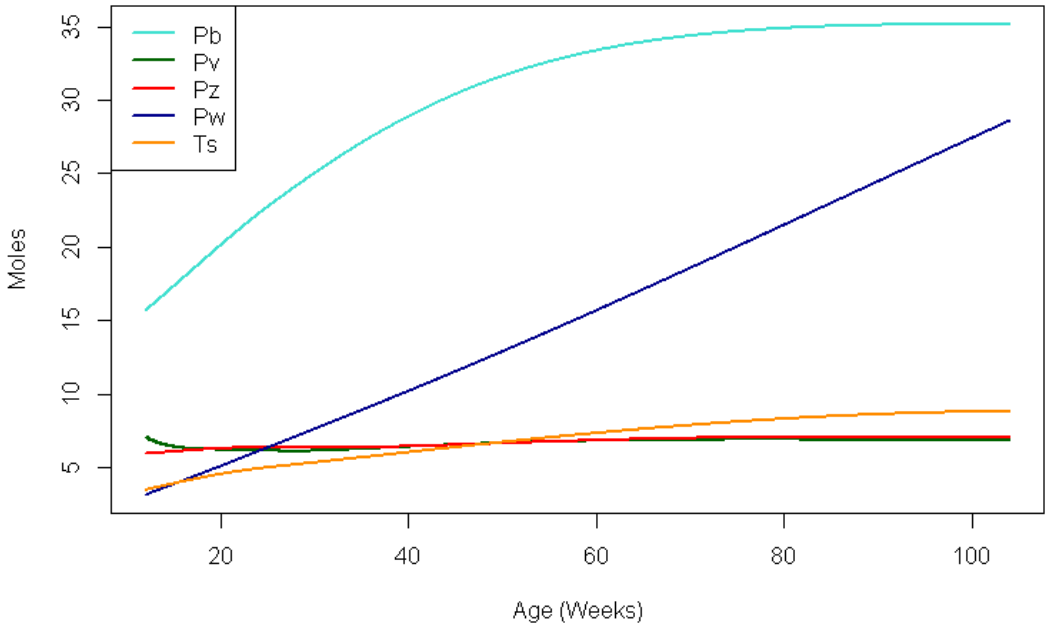

Figure 47: Storage triacylglycerol (Ts) and protein growth with F_{intake} as defined in Equation (120) and system parameters with values as given in Equation (119).

Several options for progression from this optimal control problem were considered. Problems that included the five system parameters outlined here, as well

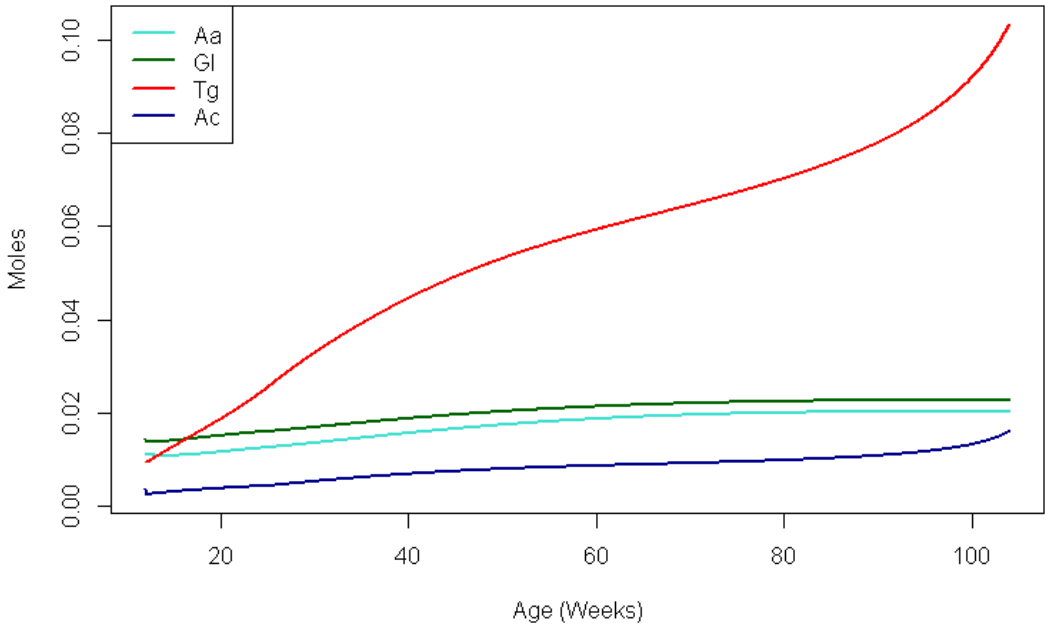

Figure 48: Circulating amino acids (Aa), glucose (Gl), lipids (Tg) and acetate (Ac) with F_{intake} as defined in Equation (120) and system parameters with values as given in Equation (119).

as a $(\frac{dTg}{dt})^2$ term in the objective functional (with various weights on this term) either failed to make an impact on the result (where the weight was perhaps too low), or resulted in final growth of acetate well beyond a reasonable level. Adding a $(\frac{dAc}{dt})^2$ term to the objective functional was not possible due to convergence errors. Therefore, scenarios with additional model parameters added to the system parameters were considered, with those related to the oxidation (output) of Tg and Ac potentially being the key to a steady-state solution for all state variables.

7.3 Nutrient Intake, Oxidation and Energy Expenditure

The previous Section (7.2) made progress towards defining control and system parameter selections that may produce a growth model for sheep that could extend into steady-state. The main issues that remain following these results are continual growth of circulating lipids and, to a lesser extent, acetate. Whilst the system parameters of D_{Tg} and D_{Ac} allowed for some variation in the way the feed intake is distributed to these pools, it may be beneficial to also include parameters relating to the utilisation of these nutrients. For both lipids and acetate, the two types of utilisation present in their respective dynamics are in lipogenesis (conversion to storage fat) and oxidation (conversion to carbon dioxide, an output of the body). By focussing on the oxidation of these nutrients, the adjustments

made to the relevant parameters should provide an outlet external to the body rather than to storage fat. Conceptually, an increase near the end of the time period in $U_{Tg,TgCd}$ and/or $U_{Ac,AcCd}$ may solve the growth issues for these nutrients. However, the model is complex and it should also be noted that acetate is *produced* in the $Tg \rightarrow Cd$ reaction. The logical choices for additional system parameters are the Michaelis-Menton constants of k_{TgCd} and k_{AcCd}, which were initially set at 0.0038 and 0.001 by Sainz and Wolff [83]. The optimal control problems in this Section have these two model parameters added to the system parameters.

7.3.1 Aiming for Steady-State - Optimal Parameter Selection of $K_{carcass}$, $K_{viscera}$, K_{other}, D_{Tg}, D_{Ac}, k_{TgCd} and k_{AcCd} with Optimal Control of F_{intake}

With the additional system parameters of k_{TgCd} and k_{AcCd}, the resulting problem may be defined as:

Minimise

$$g(u(t), \mathbf{z}) = \Sigma_{i=1}^{12} a_i \left(f_i(T)\right)^2,$$

where

$$a_i \geq 0, \ i = 1, 2, \ldots, 12.$$

The state variables are

$$\mathbf{x} = [Aa, Gl, Tg, Ac, Pb, Pv, Pz, Pw, Ts, Db, Dv, Dz]^\top,$$

and

$$\mathbf{f} = \frac{d\mathbf{x}}{dt} = \left[\frac{dAa}{dt}, \frac{dGl}{dt}, \frac{dTg}{dt}, \frac{dAc}{dt}, \frac{dPb}{dt}, \frac{dPv}{dt}, \frac{dPz}{dt}, \frac{dPw}{dt}, \frac{dTs}{dt}, \frac{dDb}{dt}, \frac{dDv}{dt}, \frac{dDz}{dt}\right]^\top,$$

are the state dynamics as defined in Equations (58) through (65),

$$\mathbf{x}(0) = \big[0.01131, 0.01447, 9.605 \times 10^{-3}, 3.772 \times 10^{-3}, 15.727, 7.0709,$$

$$5.972, 3.167, 3.493, 6.144 \times 10^{-3}, 7.628 \times 10^{-3}, 4.53 \times 10^{-3}\big]^\top, \quad (121)$$

$$t \in [0, T], \text{ where } T = 644. \quad (122)$$

System parameters are defined as

$$\mathbf{z} = [K_{carcass}, K_{viscera}, K_{other}, D_{Tg}, D_{Ac}, k_{TgCd}, k_{AcCd}]^\top,$$

with a single control variable of

$$u(t) = F_{intake},$$

where F_{intake} is piecewise linear across two fixed intervals. Constraints on the values at the end points of these intervals ($t = 0$, $t = 98$ and $t = 644$), as well as the constraints on the system parameters z are given in Table 33.

The model parameters referenced in Equations (58) through (65), with the exception of $V'_{AaPw} = 3.0405$ and those in $\mathbf{z}$, are as defined in Table 43. The model parameters, system parameters and the control variable influence the dynamics of the model as specified within Equations (58) through (65). The weights of the objective functional terms are:

$$\mathbf{a} = [0, 0, 0, 0, 1, 1, 1, 0, 1, 0, 0, 0]^\top,$$

such that the objective functional can be simplified to:

$$g(u(t), \mathbf{z}) = \left(\frac{dPb}{dt}(T)\right)^2 + \left(\frac{dPv}{dt}(T)\right)^2 + \left(\frac{dPz}{dt}(T)\right)^2 + \left(\frac{dTs}{dt}(T)\right)^2. \quad (123)$$

An optimal solution on the interior of the bounds resulted for (123):

$$\begin{aligned} g^* = \; & (1.324 \times 10^{-4})^2 + (1.331 \times 10^{-5})^2 + (-2.597 \times 10^{-4})^2 \\ & + (-3.477 \times 10^{-6})^2 \\ = \; & 8.52 \times 10^{-8}, \end{aligned} \quad (124)$$

where optimal parameter and control selection is given in Table 33. This results in the piecewise linear definition of F_{intake} as given in Equation (125).

$$F_{intake} = \begin{cases} 1.478 - (3.484 \times 10^{-3)}t, & 0 \leq t < 98, \\ 1.166 - (3.037 \times 10^{-4})t, & 98 \leq t < 644, \\ 0.971 & t \geq 644. \end{cases} \quad (125)$$

When comparing this result with that of Section 7.2.2, it can be noted that the optimal solution is 8.2% lower, at just 8.52×10^{-8}. The final growth of the body protein and the storage fat variables is very close to steady-state. The cost of this is that the final growth in lipids and acetate is even higher than they were in the result from 7.2.2, with the final value of lipids also being greater than

Term	Lower Bound	Initial Value	Upper Bound	Optimal
$K_{carcass}$	0.25	0.3596	0.68	0.3598
$K_{viscera}$	0.97	1.9448	3.92	1.9448
K_{other}	0.485	0.9745	1.94	0.9745
D_{Tg}	4.5×10^{-4}	4.5035×10^{-4}	6.0×10^{-4}	4.9387×10^{-4}
D_{Ac}	0.14	0.1500	0.20	0.1496
k_{TgCd}	3.4×10^{-3}	4.0903×10^{-3}	4.2×10^{-3}	3.8582×10^{-3}
k_{AcCd}	7.0×10^{-4}	1.0000×10^{-3}	1.1×10^{-3}	7.6948×10^{-4}
$F_{intake_{t=0}}$	1.40	1.4779	1.60	1.4779
$F_{intake_{t=98}}$	1.10	1.1365	1.30	1.1365
$F_{intake_{t=644}}$	0.85	0.9708	1.00	0.9707

Table 33: Initial values, bounds and optimal solution results for system parameters and feed intake values for problem 7.3.1.

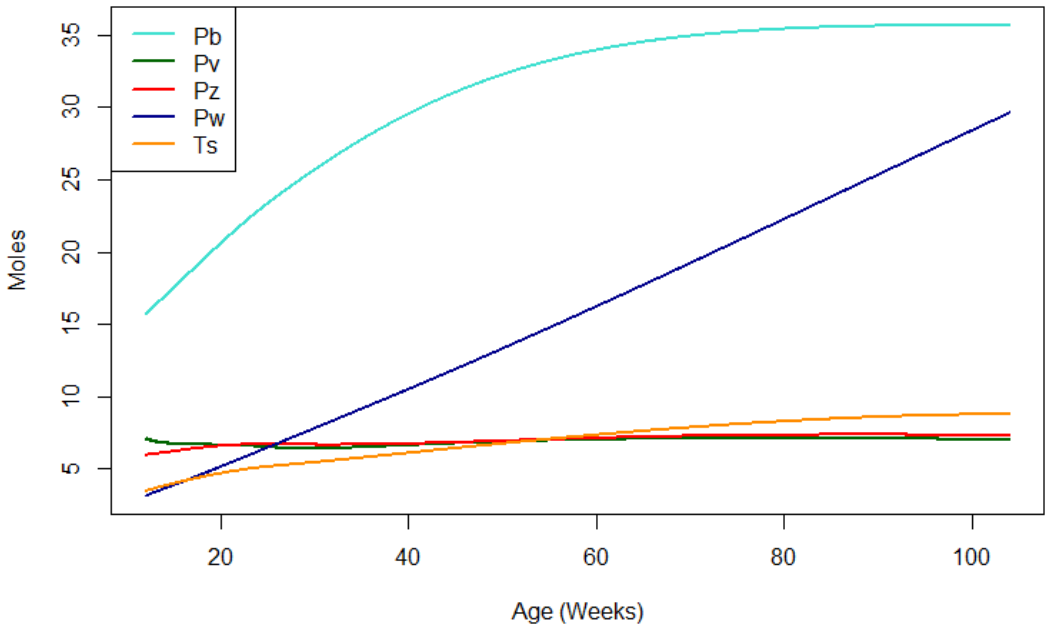

Figure 49: Storage triacylglycerol (Ts) and protein growth with F_{intake} as defined in Equation (125) and system parameters with values as given in Table 33.

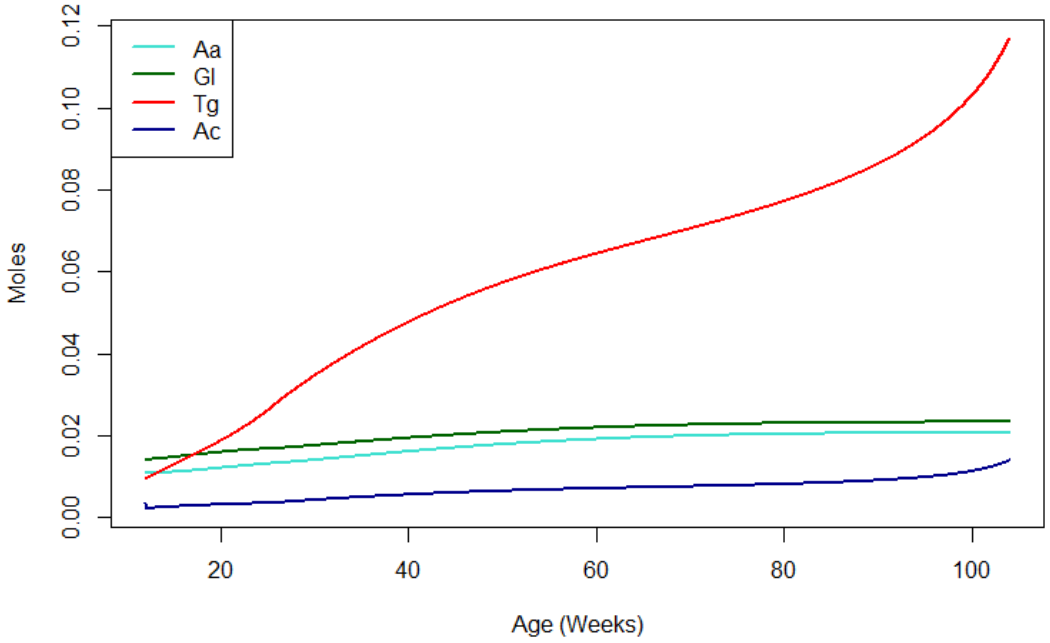

Figure 50: Circulating amino acids (Aa), glucose (Gl), lipids (Tg) and acetate (Ac) with F_{intake} as defined in Equation (125) and system parameters with values as given in Table 33.

has been seen in either of the solutions in Section 7.2. These observations can be noted in both the optimal solution in Equation (124) and Figures 49 and 50. The improvement in the optimal solution from 7.2.1 to 7.2.2 happened to also be associated with an improvement in the final growth and state of lipids and acetate, even without terms relating to these state variables being present in the objective functional. However, this is no longer the case for the results here.

Again, several options for progression from this stage were considered. Due to the instability issues associated with adding more terminal rate terms to the objective, we next look at adding terms that penalise deviation from desired final states.

7.3.2 Aiming for Steady-State and a Desired Final State - Optimal Parameter Selection of $K_{carcass}$, $K_{viscera}$, K_{other}, D_{Tg}, D_{Ac}, k_{TgCd} and k_{AcCd} with Optimal Control of F_{intake}

In this Section, we modify the objective by adding terms which will drive several of the states towards desirable terminal values which correspond to an average adult sheep. In order to find a steady-state solution for all state variables, it is clear that desired final states for Tg and Ac should be implemented. However, it may also be necessary to add desired final state conditions for the state variables

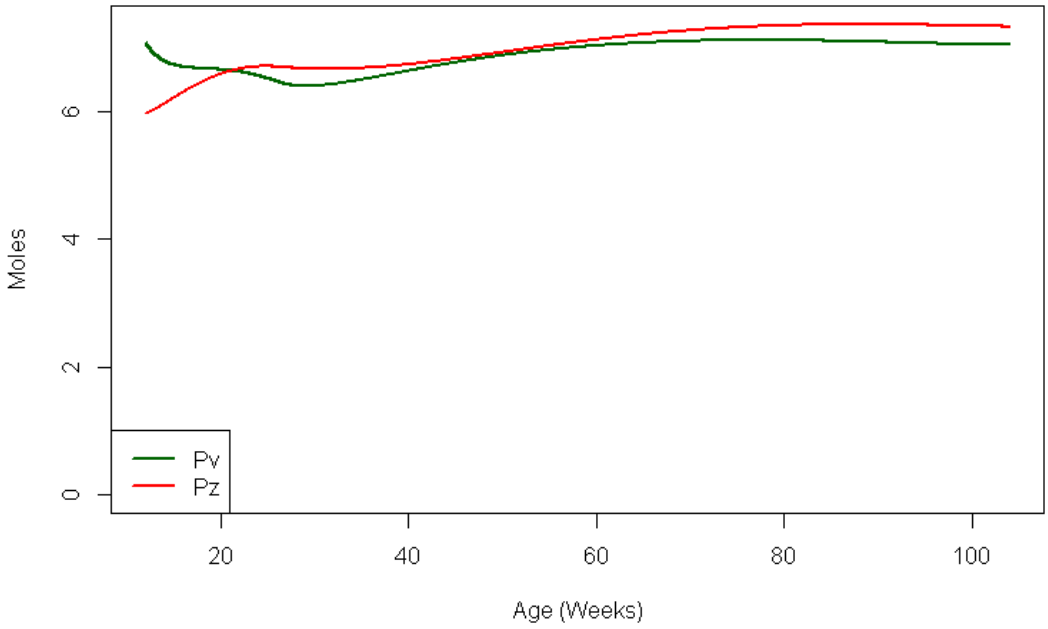

Figure 51: Growth of protein in viscera (Pv) and protein in other tissues (Pz) with F_{intake} as defined in Equation (125) and system parameters with values as given in Table 33.

affecting body weight (Pb, Pv, Pz and Ts) to ensure that the proportions of the body in the steady-state solution are sensible. If we consider the trajectories of protein in viscera (Pv) and protein in other tissues (Pz) from the solution in 7.3.1, a decline in the initial growth for Pv can be identified, and their is also a period of non-growth in Pz. This is more clearly presented in Figure 51, and is indicative of insufficient growth in these protein pools.

The final empty body weight for the solution in 7.3.1 is 38.35kg. If we re-consider the proportions of a 40kg empty body weight sheep according to the Sainz and Wolff [83] model (see Table 26 in Chapter 6), it can be shown that the proportion of body weight that is attributed to the protein pools of Pv and Pz was expected to be considerably higher. The final state values from Section 7.3.1 and their percentage of empty body weight (for Pb, Pv, Pz and Ts) or their percentage of circulating fluids (v_{ECF}, for Aa, Gl, Tg and Ac) are compared with the equivalent statistics from Sainz and Wolff [83] in Table 34. Whilst there are some differences between the two outputs for Aa and Gl, discrepancies are considerably higher (in relative and actual terms) for the other state variables. Therefore, the addition of desired final state terms for Tg, Ac, Pb, Pv, Pz and Ts are considered.

The Sainz and Wolff [83] results for $W_{EB} = 40$kg equates to 40.4kg if Equation (68) is applied. The aim of Sainz and Wolff [83] was to model lamb growth, and it

State Variable	**S&W [83]** W_{EB}**=40kg**	**7.3.1** W_{EB}**=38.35kg**	**S&W [83] % of** W_{EB}/v_{ECF}	**7.3.1 % of** W_{EB}/v_{ECF}
Aa	0.02403mol	0.02054mol	0.2503	0.2140
Gl	0.02858mol	0.02342mol	0.2977	0.2545
Tg	0.02206mol	0.1169mol	0.2298	1.270
Ac	0.00953mol	0.01411mol	0.09927	0.1533
Pb	3.819kg	4.350kg	9.548	11.34
Pv	1.277kg	0.8732kg	3.192	2.277
Pz	1.196kg	0.8943kg	2.990	2.332
Ts	9.755kg	7.477kg	24.39	19.50

Table 34: Final state values for Section 7.3.1 as compared to Sainz and Wolff [83].

State Variable	**S&W [83] % of** W_{EB}/v_{ECF}	**Desired Final State (Rounded)**
Tg	0.2298	0.023mol
Ac	0.09927	0.010mol
Pb	9.548	32mol
Pv	3.192	10.5mol
Pz	2.990	10mol
Ts	24.39	12mol

Table 35: Desired final state values for Section 7.3.2 ($W_{EB} = 41.5$kg) as compared to Sainz and Wolff [83] 40kg sheep attributes.

is unlikely the 40kg was anticipated to be the final sheep adult weight. However, the cautious approach would be to not extrapolate too far from the 40kg end point of Sainz and Wolff. Therefore it is reasonable to aim for a steady-state condition at about 41.5kg, according to our Equation (68). By applying the percentages of either W_{EB} or v_{ECF} to a 41.5kg empty body weight (9.96kg circulating fluid) sheep, and rounding to avoid what would be false precision, desired final states for the selected variables are determined. These are presented in Table 35.

As equal weights for the final growth terms in the objective resulted in low final growth in all of the relevant state variables (Pb, Pv, Pz and Ts) in the previous solutions in this Chapter, this was maintained. The desired final state terms - defined as the square of the difference between the actual and the desired final state - were initially all divided by the desired final state, such that they could be interpreted as equally weighted, and as relative square differences. However, the solution to this problem resulted in a final Ts state significantly larger than its desired final state, and so the $\frac{1}{12}$ weight on the difference term was replaced with 1.

Therefore, the problem is to:

Minimise

$$g(u(t), \mathbf{z}) = \Sigma_{i=1}^{12} \left[a_i \left(f_i(T) \right)^2 + b_i \left(x_i(T) - c_i \right)^2 \right],$$

where

$$a_i \geq 0,\ b_i \geq 0,\ c_i \geq 0,\ i = 1, 2, \ldots, 12.$$

The state variables are

$$\mathbf{x} = [Aa, Gl, Tg, Ac, Pb, Pv, Pz, Pw, Ts, Db, Dv, Dz]^\top,$$

and

$$\mathbf{f} = \frac{d\mathbf{x}}{dt} = \left[\frac{dAa}{dt}, \frac{dGl}{dt}, \frac{dTg}{dt}, \frac{dAc}{dt}, \frac{dPb}{dt}, \frac{dPv}{dt}, \frac{dPz}{dt}, \frac{dPw}{dt}, \frac{dTs}{dt}, \frac{dDb}{dt}, \frac{dDv}{dt}, \frac{dDz}{dt} \right]^\top,$$

are the state dynamics as defined in Equations (58) through (65),

$$\mathbf{x}(0) = \big[0.01131, 0.01447, 9.605 \times 10^{-3}, 3.772 \times 10^{-3}, 15.727, 7.0709,$$

$$5.972, 3.167, 3.493, 6.144 \times 10^{-3}, 7.628 \times 10^{-3}, 4.53 \times 10^{-3}\big]^\top, \quad (126)$$

$$t \in [0, T],\ \text{where } T = 644. \quad (127)$$

System parameters are defined as

$$\mathbf{z} = [K_{carcass}, K_{viscera}, K_{other}, D_{Tg}, D_{Ac}, k_{TgCd}, k_{AcCd}]^\top,$$

with a single control variable of

$$u(t) = F_{intake},$$

where F_{intake} is piecewise linear across two fixed intervals. Constraints on the values at the end points of these intervals ($t = 0$, $t = 98$ and $t = 644$), as well as the constraints on the system parameters z are given in Table 36.

The model parameters referenced in Equations (58) through (65), with the exception of $V'_{AaPw} = 3.0405$ and those in $\mathbf{z}$, are as defined in Table 43. The model parameters, system parameters and the control variable influence the dynamics of the model as specified within Equations (58) through (65). The weights of the objective functional terms are:

$$\mathbf{a} = [0, 0, 0, 0, 1, 1, 1, 0, 1, 0, 0, 0]^\top,$$

$$\mathbf{b} = [0, 0, \frac{1}{0.023}, \frac{1}{0.01}, \frac{1}{32}, \frac{1}{10.5}, \frac{1}{10}, 0, 1, 0, 0, 0]^\top,$$
$$\mathbf{c} = [0, 0, 0.023, 0.01, 32, 10.5, 10, 0, 12, 0, 0, 0]^\top,$$

such that the objective functional can be simplified to:

$$g(u(t), \mathbf{z}) = \left(\frac{dPb}{dt}(T)\right)^2 + \left(\frac{dPv}{dt}(T)\right)^2 + \left(\frac{dPz}{dt}(T)\right)^2 + \left(\frac{dTs}{dt}(T)\right)^2$$
$$+\frac{1}{32}(Pb - 32)^2 + \frac{1}{10.5}(Pv - 10.5)^2 + \frac{1}{10}(Pz - 10)^2 + (Ts - 12)^2$$
$$+\frac{1}{0.023}(Tg - 0.023)^2 + \frac{1}{0.01}(Ac - 0.01)^2. \tag{128}$$

The ideal would be where the solution did not yield an optimal parameter value at one of the bounds. However, this was not achievable in this problem. The optimal solution for (128) was:

$$\begin{aligned} g^* = \; & (3.43 \times 10^{-3})^2 + (1.12 \times 10^{-3})^2 + (1.99 \times 10^{-3})^2 \\ & + (1.51 \times 10^{-2})^2 + \tfrac{1}{32}(40.43 - 32)^2 + \tfrac{1}{10.5}(9.328 - 10.5)^2 \\ & + \tfrac{1}{10}(10.26 - 10)^2 + (12.02 - 12)^2 + \tfrac{1}{0.023}(0.041 - 0.023)^2 \\ & + \tfrac{1}{0.01}(0.004239 - 0.01)^2 \\ = \; & 2.376, \end{aligned} \tag{129}$$

where optimal parameter and control selection is given in Table 36. This results in the piecewise linear definition of F_{intake} as given in Equation (130).

$$F_{intake} = \begin{cases} 1.55 - (1.53 \times 10^{-3)}t, & 0 \le t < 98, \\ 1.418 - (1.831 \times 10^{-4})t, & 98 \le t < 644, \\ 1.30, & t \ge 644. \end{cases} \tag{130}$$

As in Sections 7.2.1, 7.2.2 and 7.3.1, bounds for the system parameters and the values of F_{intake} at the nodes were incrementally adjusted. Details are outlined in Table 36. Note that F_{intake} remains piecewise linear, and follows a similar set-up as used in Section 7.2, with initial high growth decreasing linearly.

Whilst it is not meaningful to compare the optimal objective value as it stands with that in Section 7.3.1, it can be noted that the sum of squares of the final growth for body protein and storage fat in this problem is 2.45×10^{-4}, more than 2,500 times that in 7.3.1 (8.52×10^{-6}). However, the sum of squares of the

Term	Lower Bound	Initial Value	Upper Bound	Optimal
$K_{carcass}$	0.43	0.4602	0.47	0.43
$K_{viscera}$	1.75	1.85	1.95	1.8788
K_{other}	1.02	1.04	1.06	1.02
D_{Tg}	4.2×10^{-4}	4.4×10^{-4}	4.6×10^{-4}	4.2×10^{-4}
D_{Ac}	0.11	0.12	0.13	0.11
k_{TgCd}	5.4×10^{-3}	5.5×10^{-3}	5.6×10^{-3}	5.4×10^{-3}
k_{AcCd}	9.0×10^{-4}	1.0×10^{-3}	1.1×10^{-3}	9.0×10^{-4}
$F_{intake_{t=0}}$	1.55	1.60	1.65	1.55
$F_{intake_{t=98}}$	1.40	1.45	1.50	1.40
$F_{intake_{t=644}}$	1.10	1.20	1.30	1.30

Table 36: Initial values, bounds and optimal solution results for system parameters and feed intake values for problem 7.3.2.

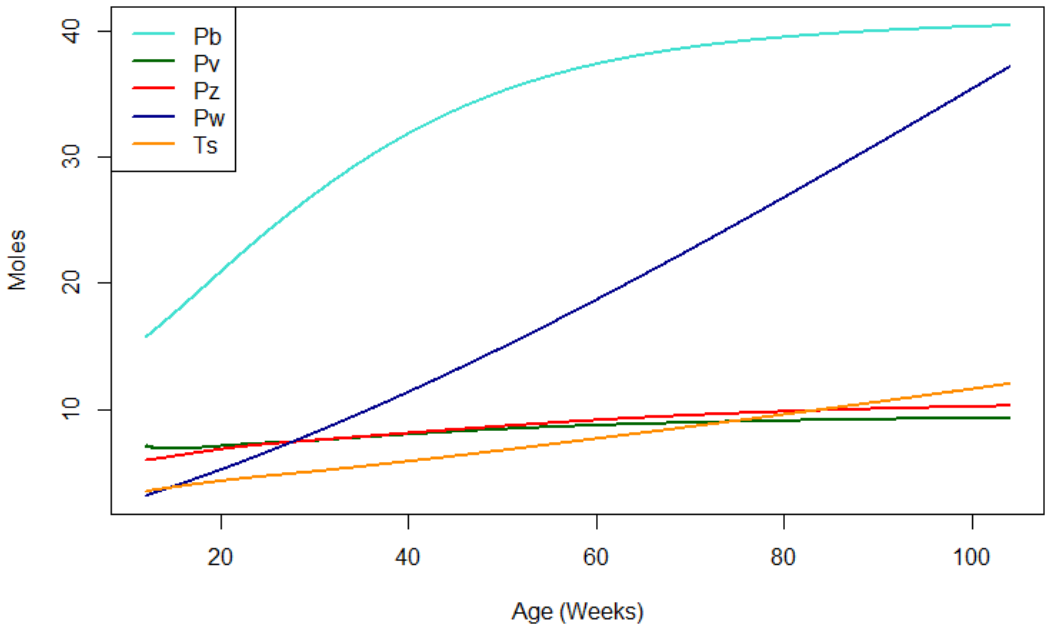

Figure 52: Storage triacylglycerol (Ts) and protein growth with F_{intake} as defined in Equation (130) and system parameters with values as given in Table 36.

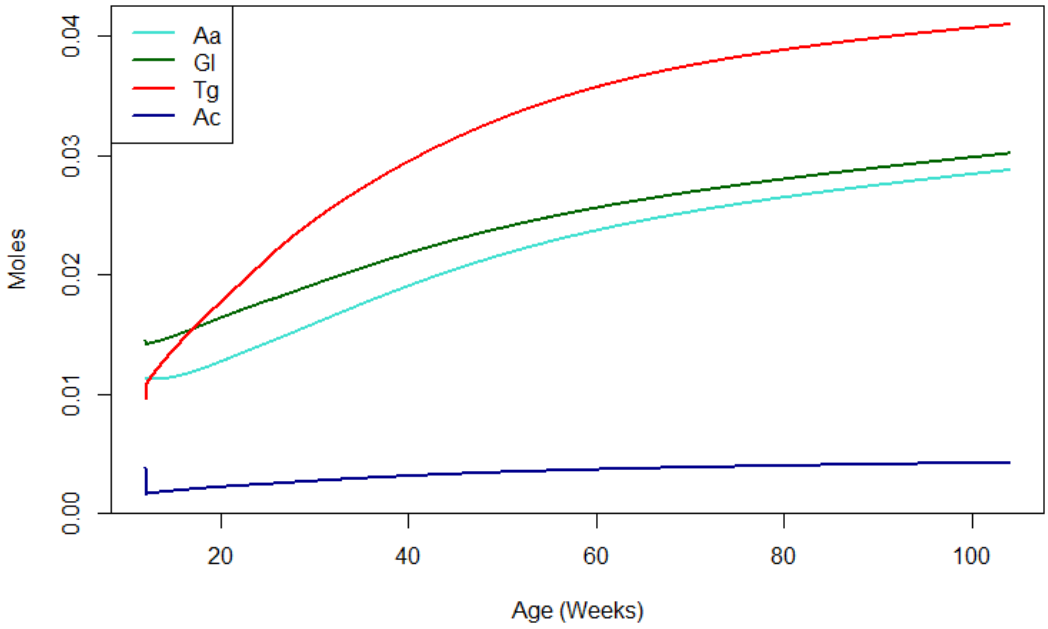

Figure 53: Circulating amino acids (Aa), glucose (Gl), lipids (Tg) and acetate (Ac) with F_{intake} as defined in Equation (130) and system parameters with values as given in Table 36.

final growth of these terms is still very low. Whilst all final growth terms of the body protein and the storage fat have magnitudes further from zero that those in 7.3.1, it is the magnitude of final storage fat growth that differs the greatest. In fact, it is clear from Figure 52 that storage fat is not rounding off to steady-state as neatly as was observed in Figure 49. However, the final growth in lipids and acetate in this solution are approaching steady-state, as can be seen in Figure 53. As was identified in Section 7.2.2, there is tick-like behaviour for acetate (see Figure 53), which indicates that this solution is only feasible with a lowering of the initial condition for acetate.

It can be noted that the final empty body weight is 45.92kg. Whilst this is higher than the intended 41.5kg (all but Pv ended higher than the desired state, for those variables contributing to empty body weight), this is not an unreasonable weight for an average adult sheep. In fact, according to the Department of Agriculture, Fisheries and Forestry in the Queensland Government [90], a typical Queensland adult Merino sheep weighs about 45kg. This may be live weight rather than empty weight, but with some variation expected around the average, and considering the existence of larger breeds of sheep than a Queensland Merino (Wool Producers Australia [104] claim the South Australian Merino as the largest of the strains of Merino in Australia), 45.92kg empty body weight is certainly within a reasonable range for an average adult sheep.

State Variable	**S&W [83]** W_{EB}**=40kg**	**7.3.2** W_{EB}**=45.92kg**	**S&W [83] % of** W_{EB}/v_{ECF}	**7.3.2 % of** W_{EB}/v_{ECF}
Aa	0.02403mol	0.02876mol	0.2503	0.2610
Gl	0.02858mol	0.03016mol	0.2977	0.2737
Tg	0.02206mol	0.04098mol	0.2298	0.3718
Ac	0.00953mol	0.004239mol	0.09927	0.03846
Pb	3.819kg	4.933kg	9.548	10.74
Pv	1.277kg	1.157kg	3.192	2.520
Pz	1.196kg	1.252kg	2.990	2.726
Ts	9.755kg	10.24kg	24.39	22.30

Table 37: Final state values for Section 7.3.2 as compared to Sainz and Wolff [83].

The proportions of all non-DNA state variables, of W_{EB} or v_{ECF} as appropriate, are closer to that for the Sainz and Wolff [83] 40kg sheep than the result from 7.3.1, except for acetate (see Table 37, as it compares to Table 34). Whilst the proportion of acetate to circulating fluids has dropped - it is now less than half of that from Sainz and Wolff [83] - it has been noted throughout the solutions of this Chapter that steady-state only seems to be achievable via a drop in acetate levels. Given that Sainz and Wolff [83] state that originally their model did not include endogenous acetate entry (internally produced), and measures such as inflating the size of the acetate pool by 100-fold were considered in order to stabilse the acetate pool, a variation of this magnitude from that presented by Sainz and Wolff [83] for final acetate levels is not a cause for immediate concern. When comparing Figure 54 with Figure 51, it can also be noted that the growth trajectories for Pv and Pz are considerably more reflective of the natural, moderately positive growth expected for these pools in 7.3.2 as compared to 7.3.1.

Another version of the problem also including a final rate term for circulating lipids in the objective functional was solved. However, the resulting solution actually produced less desirable results for lipids growth. This is possibly due to the limited combinations of desired final states and weightings that would converge to a solution in MISER3.3, or possibly due to MISER3.3 converging to a suboptimal local solution.

The solution determined in Section 7.3.2 produced the most promising results for a steady-state for all state variables out of the numerous objective formulations tested. Whilst the storage fat final growth was higher than the ideal, it was of interest to extend the time horizon even further, to investigate how the growth across all state variables would behave past the terminal time T, that is when $t > 644$. This is covered in Section 7.4.

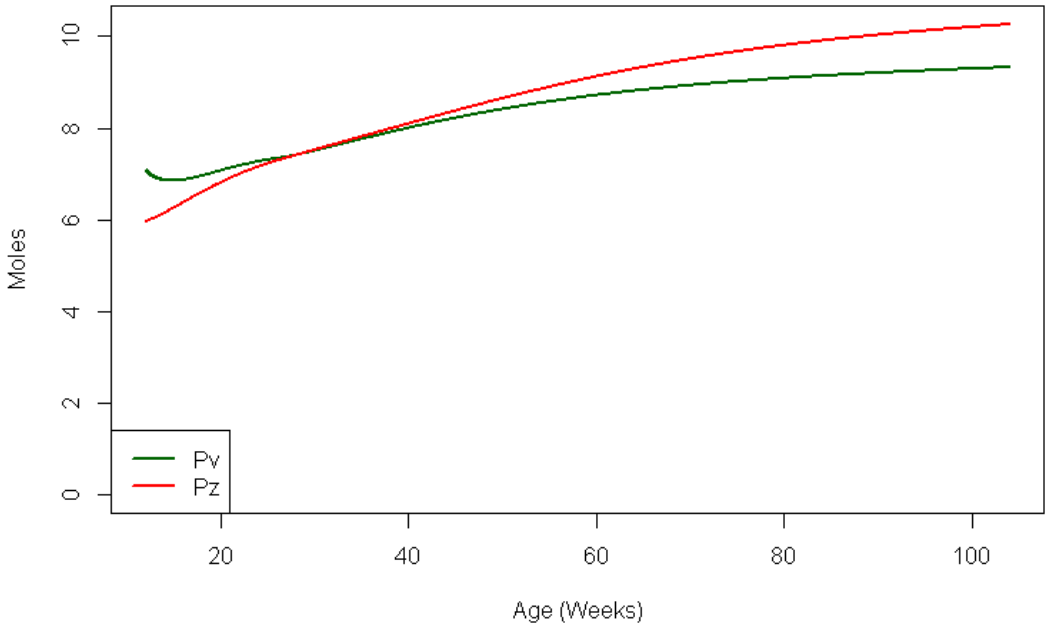

Figure 54: Growth of protein in viscera (Pv) and protein in other tissues (Pz) with F_{intake} as defined in Equation (130) and system parameters with values as given in Table 36.

7.4 Maintaining Steady-State for all State Variables

As discussed in Section 7.3, the most promising optimal control problem solution for achieving steady-state for all state variables was found in 7.3.2. The optimal control values and system parameters were simulated in MISER3.3 with the time-frame extended to reach three years of age, and the objective functional removed (such that MISER3.3 is acting simply as an integration tool, that is, an optimal control problem is not being solved). The resulting state variable trajectories are given in Figures 55 and 56. Whilst most of the state variables are maintaining steady-state through to three years of age, storage fat, glucose and amino acids are all still increasing substantially between the ages of two to three years. The optimal model parameters obtained in Section 7.3.2 were maintained, but due to the longer time horizon, our formulation of F_{intake} needs to be revised. Rather than solving a sequence of complex optimal parameter solution problems, a simple trial-and-error approach of adjusting the value of the feed intake at $t = 644$ (two years of age - denoted as x_1) and $t = 1,008$ (three years of age - denoted as x_2) was adopted to determine whether a satisfactory steady-state from two to three years of age could be achieved. That is, the values of x_1 and x_2 in the generic definition of the feed intake in Equation (131) were incrementally adjusted in the search for a reasonable solution. Note that Equation (131) is simply

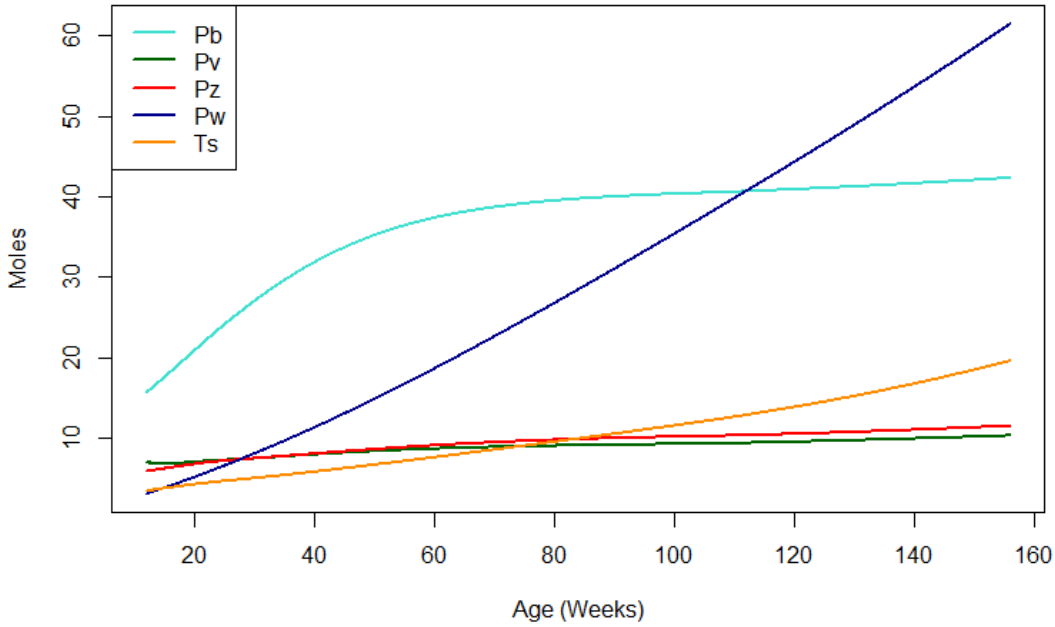

Figure 55: Extension of the result in 7.3.2 - Storage triacylglycerol (Ts) and protein growth with F_{intake} as defined in Equation (130) and system parameters with values as given in Table 36.

representative of linear interpolation between $F_{intake_{t=0}} = 1.55$, $F_{intake_{t=98}} = 1.4$, $F_{intake_{t=644}} = x_1$ and $F_{intake_{t=1008}} = x_2$. The initial value of acetate was also adjusted to $Ac_{t=0} = 1.57 \times 10^{-3}$ (the value of Ac at the first non-zero time value in the output from 7.3.2) to eliminate the initial jump from its trajectory. The trials of feed intake trajectories used in this approach are presented in Figure 57, with the selected trial indicated. Full details of trials are outlined in Table 38.

$$F_{intake} = \begin{cases} 1.55 - (1.53 \times 10^{-3})t, & 0 \leq t < 98, \\ (x_1 - 1.4)\left[\frac{t}{546} - \frac{7}{39}\right] + 1.4, & 98 \leq t < 644, \\ \frac{1}{364}\left[(x_2 - x_1)t + 1,008x_1 - 644x_2\right], & 644 \leq t < 1,008, \\ x_2, & t \geq 1,008. \end{cases} \tag{131}$$

The selected trial (Version 5) gave an acceptably stable result in the state variables from two to three years of age, and their trajectories can be found in Figures 58 and 59. The selected feed intake is presented via the dashed red line in Figure 57, and shows a feeding procedure that is initial high to promote growth, then slowly tapers off as the sheep ages. This is generally acknowledged as a reasonable approximate feeding pattern for any animal, and even humans, and further sophistication in the feed intake is not supported in the current model structure. The solution presented in this Section, as a culmination of work from previous Sections, results in the main aim of the thesis being achieved

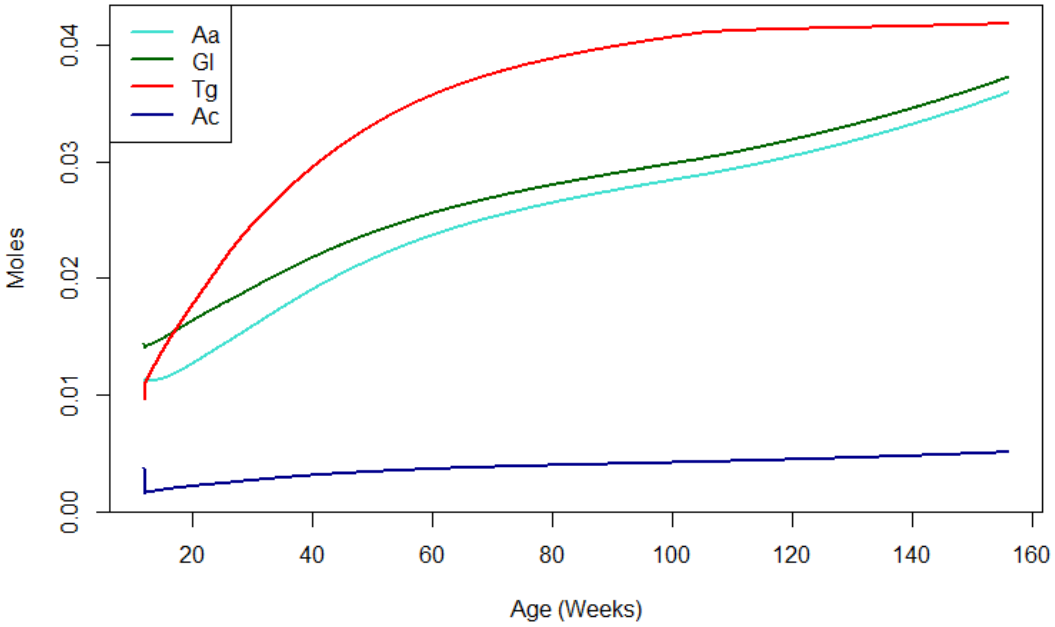

Figure 56: Extension of the result in 7.3.2 - Circulating amino acids (Aa), glucose (Gl), lipids (Tg) and acetate (Ac) with F_{intake} as defined in Equation (130) and system parameters with values as given in Table 36.

- a modelling, optimal control and simulation tool that replicates the development of a single sheep to maturity has been produced. This has the potential to be an important tool for future research in what is a multi-billion dollar industry in Australia. As an immediate next step, this development of a model definition that grows reasonably into steady-state allows for further experimentation on specific effects of other factors in the model, and further model improvements. This is explored in Chapter 8.

Version	x_1	x_2
0	1.3	1.3
1	1.25	1.25
2	1.25	1.20
3	1.25	1.15
4	1.26	1.16
5	1.25	1.16
6	1.25	1.17
7	1.26	1.18
8	1.26	1.175

Table 38: Combinations of x_1 and x_2 used in Equation (131) with model 7.3.2.

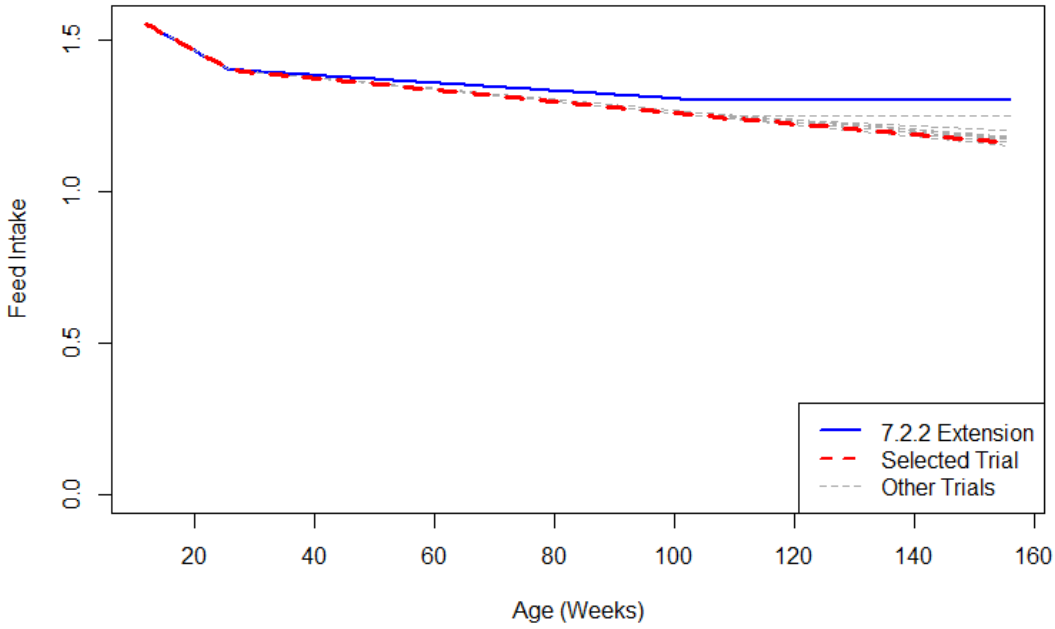

Figure 57: Trajectories of F_{intake} investigated in the trial-and-error approach to achieving long term steady-state for all state variables, using the result from 7.3.2 as a base.

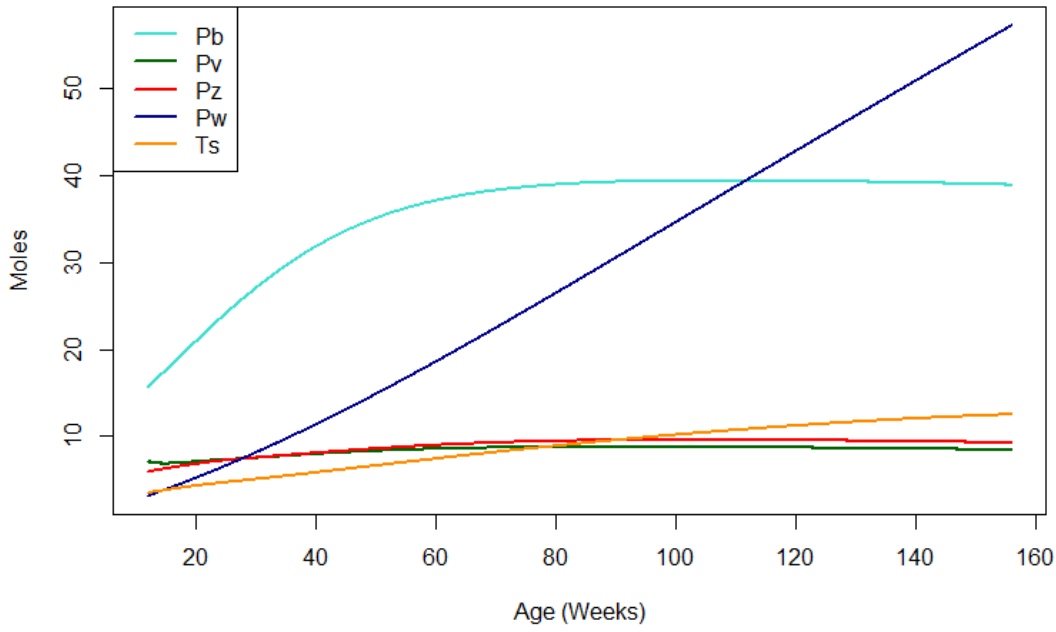

Figure 58: Storage triacylglycerol (Ts) and protein growth with F_{intake} as defined in Equation (131) with $x_1 = 1.25$ and $x_2 = 1.16$, and system parameters with values as given in Table 36.

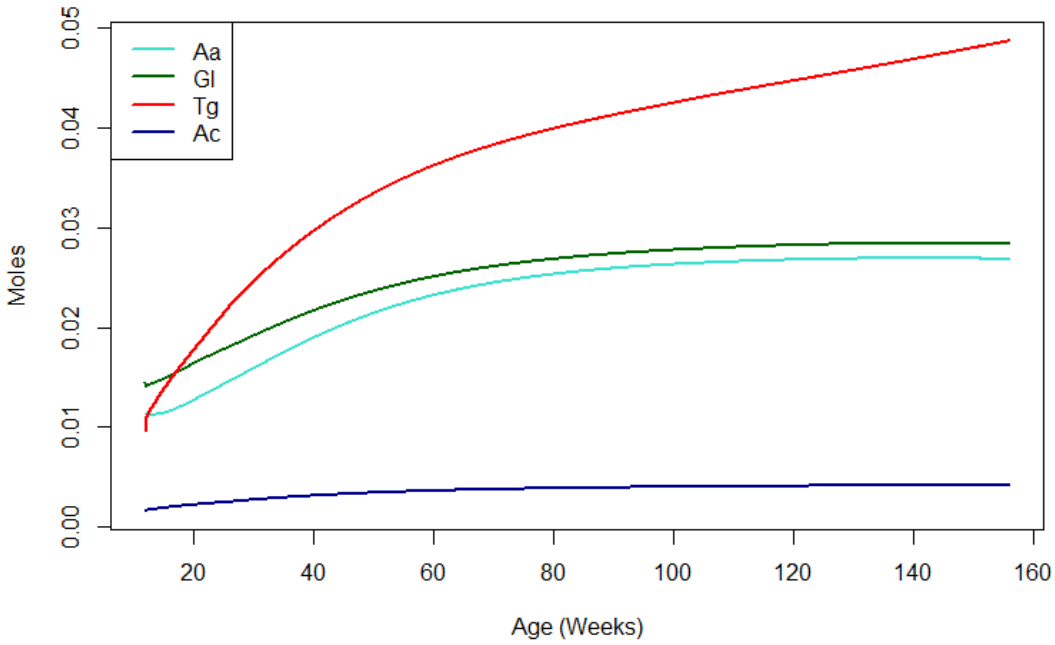

Figure 59: Circulating amino acids (Aa), glucose (Gl), lipids (Tg) and acetate (Ac) with F_{intake} as defined in Equation (131) with $x_1 = 1.25$ and $x_2 = 1.16$, and system parameters with values as given in Table 36.

8 Experimentation with the Model

The model developed in Chapter 7 provides an acceptable approximation of a lamb's growth into maturity and steady-state. This now allows for a wide variety of experimentation with many aspects of the model. While this would be best carried out by people with a deeper understanding of the biological processes underlying the model, a few examples of such experimentation are illustrated in this Chapter.

8.1 Sensitivity to Lactate Utilisation Parameters

In Section 3.8, assumptions relating to zero pools in the model defined by Sainz and Wolff [83] are described. This includes those relating to utilisation of the lactate pool, where half is assumed to be converted to glucose, and the other half is oxidised. However, these proportions are arbitrary. Sainz and Wolff state that the effect on the model behaviour (relating to adjustments to these proportions) is expected to be negligible. In order to test this theory, several different variations of these proportions were run through the model described in Section 7.3.2, via MISER3.3 with the optimisation disabled.

Version	y_1	y_2
0	0.50	0.50
1	0.25	0.75
2	0.45	0.55
3	0.55	0.45
4	0.60	0.40
5	0.67	0.33
6	0.75	0.25

Table 39: Combinations of y_1 and y_2 used in Equation (132) with model 7.3.2.

The parameters being adjusted are y_1 and y_2 as defined in Equation (132), and the combinations tested are provided in Table 39.

$$\begin{aligned} U_{La,LaGl} &= y_1 P_{La,TpLa}, \\ U_{La,LaCd} &= y_2 P_{La,TpLa}, \\ y_1 + y_2 &= 1. \end{aligned} \tag{132}$$

Various cases of y_1 and y_2 produced substantially different results, although none of these appeared to yield a more satisfactory representation of steady-state than the original ones. To illustrate the impact of adjustments to y_1 and y_2, figures of the state trajectories for the two most extreme versions (1 and 6) are presented in Figures 60 and 62 for Version 1 and Figures 61 and 65 for Version 6. Two zoomed-in versions of Figure 62 are given in Figures 63 and 64 to clearly present the state trajectories of lipids (Tg), glucose (Gl) and amino acids (Aa). Further investigation into the effects of the lactate utlisation parameters is a consideration for future work, but the results in this Section clearly demonstrate that they are not negligible.

8.2 Restricted Feed Intake

The control scenarios examined in the work thus far are designed to replicate "normal" sheep feed conditions. That is, feed conditions that allow a sheep to grow in a natural fashion. However, sheep response to fasting, be it due to drought or as part of a superfine wool growth operation, is a potential research interest. Therefore it follows that the model should be simulated under such conditions. The model in 7.3.2 has a number of nodes at which the piecewise linear value of the feed intake can be adjusted. This Section considers model performance with three cases of an instantaneous feed intake rate of zero at $t = 98$, $t = 644$ and $t = 1008$ in turn. This can be represented by the feed intake definitions given in Equations (133), (134) and (135) respectively, which are also shown in Figure 66.

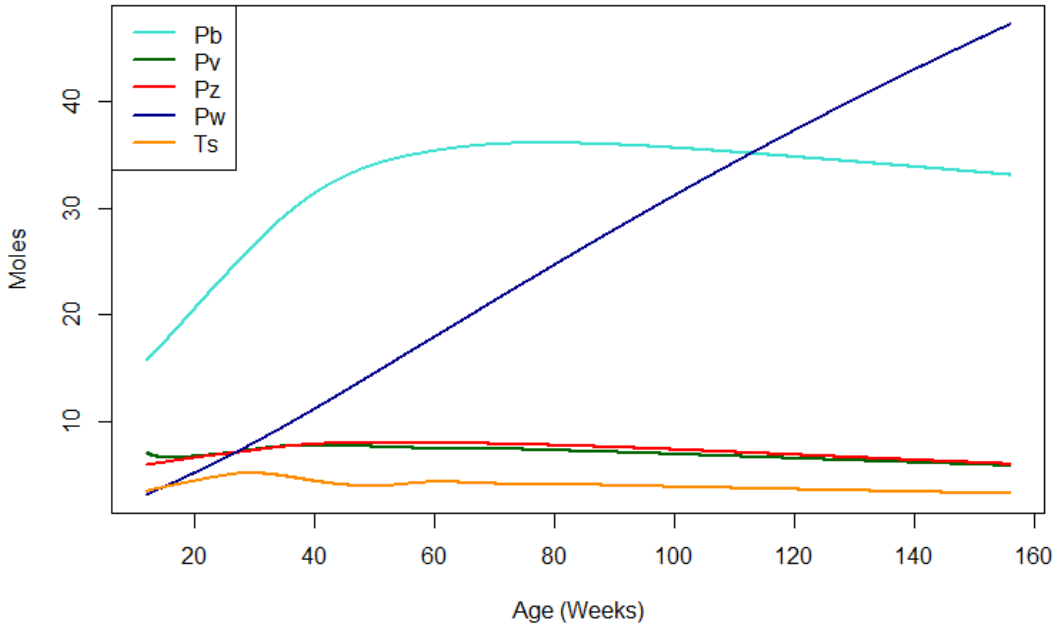

Figure 60: Storage triacylglycerol (Ts) and protein growth with F_{intake} as defined in Equation (131) with $x_1 = 1.25$ and $x_2 = 1.16$, system parameters with values as given in Table 36, and Version 1 of the lactate utilisation parameters.

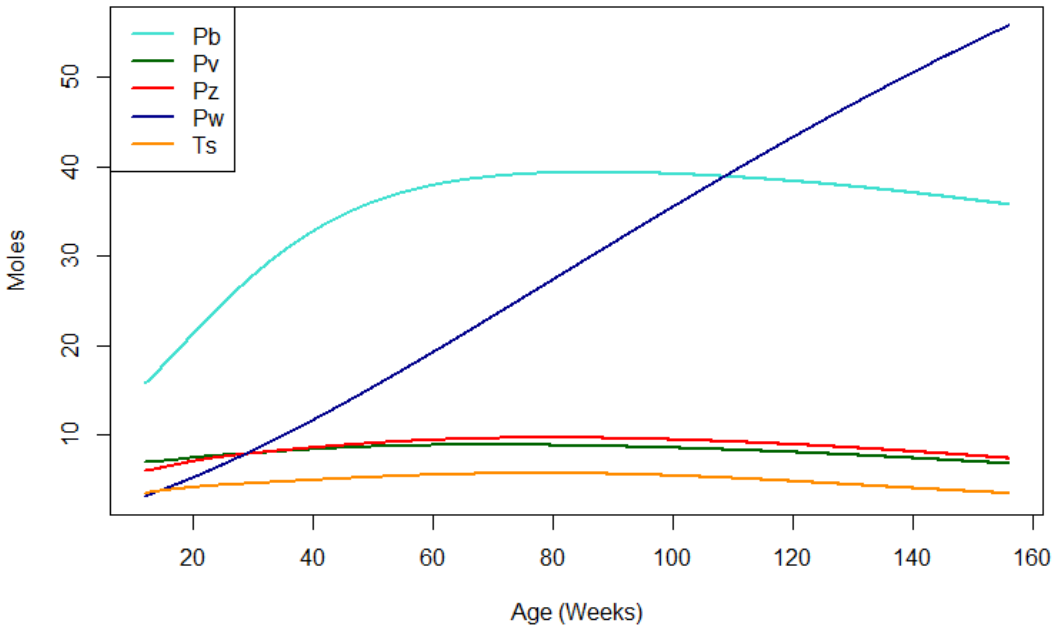

Figure 61: Storage triacylglycerol (Ts) and protein growth with F_{intake} as defined in Equation (131) with $x_1 = 1.25$ and $x_2 = 1.16$, system parameters with values as given in Table 36, and Version 6 of the lactate utilisation parameters.

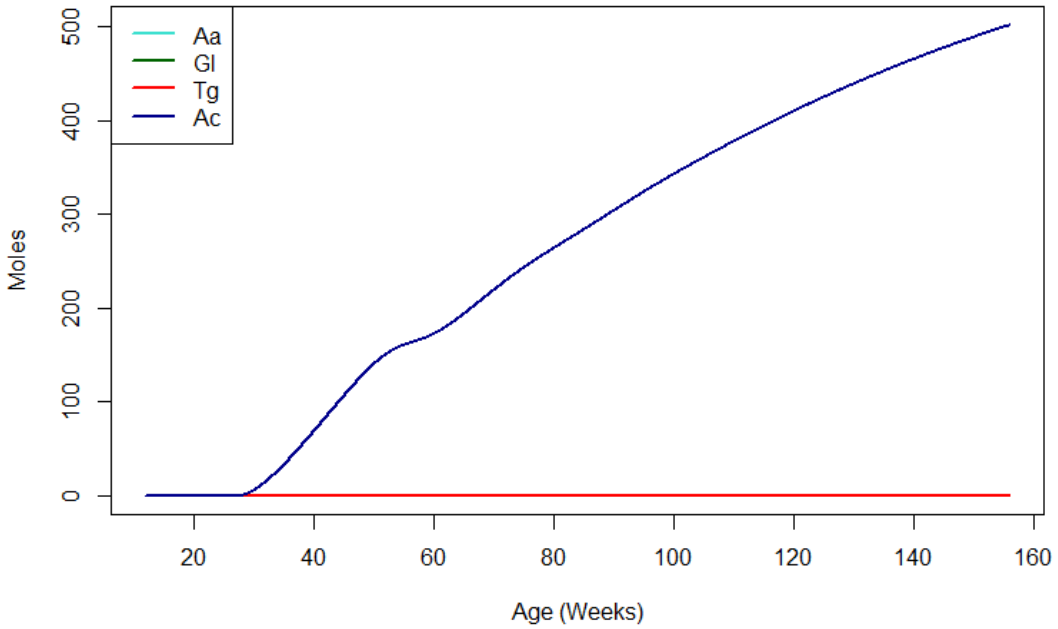

Figure 62: Circulating amino acids (Aa), glucose (Gl), lipids (Tg) and acetate (Ac) with F_{intake} as defined in Equation (131) with $x_1 = 1.25$ and $x_2 = 1.16$, system parameters with values as given in Table 36, and Version 1 of the lactate utilisation parameters.

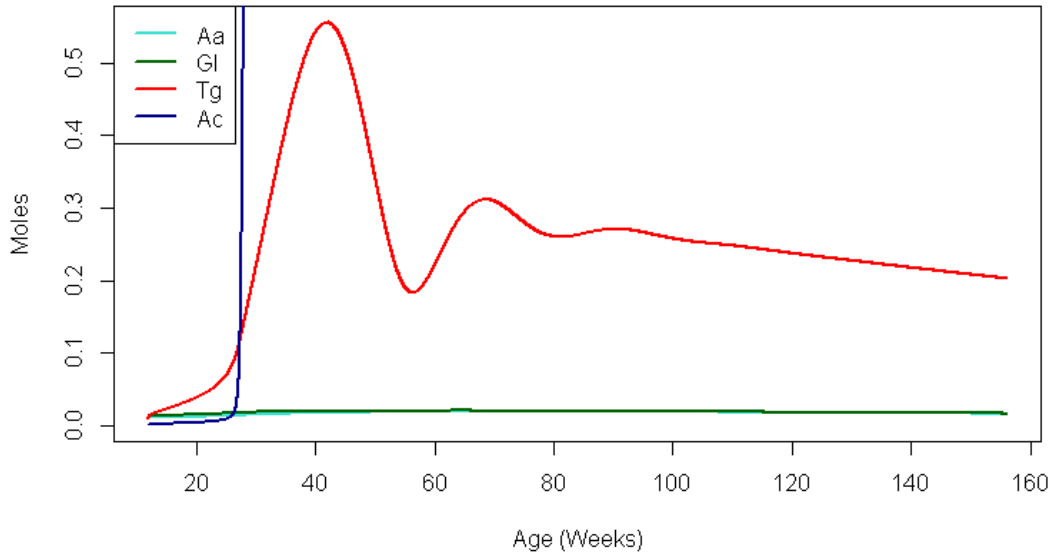

Figure 63: Circulating amino acids (Aa), glucose (Gl), lipids (Tg) and acetate (Ac) with F_{intake} as defined in Equation (131) with $x_1 = 1.25$ and $x_2 = 1.16$, system parameters with values as given in Table 36, and Version 1 of the lactate utilisation parameters (zoom 1).

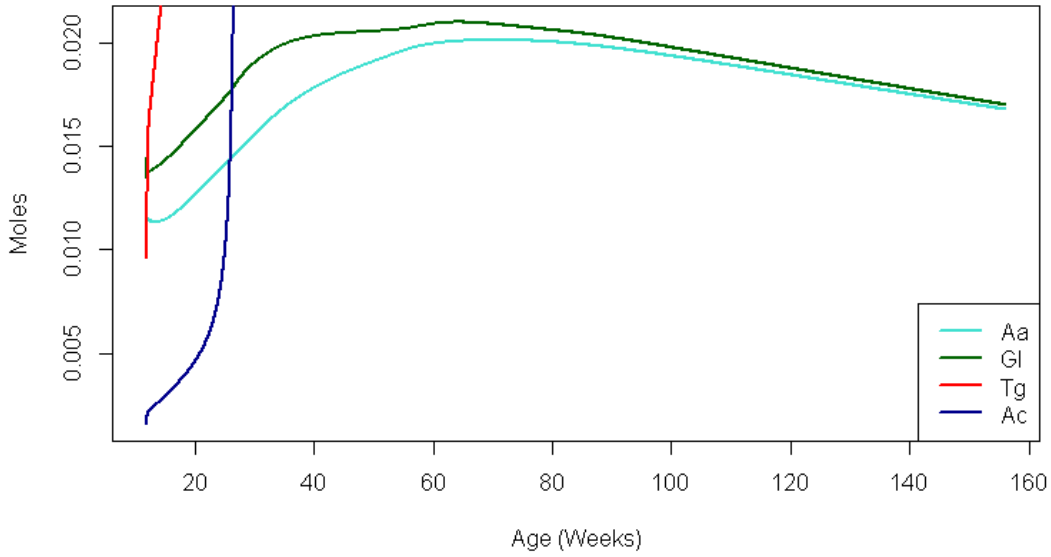

Figure 64: Circulating amino acids (Aa), glucose (Gl), lipids (Tg) and acetate (Ac) with F_{intake} as defined in Equation (131) with $x_1 = 1.25$ and $x_2 = 1.16$, system parameters with values as given in Table 36, and Version 1 of the lactate utilisation parameters (zoom 2).

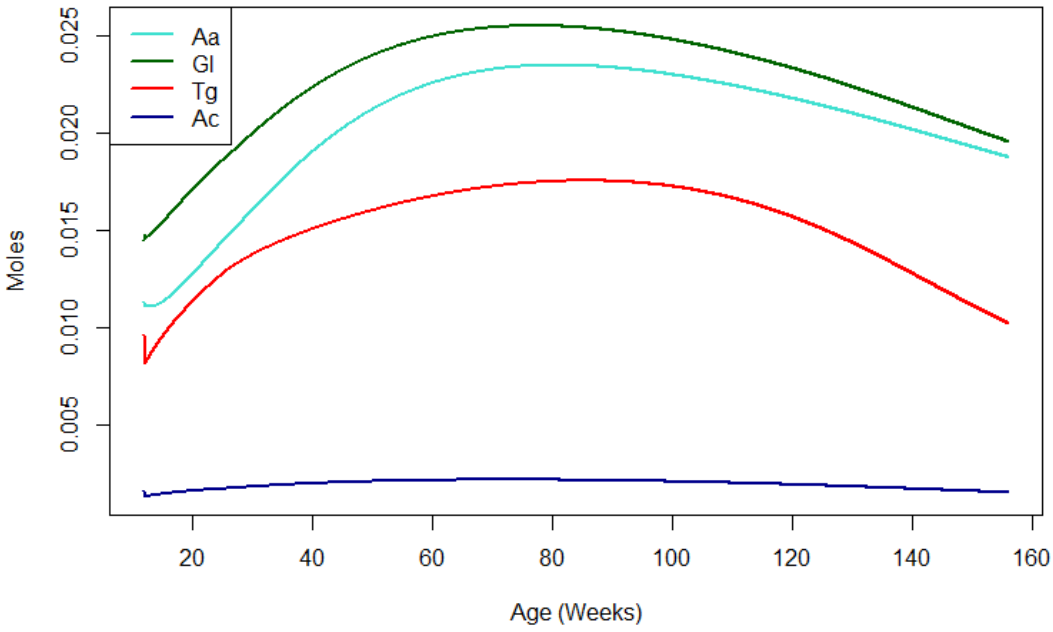

Figure 65: Circulating amino acids (Aa), glucose (Gl), lipids (Tg) and acetate (Ac) with F_{intake} as defined in Equation (131) with $x_1 = 1.25$ and $x_2 = 1.16$, system parameters with values as given in Table 36, and Version 6 of the lactate utilisation parameters.

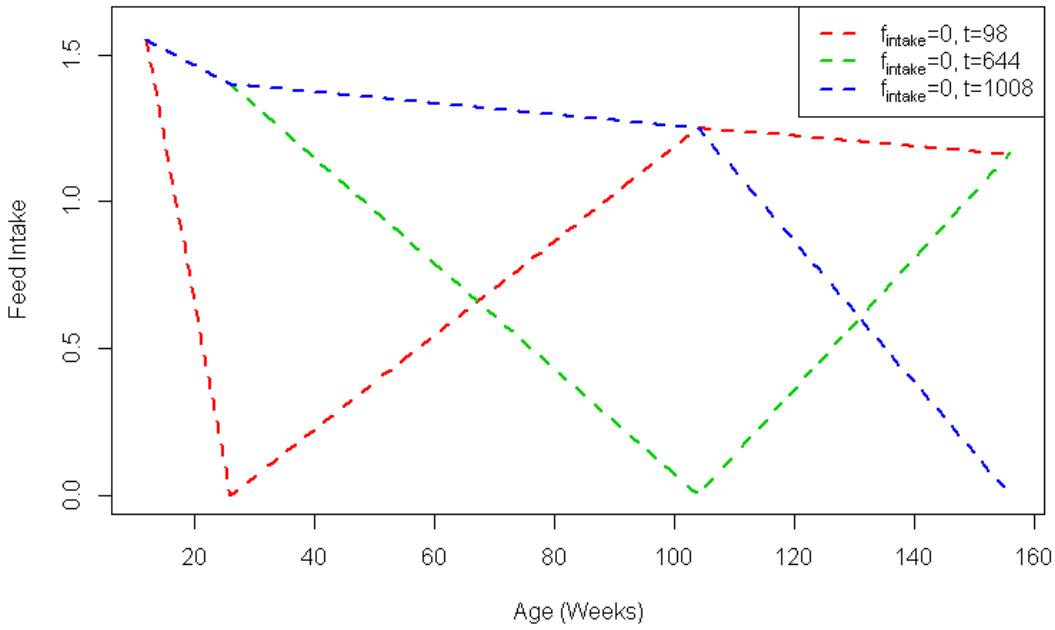

Figure 66: Restricted feed intake scenarios, as defined in Equations (133), (134) and (135).

The resulting state variable trajectories are presented in Figures 67 to 73.

$$F_{intake} = \begin{cases} 1.55 - (1.582 \times 10^{-2)}t, & 0 \leq t < 98, \\ -0.224 + (2.29 \times 10^{-3})t, & 98 \leq t < 644, \\ 1.41 - (2.47 \times 10^{-4})t, & 644 \leq t < 1,008, \\ 1.16, & t \geq 1,008. \end{cases} \tag{133}$$

$$F_{intake} = \begin{cases} 1.55 - (1.53 \times 10^{-3)}t, & 0 \leq t < 98, \\ 1.65 - (2.56 \times 10^{-3})t, & 98 \leq t < 644, \\ -2.05 + (3.19 \times 10^{-3})t, & 644 \leq t < 1,008, \\ 1.16, & t \geq 1,008. \end{cases} \tag{134}$$

$$F_{intake} = \begin{cases} 1.55 - (1.53 \times 10^{-3)}t, & 0 \leq t < 98, \\ 1.427 - (2.75 \times 10^{-4})t, & 98 \leq t < 644, \\ 3.46 - (3.43 \times 10^{-3})t, & 644 \leq t < 1,008, \\ 0, & t \geq 1,008. \end{cases} \tag{135}$$

It can be seen from these results that acetate and lipid levels can increase beyond realistic proportions when the sheep is experiencing high levels of degradation of protein and storage fat. This indicates a potential for further development in the definition of oxidation of circulating metabolites. In addition, Figure 71 clearly shows that the DNA pools, once the maximum is reached, do not then lower during periods of insufficient feed intake. The implication of this is that the

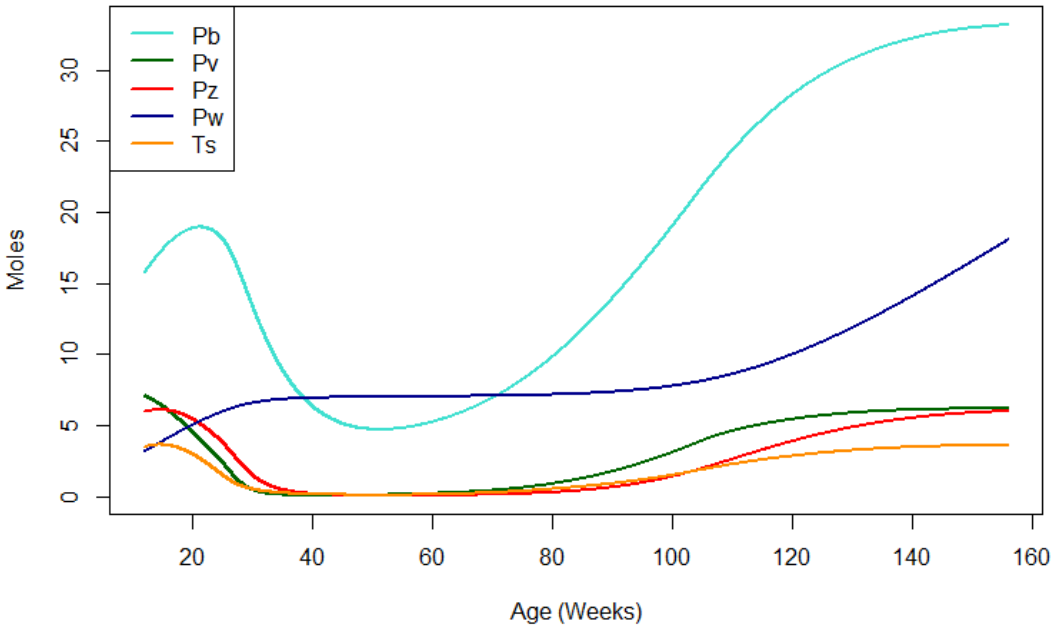

Figure 67: Storage triacylglycerol (Ts) and protein growth with F_{intake} as defined in Equation (133) and system parameters with values as given in Table 36.

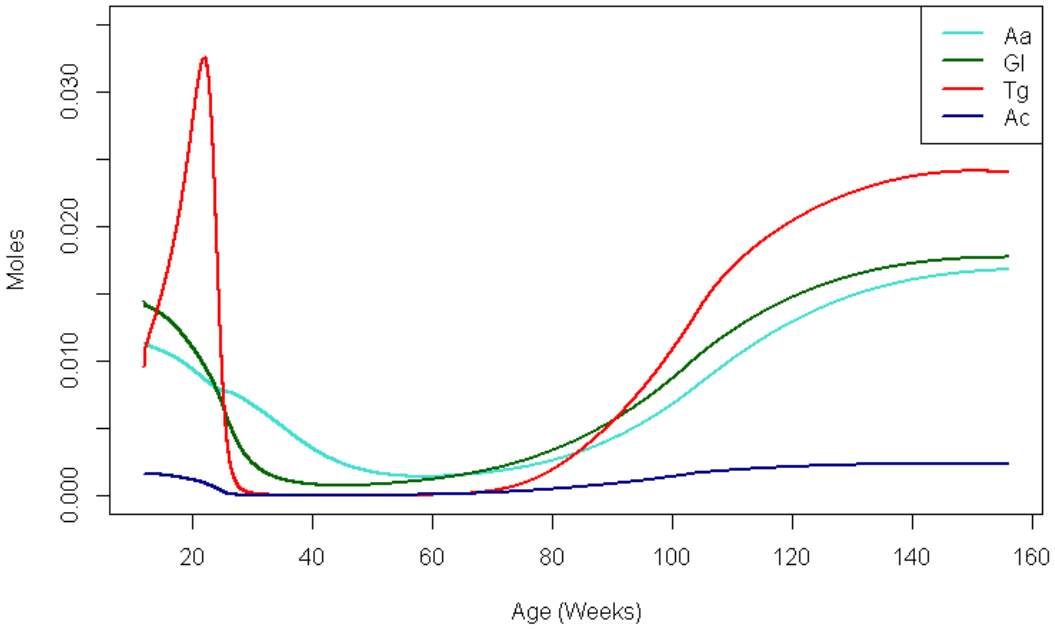

Figure 68: Circulating amino acids (Aa), glucose (Gl), lipids (Tg) and acetate (Ac) with F_{intake} as defined in Equation (133) and system parameters with values as given in Table 36.

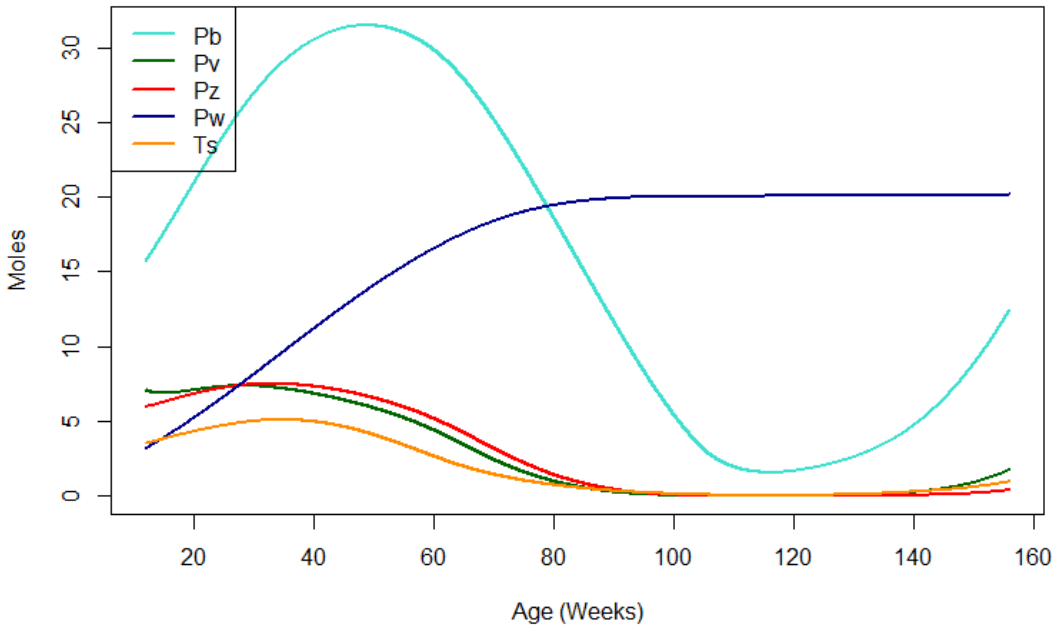

Figure 69: Storage triacylglycerol (Ts) and protein growth with F_{intake} as defined in Equation (134) and system parameters with values as given in Table 36.

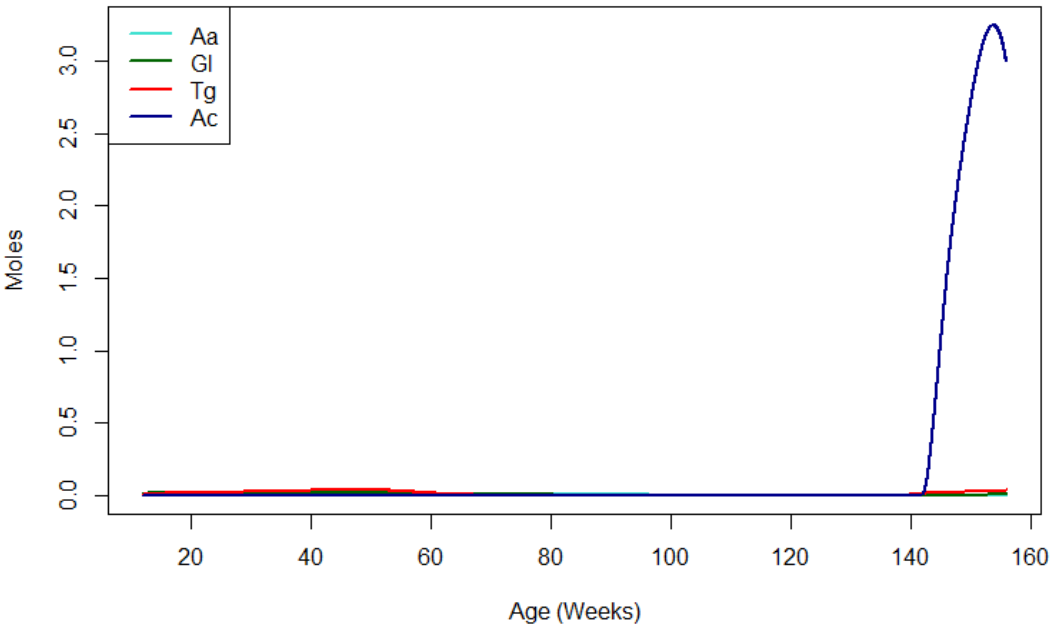

Figure 70: Circulating amino acids (Aa), glucose (Gl), lipids (Tg) and acetate (Ac) with F_{intake} as defined in Equation (134) and system parameters with values as given in Table 36.

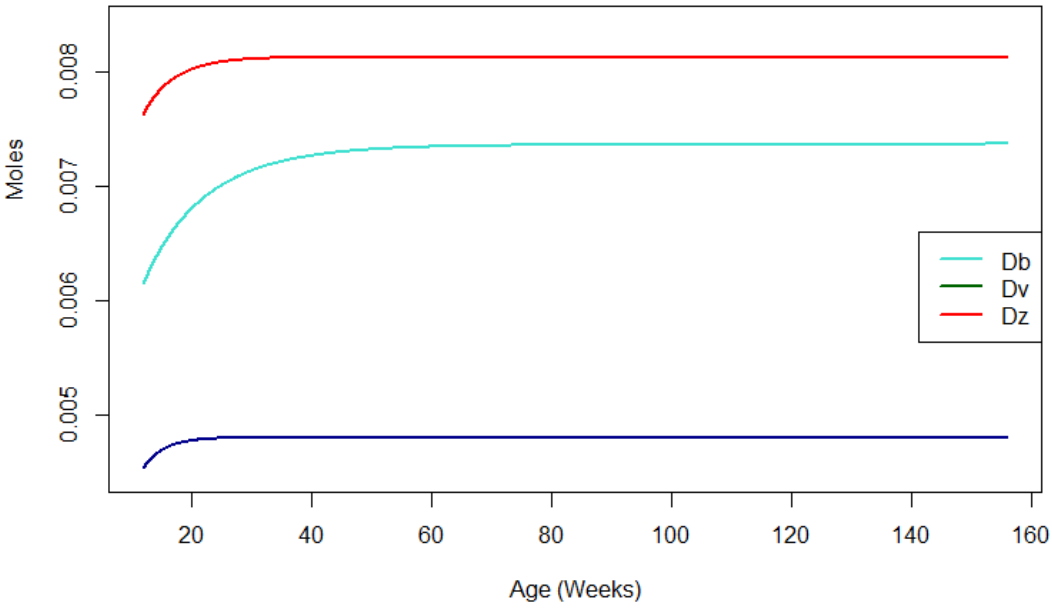

Figure 71: DNA pools corresponding to carcass (Db), viscera (Dv) and other tissues (Dz) with F_{intake} as defined in Equation (134) and system parameters with values as given in Table 36.

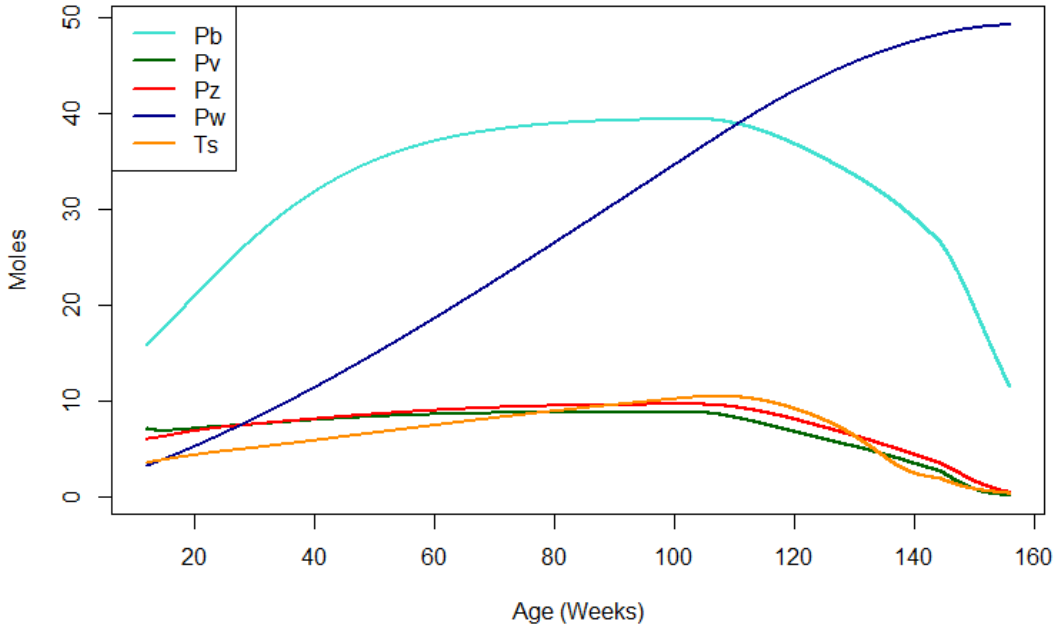

Figure 72: Storage triacylglycerol (Ts) and protein growth with F_{intake} as defined in Equation (135) and system parameters with values as given in Table 36.

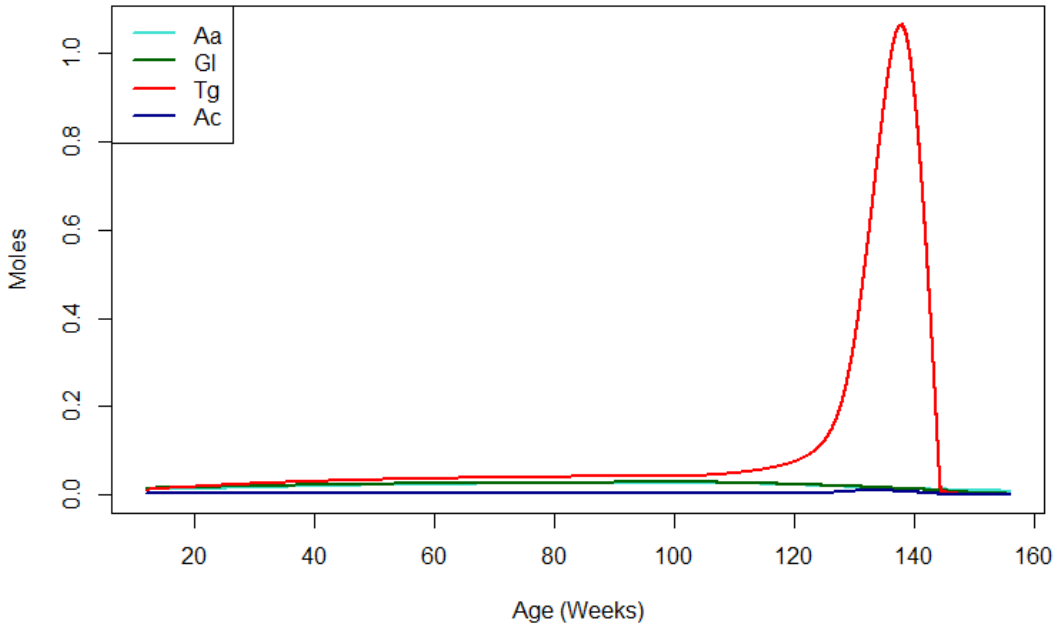

Figure 73: Circulating amino acids (Aa), glucose (Gl), lipids (Tg) and acetate (Ac) with F_{intake} as defined in Equation (135) and system parameters with values as given in Table 36.

"make-up" growth undertaken by body proteins after this period may be slower in the model than in practice. In fact, it is quite clear from the equation determining the rate of change of DNA in the carcass ($\frac{dDb}{dt} = K_{Db}\,(Db_{MAX} - Db)\,H_A$ from Equation (65)) that Db can never decrease. As $\frac{dDv}{dt}$ and $\frac{dDz}{dt}$ are similarly defined, the same conclusion of non-negative growth applies to these pools. Further investigation into the effects of feed intake restriction is a consideration for future work, but the results in this Section demonstrate that there is significant potential for improvements in the model in this respect.

9 Conclusions

The aim of this study has been achieved - a modelling, optimal control and simulation approach to the understanding of the development of a single sheep to maturity is presented. In the absence of published refinements to the Sainz and Wolff [83] model since 1990, and previous attempts to implement the model into MISER3.3 and perform optimal control problems being unsuccessful (Hon [45] and Ramsey [78]), this is a significant achievement.

Due to the importance of the sheep industry in Australia (valued at over $5 billion in 2012 - see Figures 4 and 5), and the numerous advantages that an accepted and reliable model could have (e.g. as a supplement to or replacement for field testing), this is a major step forward in this research area. The work has overcome a long standing stagnation in the development of the model by demostrating that optimal control problems relating to complex biological systems can be solved with the appropriate mathematical and programming expertise.

9.1 Summary

A summary of the work and achievements of this thesis is given below.

- Review of publications up to 2013 to identify the more sophisticated models of whole-body metabolism that are publicly available, particulary sheep metabolism. This led to confirmation of the Sainz and Wolff [83] model as a reasonable starting point for developing a deterministic model for sheep metabolism.

- Demonstration of the need for numerical solution techniques, and identification of the suitability of the control parameterisation method to solve optimal control problems with respect to whole-body metabolism models.

- Review of the specifics of the Sainz and Wolff [83] model dynamics and confirmation that the coding of the model dynamics into MISER3.3 (Fortran) from previous work (Hon [45]) was correct. Identification of inconsistencies and the existence of errors in the presentation of rate values in the Sainz and Wolff [83] paper and correction thereof - where possible (e.g. inconsistent rounding issues and the adjustment of V'_{AaPw}).

- Development of futher aspects required to run the model simulation in a fully documented, reviewed and repeatable manner, including definition of an empty body weight formula and the review and selection of appropriate initial conditions. This work included determining molecular weights for body proteins, wool protein and storage fat, as well as the translation of

wool protein mass into CFW and GFW, aiding comparison of model output to published results.

- Identification of sensitivities of initial growth rates for circulating metabolites and hormonal controls to the initial conditions.

- Development of coding of the derivatives of the state dynamics and the objective functionals with respect to the states, system parameters and controls (where relevant) such that errors were minimal and could be safely assumed to be due to fuzziness in MISER3.3's internal derivative estimates. As a result of this achievement, a workable optimal control and optimal parameter selection model was established.

- Replication of growth in the scope of the Sainz and Wolff [83] parameters (20 to 40kg empty body weight). Extension of the time frame of the simulation and idenitification of limitations in the model post 40kg.

- Use of literature results to determine basic feed intake structure, followed by the application of optimal parameter selections techniques to develop the model into that which would adequately represent steady-state growth into adulthood.

- Highlighting of ways in which this developed model could be improved with specific examples of limitations still present (e.g. definition of lactate utilisation parameters, representation of growth with restricted feed intake).

- Provision of considered suggestions of future work and developments (presented in Section 9.2 below).

9.2 Future Work

There are many different potential items for future endeavours that are now possible due to the achievements of this work (outlined in Section 9.1). Progression from the results presented here is likely to extend beyond the scope of a mathematical body of work. Therefore, many of the items discussed below would also require collaboration with those with biological, agricultural and/or biochemical expertise. With regard to the general circulation structure, as presented in Figure 11, it has been suggested that as wool growth requires energy, there should be a link between glucose and protein in wool. Similarly, including representation of the recycling of urea (from blood to the digestive system) may make for a more complete model.

Initial investigations into the sensitivity of the model to lactate utilisation parameters were conducted in Section 8.1. The aim of this Section was to simply demonstrate that the impact of the selection of these parameters on the model was not negligible, as Sainz and Wollf [83] had suggested. Therefore, the arbitrary selection of 0.5 for the coefficients of $P_{La,TpLa}$ in the equations governing $U_{La,LaGl}$ and $U_{La,LaCd}$ may not be the ideal for model accuracy. A potential area of future work would be to further investigate the effects of different selections of these coefficients, and providing a recommendation for their selection. These parameters were not the only ones that appeared to have been crudely estimated. Whilst this work investigated and adjusted a selection of parameters of the model, further consideration could be given to other parameters, and their appropriateness. There is also the potential to allow for functions (of time, age or other attributes of the sheep) to replace constant parameter values. An example to consider is the adaption of absorption parameters such as D_{Tg} or D_{Ac} to take into account current concentrations of these metabolites in circulating fluids.

As was demonstrated in Section 8.2, the model as it currently stands is limited in its ability to replicate sheep body response to periods of restricted feed intake. This is, in part, due to the simple nature of the DNA pool dynamics meaning they may not respond appropriately to such conditions. However, very high concentrations of circulating metabolites were noted in the examples presented in Section 8.2, which indicates that there are also limitations in the dynamics of other state variables as body degradation occurs. The model is also limited with respect to periods of very high feed intake. The incorporation of biological mechanisms preventing sheep from eating excessively into the model is a potential area for future research.

The definition of energy expenditure is somewhat vague in this model. The impact of varying levels of animal behaviour is not considered. Animal behaviour is, at least in part, an environmental factor - where sheep in a pen, for example, may require less feed for maintenance than those in a field or paddock. In addition, the energy requirements for thermoregulation of the body are also not explicitly considered here.

The model is quite simplistic in the way it represents wool growth. It is simply concerned with the number of moles of protein in the pool (and perhaps should have a link from circulating glucose as well), and relates directly to the number of moles of protein in the other tissues protein pool (includes, but is not limited to, skin). It has been demonstrated that other attributes of the skin (see [103]) can influence wool growth, and it is also likely to be influenced by environmental conditions and ageing. Also, other attributes of wool, apart from quantity, that are of strong interest to the industry, such as fibre quality, may be able to be

linked with other attributes of the sheep.

As a final point, there is potential to use the model developed as a component in a sheep flock growth model, taking into account elements such as stocking rates and the types of feed available (see Bowman, Cottle, White and Bywater [20]). This could be extended further to include other environmental conditions such as weather. In addition to the environmental factors, there are other factors at play not yet considered explicitly in this model. This includes: breed and genetic predispositions; disease and pests; pregnancy and lactation; and many others.

References

[1] N.R. Adams, J.R. Briegel and D. Blache, *Feed intake, liveweight and wool growth rate in Merino sheep with different responses to low- and high-quality feed*, Aust. J. of Exp. Agric., **42** (2002), 399–405.

[2] N.R. Adams and S.M. Liu, *Principles of nutrient partitioning for wool, growth and reproduction: Implications for nematode parasitism*, Aust. J. of Exp. Agric., **43** (2003), 1399–1407.

[3] N.R. Adams, S.M. Liu, J.R. Briegel and J.C. Greeff, *Protein metabolism in skin and muscle of sheep selected for or against staple strength*, Aust. J. Agric. Res., **51** (2000), 541–546.

[4] J. Aerssens, S. Boonen, G. Lowet and J. Dequekker, *Interspecies differences in bone composition, density, and quality: Potential implications for in vivo bone research*, Endocrinology, **139** (1998), 663–670.

[5] Agricultural Research Council, "The Nutrient Requirements of Ruminant Livestock", Commonwealth Agricultural Bureaux, Farnham Royal, 1980.

[6] B.J. Anderson and N.H. Holford, *Mechanism-based concepts of size and maturity in pharmacokinetics*, Annual Review of Pharmacology and Toxicology, **48** (2008), 12.1–12.30.

[7] V.O. Anosa and T.T. Isoun, *Serum proteins, blood and plasma volumes in experimental trypanosoma vivax infections of sheep and goats*, Tropical Animal Health and Production, **8** (1976), 14–19.

[8] D.G. Armstrong and K.L. Blaxter, *The heat increment of steam-volatile fatty acids in fasting sheep*, British Journal of Nutrition, **11** (1957), 247–272.

[9] D.G. Armstrong, K.L. Blaxter, N. McC. Graham and F.W. Wainman, *The utilization of the energy of two mixtures of steam-volatile fatty acids by fattening sheep*, British Journal of Nutrition, **12** (1958), 177–188.

[10] G.W. Arnold, N.A. Campbell and K.A. Galbraith, *Mathematical relationships and computer routines for a model of food intake, liveweight change and wool production in grazing sheep*, Agricultural Systems, **2** (1977), 209–226.

[11] N. Atti, F. Boucquier, M. Thériez, G. Khaldi and C. Kayouli, *In vivo estimation of body composition from the dilution space of deuterium oxide in fat-tailed barbary ewes*, Livestock Production Science, **65** (2000), 39–45.

[12] R.L. Baldwin, J. France and M. Gill, *Metabolism of the lactating cow: I. Animal elements of a mechanistic model*, Journal of Dairy Research, **54** (1987), 77–105.

[13] R.L. Baldwin and R.D. Sainz, *Energy partitioning and modeling in animal nutrition*, Annu. Rev. Nutr., **15** (1995), 191–211.

[14] D.W. Ball, J.W. Hill and R.J Scott, "The Basics of General, Organic, and Biological Chemistry", 1st Edition, Flat World Knowledge, 2011.

[15] D. Bastianelli and D. Sauvant, *Modelling the mechanisms of pig growth*, Livestock Production Science, **51** (1997), 97–107.

[16] G.C.M. Beaufort-Krol, J. Takens, G.B. Smid, M.C. Molenkamp, W.G. Zijlstra and J.R.G. Kuipers, *Lower arterial glucose concentrations in lambs with aortopulmonary shunts after an 18-hour fast*, Metabolism, **48** (1999), 1082–1088.

[17] V. Berthelot, P. Bas, P. Schmidely and C. Duvaux-Potter, *Effect of dietary propionate on intake patterns and fatty acid composition of adipose tissues in lambs*, Small Ruminant Research, **40** (2001), 29–39.

[18] N. Bhaskar, V.K. Modi, K. Govindaraju, C. Radha and R.G. Lalitha, *Utilization of meat industry by products: Protein hydrolysate from sheep visceral mass*, Bioresource Technology, **98** (2007), 388–394.

[19] C. Bishof, Alan Carle, P. Havland, P. Khademi, and A. Mauer, "ADIFOR 2.0 User's Guide (Revision D)," Technical Report ANL/MCS-TM-192, Argonne National Laboratory, 1994.

[20] P.J. Bowman, D.J. Cottle, D.H. White and A.C. Bywater, *Simulation of wool growth rate and fleece characteristics of Merino sheep in southern Australia. Part 1 - Model description*, Agricultural Systems, **43** (1993), 287–299.

[21] P.J. Bowman, D.H. White, D.J. Cottle and A.C. Bywater, *Simulation of wool growth rate and fleece characteristics of Merino sheep in southern Australia. Part 2 - Assessment of biological components of the model*, Agricultural Systems, **43** (1993), 301–321.

[22] T.S. Brand and F. Franck, *Production responses of two genetic different types of Merino sheep subjected to different nutritional levels*, Small Ruminant Research, **37** (2000), 85–91.

[23] B.W. Butler-Hogg, *Growth patterns in sheep: Changes in the chemical composition of the empty body and its constituent parts during weight loss and compensatory growth*, The Journal of Agricultural Science, **103** (1984), 17–24.

[24] A. Cannas, A.S. Atzori, I.A.M.A. Teixeira, R.D. Sainz and J.W. Oltjen, *The energetic cost of maintenance in ruminants: From classical to new concepts and prediction systems*, In: Energy and Protein Metabolism and Nutrition (G. M. Crovetto, Ed.), European Assoc. for Anim. Prod. Publ., **127** (2010), 531–542.

[25] D. Casamassima, R. Pizzo, M. Palazzo, A.G. D'Alessandro and G. Martemucci, *Effect of water restriction on productive performance and blood parameters in Comisana sheep reared under intensive condition*, Small Ruminant Research, **78** (2008), 169–175.

[26] M.J. Clarkson, *Blood and plasma volumes in sheep infected with trypanosoma vivax*, Journal of Comparative Pathology, **78** (1958), 189–193.

[27] S.W.P. Cloete, G.J. Delport, G.J. Erasmus, J.J. Olivier, H.J Heydenrych and E. Du Toit, *Environmental and genetic trends in clean fleece mass, live mass and fibre diameter in selection and control flocks involving a selection experiment for increased clean fleece mass in South African Merino sheep*, South African Journal of Animal Science, **22**:2 (1992), 50–57.

[28] M.C. Corfield and A. Robson, *The amino acid composition of wool*, Biochem. J., **59** (1955), 62–68.

[29] J. Cutnell and K. Johnson, "Physics", 4^{th} Edition, Wiley, 1998.

[30] A. De Angelisl, *Energy and protein value of lucerne hay and wheat straw diets for lambs*, In: Energy and Protein Metabolism and Nutrition (G. M. Crovetto, Ed.), European Assoc. for Anim. Prod. Publ., **127** (2010), 547–548.

[31] Q. Dong, H. Zang, A. Liu, G. Yang, C. Sun, L. Siu, P. Wang and L. Li, *Determination of molecular weight of hyaluronic acid by near-infrared spectroscopy*, Journal of Pharmaceutical and Biomedical Analysis, **53** (2010), 274–278.

[32] B. Elmahdi, H-P. Sallmann, H. Fuhrmann, W. Von Engelhardt and M. Kaske, *Comparative aspects of glucose tolerance in camels, sheep, and ponies*, Comp. Biochem. Physiol., **118A** (1997), 147–151.

[33] R.A. Field, M.L. Riley, F.C. Mello, M.H. Corbridge and A.W. Kotula, *Bone composition in cattle, pigs, sheep and poultry*, Journal of Animal Science, **39**:3 (1974), 493–499.

[34] R.M.T. Fleming, I. Thiele, G. Provan and H.P. Nasheuer, *Integrated stoichiometric, thermodynamic and kinetic modelling of steady state metabolism*, Journal of Theoretic Biology, **264** (2010), 683–692.

[35] R. Fletcher, "Practical Methods of Optimization", 2nd Edition, Wiley, Chichester, 1987.

[36] D.G. Fox, L.O. Tedeschi, T.P. Tylutki, J.B. Russell, M.E. Van Amburgh, L.E. Chase, A.N. Pell and T.R. Overton, *The Cornell Net Carbohydrate and Protein System model for evaluating herd nutrition and nutrient excretion*, Animal Feed Science and Technology, **112** (2004), 29–78.

[37] M. Gill, J.H.M. Thornley, J.L. Black, J.D. Oldham and D.E. Beever, *Simulation of the metabolism of absorbed energy-yielding nutrients in young sheep*, British Journal of Nutrition, **52** (1984), 621–649.

[38] N.McC. Graham, *The metabolic rate of fasting sheep in relation to total and lean body weight, and the estimation of maintenance requirements*, Australian Journal of Agricultural Research, **18** (1967), 127–136.

[39] N.McC. Graham, T.W. Searle and D.A. Griffiths, *Basal metabolic rate in lambs and young sheep*, Australian Journal of Agricultural Research, **25** (1974), 957–971.

[40] J. Hammond, "Growth and the Development of Mutton Qualities in the Sheep", Oliver and Boyd, London, 1932.

[41] M.D. Hanigan, J. Dijkstra, W.J.J. Gerrits and J. France, *Modelling post-absorptive protein and amino acid metabolism in the ruminant*, Proceedings of the Nutrition Society, **56** (1997), 631–643.

[42] J.F. Hecker, "The Sheep as an Experimental Animal", Academic Press, New York, 1983.

[43] T.P. Hilditch and R.K. Shrivastava, *The component glycerides of an Indian sheep body fat*, J. Amer. Oil Chem., **26** (1949), 1–4.

[44] A.C. Hindmarsh, *LSODE and LSODI, two new initial value ordinary differential equation solvers*, ACM SIGNUM Newsletter, **15** (1980), 10–11.

[45] T. Hon, "Modeling Protein Synthesis in Sheep", Honours Dissertation, Curtin University of Technology, Perth, Australia, 2003.

[46] J.S. Huxley, *Constant differential growth ratios and their significance*, Nature, **114**, 895–896.

[47] H.D. Jackson and V.W. Winkler, *Effects of starvation on the fatty acid composition of adipose tissue and plasma lipids of sheep*, The Journal of Nutrition, **100** (1970), 201–207.

[48] L.S. Jennings, M.E. Fisher, K.L. Teo and C.J. Goh, "MISER3 Optimal Control Software Version 3 Theory and User Manual", *http://school.maths.uwa.edu.au/∼les/miser3.3.html*, 2005.

[49] C.Y. Kaya and J.L. Noakes, *Computations and time-optimal controls*, Optimal Control Applications and Methods, **17** (1996), 171–185.

[50] C.Y. Kaya and J.L. Noakes, *Computational method for time-optimal switching control*, Journal of Optimization Theory and Applicatons, **117**:1 (2003), 69–92.

[51] E. Kebreab, J.A.N. Mills, L.A. Crompton, A. Bannink, J. Dijkstra, W.J.J. Gerrits and J. France, *An integrated mathematical model to evaluate nutrient partition in dairy cattle between the animal and its environment*, Animal Feed Science and Technology, **112** (2004), 131–154.

[52] S.M. Liu and D.G. Masters, *Amino acid utilisation for wool production*, In: Amino Acids in Animal Nutrition (J.P.F. D'Mello, Ed.), 2nd Edition, CABI International, Oxon, United Kingdom, (2003), 309–328.

[53] W. Liu and F. Tang, *Modeling a simplified regulatory system of blood glucose at molecular levels*, Journal of Theoretical Biology, **252** (2008), 608–620.

[54] C.J. Lupton, J.E. Huston, B.F. Craddock, F.A. Pfeiffer and W.L. Polk, *Comparison of three systems for concurrent production of lamb meat and wool*, Small Ruminant Research, **72** (2007), 133–140.

[55] R. Luus and T.H.I. Jaakola, *Optimization by direct search and systematic reduction in the size of search region*, AIChE J., **19** (1973), 760–766.

[56] J.P. McCann, E.N. Bergman and D.H. Beermann, *Dynamic and static phases of severe dietary obesity in sheep: Food intakes, endocrinology and carcass and organ chemical composition*, American Institute of Nutrition, **122** (1992), 496–505.

[57] B.A. McGregor, *Comparative productivity and grazing behaviour of Huacaya alpacas and Peppin Merino sheep grazed on annual pastures*, Small Ruminant Research, **44** (2002), 219–232.

[58] J.P. McNamara, *Research, improvement and application of mechanistic, biochemical, dynamic models of metabolism in lactating dairy cattle*, Animal Feed Science and Technology, **112** (2004), 155–176.

[59] J.P. McNamara and J.E. Pettigrew, *Protein and fat utilization in lactating sows: II. Challenging behaviour of a model of metabolism*, Journal of Animal Science, **80** (2002), 2452–2460.

[60] J.C. MacRae and G.E. Lobley, *Some factors which influence thermal energy losses during the metabolism of ruminants*, Livestock Production Science, **9** (1982), 447–456.

[61] J.C. MacRae, A. Walker, D. Brown and G.E. Lobley, *Accretion of total protein and individual amino acids by organs and tissues of growing lambs and the ability of nitrogen balance techniques to quantitate protein retention*, Animal Production, **53** (1993), 237–245.

[62] H.H. Meyer, M.L. Bigham, R.L. Baker, T.G. Harvey and S.M. Hickey, *Effects of Booroola Merino breeding and the* Fec^B *gene on performance of crosses with longwool breeds. 1. Effects on growth, onset of puberty, wool production and wool traits*, Livestock Production Science, **39** (1994), 183–190.

[63] L. Michaelis and M.L. Menton, *Die kinetik der invertinwirkung*, Biochem. Z., **49** (1913), 333–369.

[64] A.N. Moen and G.S. Boomer, *Modeling annual energy metabolism rhythms in mammals*, Ecological Modelling, **184** (2005), 193–202.

[65] H.N. Munro, *Evolution of protein metabolism in mammals*, In: Mammalian Protein Metabolism (H.N. Munro, Ed.), Academic Press, New York, (1969), 133–182.

[66] D.L. Nelson and M.M. Cox, "Principles of Biochemistry", 4^{th} Edition, W.H. Freeman and Company, New York, 2005.

[67] G. Offer and P. Knight, *The structural basis of water-holding in meat. Part 2: Drip losses*, In: Developments in Meat Science (R.A. Lawrie, Ed.), **4** (1988), 173–243.

[68] B.M. Ogilvie, G.L. McClymont and F.B. Shorland, *Effect of duodenal administration of highly unsaturated fatty acids on composition of ruminant depot fat*, Nature, **190** (1961), 725–726.

[69] J.W. Oltjen, A. Cannas, A.S. Atzori, L.O. Tedeschi, R.D. Sainz and D.G. Fox, *Integration of the Small Ruminant Nutrition System and of the UC Davis sheep growth model for improved predictions*, In: Energy and Protein Metabolism and Nutrition (G. M. Crovetto, Ed.), European Assoc. for Anim. Prod. Publ., **127** (2010), 553–554.

[70] L.A. Onischuk and A.D. Kennedy, *Growth hormone, insulin, prolactin and glucose levels in ewe and ram lambs during normal and compensatory growth*, Domestic Animal Endocrinology, **7** (1990), 365–381.

[71] E.R. Ørskov and D.M. Allen, *Utilization of salts of volatile fatty acids by growing sheep*, British Journal of Nutrition, **20** (1966), 295–305.

[72] M. Ozcan, B. Ekiz, A. Yilmaz and A. Ceyhan, *Genetic parameter estimates for lamb growth traits and greasy fleece weight at first shearing in Turkish Merino sheep*, Small Ruminant Research, **56** (2005), 215–222.

[73] N. Panousis, Ch. Brozos, I. Karagiannis, N.D. Giadinis, S. Lafi and M. Kritsepi-Konstantinou, *Evaluation of Precision Xceed® meter for on-site monitoring of blood β-hydroxybutyric acid and glucose concentrations in dairy sheep*, Research in Veterinary Science, **93** (2012), 435–439.

[74] K.L. Pearce, K. Rosenvold, H.J. Andersen and D.L. Hopkins, *Water distribution and mobility in meat during the conversion of muscle to meat and ageing and the impacts on fresh meat quality attributes - A review*, Meat Science, **89** (2011), 111–124.

[75] L. Petzold, *Automatic selection of methods for solving stiff and nonstiff systems of ordinary differential equations*, SIAM Journal on Scientific and Statistical Computing, **4** (1983), 136–148.

[76] L.S. Pontryagin, V.G. Boltyanskii, R.V. Gamkrelidze, and E.F. Mischenko, "The Mathematical Theory of Optimal Processes", Wiley Interscience, New York, 1962.

[77] C.A. Ramírez-Restrepo, T.N. Barry, N. López-Villalobos, P.D. Kemp and W.C. McNabb, *Use of Lotus corniculatus containing condensed tannins to increase lamb and wool production under commercial dryland farming conditions without the use of anthelmintics*, Animal Feed Science and Technology, **177** (2004), 85–105.

[78] D. Ramsey, "Implementation of Automatic Differentiation Code for a Complex Optimal Control Problem", Mathematics Project, Curtin University of Technology, Perth, Australia, 2004.

[79] S. Rehbein, H. Oertel, D. Barth, M. Visser, R. Winter, L.G. Cramer and W.K. Langholff, *Effects of Psoroptes ovis infection and its control with an ivermectin controlled-release capsule on growing sheep. 2. Evaluation of wool production and leather value*, Veterinary Parasitology, **91** (2000), 119–128.

[80] J.P Robertson, A. Faulkner and R.G. Vernon, *Regulation of glycolysis and fatty acid synthesis from glucose in sheep adipose tissue*, Biochem. J., **206** (1982), 577–586.

[81] M. Rodehutscord, P. Young, N. Phillips and C.L. White, *Wool growth in Merino wethers fed lupins untreated or treated with heat, formaldehyde, with and without a supplementation of rumen protected methionine*, Animal Feed Science and Technology, **82** (1999), 213–226.

[82] J.A.F. Rook, C.C. Balch, R.C. Campling and L.J. Fisher, *The utilization of acetic, propionic and butyric acids by growing heifers*, British Journal of Nutrition, **17** (1963), 399-406.

[83] R.D. Sainz and J.E. Wolff, *Development of a dynamic, mechanistic model of lamb metabolism and growth*, Animal Production, **51** (1990), 535–549.

[84] R.D. Sainz and J.E. Wolff, *Evaluation of hypotheses regarding mechanisms of action of growth promotants and repartitioning agents using a simulation model of lamb metabolism and growth*, British Society of Animal Production, **51** (1990), 551–558.

[85] M.R. Sanz Sampelayo, M.J. Lupiani, J.E. Guerrero and J. Boza, *A comparison of different metabolic types between goat kids and lambs: Key blood constituents at different times in the first two months after birth*, Small Ruminant Research, **31** (1998), 29–35.

[86] Z. Sarnyai and L.G. Boros, *Modeling networks of glycolysis, overall energy metabolism and drug metabolism under a systems biology approach*, Annual Reports in Medicinal Chemistry, **43** (2008), Chapter 20: 329–349.

[87] G.H. Scales, A.R. Bray, D.B. Baird, D. O'Connell and T.L. Knight, *Effect of sire breed on growth, carcass, and wool characteristics of lambs born to Merino ewes in New Zealand*, New Zealand J. of Agric. Research, **43** (2000), 93–100.

[88] T.W. Searle, *Body composition in lambs and young sheep and its prediction in vivo from tritiated water space and body weight*, Journal of Agricultural Science, Cambridge, **74** (1970), 357–362.

[89] N.K. Sinha and S.K. Singh, *Genetic and phenotypic parameters of body weights, average daily gains and first shearing wool yield in Muzaffarnagri sheep*, Small Ruminant Research, **26** (1997), 21–29.

[90] The State of Queensland (Department of Agriculture, Fisheries and Forestry), "Facts and Figures on Sheep and Wool", *http://www2.dpi.qld.gov.au/sheep/6572.html*, Archived to *http://archive.is/Vx7e*, 2005.

[91] L.O. Tedeschi, D.G. Fox, G.E. Carstens and C.L. Ferrell, *The partial efficiency of use of metabolisable energy for growth in ruminants*, In: Energy and Protein Metabolism and Nutrition (G. M. Crovetto, Ed.), European Assoc. for Anim. Prod. Publ., **127** (2010), 519–529.

[92] K.L. Teo, C.J. Goh and K.H. Wong, *A unified computational approach to optimal control problems*, In: Pittman Monographs and Surveys in Pure and Applied Mathematics 55, Longman Scientific and Technical, New York, 1991.

[93] M.K. Tripathi, A.S. Mishra, A.K. Misra, D. Mondal and S.A. Karim, *Effect of substitution of groundnut with high glucosinolate mustard (Brassica juncea) meal on nutrient utilization, growth, vital organ weight and blood composition of lambs*, Small Ruminant Research, **39** (2001), 261–267.

[94] R.N. Upton, *Organ weights and blood flows of sheep and pig for physiological pharmacokinetic modelling*, Journal of Phamacological and Toxicological Methods, **58** (2008), 198–205.

[95] I. Vetharaniam, D.G. McCall, P.F. Fennessy and D.J. Garrick, *A model of mammalian energetics and growth: Model development*, Agricultural Systems, **68** (2001), 55–68.

[96] I. Vetharaniam, D.G. McCall, P.F. Fennessy and D.J. Garrick, *A model of mammalian energetics and growth: Model testing (sheep)*, Agricultural Systems, **68** (2001), 69–91.

[97] O. Von Stryk, *Numerical solution of optimal control problems by direct collocation*, In: Optimal Control - Calculus of Variations, Optimal Control Theory and Numerical Methods (R.Bulirsch, A.Miele, J.Stoer and K-H. Well,

Eds.), International Series of Numerical Mathematics, Basel: Birkhäuser, **111** (1993), 129–143.

[98] B.C. Wang and R. Luus, *Reliability of optimization procedures for obtaining global optimum*, AICh J., **24** (1978), 619–626.

[99] S.R. West, J.H Brown and B.J Enquist, *A general model for the origin of allometric scaling laws in biology*, Science, **276** (1997), 122–126.

[100] C.L. White, L.M. Tabe, H. Dove, J. Hamblin, P. Young, N. Phillips, R. Taylor, S. Gulati, J. Ashes and T.J.V. Higgins, *Increased efficiency of wool growth and live weight gain in Merino sheep fed transgenic lupin seed containing sunflower albumin*, Journal of the Science of Food and Agriculture, **81** (2000), 147–154.

[101] D.H. White and B.J. McConchie, *Effect of stocking rate on fleece measurements and their relationships in Merino sheep*, Aust. J. Agric. Res., **27** (1976), 163–174.

[102] A.J. Williams, *Wool growth*, In: Australian Sheep and Wool Handbook (D.J. Cottle, Ed.), Inkata Press, Melbourne, Australia, (1995), 224–242.

[103] M. Wodzicka, *Studies on the thickness and chemical composition of the skin of sheep*, New Zealand Journal of Agricultural Research, **1:4** (1958), 582–591.

[104] Wool Producers Australia, "Genetics", *http://www.woolproducers.com.au/about/trade/genetics/.*

[105] T. Wuliji, K.G. Dodds, J.T.J. Land, R.N. Andrews and P.R. Turner, *Response to selection for ultrafine Merino sheep in New Zealand*, Livestock Production Science, **58** (1999), 33–44.

[106] S. Zhang, D. Blache, M.A. Blackberry and G.B. Martin, *Body reserves affect the reproductive endocrine responses to an acute change in nutrition in mature male sheep*, Animal Reproduction Science, **88** (2005), 257–269.

A Background

Tables 40 – 43 define the symbols, notation, rates and parameters of the Sainz and Wolff [83] model respectively.

Symbol	Entity	Symbol	Entity	Symbol	Entity
Aa	Amino Acids	La	Lactic Acid		DNA in:
Ac	Acetic Acid	Ox	Oxygen	Db	Carcass
Ad	ADP		Protein in:	Dv	Viscera
At	ATP	Pb	Carcass	Dz	Other tissues
Bu	Butyric Acid	Pv	Viscera	Pr	Propionic Acid
Cd	Carbon Dioxide	Pz	Other tissues	Tg	Circulating Lipids
Gl	Glucose	Pw	Wool	Tp	Triose Phosphates
Gy	Glycerol			Ts	Storage Triacylglycerol

Table 40: Symbols used for quantities in the model (Sainz and Wolff [83]).

Notation	Translation	Units
A_i	Absorption rate of i	mol i per day
$U_{i,jk}$	Utilisation of i in $j \rightarrow k$ reaction	
$P_{i,jk}$	Production of i in $j \rightarrow k$ reaction	
$R_{i,jk}$	Requirement for i in $j \rightarrow k$ reaction	mol i per mol j utilised in $j \rightarrow k$ reaction
$Y_{i,jk}$	Yield of i from $j \rightarrow k$ reaction	
K_{jk}	Rate constant for $j \rightarrow k$ reaction	1 per day or per day
V_{jk}	Maximum velocity for $j \rightarrow k$ reaction with respect to i	mol j per day
$k_{i,jk}$	Michaelis-Menton constant for $j \rightarrow k$ reaction with respect to i	mol i per 1
C_i	Concentration of i	
W_l	Weight of l (l = empty of full body,P_b, P_v, P_z, P_w, T_s)	kg
Hm	Index of hormonal state, in which m is A (anabolic) or C (catabolic)	none
v_n	Volume of distribution n (n =extra-cellular fluid (ECF), W_{EB})	1 or kg

Table 41: General Sainz and Wolff [83] model notation.

Term	Definition
W_{EB}	empty body weight (kg)
A_{Aa}	absorption of amino acids
A_{Gl}	absorption of glucose
A_{Tg}	absorption of lipids
A_{Ac}	absorption of acetate
A_{Pr}	absorption of propionate
A_{Bu}	absorption of butyrate
$U_{Bu,BuCd}$	butyrate oxidation
$U_{Aa,AaGl}$	gluconeogenesis from amino acids
$U_{Pr,PrGl}$	gluconeogenesis from propionate
$U_{La,LaGl}$	gluconeogenesis from lactate
$U_{Gy,GyGl}$	gluconeogenesis from glycerol
$U_{Gl,GlTp}$	glucose to triose phosphates
$U_{Tp,TpLa}$	triose phosphates to lactate
$U_{La,LaCd}$	lactate oxidation
$U_{Ac,AcTs}$	lipogenesis from acetate
$U_{Ts,TsTg}$	lipolysis of storage fat
$U_{Tg,TgTs}$	esterification of fatty acids
$U_{Pb,PbAa}$	carcass protein degradation
$U_{Pv,PvAa}$	visceral protein degradation
$U_{Pz,PzAa}$	“other” protein degradation
$U_{Aa,AaPb}$	carcass protein synthesis
$U_{Aa,AaPv}$	visceral protein synthesis
$U_{Aa,AaPz}$	“other” protein synthesis
$U_{Aa,AaPw}$	wool protein synthesis
	undefined energy expenditure in:
$U_{At,carcass}$	carcass
$U_{At,viscera}$	viscera
$U_{At,other}$	other tissues
$U_{At,AtAd}$	total ATP hydrolysis
$P_{At,AdAt}$	partial ATP production
$U_{Gl,GlCd}$	glucose oxidation
$U_{Tg,TgCd}$	lipid oxidation
$U_{Ac,AcCd}$	acetate oxidation

Table 42: Definitions of major rates in the Sainz and Wolff model [83].

Name	Value	Name	Value	Name	Value	Name	Value
$\theta 1$	1.0	$K_{carcass}$	0.34	D_{Aa}	0.027	$Y_{Gl,AaGl}$	0.3528
$\theta 2$	1.0	$K_{viscera}$	1.94	D_{Gl}	0.0	$Y_{Ac,AaGl}$	0.437
$\theta 3$	0.878	K_{other}	0.97	D_{Tg}	0.000556	$Y_{At,AaGl}$	3.7
$\theta 4$	0.902	K_{Db}	0.015	D_{Ac}	0.176	$Y_{Ac,TgCd}$	6.0
$\theta 5$	5.0	K_{Dv}	0.03	D_{Pr}	0.778	$Y_{At,TgCd}$	321.0
$\theta 6$	0.75	K_{Dz}	0.045	D_{Bu}	0.0273	$Y_{Gl,PrGl}$	0.5
$\theta 7$	0.682	K_{PbAa}	0.04	Db_{MAX}	0.00737	$Y_{Gl,LaGl}$	0.5
$\theta 8$	0.852	K_{PvAa}	0.3	Dv_{MAX}	0.0813	$Y_{Gl,GyGl}$	0.5
$\theta 9$	0.882	K_{PzAa}	0.1	Dz_{MAX}	0.0048	$Y_{Ac,AcTs}$	0.04167
$\theta 10$	0.916	k_{AaPw}	0.0025	$V^{'}_{AaPb}$	21.7	$Y_{Tp,GlTp}$	2.0
$K^{'}_{AaGl}$	18.0	k_{TgCd}	0.0038	$V^{'}_{AaPv}$	63.2	$Y_{At,GlCd}$	38.0
$k^{'}_{AaPb}$	0.0005	k_{AcCd}	0.001	$V^{'}_{AaPz}$	33.8	$Y_{At,AcCd}$	10.0
$k^{'}_{AaPv}$	0.0005	k_{TsTg}	0.0968	$V^{'}_{AaPw}$	0.0145	$Y_{At,GyGl}$	2.0
$k^{'}_{AaPz}$	0.0005	$k_{Tg,AcTs}$	0.0036	$V^{'}_{GlTp}$	0.0415	$Y_{At,PrCd}$	17.0
$k^{'}_{GlTp}$	0.003	$k_{Ac,AcTs}$	0.001	$V^{'}_{TgTs}$	0.00518	$Y_{At,BuCd}$	25.0
$k^{'}_{GlCd}$	0.0165	$k_{Gl,TgTs}$	0.003	$V^{'}_{AcTs}$	0.346	$Y_{At,TpLa}$	2.0
$k^{'}_{Gl,AcTs}$	0.001	$k_{Tg,TgTs}$	0.0024	$V^{'}_{TsTg}$	0.00546	$Y_{At,LaCd}$	18.0
F_{intake}	1.6	$R_{At,A_{Gl}}$	1.0	$R_{At,TgTs}$	9.0	$R_{At,TsTg}$	9.0
$C_{Aa,ref}$	0.0025	$R_{At,A_{Tg}}$	4.0	$R_{At,AcTs}$	8.5	$R_{Ox,GlCd}$	6.0
$C_{Gl,ref}$	0.003	$R_{At,AaPx}$	5.0	$R_{At,PrGl}$	2.0	$R_{Ox,TgCd}$	57.0
$R_{At,A_{Aa}}$	1.0	$R_{At,GlTp}$	2.0	$R_{At,LaGl}$	3.0	$R_{Ox,AcCd}$	2.0

Table 43: Parameter names and values (Sainz and Wolff [83]).

B Molecular Weights

Amino Acid	MW (g/mol)	Carcass	Viscera	Other	Wool
Aspartate	133	11.755	12.181	9.589	8.804
Threonine	119	5.909	6.288	4.850	7.161
Serine	105	4.171	4.915	5.486	8.741
Glutamate	147	19.707	18.274	18.433	20.937
Glycine	75	6.927	5.476	9.718	3.912
Alanine	89	7.071	6.048	7.998	3.571
Valine	117	5.693	6.475	0.367	6.454
Isoleucine	131	4.943	5.273	3.285	3.942
Leucine	131	9.757	10.942	7.803	9.723
Tyrosine	181	5.572	7.013	5.107	9.440
Phenylalanine	165	6.390	7.969	5.517	5.958
Histidine	155	4.002	4.366	2.268	1.866
Lysine	146	10.149	10.140	7.323	5.125
Arginine	174	12.614	11.036	14.364	15.882
Proline	115	6.966	6.253	9.974	7.497
Methionine	149	2.663	4.047	1.557	0.897
Cysteine	121	1.081	2.373	4.425	11.894
Hydroxyproline	131	4.033	1.980	7.803	0.000
Total		**129.40**	**131.05**	**125.86**	**131.80**

Table 44: Amino acid contribution to the weighted average molecular weights of amino acids in protein.

	Molecular Weight		
Protein Area	**Number Avg.**	**Weighted Avg.**	**PDI**
Carcass	122.13	129.42	1.0596
Viscera	123.75	131.05	1.0590
Other Tissues	122.40	125.86	1.0283
Wool	126.41	131.80	1.0427

Table 45: Polydispersity indices (PDI) for amino acids in protein.

C Growth Trajectories

Figures from Sections 5.1 and 5.2 not essential to explain the findings of these Sections are presented here.

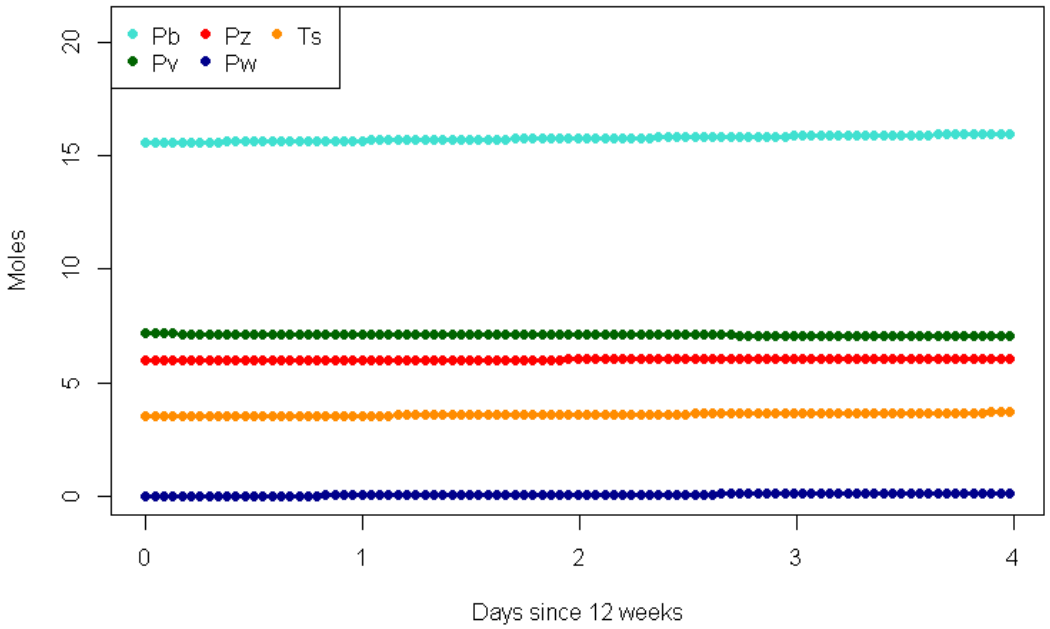

Figure 74: Protein pools and storage triacylglycerol (Ts) over first four days of simulation, using preliminary initial conditions derived from Hon [45].

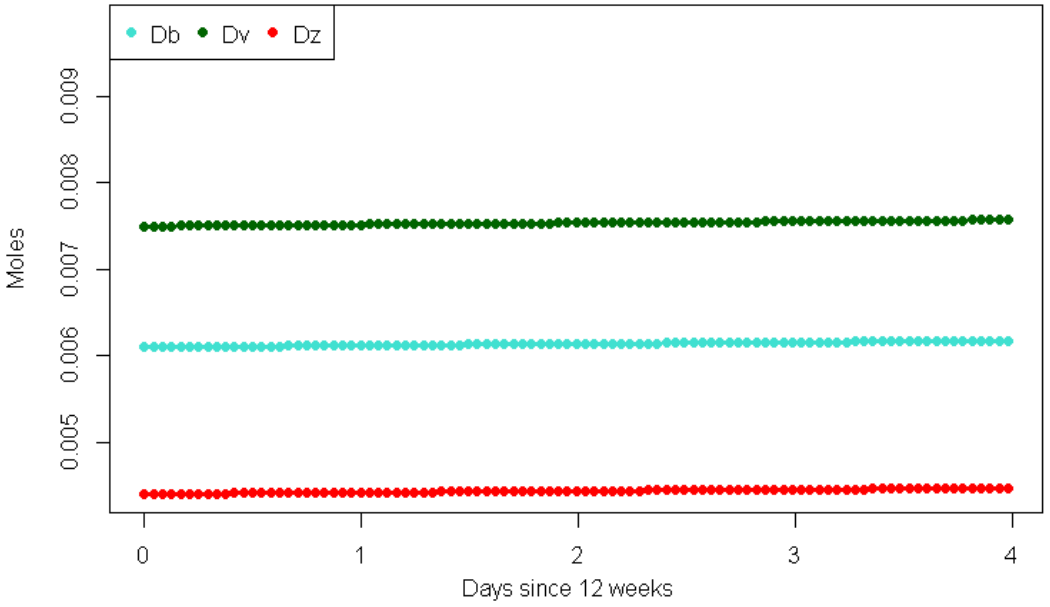

Figure 75: DNA pools over first four days of simulation, using preliminary initial conditions derived from Hon [45].

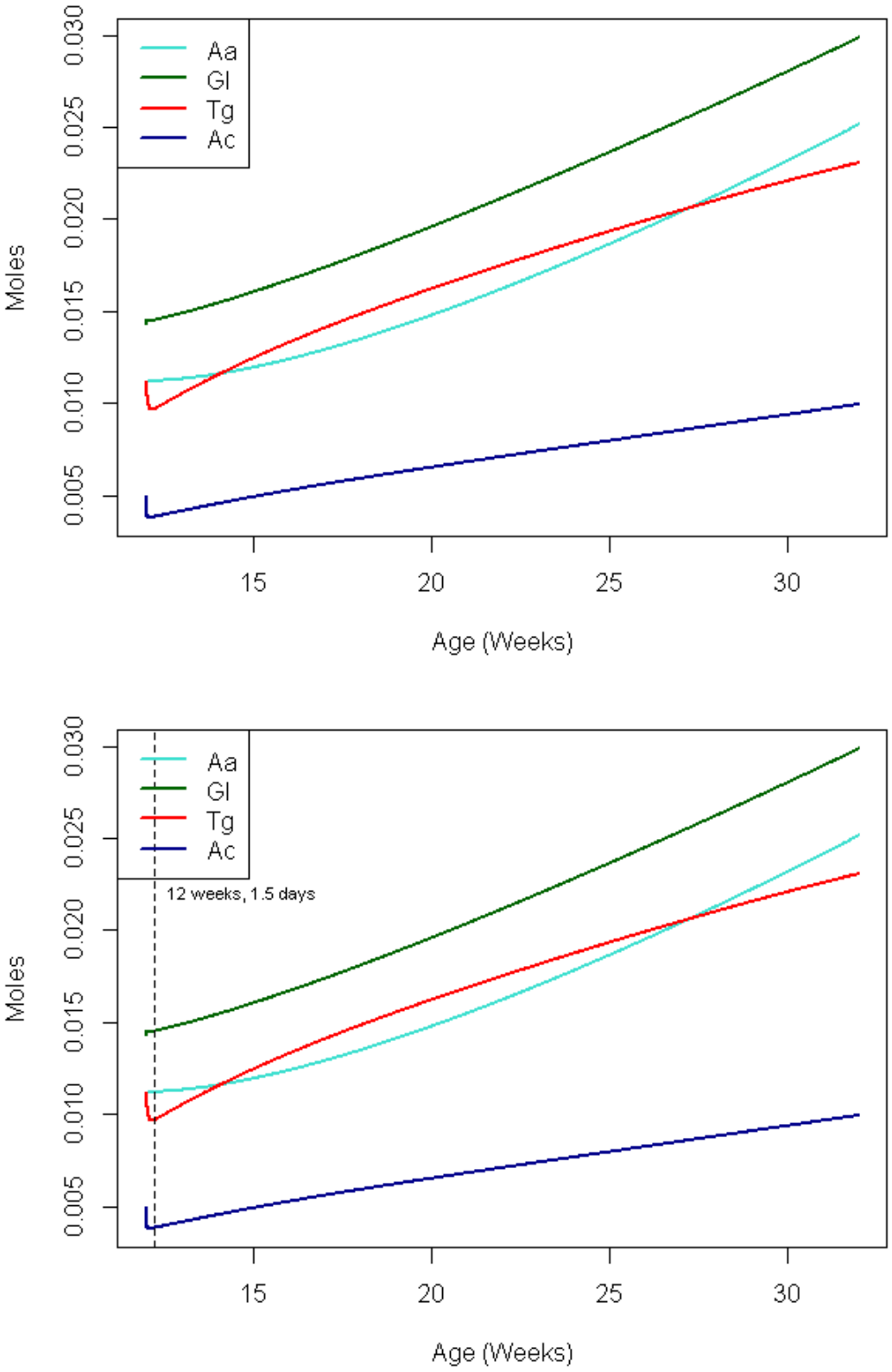

Figure 76: Circulating amino acids (Aa), glucose (Gl), lipids (Tg) and acetate (Ac), using preliminary initial conditions derived from Sainz and Wolff [83].

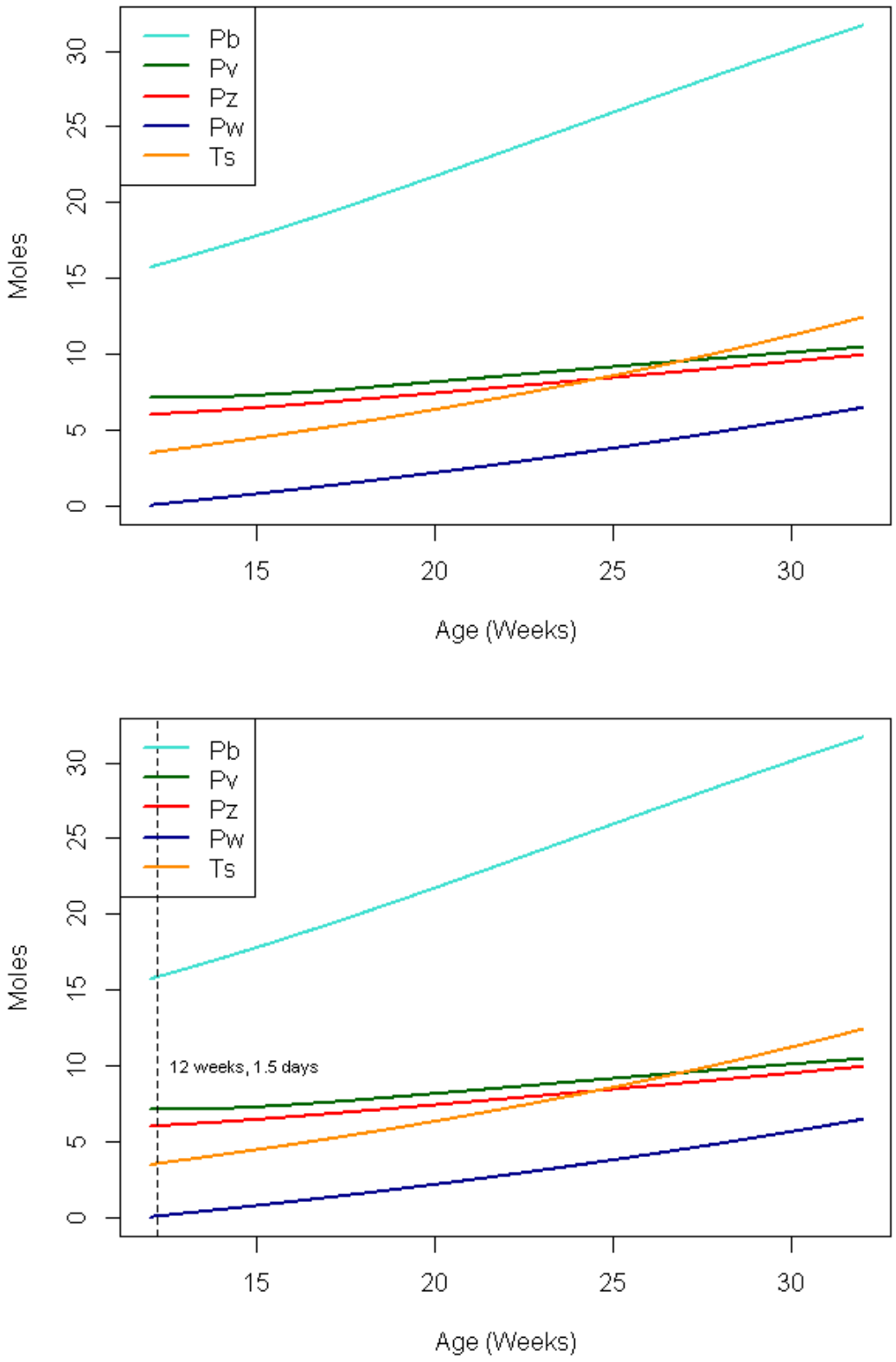

Figure 77: Protein in carcass (Pb), viscera (Pv), other tissues (Pz) and wool (Pw), and storage triacylglycerol (Ts), using preliminary initial conditions derived from Sainz and Wolff [83].

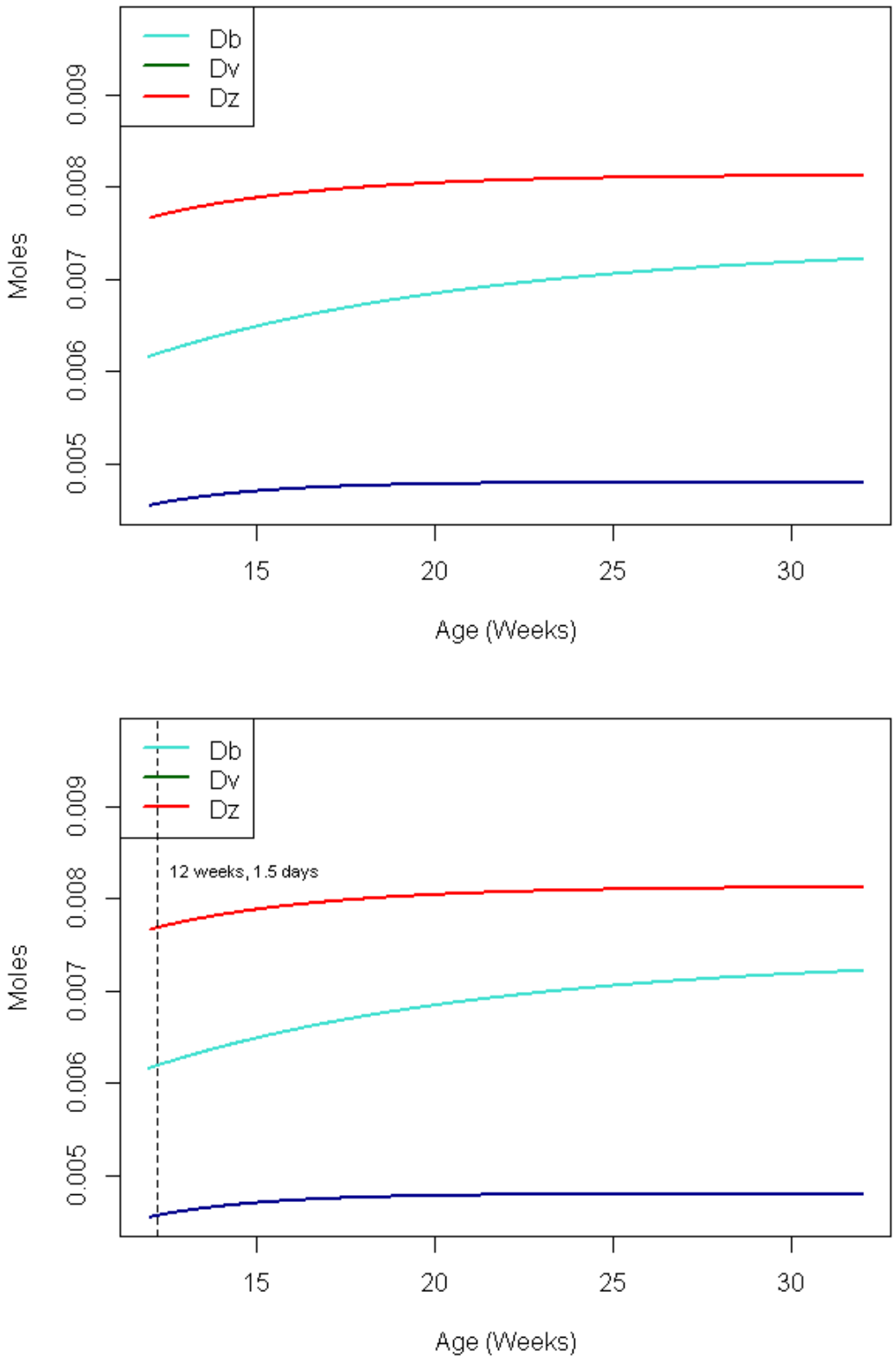

Figure 78: DNA pools corresponding to carcass (Db), viscera (Dv) and other tissues (Dz), using preliminary initial conditions derived from Sainz and Wolff [83].

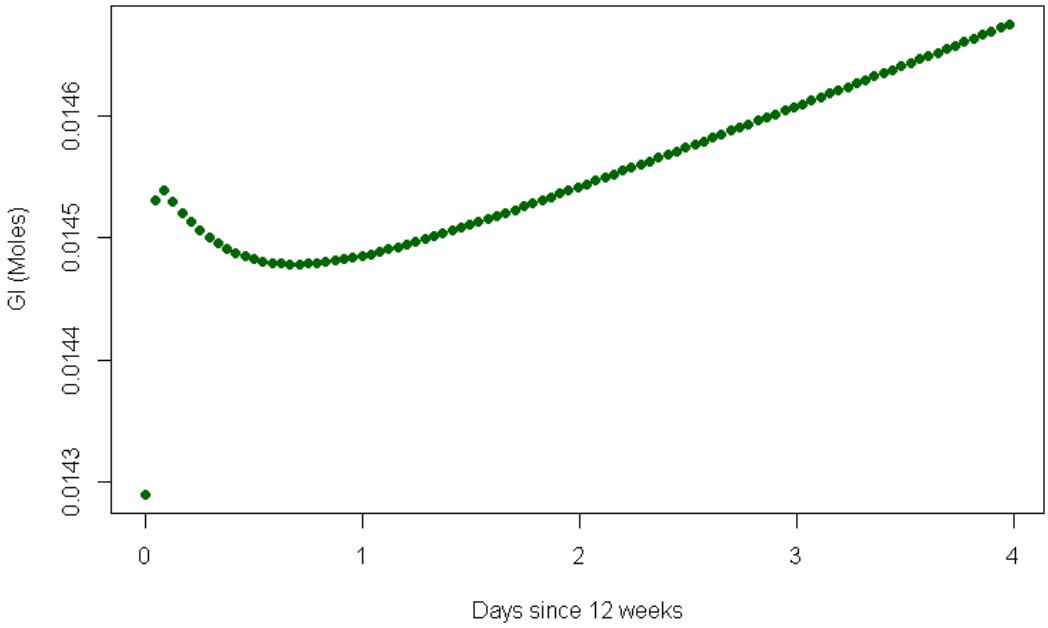

Figure 79: Glucose (Gl) over first four days of simulation, using preliminary initial conditions derived from Sainz and Wolff [83].

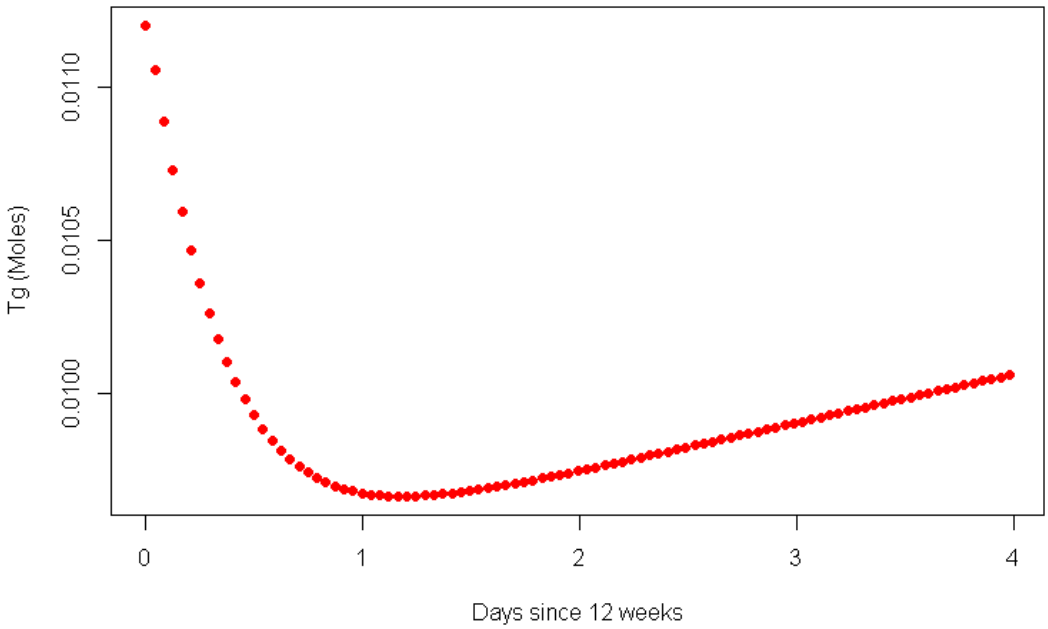

Figure 80: Lipids (Tg) over first four days of simulation, using preliminary initial conditions derived from Sainz and Wolff [83].

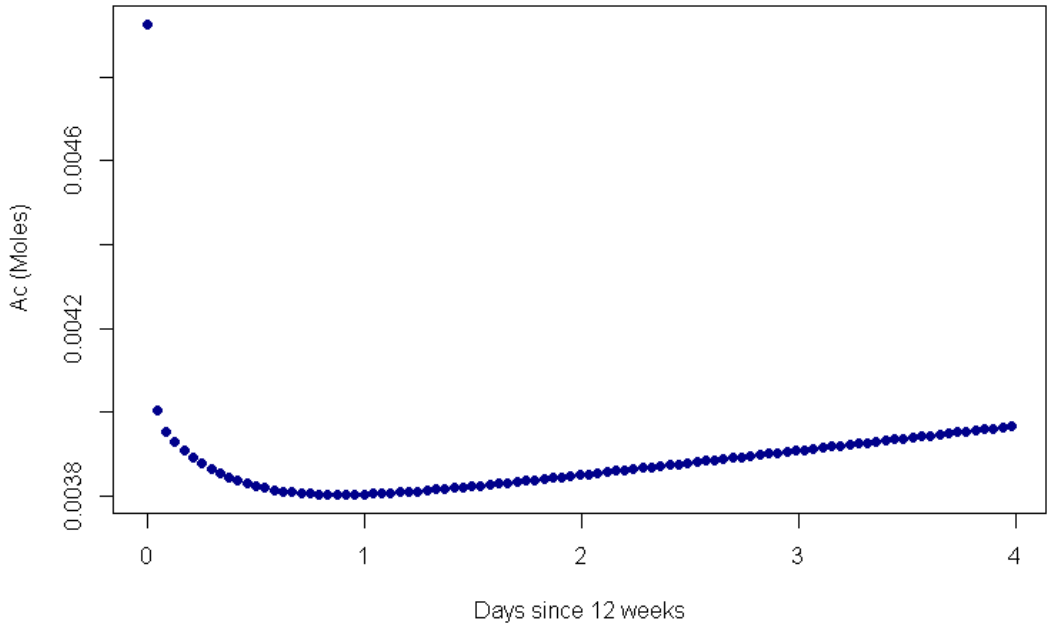

Figure 81: Acetate (Ac) over first four days of simulation, using preliminary initial conditions derived from Sainz and Wolff [83].

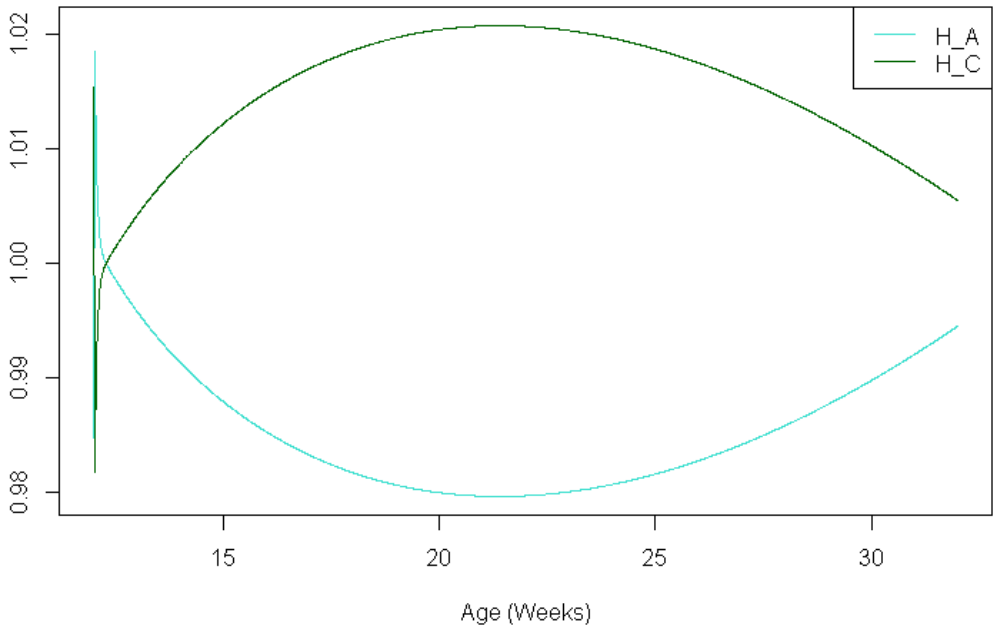

Figure 82: Anabolic (H_A) and catabolic (H_C) hormonal controls, using preliminary initial conditions derived from Sainz and Wolff [83].

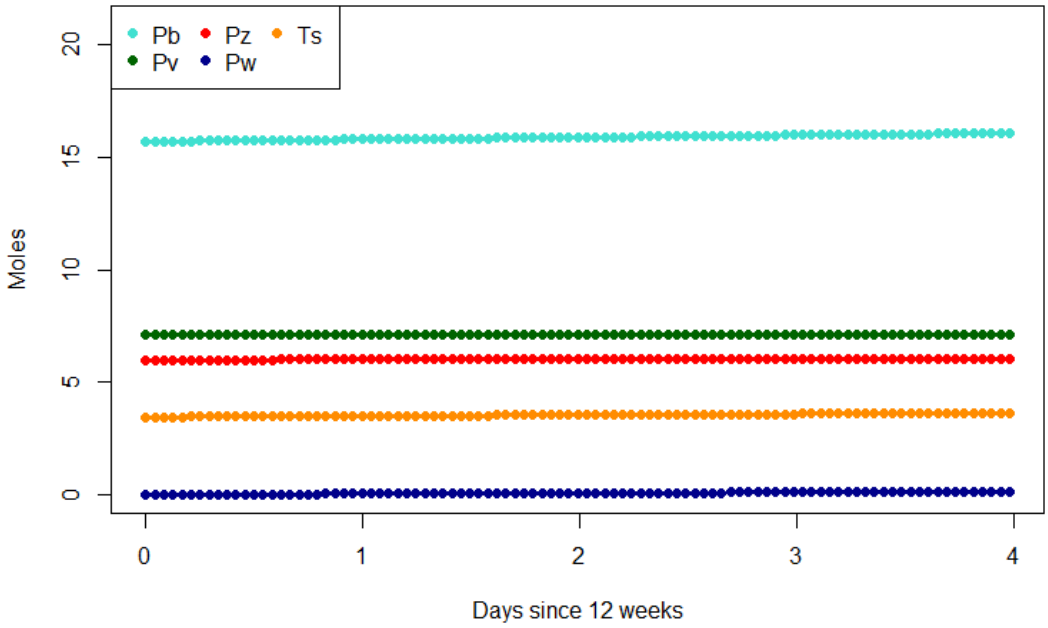

Figure 83: Protein pools and storage triacylglycerol (Ts) over first four days of simulation, using preliminary initial conditions derived from Sainz and Wolff [83].

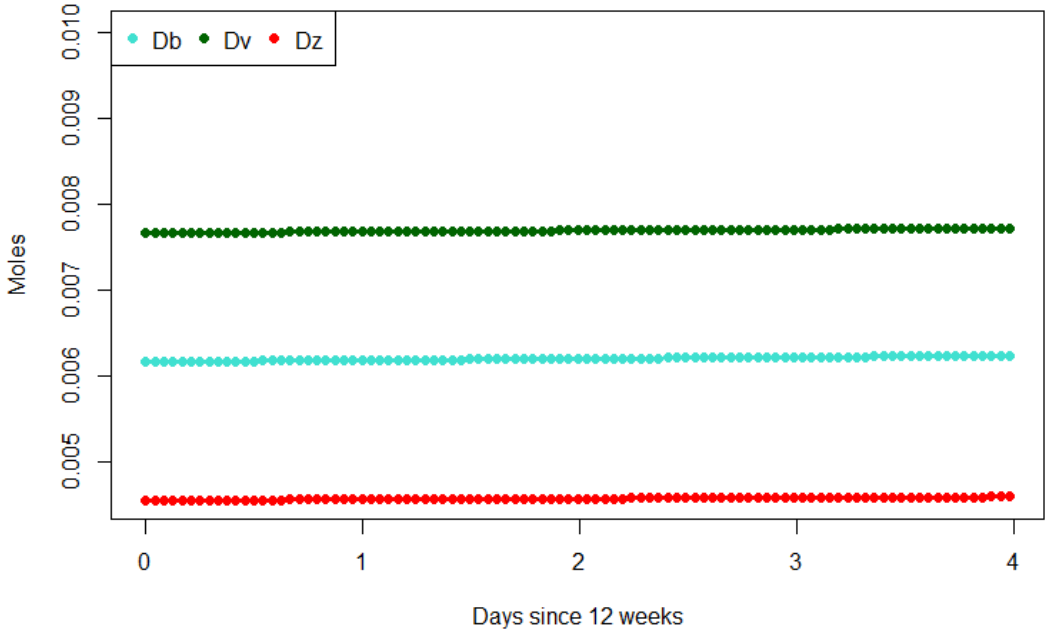

Figure 84: DNA pools over first four days of simulation, using preliminary initial conditions derived from Sainz and Wolff [83].

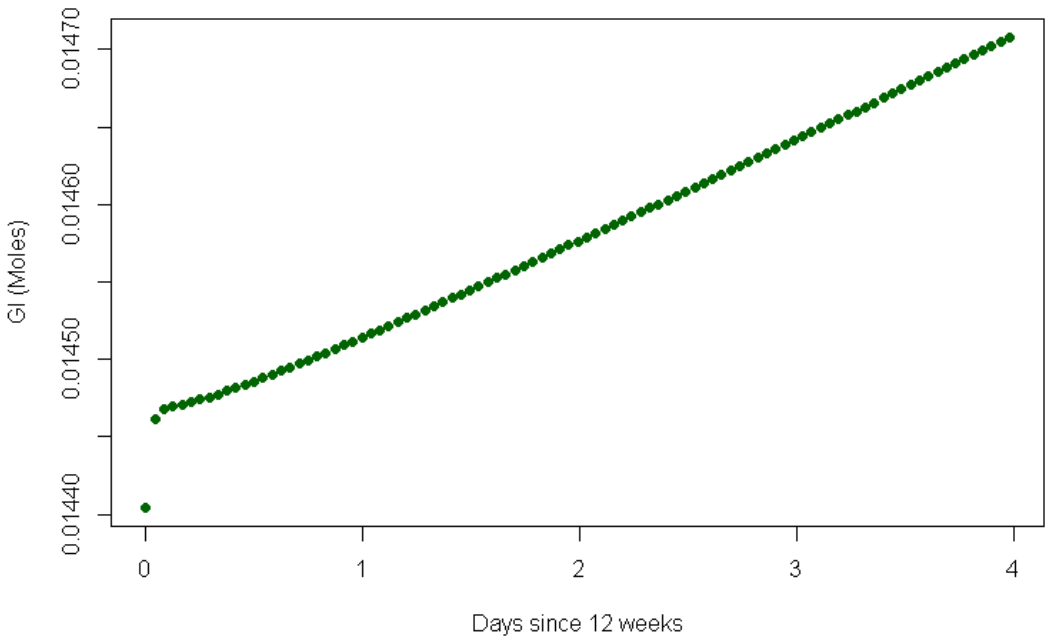

Figure 85: Glucose (Gl) over first four days of simulation, using draft revised initial conditions derived from Sainz and Wollf [83].

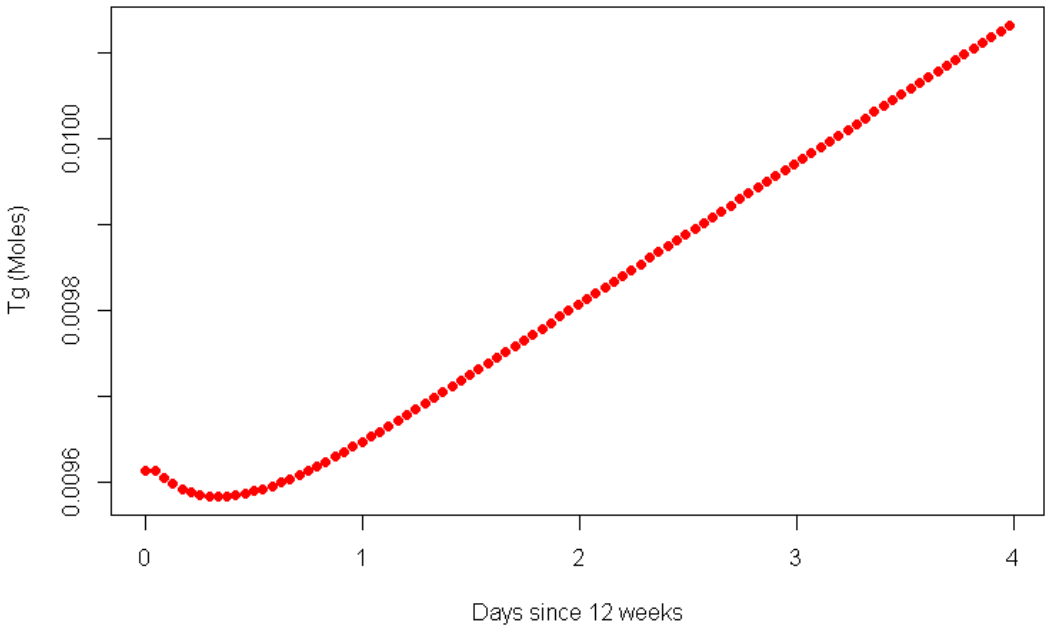

Figure 86: Lipids (Tg) over first four days of simulation, using draft revised initial conditions derived from Sainz and Wollf [83].

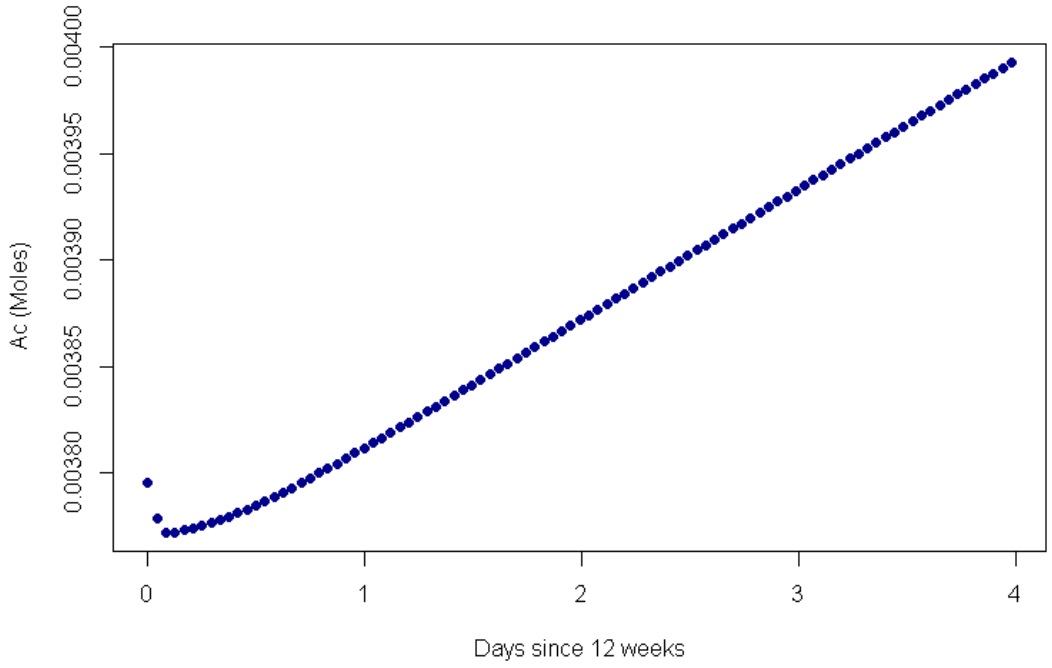

Figure 87: Acetate (Ac) over first four days of simulation, using draft revised initial conditions derived from Sainz and Wollf [83].

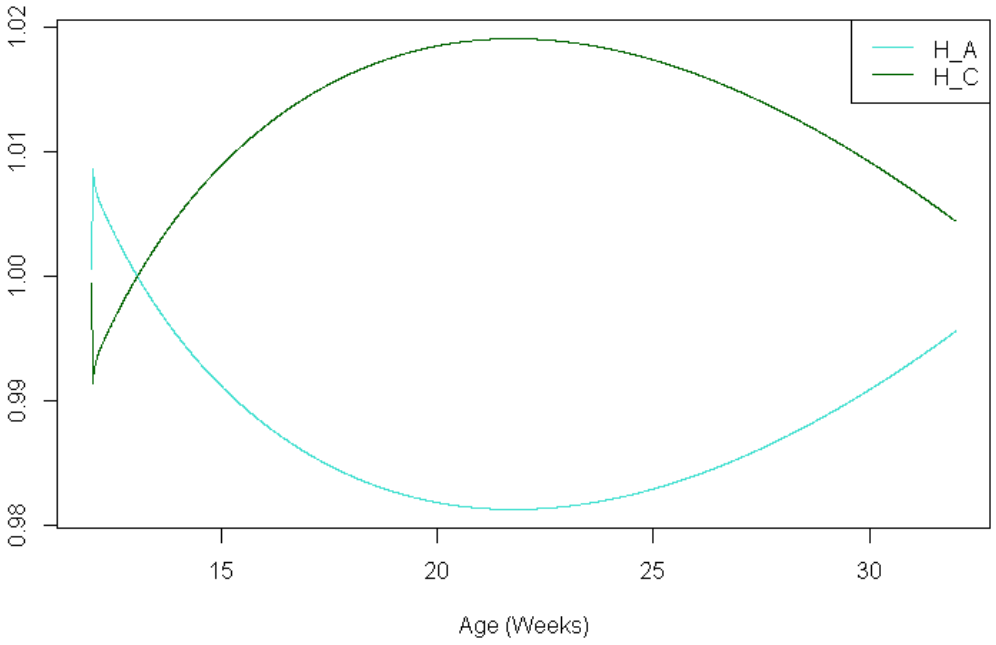

Figure 88: Anabolic (H_A) and catabolic (H_C) hormonal controls, using draft revised initial conditions derived from Sainz and Wolff [83].

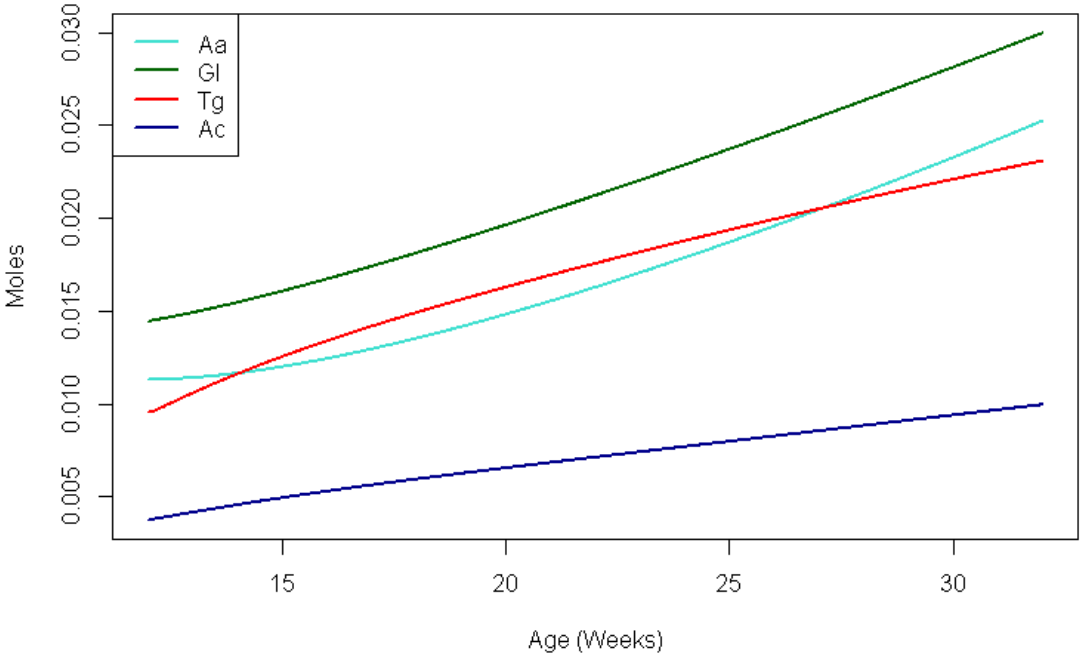

Figure 89: Circulating amino acids (Aa), glucose (Gl), lipids (Tg) and acetate (Ac), using further revised initial conditions derived from Sainz and Wolff [83].

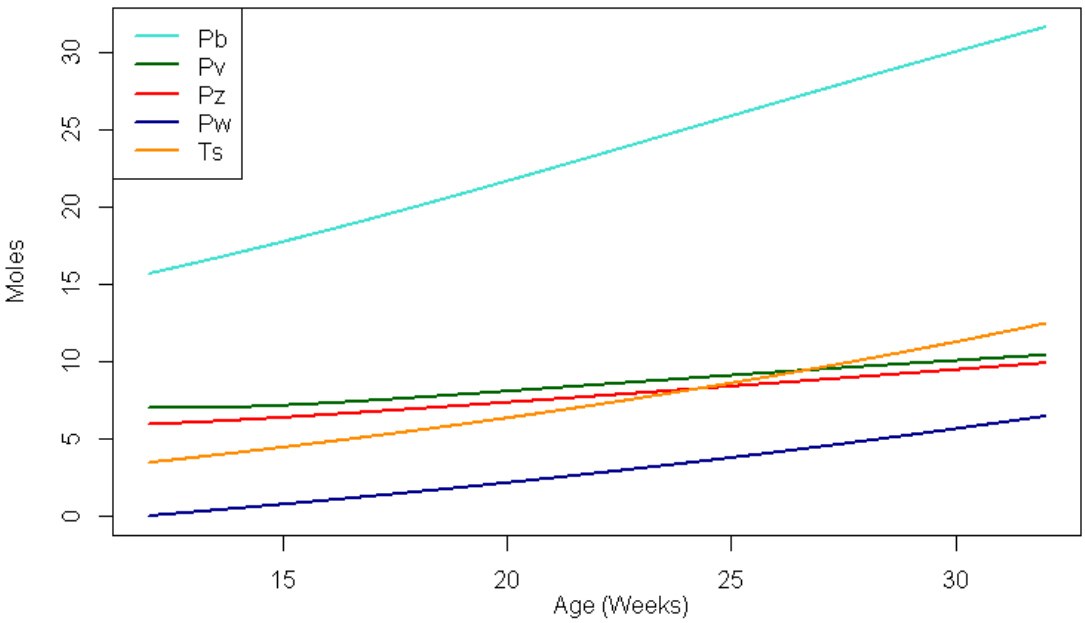

Figure 90: Protein in carcass (Pb), viscera (Pv), other tissues (Pz), wool (Pw), and storage triacylglycerol (Ts), using further revised initial conditions derived from Sainz and Wolff [83].

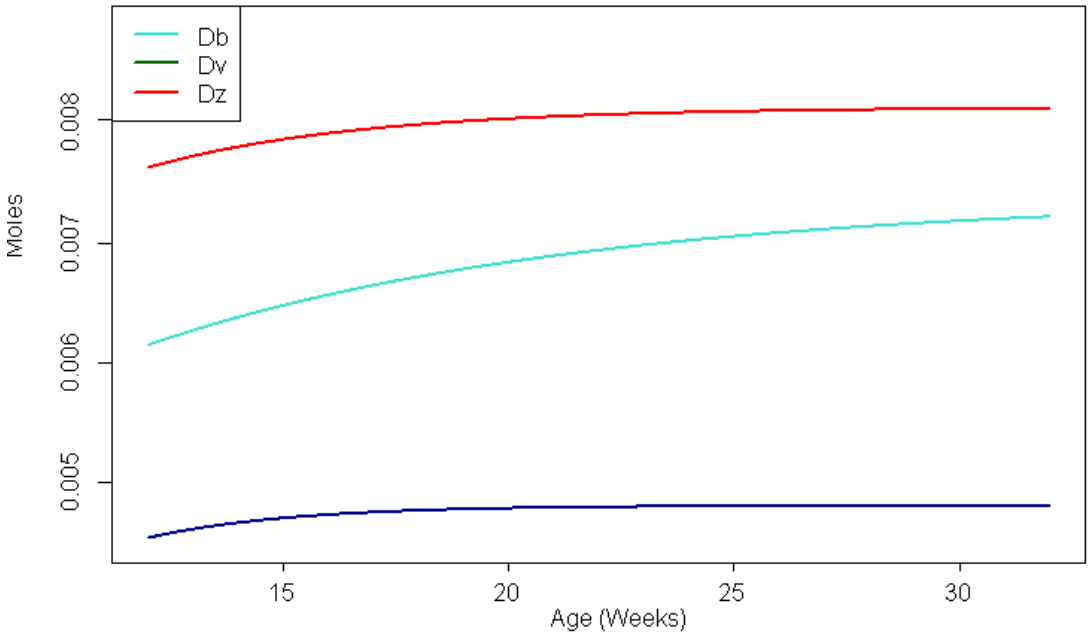

Figure 91: DNA pools corresponding to carcass (Db), viscera (Dv) and other tissues (Dz), using further revised initial conditions derived from Sainz and Wolff [83].

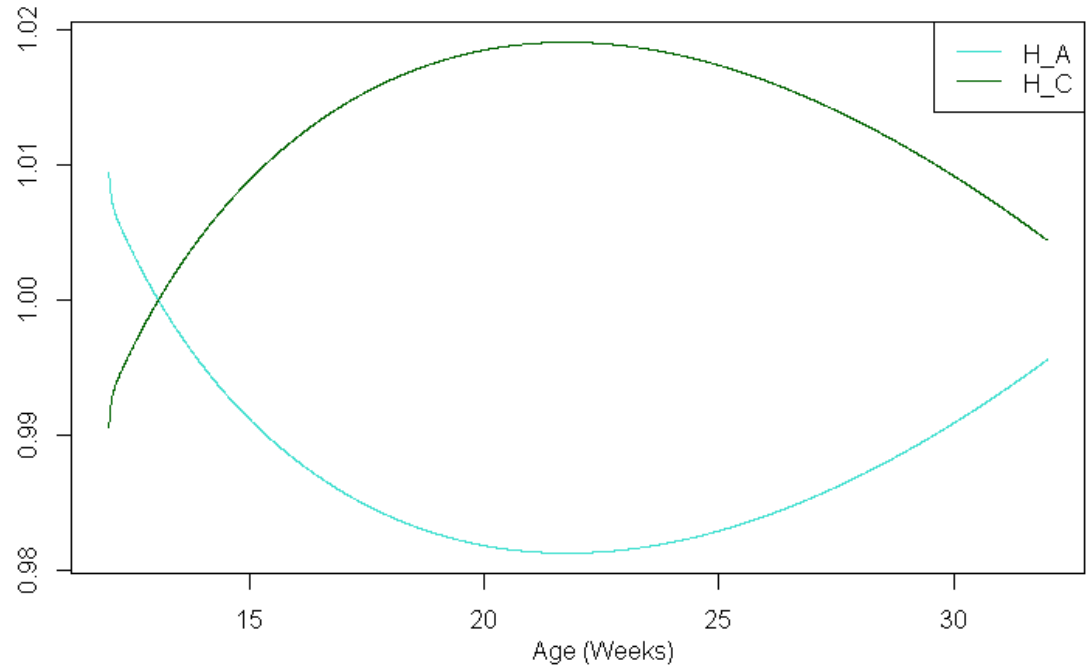

Figure 92: Anabolic (H_A) and catabolic (H_C) hormonal controls, using further revised initial conditions derived from Sainz and Wolff [83].